

# CHAPTER 1

---

## Update on Ozone-Depleting Substances (ODSs) and Other Gases of Interest to the Montreal Protocol

**Lead Authors:**

L.J. Carpenter  
S. Reimann

**Coauthors:**

J.B. Burkholder  
C. Clerbaux  
B.D. Hall  
R. Hossaini  
J.C. Laube  
S.A. Yvon-Lewis

**Contributors:**

D.R. Blake  
M. Dorf  
G.S. Dutton  
P.J. Fraser  
L. Froidevaux  
F. Hendrick  
J. Hu  
A. Jones  
P.B. Krummel  
L.J.M. Kuijpers  
M.J. Kurylo  
Q. Liang  
E. Mahieu  
J. Mühle  
S. O'Doherty  
K. Ohnishi  
V.L. Orkin  
K. Pfeilsticker  
M. Rigby  
I.J. Simpson  
Y. Yokouchi

**Chapter Editors:**

A. Engel  
S.A. Montzka

[Formatted for double-sided printing.]

From:

WMO (World Meteorological Organization), *Scientific Assessment of Ozone Depletion: 2014*, Global Ozone Research and Monitoring Project – Report No. 55, 416 pp., Geneva, Switzerland, 2014.

This chapter should be cited as:

L.J. Carpenter and S. Reimann (Lead Authors), J.B. Burkholder, C. Clerbaux, B.D. Hall, R. Hossaini, J.C. Laube, and S.A. Yvon-Lewis, Ozone-Depleting Substances (ODSs) and Other Gases of Interest to the Montreal Protocol, Chapter 1 in *Scientific Assessment of Ozone Depletion: 2014*, Global Ozone Research and Monitoring Project – Report No. 55, World Meteorological Organization, Geneva, Switzerland, 2014.

# CHAPTER 1

## UPDATE ON OZONE-DEPLETING SUBSTANCES (ODSs) AND OTHER GASES OF INTEREST TO THE MONTREAL PROTOCOL

### Contents

SCIENTIFIC SUMMARY .....	1
1.1 SUMMARY OF THE PREVIOUS OZONE ASSESSMENT .....	5
1.2 LONGER-LIVED HALOGENATED SOURCE GASES .....	5
1.2.1 Updated Observations, Lifetimes, and Emissions .....	5
1.2.1.1 Chlorofluorocarbons (CFCs) .....	6
1.2.1.2 Halons .....	21
1.2.1.3 Carbon Tetrachloride (CCl <sub>4</sub> ) .....	22
1.2.1.4 Methyl Chloroform (CH <sub>3</sub> CCl <sub>3</sub> ) .....	24
1.2.1.5 Hydrochlorofluorocarbons (HCFCs) .....	24
1.2.1.6 Methyl Chloride (CH <sub>3</sub> Cl) .....	27
1.2.1.7 Methyl Bromide (CH <sub>3</sub> Br) .....	28
1.3 VERY SHORT-LIVED HALOGENATED SUBSTANCES (VSLS) .....	31
1.3.1 Abundance, Trends, and Emissions of Very Short-Lived Source Gases .....	37
1.3.1.1 Chlorine-Containing Very Short-Lived Source Gases .....	37
1.3.1.2 Bromine-Containing Very Short-Lived Source Gases .....	38
1.3.1.3 Iodine-Containing Very Short-Lived Source Gases .....	41
1.3.2 Dynamics and Transport of VSLS .....	42
1.3.2.1 Source Gas Injection (SGI) .....	43
1.3.2.2 Product Gas Injection (PGI) .....	46
1.3.2.3 Total VSLS Halogen Input into the Stratosphere .....	47
1.3.3 Potential Influence of VSLS on Ozone .....	50
1.3.4 New Anthropogenic VSLS .....	50
1.4 CHANGES IN ATMOSPHERIC HALOGENS .....	53
1.4.1 Tropospheric and Stratospheric Chlorine Changes .....	53
1.4.1.1 Tropospheric Chlorine Changes .....	53
1.4.1.2 Stratospheric Chlorine Changes .....	55
1.4.2 Tropospheric and Stratospheric Bromine Changes .....	57
1.4.2.1 Tropospheric Bromine Changes .....	57
1.4.2.2 Stratospheric Bromine Changes .....	58
1.4.3 Tropospheric and Stratospheric Iodine Changes .....	60
1.4.3.1 Tropospheric Iodine Changes .....	60
1.4.3.2 Stratospheric Iodine Changes .....	60
1.4.4 Changes in Ozone-Depleting Halogen Abundance in the Stratosphere Based Upon Long-Lived Source Gas Measurements: Equivalent Chlorine (ECI) and Equivalent Effective Stratospheric Chlorine (EESC) .....	60
1.4.5 Fluorine in the Troposphere and Stratosphere .....	62
1.5 CHANGES IN OTHER TRACE GASES THAT INFLUENCE STRATOSPHERIC OZONE AND CLIMATE .....	63
1.5.1 Updates to Mole Fractions, Budgets, Lifetimes, and Observations .....	63
1.5.1.1 F-gases .....	64

1.5.1.2	Nitrous Oxide (N <sub>2</sub> O)	72
1.5.1.3	Methane (CH <sub>4</sub> )	73
1.5.1.4	COS, SO <sub>2</sub>	73
1.6	POLICY-RELEVANT INFORMATION HIGHLIGHTS	74
1.6.1	HCFCs Becoming a Larger Fraction of Tropospheric Chlorine; Bromine from Halons Now Decreasing	74
1.6.2	VSLs Chlorinated Compounds Become More Relevant for Stratospheric Ozone	75
1.6.3	Radiative Forcing of ODSs and ODS Replacement Compounds	75
1.6.4	GWP-Weighted Emissions of ODS and ODS Replacement Compounds	76
1.6.5	Ongoing Mismatch between Estimated Sources of CCl <sub>4</sub> from Measurements and from Inventories	77
1.6.6	Quarantine and Pre-Shipment (QPS) Consumption of CH <sub>3</sub> Br Has Exceeded Non-QPS Consumption	78
	REFERENCES	79

## SCIENTIFIC SUMMARY

*Changes in the global atmospheric abundance of a substance are determined by the balance between its emissions and removal. Declines observed for ozone-depleting substances (ODSs) controlled under the Montreal Protocol are due to global emission reductions that have made emissions smaller than removals. Most ODSs are potent greenhouse gases. As the majority of ODSs have been phased out, demand for hydrochlorofluorocarbon (HCFC) and hydrofluorocarbon (HFC) substitutes for the substances controlled under the Montreal Protocol has increased; these are also greenhouse gases. HCFCs deplete much less ozone per kilogram emitted than chlorofluorocarbons (CFCs), while HFCs essentially deplete no ozone.*

**The amended and adjusted Montreal Protocol has continued to reduce emissions and atmospheric abundances of most controlled ozone-depleting substances. By 2012, the total combined abundance of anthropogenic ODSs in the troposphere (measured as Equivalent Chlorine) had decreased by nearly 10% from its peak value in 1994.**

**The contributions to the overall decline in tropospheric chlorine (Cl) and bromine (Br) from substances and groups of substances controlled and not controlled under the Montreal Protocol have changed since the previous Assessment.** The observed declines in total tropospheric Cl and Br from controlled substances during the 5-year period 2008–2012 were  $13.4 \pm 0.9$  parts per trillion (ppt)  $\text{yr}^{-1}$  and  $0.14 \pm 0.02$  ppt  $\text{yr}^{-1}$ , respectively.<sup>1</sup>

*Substances controlled under the Montreal Protocol*

- $-13.5 \pm 0.5$  ppt Cl  $\text{yr}^{-1}$  from chlorofluorocarbons (CFCs)
- $-4.1 \pm 0.2$  ppt Cl  $\text{yr}^{-1}$  from methyl chloroform ( $\text{CH}_3\text{CCl}_3$ )
- $-4.9 \pm 0.7$  ppt Cl  $\text{yr}^{-1}$  from carbon tetrachloride ( $\text{CCl}_4$ )
- $-0.07 \pm 0.01$  ppt Cl  $\text{yr}^{-1}$  from halon-1211
- $+9.2 \pm 0.3$  ppt Cl  $\text{yr}^{-1}$  from hydrochlorofluorocarbons (HCFCs)
- $-0.06 \pm 0.02$  ppt Br  $\text{yr}^{-1}$  from halons
- $-0.08 \pm 0.02$  ppt Br  $\text{yr}^{-1}$  from methyl bromide ( $\text{CH}_3\text{Br}$ )

*Substances not controlled under the Montreal Protocol*

- $-1.7 \pm 1.3$  ppt Cl  $\text{yr}^{-1}$  from methyl chloride ( $\text{CH}_3\text{Cl}$ )
- $+1.3 \pm 0.2$  ppt Cl  $\text{yr}^{-1}$  from very short-lived chlorine compounds (predominantly dichloromethane,  $\text{CH}_2\text{Cl}_2$ )

### Tropospheric Chlorine

**Total tropospheric chlorine from ODSs continued to decrease between 2009 and 2012 to 3300 parts per trillion (ppt) in 2012.** The observed decline in controlled substances of  $13.4 \pm 0.9$  ppt Cl  $\text{yr}^{-1}$  during 2008–2012 was in line with the A1 (baseline) scenario of the 2010 Assessment.

**Of total tropospheric Cl in 2012:**

- **CFCs, consisting primarily of CFC-11, -12, and -113, accounted for  $204 \pm 5$  ppt (about 61%) and are declining.** Their relative contribution is essentially unchanged from the 2010 Assessment (62% in 2008).
- **$\text{CCl}_4$  accounted for  $339 \pm 5$  ppt (about 10%).** While our current understanding of the budget of  $\text{CCl}_4$  is incomplete, mole fractions of  $\text{CCl}_4$  declined largely as projected based on prior observations and the A1 scenario of the 2010 Assessment during 2009–2012.
- **HCFCs accounted for  $286 \pm 4$  ppt (8.7%).** In total, the rate of increase for the sum of HCFCs has slowed by 25% since 2008 and has been lower than projected in the 2010 Assessment.

<sup>1</sup> All uncertainties are one standard deviation unless otherwise specified.

- **CH<sub>3</sub>CCl<sub>3</sub>, the largest contributor to the decrease in total tropospheric chlorine until around 2005, accounted for only 16 ± 1 ppt (0.5%).** This is 50% less than in 2008 (32 ppt) and a 95% reduction from its mean contribution to the total Cl decline during the 1980s. The fraction is declining in line with the A1 scenario of the 2010 Assessment.
- **CH<sub>3</sub>Cl accounted for 540 ± 5 ppt (about 16%) and has remained essentially constant since 2008.** This gas is emitted predominantly from natural sources.
- **Very short-lived compounds (VSLS) contribute approximately 3%.**

**Global emissions of HCFCs remain substantial, but relative emissions of individual constituents have changed notably since the last Assessment.** Emissions of HCFC-22 have stabilized since 2008 at around 370 gigagrams per year (Gg yr<sup>-1</sup>). HCFC-142b emissions decreased in the same period. In contrast emissions of HCFC-141b have increased since the last Assessment, in parallel with reported production and consumption in Article 5 Parties.

**Estimated sources and sinks of CCl<sub>4</sub> remain inconsistent with observations of its abundance.** The estimate of the total global lifetime (26 years) combined with the observed CCl<sub>4</sub> trend in the atmosphere (-1.1 to -1.4 ppt yr<sup>-1</sup> in 2011–2012) implies emissions of 57 (40–74) Gg yr<sup>-1</sup>, which cannot be reconciled with estimated emissions from net reported production. New evidence indicates that other poorly quantified sources, unrelated to reported production, could contribute to the currently unaccounted emissions.

**Three CFCs (CFC-112, -112a, -113a) and one HCFC (HCFC-133a) have recently been detected in the atmosphere.** These four chlorine-containing compounds are listed in the Montreal Protocol and contribute about 4 ppt or ~ 0.1% toward current levels of total chlorine, currently adding less than 0.5 ppt Cl yr<sup>-1</sup>. Abundances of CFC-112 and CFC-112a are declining and those of CFC-113a and HCFC-133a are increasing. The sources of these chemicals are not known.

### Stratospheric Inorganic Chlorine and Fluorine

**Hydrogen chloride (HCl) is the major reservoir of inorganic chlorine (Cl<sub>y</sub>) in the mid- to upper stratosphere. Satellite-derived measurements of HCl (50°N–50°S) in the mid- to upper stratosphere show a mean decline of 0.6% ± 0.1% yr<sup>-1</sup> between 1997 and 2012. This is consistent with the measured changes in controlled chlorinated source gases.** Variability in this decline is observed over shorter time periods based on column measurements above some ground-based sites, likely due to dynamic variability.

**Measured abundances of stratospheric fluorine product gases (HF, COF<sub>2</sub>, COClF) increased by about 1% yr<sup>-1</sup> between 2008 and 2012.** This is consistent with increases in measured abundances of fluorinated compounds and their degradation products. The increase was smaller than in the beginning of the 1990s, when the concentrations of fluorine-containing ODSs were increasing more rapidly.

### Tropospheric Bromine

**Total organic bromine from controlled ODSs continued to decrease in the troposphere and by 2012 was 15.2 ± 0.2 ppt, approximately 2 ppt below peak levels observed in 1998.** This decrease was close to that expected in the A1 scenario of the 2010 Assessment and was primarily driven by declines in methyl bromide (CH<sub>3</sub>Br), with some recent contribution from an overall decrease in halons. Total bromine from halons had stopped increasing at the time of the last Assessment, and a decrease is now observable.

**CH<sub>3</sub>Br mole fractions continued to decline during 2008–2012, and by 2012 had decreased to 7.0 ± 0.1 ppt, a reduction of 2.2 ppt from peak levels measured during 1996–1998.** These atmospheric declines are driven primarily by continued decreases in total reported consumption of CH<sub>3</sub>Br from fumigation. As of 2009, reported consumption for quarantine and pre-shipment (QPS) uses, which are exempted uses (not controlled) under the Montreal Protocol, surpassed consumption for controlled (non-

QPS) uses. As a result of the decrease in atmospheric CH<sub>3</sub>Br, the natural oceanic source is now comparable to the oceanic sink.

### Stratospheric Inorganic Bromine

**Total inorganic stratospheric bromine (Br<sub>y</sub>), derived from observations of bromine monoxide (BrO), was 20 (16–23) ppt in 2011, and had decreased at  $\sim 0.6 \pm 0.1\%$  yr<sup>-1</sup> between peak levels observed in 2000–2001 and 2012.** This decline is consistent with the decrease in total tropospheric organic Br based on measurements of CH<sub>3</sub>Br and the halons.

### Equivalent Effective Stratospheric Chlorine (EESC)

*EESC is a sum of chlorine and bromine derived from ODS tropospheric abundances weighted to reflect their expected depletion of stratospheric ozone. The growth and decline in EESC depends on a given tropospheric abundance propagating to the stratosphere with varying time lags (on the order of years) associated with transport. Therefore the EESC abundance, its peak timing, and its rate of decline, are different in different regions of the stratosphere.*

**By 2012, EESC had declined by about 10% in polar regions and about 15% in midlatitudes from their peak values, with CH<sub>3</sub>CCl<sub>3</sub>, CH<sub>3</sub>Br, and CFCs contributing approximately equally to these declines.** This drop is about 40% of the decrease required for EESC in midlatitudes to return to the 1980 benchmark level, and about 20% of the decrease required for EESC in polar regions to return to the 1980 benchmark level.

### Very Short-Lived Halogenated Substances (VSLS)

*VSLS are defined as trace gases whose local lifetimes are comparable to, or shorter than, interhemispheric transport timescales and that have non-uniform tropospheric abundances. These local lifetimes typically vary substantially over time and space. As in prior Assessments, we consider species with annual mean lifetimes less than approximately 6 months to be VSLS. Of the VSLS identified in the current atmosphere, brominated and iodinated species are predominantly of oceanic origin, while the chlorinated species have significant industrial sources. These compounds will release their halogen atoms nearly immediately once they enter the stratosphere. The current contribution of chlorinated VSLS to Equivalent Chlorine (ECl) is about one-third as large as the contribution of VSLS brominated gases. Iodine from VSLS likely makes a minor contribution to ECl.*

**Total chlorinated VSLS source gases increased from 84 (70–117) ppt in 2008 to 91 (76–125) ppt in 2012 in the lower troposphere.** Dichloromethane (CH<sub>2</sub>Cl<sub>2</sub>), a VSLS that has predominantly anthropogenic sources, accounted for the majority of this change, with an increase of  $\sim 60\%$  over the last decade.

**The estimated contribution of chlorinated VSLS to total stratospheric chlorine remains small.** A lack of data on their concentrations in the tropical tropopause layer (TTL) limits our ability to quantify their contribution to the inorganic chlorine loading in the lower stratosphere. Current tropospheric concentrations of chlorinated VSLS imply a source gas injection of 72 (50–95) ppt, with 64 ppt from anthropogenic emissions (e.g., CH<sub>2</sub>Cl<sub>2</sub>, CHCl<sub>3</sub>, 1,2 dichloroethane (CH<sub>2</sub>ClCH<sub>2</sub>Cl), tetrachloroethene (CCl<sub>2</sub>CCl<sub>2</sub>)). The product gases are estimated to contribute 0–50 ppt giving a total of  $\sim 95$  ppt (50–145 ppt) against a total of 3300 ppt of chlorine from long-lived ODSs entering the stratosphere.

**There is further evidence that VSLS contribute  $\sim 5$  (2–8) ppt to a total of  $\sim 20$  ppt of stratospheric bromine.** Estimates of this contribution from two independent approaches are in agreement. New data suggest that previous estimates of stratospheric Br<sub>y</sub> derived from BrO observations may in some cases have been overestimated, and imply a contribution of  $\sim 5$  (2–8) ppt of bromine from VSLS. The second approach sums the quantities of observed, very short-lived source gases around the tropical tropopause with improved modeled estimates of VSLS product gas injection into the stratosphere, also giving a total contribution of VSLS to stratospheric bromine of  $\sim 5$  (2–8) ppt.

## Updated Lifetime Estimates

The uncertainties of estimated lifetimes for key long-lived ozone-depleting and related substances are better quantified following the SPARC Lifetimes Assessment (Stratosphere-troposphere Processes And their Role in Climate, 2013). Of note is the change in the estimated lifetime of CFC-11 (revised from 45 yr to 52 yr). The estimate of the total global lifetime of CCl<sub>4</sub> (26 yr) remains unchanged from the previous Assessment, although estimates of the relative importance of the multiple loss processes have been revised.

## Other Trace Gases That Directly Affect Ozone and Climate

The emissions of CFCs, HCFCs, and HFCs in terms of their influence on climate (as measured by gigatonnes of carbon dioxide (CO<sub>2</sub>)-equivalent emissions) were roughly equal in 2012. However, the emissions of HFCs are increasing rapidly, while the emissions of CFCs are going down and those of HCFCs are essentially unchanged. The 100-year GWP-weighted emissions for the sum of CFC, HCFC, and HFC emissions was 2.2 Gt CO<sub>2</sub>-equivalent in 2012. The sum of GWP-weighted emissions of CFCs was  $0.73 \pm 0.25$  Gt CO<sub>2</sub>-equivalent yr<sup>-1</sup> in 2012 and has decreased on average by  $11.0 \pm 1.2\%$  yr<sup>-1</sup> from 2008 to 2012. The sum of HCFC emissions was  $0.76 \pm 0.12$  Gt CO<sub>2</sub>-equivalent yr<sup>-1</sup> in 2012 and has been essentially unchanged between 2008 and 2012. Finally, the sum of HFC emissions was  $0.69 \pm 0.12$  Gt CO<sub>2</sub>-equivalent yr<sup>-1</sup> in 2012 and has increased on average by  $6.8 \pm 0.9\%$  yr<sup>-1</sup> from 2008 to 2012. The HFC increase partially offsets the decrease by CFCs. Current emissions of HFCs are, however, are less than 10% of peak CFC emissions in the early 1990s (>8 Gt CO<sub>2</sub>-equivalent yr<sup>-1</sup>).

From 2008 to 2012 the global mean mole fraction of nitrous oxide (N<sub>2</sub>O), which leads to ozone depletion in the stratosphere, increased by 3.4 parts per billion (ppb), to 325 ppb. With the atmospheric burden of CFC-12 decreasing, N<sub>2</sub>O is currently the third most important long-lived greenhouse gas contributing to radiative forcing (after CO<sub>2</sub> and methane (CH<sub>4</sub>)).

Methane (CH<sub>4</sub>) is an important greenhouse gas and influences stratospheric ozone. In 2012 the average background global mole fraction of CH<sub>4</sub> was 1808 ppb, with a growth rate of 5–6 ppb yr<sup>-1</sup> from 2008 to 2012. This is comparable to the 2006–2008 period when the CH<sub>4</sub> growth rate began increasing again after several years of near-zero growth. The renewed increase is thought to result from a combination of increased CH<sub>4</sub> emissions from tropical and high-latitude wetlands together with increasing anthropogenic (fossil fuel) emissions, though the relative contribution of the wetlands and fossil fuel sources is uncertain.

Hydrofluorocarbons (HFCs) used as ODS substitutes are increasing in the global atmosphere. The most abundant HFC, HFC-134a, reached a mole fraction of nearly 68 ppt in 2012 with an increase of 5 ppt yr<sup>-1</sup> (7.6%) in 2011–2012. HFC-125, -143a, and -32 have similar or even higher relative growth rates than HFC-134a, but their current abundances are considerably lower.

Worldwide emissions of HFC-23, a potent greenhouse gas and by-product of HCFC-22 production, reached a maximum of ~15 Gg in 2006, decreased to ~9 Gg in 2009, and then increased again to reach ~13 Gg yr<sup>-1</sup> in 2012. While efforts in non-Article 5 Parties mitigated an increasing portion of HFC-23 emissions through 2004, the temporary decrease in emissions after 2006 is consistent with destruction of HFC-23 in Article 5 Parties owing to the Clean Development Mechanism (CDM) of the Kyoto Protocol. The average global mole fraction of HFC-23 reached 25 ppt in 2012, with an increase of nearly 1 ppt yr<sup>-1</sup> in recent years.

Mole fractions of sulfur hexafluoride (SF<sub>6</sub>), nitrogen trifluoride (NF<sub>3</sub>), and sulfuryl fluoride (SO<sub>2</sub>F<sub>2</sub>) increased in recent years. Global averaged mole fractions of SF<sub>6</sub> reached 7.6 ppt in 2012, with an annual increase of 0.3 ppt yr<sup>-1</sup> (4% yr<sup>-1</sup>). Global averaged mole fractions of NF<sub>3</sub> reached 0.86 ppt in 2011, with an annual increase of 0.1 ppt yr<sup>-1</sup> (12% yr<sup>-1</sup>). Global averaged mole fractions of SO<sub>2</sub>F<sub>2</sub> reached 1.8 ppt in 2012, with an annual increase of 0.1 ppt yr<sup>-1</sup> (5% yr<sup>-1</sup>). The considerable increases for these entirely anthropogenic, long-lived substances are caused by ongoing emissions.

## 1.1 SUMMARY OF THE PREVIOUS OZONE ASSESSMENT

Chapter 1 of the 2010 Assessment report (Montzka and Reimann et al., 2011) provided evidence of continued reductions of the atmospheric abundance of most ozone-depleting substances (ODSs), resulting from phase-out of controlled ODS production and consumption under the Montreal Protocol. Total tropospheric chlorine and bromine from long-lived chemicals continued to decrease between 2005 and 2008. The atmospheric reservoir for methyl chloroform ( $\text{CH}_3\text{CCl}_3$ ) had reduced to the point that its contribution to the chlorine decline was surpassed by the chlorofluorocarbons (CFCs). Mole fractions of CFC-12, the single largest contributor to the atmospheric chlorine loading, declined for the first time in this period. The total tropospheric chlorine decline was however slower than expected because the sum of the CFC mole fractions did not drop as rapidly as projected and increases in hydrochlorofluorocarbons (HCFCs) were larger than anticipated. The stratospheric chlorine burden declined in accordance with the tropospheric decrease, within expected uncertainties. Chlorine-containing very short-lived substances (VSLS) and their degradation products contributed approximately 80 ppt (parts per trillion) of chlorine to the stratosphere, which was about 2% of the contribution from the longer-lived ODSs.

Chapter 1 of the 2010 Assessment documented the continued discrepancy between emissions of carbon tetrachloride ( $\text{CCl}_4$ ) inferred from observed global trends with the much lower and more variable emissions derived from data reported to the United Nations Environment Programme (UNEP). These differences could not solely be explained by scaling the atmospheric lifetime. For other important ODSs (e.g., CFC-11), there was evidence that atmospheric lifetimes might be longer than reported in previous Assessments.

Tropospheric mole fractions of hydrofluorocarbons (HFCs), used as non-ozone-depleting ODS substitutes, continued to increase, which was reflected by an increase in column abundances of hydrogen fluoride (HF), one of their major degradation products. In total the sum of HFC emissions used as ODS replacements, weighted by direct, 100-year Global Warming Potentials (GWPs), increased by nearly 10%  $\text{yr}^{-1}$  from 2004 to 2008. In addition, emissions of the very potent greenhouse gas HFC-23 ( $\text{CHF}_3$ ), which was mainly released from the production of HCFC-22 and therefore not labeled as an ODS replacement, had increased despite efforts to curb HFC-23 emissions.

The only regulated bromine compound still not decreasing in 2008 was halon-1301. The total tropospheric bromine levels from long-lived ODSs, however, continued to decrease because of the declining abundance of methyl bromide ( $\text{CH}_3\text{Br}$ ) and because the sum of halons had stopped increasing. For the first time, measurements of stratospheric bromine showed a slight decrease over this period. Slightly more than 50% of the atmospheric bromine stemmed from sources not controlled by the Montreal Protocol (i.e., from natural sources and from quarantine and pre-shipment (QPS) uses of  $\text{CH}_3\text{Br}$ ). The contribution from mostly natural short-lived compounds such as dibromomethane ( $\text{CH}_2\text{Br}_2$ ) and tribromomethane ( $\text{CHBr}_3$ ) and their degradation products to stratospheric bromine was estimated to be 1–8 ppt, which contributed substantially to the estimated total of 22.5 ppt of bromine in the stratosphere in 2008.

Equivalent Effective Stratospheric Chlorine (EESC) represents the overall influence on stratospheric ozone levels from the sum of the tropospheric abundances of chlorine and bromine ODSs. A discussion of the EESC concept can be found in Box 8-1 of the 2006 Assessment (Daniel and Velders, 2007). By the end of 2008, the EESC abundance in the midlatitude stratosphere had decreased by about 11% from its peak value in 1997. This represented 28% of the decrease required for EESC in the midlatitude stratosphere to return to the 1980 benchmark level. In the polar stratosphere, EESC had decreased by about 5% from its peak value in 2002, which is 10% of the decrease required for EESC in polar regions to return to the 1980 benchmark level.

## 1.2 LONGER-LIVED HALOGENATED SOURCE GASES

### 1.2.1 Updated Observations, Lifetimes, and Emissions

Global tropospheric observations of ODSs have been performed and updated by independent groups using both in situ and flask measurements as early as the late 1970s (Figure 1-1, Table 1-1). Data

from networks with global coverage (AGAGE: Advanced Global Atmospheric Gases Experiment; NOAA: National Oceanic and Atmospheric Administration; UCI: University of California, Irvine) are discussed primarily, except for substances where data from only one global network are available. For some ODSs, surface observations have been complemented with trends of total column measurements using satellite- and ground-based remote sensing techniques (Table 1-2).

Global steady-state lifetime estimates of the main ODSs and related substances appear in Table 1-3. Most are taken directly from SPARC (2013) and were derived from a weighted average of the lifetimes using different methods. Global steady-state lifetimes are derived from a combination of partial lifetimes for tropospheric hydroxyl radical (OH) reactive loss, stratospheric loss, and ocean and soil loss. Furthermore, updates to atmospheric budgets (emissions and sinks) of ODSs are discussed. Global mean mole fractions, trends, and emissions were calculated by combining the global network data with a two-dimensional model (Rigby et al., 2013, 2014).

### 1.2.1.1 CHLOROFLUOROCARBONS (CFCs)

#### **Observations**

The global surface mean dry air mole fractions of the three most abundant chlorofluorocarbons (CFC-12 ( $\text{CCl}_2\text{F}_2$ ), CFC-11 ( $\text{CCl}_3\text{F}$ ), and CFC-113 ( $\text{CCl}_2\text{FCClF}_2$ )) continued to decline since the last Assessment (Figure 1-1 and Table 1-1). Between 2008 and 2012 the trends observed for these three ODSs are consistent (within uncertainties) with those anticipated in the A1-2010 scenario (Daniel and Velders et al., 2011). For these three ODSs, differences in global abundances estimated by the three global networks in Table 1-1 were less than 1% in 2011–2012. This is comparable to differences of 1–2% for the measurement of these substances evaluated within the International Halocarbons in Air Comparison Experiment (IHALACE) (Hall et al., 2014). Differences between the global networks are used not only for estimating the uncertainty of the measurement data themselves, but also for assessing the accuracy and reliability of global emission estimates, which make use of these data.

Recent changes in the Northern Hemisphere abundances of CFC-11, CFC-12, and CFC-113 measured by ground-based infrared solar absorption spectroscopy (e.g., Zander et al., 2008) and space-based instruments (Brown et al., 2011; Kellmann et al., 2012) are largely consistent (within uncertainties) with those measured at the surface between 2004 and 2010 (Figure 1-2 and Table 1-2). Only CFC-113 from Atmospheric Chemistry Experiment-Fourier Transform Spectrometer (ACE-FTS) (Brown et al., 2011) shows a faster decrease than the ground-based measurements, which could be caused by measurement issues in the space-based instrument for this compound.

Global mole fractions of both CFC-114 ( $\text{CClF}_2\text{CClF}_2$ ) and CFC-115 ( $\text{CClF}_2\text{CF}_3$ ) have remained nearly constant since 2008 (Table 1-1). Measurements of CFC-114 include a fraction due to CFC-114a ( $\text{CCl}_2\text{FCF}_3$ ), which is estimated to be around 10%, based on measurements in the 1990s (Oram, 1999). Furthermore, CFC-112 ( $\text{CCl}_2\text{FCCl}_2\text{F}$ ), -112a ( $\text{CClF}_2\text{CCl}_3$ ), -113a ( $\text{CCl}_3\text{CF}_3$ ), and HCFC-133a ( $\text{CH}_2\text{ClCF}_3$ ) (Section 1.2.1.5) were recently determined to be present in the atmosphere, with mole fractions of less than 1 ppt in 2010 (Laube et al., 2014). Abundances of CFC-112 and CFC-112a are declining but those of CFC-113a (and HCFC-133a) are increasing. These newly detected ODSs are listed in the Montreal Protocol and contribute about 4 ppt or  $\sim 0.1\%$  toward current levels of total chlorine, currently adding less than 0.5 ppt  $\text{Cl yr}^{-1}$ .

#### **Lifetimes and emissions**

For CFC-11, a longer steady-state lifetime of 52 (43–67) years was recommended by SPARC (2013) compared with the 45-year lifetime used in the previous Assessments. Since the SPARC (2013) evaluation, a new CFC-11 UV absorption spectrum data set was reported by McGillen et al. (2013) that significantly reduced the overall estimated uncertainty in the CFC-11 spectrum from  $\sim 20\%$ , as reported in SPARC (2013), to  $\sim 4\%$ . This leads to a substantially reduced contribution to the CFC-11 lifetime uncertainty due to uncertainties in CFC-11 photolysis. The recommended CFC-11 steady-state lifetime of SPARC (2013) and its estimated uncertainty range, however, do not change significantly as a result. In

SPARC (2013) the lifetime and its range were primarily determined by the differences between observational data and various 3-D model calculations.

Another notable change discussed in SPARC (2013) was for CFC-115, for which the total lifetime was revised from 1020 to 540 years based on new  $O(^1D) + CFC-115$  reaction rate data from Baasandorj et al. (2013).

Results since SPARC (2013) include a suggested revision of the CFC-113a lifetime from ~45 to 59 (31–305) years by Laube et al. (2014), although uncertainties of the new estimate include the old number.

Global top-down emissions of CFC-11 derived from atmospheric observations, considering its new lifetime of 52 years, have been declining slowly over the past decade and are estimated to have been 57 (46–68) Gg in 2012 (Figure 1-3). Bottom-up estimated emissions are only available until 2003 and averaged 73 Gg yr<sup>-1</sup> in the period 2000–2003 (UNEP, 2006). This was 19 Gg yr<sup>-1</sup> smaller than estimated emissions using measurement-based top-down methods and a 52-year lifetime (Figure 1-3). The increase of the lifetime estimate from 45 years to 52 years considerably reduces the gap for CFC-11 emission estimates by the two methods from the previous Assessment (Montzka and Reimann et al., 2011).

Global CFC-12 emissions have been declining more rapidly than those of CFC-11. Top-down estimates (Figure 1-3) indicate emissions of CFC-12 were decreasing at a rate of ~7 Gg yr<sup>-1</sup> in recent years to 40 (26–54) Gg in 2012. Global CFC-113 emissions have been consistently lower than 5 Gg yr<sup>-1</sup> over recent years.

Emissions of the newly detected CFC-113a were estimated at 2 Gg in 2012 (Figure 1-3) and they could be caused by its usage as an intermediate in agrochemical production (Laube et al., 2014) or as a feedstock for HFC-125 (CHF<sub>2</sub>CF<sub>3</sub>) and HFC-134a (CH<sub>2</sub>FCF<sub>3</sub>) production (UNEP, 2013a). Although global production numbers for these HFCs are not available, the rapid increases in mole fractions and global emissions of HFC-125 and HFC-134a in the atmosphere (Figures 1-24, 1-25, and Table 1-14) indicate the potential for increasing releases of CFC-113a.

Measurements within specific regions and meteorological models are used to estimate emissions of ODSs and other halocarbons on regional scales. These regional source estimates are prone to considerable uncertainties due to inaccuracies in meteorological data, transport models, and in some instances, seasonal variations of emission. The summed effect of the errors in these parameters and their extrapolations can lead to large uncertainties for estimated regional emissions (see, e.g., Figure 1-4). When studied regions are substantially different from national scales, additional errors can be introduced by extrapolation of the regional estimates to national scales, which are often compared to national inventory-based estimates. Regional emissions of CFC-11, -12, and -113 were predominantly estimated to be from East Asia in recent years, due to the phase-out of these compounds in important Article 5 countries in 2010. In Figure 1-4 historical and projected bottom-up emissions in China (Wan et al., 2009) are compared with top-down regional emissions derived from atmospheric measurements (Palmer et al., 2003; Vollmer et al., 2009; Kim et al., 2010; An et al., 2012; Fang et al., 2012). The concurrent decline of emissions seen by both independent methods (top-down and bottom-up) shows the success of the Montreal Protocol in substantially decreasing CFC emissions in China. In 2000 CFC-12 top-down emission estimates were more than a factor of two higher than inventory-based estimates, but both estimates compare better in most recent years. Whereas CFC-11 emissions are still substantial but also declining, both top-down and bottom-up emissions of CFC-113, which was mostly used as a solvent, were found to be consistently small in recent years. However, measurements of these CFCs in urban environments in China, for example in the Pearl River Delta (Shao et al., 2011; Wu et al., 2014), still show mole fraction enhancements above background levels, indicating ongoing emissions from in-use equipment.

Recent estimates of emissions of CFC-11 and CFC-12 in the U.S. and Europe (Millet et al., 2009; Miller et al., 2012; Keller et al., 2012) were still comparable to those in China, although new production of CFCs for use was restricted in the U.S. and Europe in 1996/1995 (i.e., 14/15 years ahead of restrictions in China). For CFC-113, enhancements above background levels were not detected in the U.S. by Gentner et al. (2010) or Millet et al. (2009), suggesting very low emissions in this region of the world. In a source-specific study, Hodson et al. (2010) found that landfills were only small sources of CFC-11, CFC-12, and CFC-113 in the U.S. and in the United Kingdom.

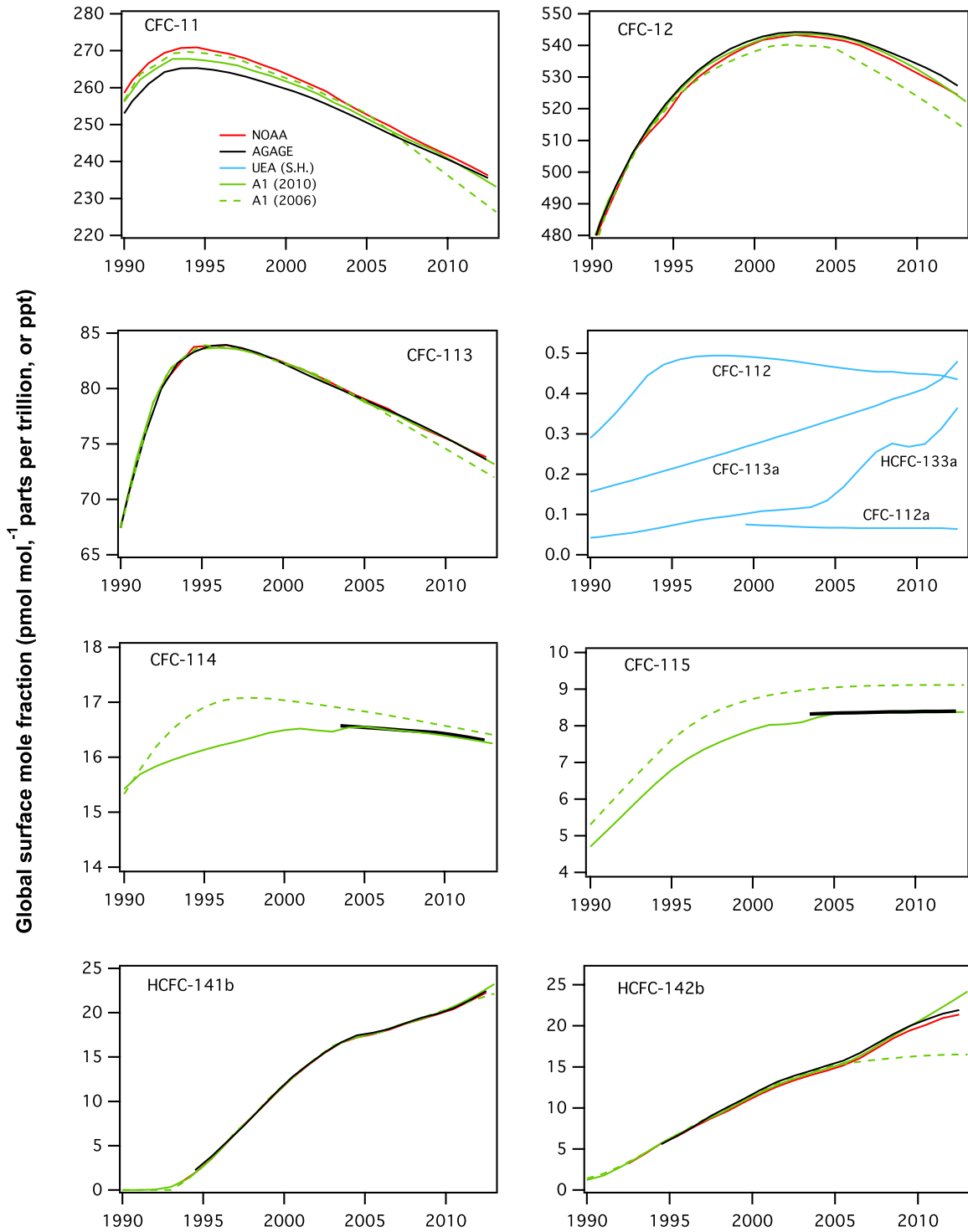


**Figure 1-1.** Mean global surface mole fractions (expressed as dry air mole fractions in parts per trillion or ppt) of ozone-depleting substances from independent sampling networks and from scenario A1 of the previous Ozone Assessments (Daniel and Velders et al., 2007, 2011) over the past 22 years (1990–2012). Measured global surface annual means are shown as red lines (NOAA data), black lines (AGAGE data), and blue lines (University of East Anglia (UEA) Southern Hemisphere (S.H.) data), *(continued next page)*

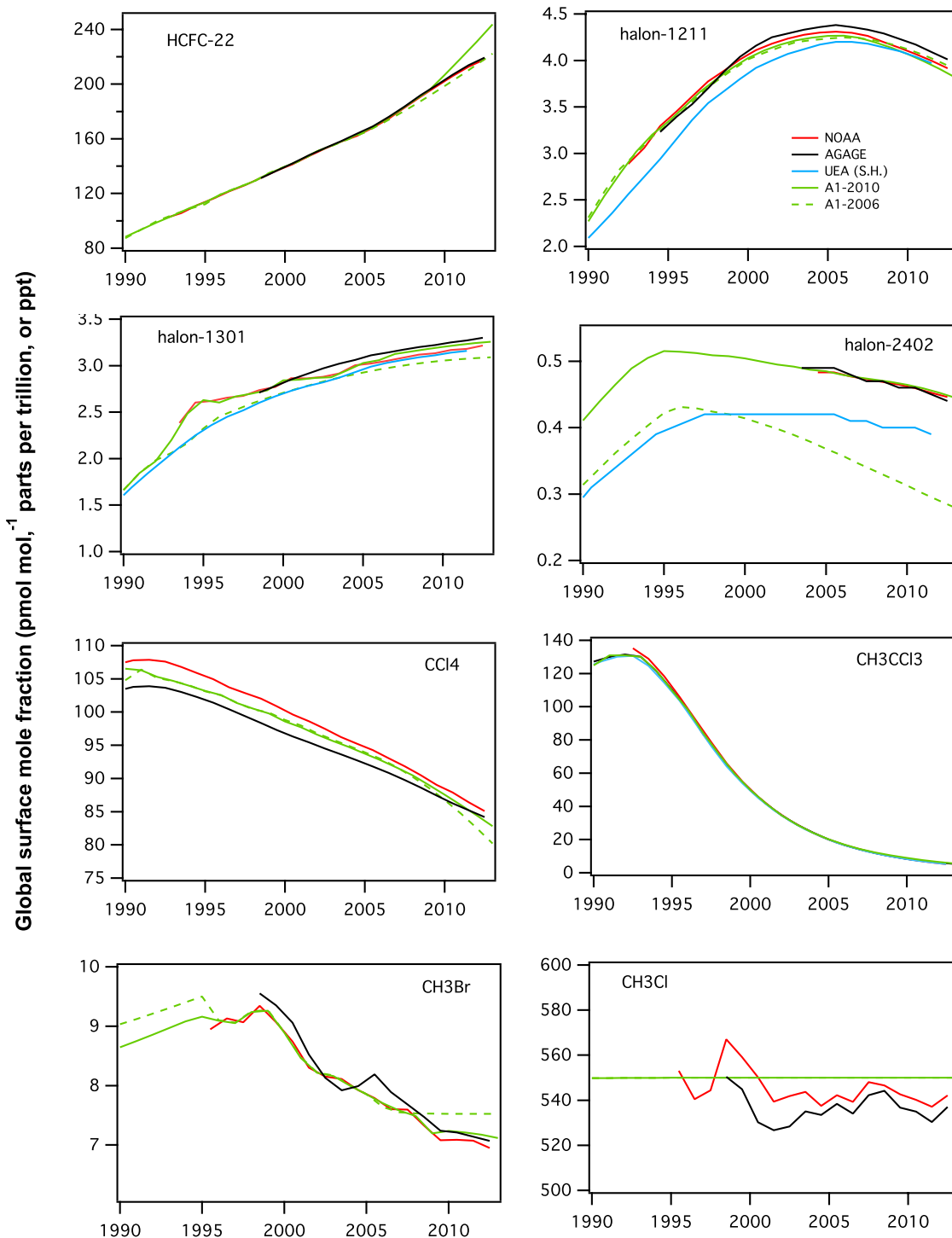


**(Figure 1-1, continued)** using Cape Grim archived air). Mole fractions from scenario A1 from the previous assessment (green lines) were derived to match observations in years before 2009 (Daniel and Velders et al., 2011). The scenario A1-2010 results shown in years after 2008 are projections made for 2009. Mole fractions from scenario A1 from the 2006 Assessment (green-dashed lines) were derived to match observations in years before 2005 (Daniel and Velders et al., 2007). The scenario A1-2006 results shown in years after 2004 are projections made in 2005.

**Table 1-1. Measured mole fractions and changes of ozone-depleting gases from ground-based sampling networks.**

Chemical Formula	Common or Industrial Name	Annual Mean Mole Fraction (ppt)			Change (2011–2012)		Network, Method
		2008	2011	2012	(ppt yr <sup>-1</sup> )	(% yr <sup>-1</sup> )	
<b>CFCs</b>							
CCl <sub>3</sub> F	CFC-11	243.4	237.6	235.5	-2.1	-0.9	AGAGE, in situ <sup>1</sup>
		244.8	238.6	236.3	-2.3	-1.0	NOAA, flask & in situ
		244.2	237.9	235.3	-2.6	-1.1	UCI, flask
CCl <sub>2</sub> F <sub>2</sub>	CFC-12	537.5	530.4	527.5	-2.9	-0.5	AGAGE, in situ
		535.3	527.2	524.4	-2.9	-0.5	NOAA, flask & in situ
		532.6	525.3	522.5	-2.8	-0.5	UCI, flask
CCl <sub>2</sub> FCCl <sub>2</sub> F	CFC-112	0.45	0.45	0.44	-0.01	-2	UEA, flask (Cape Grim)
CCl <sub>3</sub> CClF <sub>2</sub>	CFC-112a	0.065	0.066	0.064	-0.002	-3	UEA, flask (Cape Grim)
CCl <sub>2</sub> FCClF <sub>2</sub>	CFC-113	76.7	74.4	73.6	-0.8	-1.1	AGAGE, in situ
		76.5	74.5	73.8	-0.6	-0.8	NOAA, flask & in situ
		77.1	74.9	74.2	-0.7	-0.9	UCI, flask
CCl <sub>3</sub> CF <sub>3</sub>	CFC-113a	0.39	0.44	0.48	0.04	10	UEA, flask (Cape Grim)
CClF <sub>2</sub> CClF <sub>2</sub>	CFC-114 <sup>2</sup>	16.46	16.37	16.33	-0.04	-0.2	AGAGE, in situ
		15.95	15.77	15.75	-0.02	-0.1	NIES, in situ (Japan)
CClF <sub>2</sub> CF <sub>3</sub>	CFC-115	8.38	8.39	8.40	0.01	0.2	AGAGE, in situ
		8.32	8.44	8.48	0.04	0.5	NIES, in situ (Japan)
<b>HCFCs</b>							
CHClF <sub>2</sub>	HCFC-22	191.8	214.2	219.8	5.6	2.6	AGAGE, in situ
		190.9	212.7	218.0	5.3	2.5	NOAA, flask
		188.3	209.0	214.5	5.5	2.6	UCI, flask
CHClFCF <sub>3</sub>	HCFC-124	1.48	1.34	1.30	-0.04	-3	AGAGE, in situ
CH <sub>2</sub> ClCF <sub>3</sub>	HCFC-133a	0.275	0.313	0.365	0.052	17	UEA, flask (Cape Grim)
CH <sub>3</sub> CCl <sub>2</sub> F	HCFC-141b	19.5	21.4	22.5	1.1	5.1	AGAGE, in situ
		19.3	21.3	22.3	1.0	4.4	NOAA, flask
		18.8	20.8	21.8	1.0	4.8	UCI, flask
CH <sub>3</sub> CClF <sub>2</sub>	HCFC-142b	19.0	21.5	22.0	0.5	2.4	AGAGE, in situ
		18.5	20.9	21.3	0.4	2.0	NOAA, flask
		18.0	21.0	21.8	0.8	3.8	UCI, flask
<b>Halons</b>							
CBr <sub>2</sub> F <sub>2</sub>	halon-1202	0.026	0.020	0.019	-0.001	-5	UEA, flask (Cape Grim)

*(continued next page)*

Chemical Formula	Common or Industrial Name	Annual Mean Mole Fraction (ppt)			Change (2011–2012)		Network, Method
		2008	2011	2012	(ppt yr <sup>-1</sup> )	(% yr <sup>-1</sup> )	
<i>Table 1-1, continued.</i>							
CBrClF <sub>2</sub>	halon-1211	<b>4.29</b>	<b>4.09</b>	<b>4.01</b>	<b>-0.08</b>	<b>-2.0</b>	AGAGE, in situ
		<b>4.20</b>	<b>4.00</b>	<b>3.92</b>	<b>-0.08</b>	<b>-2.0</b>	NOAA, flask <sup>3</sup>
		<b>4.25</b>	<b>4.03</b>	<b>3.96</b>	<b>-0.07</b>	<b>-1.7</b>	NOAA, in situ
		<b>4.24</b>	<b>4.18</b>	<b>4.14</b>	<b>-0.04</b>	<b>-1.0</b>	UCI, flask
CBrF <sub>3</sub>	halon-1301	<b>3.20</b>	<b>3.27</b>	<b>3.30</b>	<b>0.03</b>	<b>0.9</b>	AGAGE, in situ
		<b>3.12</b>	<b>3.18</b>	<b>3.22</b>	<b>0.04</b>	<b>1.1</b>	NOAA, flask
CBrF <sub>2</sub> CBrF <sub>2</sub>	halon-2402	<i>0.47</i>	<i>0.45</i>	<i>0.44</i>	<i>-0.01</i>	<i>-1.3</i>	AGAGE, in situ <sup>4</sup>
		<b>0.47</b>	<b>0.45</b>	<b>0.44</b>	<b>-0.01</b>	<b>-1.4</b>	NOAA, flask
		<i>0.41</i>	<i>0.394</i>	<i>0.387</i>	<i>-0.007</i>	<i>-2</i>	UEA, flask (Cape Grim)
<b>Chlorocarbons</b>							
CH <sub>3</sub> Cl	methyl chloride	<b>544.2</b>	<b>530.3</b>	<b>537.1</b>	<b>6.8</b>	<b>1.3</b>	AGAGE, in situ
		<b>546.6</b>	<b>537.1</b>	<b>542.2</b>	<b>5.0</b>	<b>0.9</b>	NOAA, flask
		<b>546</b>	-	-	-	-	NOAA, in situ
CCl <sub>4</sub>	carbon tetrachloride	<b>88.6</b>	<b>85.2</b>	<b>84.2</b>	<b>-1.1</b>	<b>-1.2</b>	AGAGE, in situ
		<b>90.5</b>	<b>86.4</b>	<b>85.1</b>	<b>-1.4</b>	<b>-1.6</b>	NOAA, flask & in situ
		<b>91.5</b>	<b>87.8</b>	<b>86.7</b>	<b>-1.1</b>	<b>-1.3</b>	UCI, flask
CH <sub>3</sub> CCl <sub>3</sub>	methyl chloroform	<b>10.6</b>	<b>6.26</b>	<b>5.20</b>	<b>-1.06</b>	<b>-17</b>	AGAGE, in situ
		<b>10.8</b>	<b>6.31</b>	<b>5.25</b>	<b>-1.06</b>	<b>-17</b>	NOAA, flask
		<b>11.5</b>	<b>6.8</b>	<b>5.7</b>	<b>-1.1</b>	<b>-16</b>	UCI, flask
<b>Bromocarbons</b>							
CH <sub>3</sub> Br	methyl bromide	<b>7.47</b>	<b>7.14</b>	<b>7.07</b>	<b>-0.11</b>	<b>-1.0</b>	AGAGE, in situ
		<b>7.33</b>	<b>7.07</b>	<b>6.95</b>	<b>-0.12</b>	<b>-1.7</b>	NOAA, flask

Mole fractions in this table represent independent estimates measured by different groups for the years indicated. Results in bold text are estimates of global surface mean mole fractions. Regional data from relatively unpolluted sites are shown (in italics) where global estimates are not available, where global estimates are available from only one network, or where data from global networks do not represent independent calibration scales (e.g., halon-2402). Absolute changes (ppt yr<sup>-1</sup>) are calculated as the difference in annual means; relative changes (% yr<sup>-1</sup>) are the same difference relative to the 2011 value. Small differences between values from previous Assessments are due to changes in calibration scale and methods for estimating global mean mole fractions from a limited number of sampling sites.

These observations are updated from the following sources: Rowland et al. (1982); Butler et al. (1998); Fraser et al. (1999); Montzka et al. (1999); Oram (1999); Montzka et al. (2000); Prinn et al. (2000); Montzka et al. (2003); O'Doherty et al. (2004); Yokouchi et al. (2006); Simpson et al. (2007); Miller et al. (2008); Montzka et al. (2009); Newland et al. (2013); Laube et al. (2014). AGAGE, Advanced Global Atmospheric Gases Experiment (<http://agage.eas.gatech.edu/>); NOAA, National Oceanic and Atmospheric Administration, U.S. (<http://www.esrl.noaa.gov/gmd/dv/site/>); UEA, University of East Anglia, United Kingdom (<http://www.uea.ac.uk/environmental-sciences/research/marine-and-atmospheric-sciences-group>); UCI, University of California, Irvine, U.S. ([http://ps.uci.edu/~rowlandblake/research\\_atmos.html](http://ps.uci.edu/~rowlandblake/research_atmos.html)); NIES, National Institute for Environmental Studies, Japan (<http://db.cger.nies.go.jp/gem/moni-e/warm/Ground/st01.html>). Cape Grim: Cape Grim Baseline Air Pollution Station, Australia.

Notes: <sup>1</sup>Global mean estimates from AGAGE are calculated using atmospheric data and a 12-box model (Cunnold et al., 1983; Rigby et al., 2013). AGAGE calibrations as specified in CDIAC (2014) and related primary publications. <sup>2</sup>Measurements of CFC-114 are a combination of CFC-114 and the CFC-114a isomer, with an assumed relative contribution of 10% CFC-114a (Oram, 1999). <sup>3</sup>The NOAA halon-1211 data have been updated following an instrument change in 2009. <sup>4</sup>AGAGE halon-2402 data are on the NOAA scale.

**Table 1-2. Comparison of annual trends of ODSs, HFC-23, CF<sub>4</sub>, and SF<sub>6</sub> from in-situ measurements vs. remote sensing measurements.** Relative trends in ODSs and halogenated greenhouse gases for the common 2004–2010 time period (except when specified) derived from in-situ surface measurements and remote sensing observations from the ground and from space. Surface trends were derived from monthly mean mole fractions, weighted by surface area in the region 30°N–90°N. Shown are the average and standard deviation of trends derived independently from NOAA and AGAGE data (% yr<sup>-1</sup> relative to 2007 annual mean). For CF<sub>4</sub> and HFC-23, only AGAGE data were used, and the uncertainty was derived from uncertainties (one standard deviation) in the slope and 2007 annual mean. For HFC-23, global mean data were used from 2007 through 2010, supplemented with data from Miller et al. (2010) for 2004–2007. Ground-based remote sensing trends were derived from daily mean total column measurements performed at Jungfraujoch (46.5°N). The ACE-FTS trends were determined using tropical occultations (30°N–30°S), after averaging the mixing ratios in molecule-dependent altitude ranges (Brown et al., 2011). For HFC-23, the 40°N–40°S occultations were considered in the 10–25 km altitude range. For MIPAS CFC-11 and -12, mean rates of change for the 20°N–20°S and 10–15 km altitude range are provided, including observations between 2002 and 2011 (Kellmann et al., 2012). For SF<sub>6</sub>, the trend characterizes the 2006–2009 time period between 17.5°N–17.5°S latitude and 9–15 km altitude (Stiller et al., 2012).

Substance	Annual Trend 2004–2010 (% yr <sup>-1</sup> relative to 2007)			Data Sources
	In-situ 30°N–90°N	Remote sensing ground (total columns)	Remote sensing satellite	
CFC-11	-0.84 ± 0.09	-0.99 ± 0.10	MIPAS: -1.03 ± 0.09  ACE-FTS: -0.9 ± 0.1	NOAA, AGAGE Zander et al., 2008 Kellmann et al., 2012 Brown et al., 2011
CFC-12	-0.39 ± 0.05	-0.38 ± 0.07	MIPAS: -0.51 ± 0.09  ACE-FTS: -0.4 ± 0.1	NOAA, AGAGE Zander et al., 2008 Kellmann et al., 2012 Brown et al., 2011
CFC-113	-0.93 ± 0.02		ACE-FTS: -1.2 ± 0.1	NOAA, AGAGE Brown et al., 2011
CCl <sub>4</sub>	-1.35 ± 0.08	-1.31 ± 0.15	ACE-FTS -1.2 ± 0.1	NOAA, AGAGE Rinsland et al., 2012 Brown et al., 2011
HCFC-22	3.97 ± 0.06	3.52 ± 0.08	ACE-FTS 3.7 ± 0.1	NOAA, AGAGE Zander et al., 2008 Brown et al., 2011
HCFC-141b	2.57 ± 0.07		ACE-FTS 0.74 ± 0.5	NOAA, AGAGE Brown et al., 2011
HCFC-142b	5.44 ± 0.03		ACE-FTS 7.0 ± 0.4	NOAA, AGAGE Brown et al., 2011
HFC-23	4.2 ± 0.2		ACE-FTS 3.9 ± 1.2	AGAGE Harrison et al., 2012
CF <sub>4</sub>	0.86 ± 0.01	1.02 ± 0.05	ACE-FTS 0.74 ± 0.04	AGAGE Mahieu et al., 2014 Brown et al., 2011
SF <sub>6</sub>	4.27 ± 0.07	4.14 ± 0.32	MIPAS 4.3  ACE-FTS: 4.2 ± 0.1	NOAA, AGAGE Zander et al., 2008 Stiller et al., 2012 Brown et al., 2011

**Table 1-3. Steady-state lifetimes for selected long-lived halocarbons (total lifetimes greater than 0.5 years).** Total and partial lifetimes are defined in Box 1-1. Compounds included in the SPARC (2013) lifetime report are given in bold with the total lifetimes calculated using the SPARC (2013) atmospheric partial lifetime recommendation and the ocean and soil partial lifetimes reported here; stratospheric partial lifetimes for these compounds were taken from the SPARC (2013) model-mean unless noted otherwise. The footnotes contain specific details for each compound in the table. See Table 1-5 in Section 1.3 for local lifetime estimates for very short-lived substances (VLSLs) and Table 1-11 in Section 1.3 for lifetimes of potential ODS replacement compounds.

Industrial Designation or Common Name	Chemical Formula	WMO (2011) Total Lifetime (years)	New Total Lifetime <sup>a</sup> (years)	SPARC (2013) Atmospheric Partial Lifetime & Estimated Uncertainty Range <sup>b</sup> (years)	Tropo-spheric OH Partial Lifetime <sup>c</sup> (years)	Strato-spheric Partial Lifetime (years)	Ocean Partial Lifetime (years) <sup>d</sup>	Notes
<b>Halogenated Methanes</b>								
HFC-41	CH <sub>3</sub> F	2.8	2.8		2.9	~65	1340	1, 2
<b>HFC-32</b>	<b>CH<sub>2</sub>F<sub>2</sub></b>	5.2	5.4	5.4 [4.0–8.2]	5.5	124		1
<b>HFC-23</b>	<b>CHF<sub>3</sub></b>	222	228	228 [160–394]	243	4420		1
PFC-14 (Carbon tetrafluoride)	CF <sub>4</sub>	>50,000	>50,000					3
<b>Methyl chloride</b>	<b>CH<sub>3</sub>Cl</b>	1.0	0.9	1.3 [0.9–2.0]	1.57	30.4 <sup>e</sup>	12	4–7
<b>Carbon tetrachloride</b>	<b>CCl<sub>4</sub></b>	26	26	44 (36–58) [33–67]		44 <sup>f</sup>	94	7
HCFC-31	CH <sub>2</sub> ClF	1.3	1.2		1.3	~35		1, 2, 8
<b>HCFC-22</b>	<b>CHClF<sub>2</sub></b>	11.9	11.9	12 [9.3–18]	13.0	161	1174	4
HCFC-21	CHCl <sub>2</sub> F	1.7	1.7		1.8	~35	673	1, 2, 8
<b>CFC-11</b>	<b>CCl<sub>3</sub>F</b>	45	52	52 (43–67) [35–89]		55		9
<b>CFC-12</b>	<b>CCl<sub>2</sub>F<sub>2</sub></b>	100	102	102 (88–122) [78–151]		95.5		9
CFC-13	CClF <sub>3</sub>	640	640					3
<b>Methyl bromide</b>	<b>CH<sub>3</sub>Br</b>	0.8	0.8	1.5 [1.1–2.3]	1.8	26.3 <sup>e</sup>	3.1	4, 7, 10
Halon-1201	CHBrF <sub>2</sub>	5.2	5.1		6.0	~35		1, 2, 8
<b>Halon-1301</b>	<b>CBrF<sub>3</sub></b>	65	72	72 (61–89) [58–97]		73.5		9
<b>Halon-1211</b>	<b>CBrClF<sub>2</sub></b>	16	16	16 [10–39]		41		11
<b>Halon-1202</b>	<b>CBr<sub>2</sub>F<sub>2</sub></b>	2.9	2.5	2.5 [1.5–7.3]		36		11
<b>Halogenated Ethanes</b>								
<b>HFC-152a</b>	<b>CH<sub>3</sub>CHF<sub>2</sub></b>	1.5	1.6	1.6 [1.2–2.2]	1.55	39	1958	1
HFC-143	CH <sub>2</sub> FCHF <sub>2</sub>	3.5	3.5		3.70	~75		1, 2
<b>HFC-143a</b>	<b>CH<sub>3</sub>CF<sub>3</sub></b>	47.1	51	51 [38–81]	57	612		1
HFC-134	CHF <sub>2</sub> CHF <sub>2</sub>	9.7	9.7		10.5	~135		1, 2
<b>HFC-134a</b>	<b>CH<sub>2</sub>FCF<sub>3</sub></b>	13.4	14	14 [10–21]	14.1	267	5909	4
<b>HFC-125</b>	<b>CHF<sub>2</sub>CF<sub>3</sub></b>	28.2	31	31 [22–48]	32	351	10650	1
PFC-116 (Perfluoroethane)	CF <sub>3</sub> CF <sub>3</sub>	>10,000	>10,000					3
<b>Methyl chloroform</b>	<b>CH<sub>3</sub>CCl<sub>3</sub></b>	5.0	5.0 <sup>g</sup>	6.1 [4.7–5.4]	6.1 <sup>f</sup>	38	94	12
<b>HCFC-141b</b>	<b>CH<sub>3</sub>CCl<sub>2</sub>F</b>	9.2	9.4	9.4 [7.2–18]	10.7	72.3	9190	1
<b>HCFC-142b</b>	<b>CH<sub>3</sub>CClF<sub>2</sub></b>	17.2	18	18 [14–25]	19.3	212	122200	1
HCFC-133a	CH <sub>2</sub> ClCF <sub>3</sub>	4.3	4.0		4.5	41		1, 2, 13
HCFC-123	CHCl <sub>2</sub> CF <sub>3</sub>	1.3	1.3		1.35	36		1, 14
HCFC-123a	CHClFClF <sub>2</sub>	4.0	4.0		4.3	~65		1, 2, 8
HCFC-123b	CHF <sub>2</sub> CCl <sub>2</sub> F	6.2	~6		~7	~50		2, 8, 15
HCFC-124	CHClFClF <sub>3</sub>	5.9	5.9		6.3	111	1855	1, 14

(continued next page)

Industrial Designation or Common Name	Chemical Formula	WMO (2011) Total Lifetime (years)	New Total Lifetime <sup>a</sup> (years)	SPARC (2013) Atmospheric Partial Lifetime & Estimated Uncertainty Range <sup>b</sup> (years)	Tropospheric OH Partial Lifetime <sup>c</sup> (years)	Stratospheric Partial Lifetime (years)	Ocean Partial Lifetime (years) <sup>d</sup>	Notes
HCFC-124a	CHF <sub>2</sub> CClF <sub>2</sub>	9.1	~9.2		~10	~120		2, 16
CFC-112	CCl <sub>2</sub> FCCl <sub>2</sub> F		59			59		13
CFC-112a	CClF <sub>2</sub> CCl <sub>3</sub>		51			51		13
<b>CFC-113</b>	<b>CCl<sub>2</sub>FCClF<sub>2</sub></b>	85	93	93 (82–109) [69–138]		88.4		9, 17
CFC-113a	CCl <sub>3</sub> CF <sub>3</sub>	~45	59			59		13
<b>CFC-114</b>	<b>CClF<sub>2</sub>CClF<sub>2</sub></b>	190	189	189 [153–247]		191		9, 17
CFC-114a	CCl <sub>2</sub> FCF <sub>3</sub>	~100	~100			~100		18
<b>CFC-115</b>	<b>CClF<sub>2</sub>CF<sub>3</sub></b>	1020	540	540 [404–813]		664		19
Halon-2311 (Halothane)	CHBrClCF <sub>3</sub>	1.0	1.0		1.1	~16		1, 2, 8
<b>Halon-2402</b>	<b>CBrF<sub>2</sub>CBrF<sub>2</sub></b>	20	28	28 [20–45]		41		11
<b>Halogenated Propanes</b>								
HFC-263fb	CH <sub>3</sub> CH <sub>2</sub> CF <sub>3</sub>	1.2	1.1		1.16	~40		1, 2
HFC-245ca	CH <sub>2</sub> FCF <sub>2</sub> CHF <sub>2</sub>	6.5	6.5		6.9	~105		1, 2
HFC-245ea	CHF <sub>2</sub> CHFCHF <sub>2</sub>	3.2	3.2		3.4	~70		1, 2
HFC-245eb	CH <sub>2</sub> FCHFCF <sub>3</sub>	3.1	3.2		3.3	~70		1, 2
<b>HFC-245fa</b>	<b>CHF<sub>2</sub>CH<sub>2</sub>CF<sub>3</sub></b>	7.7	7.9	7.9 [5.5–14]	8.2	149		1
HFC-236cb	CH <sub>2</sub> FCF <sub>2</sub> CF <sub>3</sub>	13.1	~13		~14	~240		20
HFC-236ea	CHF <sub>2</sub> CHF <sub>2</sub> CF <sub>3</sub>	11.0	11.0		11.9	~145		1, 2
HFC-236fa	CF <sub>3</sub> CH <sub>2</sub> CF <sub>3</sub>	242	222		253	~1800		1, 21
<b>HFC-227ea</b>	<b>CF<sub>3</sub>CHFCF<sub>3</sub></b>	38.9	36	36 [25–61]	37.5	673		4, 22
PFC-218 (Perfluoropropane)	CF <sub>3</sub> CF <sub>2</sub> CF <sub>3</sub>	2,600	~7,000					23
PFC-c216 (Perfluorocyclopropane)	c-C <sub>3</sub> F <sub>6</sub>	~3,000	~4,000					23
HCFC-243cc	CH <sub>3</sub> CF <sub>2</sub> CCl <sub>2</sub> F	19.5	19.5		27.1	~70		1, 2, 8
HCFC-234fb	CF <sub>3</sub> CH <sub>2</sub> CCl <sub>2</sub> F	49	~45		98	~85		1, 2, 8
HCFC-225ca	CHCl <sub>2</sub> CF <sub>2</sub> CF <sub>3</sub>	1.9	1.9		2.0	44		1, 14
HCFC-225cb	CHClFCF <sub>2</sub> CClF <sub>2</sub>	5.9	5.9		6.3	101		1, 14
<b>Halogenated Higher Alkanes</b>								
HFC-365mfc	CH <sub>3</sub> CF <sub>2</sub> CH <sub>2</sub> CF <sub>3</sub>	8.7	8.7		9.3	~125		1, 2
HFC-356mcf	CH <sub>2</sub> FCH <sub>2</sub> CF <sub>2</sub> CF <sub>3</sub>	1.3	1.2		1.26	~40		1, 2
HFC-356mff	CF <sub>3</sub> CH <sub>2</sub> CH <sub>2</sub> CF <sub>3</sub>	8.3	8.3		8.9	~120		1, 2
HFC-338pcc	CHF <sub>2</sub> CF <sub>2</sub> CF <sub>2</sub> CHF <sub>2</sub>	12.9	12.9		14.0	~160		1, 2
HFC-329p	CHF <sub>2</sub> CF <sub>2</sub> CF <sub>2</sub> CF <sub>3</sub>	28.4	~30		~34	~260		2, 24
PFC-C318 (Perfluorocyclobutane)	c-C <sub>4</sub> F <sub>8</sub>	3,200	3,200					3
PFC-31-10 (Perfluorobutane)	C <sub>4</sub> F <sub>10</sub>	2,600	~5,000					23
( <i>E</i> )-R316c (( <i>E</i> )-1,2-dichlorohexafluorocyclobutane)	( <i>E</i> )-1,2-c-C <sub>4</sub> F <sub>6</sub> Cl <sub>2</sub>		75			76		9, 25
( <i>Z</i> )-R316c (( <i>Z</i> )-1,2-dichlorohexafluorocyclobutane)	( <i>Z</i> )-1,2-c-C <sub>4</sub> F <sub>6</sub> Cl <sub>2</sub>		114			115		9, 25

(continued next page)

Industrial Designation or Common Name	Chemical Formula	WMO (2011) Total Lifetime (years)	New Total Lifetime <sup>a</sup> (years)	SPARC (2013) Atmospheric Partial Lifetime & Estimated Uncertainty Range <sup>b</sup> (years)	Tropo-spheric OH Partial Lifetime <sup>c</sup> (years)	Strato-spheric Partial Lifetime (years)	Ocean Partial Lifetime (years) <sup>d</sup>	Notes
HFC-43-10mee	CF <sub>3</sub> CHFCHFCF <sub>2</sub> CF <sub>3</sub>	16.1	16.1		17.9	157		1, 14
HFC-458mfcf	CF <sub>3</sub> CH <sub>2</sub> CF <sub>2</sub> CH <sub>2</sub> CF <sub>3</sub>	22.9	22.9		25.5	~225		1, 2
PFC-41-12 (Perfluoropentane)	C <sub>5</sub> F <sub>12</sub>	4,100	4,100					3
HFC-55-10mccf	CF <sub>3</sub> CF <sub>2</sub> CH <sub>2</sub> CH <sub>2</sub> CF <sub>2</sub> CF <sub>3</sub>	7.5	7.5		8.0	~115		1, 2
HFC-52-13p	CHF <sub>2</sub> CF <sub>2</sub> CF <sub>2</sub> CF <sub>2</sub> CF <sub>2</sub> CF <sub>3</sub>	32.2	32.7		37.0	~280		2, 26
PFC-51-14 (Perfluorohexane)	C <sub>6</sub> F <sub>14</sub>	3,100	3,100					3
PFC-61-16 (Perfluoroheptane)	C <sub>7</sub> F <sub>16</sub>	~3,000	~3,000					23
PFC-71-18 (Perfluorooctane)	C <sub>8</sub> F <sub>18</sub>		~3,000					23
Perfluorodecalin	C <sub>10</sub> F <sub>18</sub> , ( <i>E</i> )- and ( <i>Z</i> )-isomers	~2,000	~2,000					23
<b>Fluorinated Alcohols</b>								
1,1,1,3,3,3-hexa-fluoroisopropanol	(CF <sub>3</sub> ) <sub>2</sub> CHOH	1.9	1.9		2.0	~50		1, 2
<b>Halogenated Ethers</b>								
HFE-143a	CH <sub>3</sub> OCF <sub>3</sub>	4.8	4.8		5.1	~90		1, 2
HFE-134	CHF <sub>2</sub> OCHF <sub>2</sub>	24.4	25.4		28.4	~240		1, 2
HFE-125	CHF <sub>2</sub> OCF <sub>3</sub>	119	119		147	~620		1, 2
HFE-227ea	CF <sub>3</sub> OCHF <sub>2</sub> CF <sub>3</sub>	51.6	46.7		54	~345		1, 2
HCFE-235da2 (Isoflurane)	CHF <sub>2</sub> OCHClCF <sub>3</sub>	3.5	3.5		3.7	~55		1, 2, 27
HFE-236ea2 (Desflurane)	CHF <sub>2</sub> OCHF <sub>2</sub> CF <sub>3</sub>	10.8	10.8		11.7	~145		1, 2
HFE-236fa	CF <sub>3</sub> OCH <sub>2</sub> CF <sub>3</sub>	7.5	~7.5		~8	~115		2, 28
HFE-245fa1	CF <sub>3</sub> OCH <sub>2</sub> CHF <sub>2</sub>	6.6	~6.6		~7	~105		2, 29
HFE-245fa2	CHF <sub>2</sub> OCH <sub>2</sub> CF <sub>3</sub>	5.5	5.5		5.8	~95		1, 2
HFE-245cb2	CH <sub>3</sub> OCF <sub>2</sub> CF <sub>3</sub>	4.9	5.0		5.24	~90		1, 2
HFE-254cb2	CH <sub>3</sub> OCF <sub>2</sub> CHF <sub>2</sub>	2.5	2.5		2.62	~60		1, 2
HFE-236ca	CHF <sub>2</sub> OCF <sub>2</sub> CHF <sub>2</sub>	20.8	20.8		23.1	~210		1, 2
HFE-235ca2 (Enflurane)	CHF <sub>2</sub> OCF <sub>2</sub> CHCl	4.3	4.3		4.62	~70		2, 8, 30
HFE-329mcc2	CF <sub>3</sub> CF <sub>2</sub> OCF <sub>2</sub> CHF <sub>2</sub>	22.5	~25		23–34	~220		2, 31
HFE-338mcf2	CF <sub>3</sub> CF <sub>2</sub> OCH <sub>2</sub> CF <sub>3</sub>	7.5	~7.5		~8	~130		2, 32
HFE-347mcc3	CH <sub>3</sub> OCF <sub>2</sub> CF <sub>2</sub> CF <sub>3</sub>	5.0	5.0		5.3	~90		1, 2
HFE-347mcf2	CF <sub>3</sub> CF <sub>2</sub> OCH <sub>2</sub> CHF <sub>2</sub>	6.6	~6.6		~7	~105		2, 33
HFC-347mcf	CHF <sub>2</sub> OCH <sub>2</sub> CF <sub>2</sub> CF <sub>3</sub>	5.7	5.6		6.0	~95		1, 2
HFE-347pcf2	CF <sub>3</sub> CH <sub>2</sub> OCF <sub>2</sub> CHF <sub>2</sub>	6.0	5.9		6.3	~100		1, 2
HFE-356mcc3	CH <sub>3</sub> OCF <sub>2</sub> CHFCF <sub>3</sub>	~3	~3		~3	~65		2, 34
HFE-356pcc3	CH <sub>3</sub> OCF <sub>2</sub> CF <sub>2</sub> CHF <sub>2</sub>	~3	~3		~3	~65		2, 34
HFE-356pcf2	CHF <sub>2</sub> CH <sub>2</sub> OCF <sub>2</sub> CHF <sub>2</sub>	5.7	~6		~6	~95		2, 35
HFE-356pcf3	CHF <sub>2</sub> OCH <sub>2</sub> CF <sub>2</sub> CHF <sub>2</sub>	3.5	3.5		3.7	~75		1, 2
HFE-347mmz1 (Sevoflurane)	(CF <sub>3</sub> ) <sub>2</sub> CHOCH <sub>2</sub> F	2.2	~2		~2	~50		2, 36
HFE-338mmz1	(CF <sub>3</sub> ) <sub>2</sub> CHOCHF <sub>2</sub>	21.2	21.2		23.5	~215		1, 2

(continued next page)

Industrial Designation or Common Name	Chemical Formula	WMO (2011) Total Lifetime (years)	New Total Lifetime <sup>a</sup> (years)	SPARC (2013) Atmospheric Partial Lifetime & Estimated Uncertainty Range <sup>b</sup> (years)	Tropo-spheric OH Partial Lifetime <sup>c</sup> (years)	Strato-spheric Partial Lifetime (years)	Ocean Partial Lifetime (years) <sup>d</sup>	Notes
Perfluoroisopropyl methyl ether	(CF <sub>3</sub> ) <sub>2</sub> CFOCH <sub>3</sub>	3.7	3.6		3.8	~75		1, 2
HFE-7100	CH <sub>3</sub> O(CF <sub>2</sub> ) <sub>3</sub> CF <sub>3</sub>	4.7	4.7		5.0	~85		1, 2
HFE-54-11meef	CF <sub>3</sub> CHF <sub>2</sub> CF <sub>2</sub> OCH <sub>2</sub> CF <sub>2</sub> CF <sub>3</sub>	8.8	8.8		9.5	~125		2, 37
HFE-569sf2	CH <sub>3</sub> CH <sub>2</sub> O(CF <sub>2</sub> ) <sub>3</sub> CF <sub>3</sub>	0.8	~0.8		~0.8	~30		2, 38
HFE-236ca12	CHF <sub>2</sub> OCF <sub>2</sub> OCHF <sub>2</sub>	25.0	25.0		28.0	235		1, 2
HFE-338pcc13	CHF <sub>2</sub> OCF <sub>2</sub> CF <sub>2</sub> OCHF <sub>2</sub>	12.9	12.9		14.0	~160		1, 2
HFE-43-10pccc	CHF <sub>2</sub> OCF <sub>2</sub> OCF <sub>2</sub> CF <sub>2</sub> OCHF <sub>2</sub>	13.5	13.5		14.7	~165		1, 2
Trifluoromethyl formate	CF <sub>3</sub> OC(O)H	<3.5	<3.5		3.7	~75		2, 39, 40
Perfluoroethyl formate	C <sub>2</sub> F <sub>5</sub> OC(O)H	<3.5	<3.5		3.7	~75		2, 40, 41
Perfluoro-n-propyl formate	n-C <sub>3</sub> F <sub>7</sub> OC(O)H	<2.6	<2.6		2.7	~60		2, 40, 41
<b>Other Fluorinated Compounds</b>								
Trifluoromethyl-sulfurpentafluoride	SF <sub>5</sub> CF <sub>3</sub>	650–950	650–950					42
Sulfur hexafluoride	SF <sub>6</sub>	3,200	3,200					3
<b>Nitrogen trifluoride</b>	NF <sub>3</sub>	500	569			740		43
Sulfuryl fluoride	SO <sub>2</sub> F <sub>2</sub>	36	36		>300	630	40	44

<sup>a</sup> Total lifetime includes tropospheric OH and Cl atom reaction and photolysis loss, stratospheric loss due to reaction (OH and O(<sup>1</sup>D)) and photolysis, and ocean and soil uptake as noted in the table.

<sup>b</sup> The lifetimes given in parenthesis ( ) represent the “most likely” lifetime range, while the lifetimes given in brackets [ ] represent the “possible” lifetime range, see SPARC (2013).

<sup>c</sup> Lifetime for tropospheric loss due to reaction with OH calculated relative to the lifetime for CH<sub>3</sub>CCl<sub>3</sub>, (6.1 years) and a temperature of 272 K (see Box 1-1).

<sup>d</sup> Ocean lifetimes were taken from Yvon-Lewis and Butler (2002) unless noted otherwise.

<sup>e</sup> Stratospheric lifetime from Chapter 5 of SPARC (2013).

<sup>f</sup> Stratospheric lifetime from SPARC (2013) was based on both tracer (40 years) and model-mean (49 years) derived lifetimes.

<sup>g</sup> The value of τ<sub>OH</sub> of 6.1 years for methyl chloroform was derived from its measured overall lifetime of 5.0 years (Prinn et al., 2005; Clerbaux and Cunnold et al., 2007), taking into account an ocean partial lifetime of 94 years and stratospheric partial lifetime of 38 years.

#### Notes

- OH rate coefficient data taken from Sander et al. (2011).
- Stratospheric reactive loss (O(<sup>1</sup>D) and OH) partial lifetime estimate was based on an empirical correlation derived from data reported in Naik et al. (2000);  $\log(\text{Stratospheric reactive partial lifetime}) = 1.537 + 0.5788 \cdot \log(\text{Tropospheric OH partial lifetime})$ . This correlation was used in WMO (2011).
- Total lifetime is a best estimate taken from Ravishankara et al. (1993) that includes mesospheric loss due to Lyman- $\alpha$  (121.567 nm) photolysis.
- OH rate coefficient data taken from SPARC (2013) Chapter 3.
- Lifetime due to reaction with Cl atom of 259 years taken from the SPARC (2013) Chapter 5 model-mean.
- Ocean lifetime taken from Hu et al. (2013).
- Total lifetime also includes soil uptake partial lifetimes: 4.2 years for CH<sub>3</sub>Cl (Hu, 2012), 195 years for CCl<sub>4</sub> (Montzka and Reimann et al., 2011), and 3.35 years for CH<sub>3</sub>Br (Montzka and Reimann et al., 2011).
- Stratospheric photolysis lifetime was estimated using the empirical relationship given in Orkin et al. (2013a).
- Tropospheric UV photolysis partial lifetime: 1870 years for CFC-11, 11600 years for CFC-12, 4490 years for halon-1301, 7620 years for CFC-113, 19600 years for CFC-114, 3600 years for (*E*)-R316c, and 10570 years for (*Z*)-R316c.
- Ocean lifetime taken from Hu et al. (2012).
- Lifetimes from 2-D model calculations using cross section data from Papanastasiou et al. (2013). The total lifetime includes a tropospheric photolysis partial lifetimes: 27.2 years for halon-1211, 2.74 years for halon-1202, and 85.5 years for halon-2402.
- Tropospheric OH partial lifetime calculated from an overall lifetime of 5.0 years derived from the AGAGE and NOAA networks using a stratospheric partial lifetime of 38 years and an ocean partial lifetime of 94 years (Prinn et al., 2005).
- Stratospheric partial lifetime of 51 (27–264) years taken from Laube et al. (2014) and scaled to a CFC-11 lifetime of 52 years.
- Stratospheric partial lifetime taken from Naik et al. (2000).
- Stratospheric OH partial lifetime estimated from that for CHF<sub>2</sub>CF<sub>3</sub> taking into account the effects of chlorine substitution on the rate coefficients for CH<sub>3</sub>CF<sub>3</sub> and CH<sub>3</sub>CFCl<sub>2</sub>.
- Tropospheric OH partial lifetime estimated from that for CHF<sub>2</sub>CF<sub>3</sub> taking into account the effects of chlorine substitution on the rate coefficients for CH<sub>3</sub>CF<sub>3</sub> and CH<sub>3</sub>CF<sub>2</sub>Cl; stratospheric photolysis estimated to be the same as for CF<sub>3</sub>CF<sub>2</sub>Cl of 1590 years from SPARC (2013) Chapter 5 model mean.
- The revised O(<sup>1</sup>D) rate coefficient recommended in SPARC (2013) Chapter 3 would decrease the model calculated stratospheric partial lifetime slightly.
- UV photolysis is the expected predominant stratospheric loss process, however, no UV absorption spectrum data are available. Lifetimes assumed to be similar to CFC-12.

19. Stratospheric partial lifetime from 2-D model calculations using  $O(^1D)$  rate coefficient data from Baasandorj et al. (2013). The total lifetime includes mesospheric loss due to Lyman- $\alpha$  (121.567 nm) photolysis.
20. Lifetimes estimated to be similar to that of HFC-134a ( $CH_2FCF_3$ ).
21. Stratospheric partial lifetime estimated based on a reactivity comparison with  $CH_2F_2$  and  $CF_3CHF_2$ .
22. Stratospheric partial lifetime calculated using 2-D model with OH and  $O(^1D)$  rate coefficients recommended in SPARC (2013) Chapter 3.
23. Total lifetime estimated based on the increase in Lyman- $\alpha$  (121.567 nm) cross section with increasing number of  $-CF_2-$  groups in the perfluorocarbon.
24. OH rate coefficient from Young et al. (2009) and an assumed temperature dependence the same as for  $CHF_2CF_3$ .
25. Lifetimes taken from the 2-D model calculations in Papadimitriou et al. (2013b).
26. OH rate coefficient data taken from Atkinson et al. (2008).
27. Stratospheric partial lifetime assumed to be the same as for HCFC-133a ( $CH_2ClCF_3$ ).
28. Tropospheric OH partial lifetime estimated from that for  $CF_3CH_2OCF_2CHF_2$  by adjusting for the reactivity contribution of  $-CF_2CHF_2$  determined from the reactivity of  $CF_3CF_2OCF_2CHF_2$ .
29. Tropospheric OH partial lifetime estimated from those for  $CF_3OCH_3$  and  $CHF_2CH_2CF_3$ .
30. OH rate coefficient taken from Tokuhashi et al. (1999).
31. Tropospheric OH partial lifetime estimated as being greater than that of  $CHF_2CF_2OCHF_2$  and less than that of  $CHF_2CF_2CF_2CF_3$ .
32. Tropospheric OH partial lifetime assumed to be the same as that of  $CF_3OCH_2CF_3$ .
33. Tropospheric OH partial lifetime assumed to be the same as for  $CHF_2CH_2OCF_3$ .
34. Tropospheric OH partial lifetime assumed to be approximately that of  $CH_3OCF_2CHF_2$ .
35. Tropospheric OH partial lifetime estimated from the sum of the OH reaction loss of  $CF_3CF_2OCF_2CHF_2$  and  $CF_3CF_2OCH_2CHF_2$ .
36. OH rate coefficient from the 298 K studies of Langbein et al. (1999) and Sulbaek Andersen et al. (2012) and an assumed  $E/R$  of 1500 K.
37. OH rate coefficient from Chen et al. (2005a).
38. OH rate coefficient from the 295 K study of Christensen et al. (1998) and an assumed  $E/R$  of 1000 K.
39. OH rate coefficient taken from Chen et al. (2004b).
40. Ocean loss for perfluoro esters has been estimated from hydrolysis and solubility data for non-fluorinated and partially fluorinated esters by Kutsuna et al. (2005). These authors suggest that the ocean sink can be comparable to the tropospheric reaction sink for perfluoro esters, thereby reducing the total lifetimes given in this table by as much as a factor of 2.
41. OH rate coefficient from Chen et al. (2004a).
42. Total lifetime taken from Table 1-4 in Clerbaux and Cunnold et al. (2007).
43. Lifetimes calculated based on 2-D model from Papadimitriou et al. (2013a); total lifetime includes tropospheric (84150 years) and mesospheric (2531 years) partial lifetimes.
44. From Papadimitriou et al. (2008) and Mühle et al. (2009).

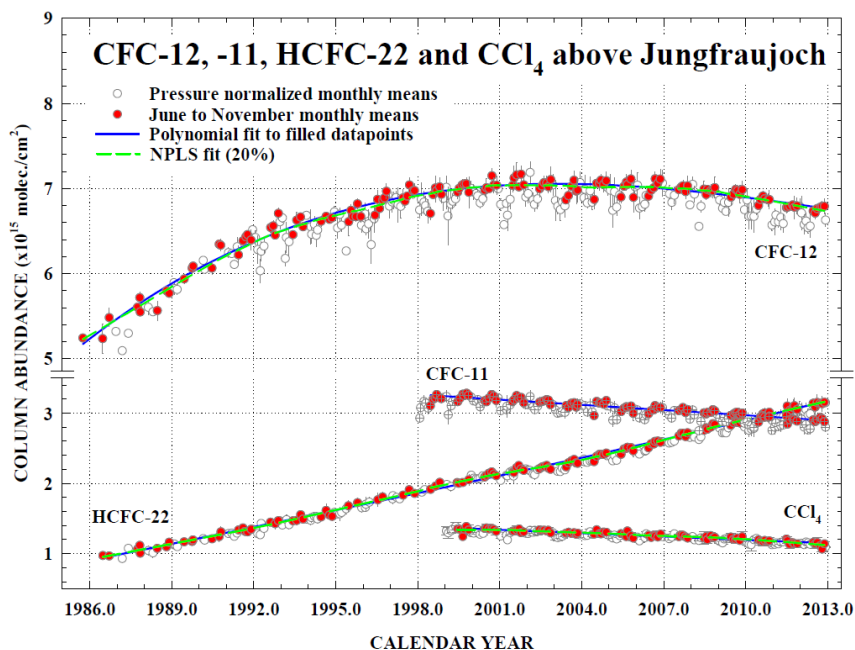


**Figure 1-2.** Time evolution of monthly-mean total vertical column abundances (in molecules per square centimeter) for CFC-12, CFC-11,  $CCl_4$ , and HCFC-22 above the Jungfraujoch station, Switzerland, through 2012 (updated from Zander et al. (2008), using the bootstrap resampling tool described by Gardiner et al. (2008) for the trend evaluations and Rinsland et al. (2012)). Note the discontinuity in the vertical scale. Solid blue lines show polynomial fits to the columns measured in June to November only so as to mitigate the influence of variability caused by atmospheric transport and tropopause subsidence during winter and spring (open circles) on derived trends. Dashed green lines show nonparametric least-squares fits (NPLS) to the June to November data.

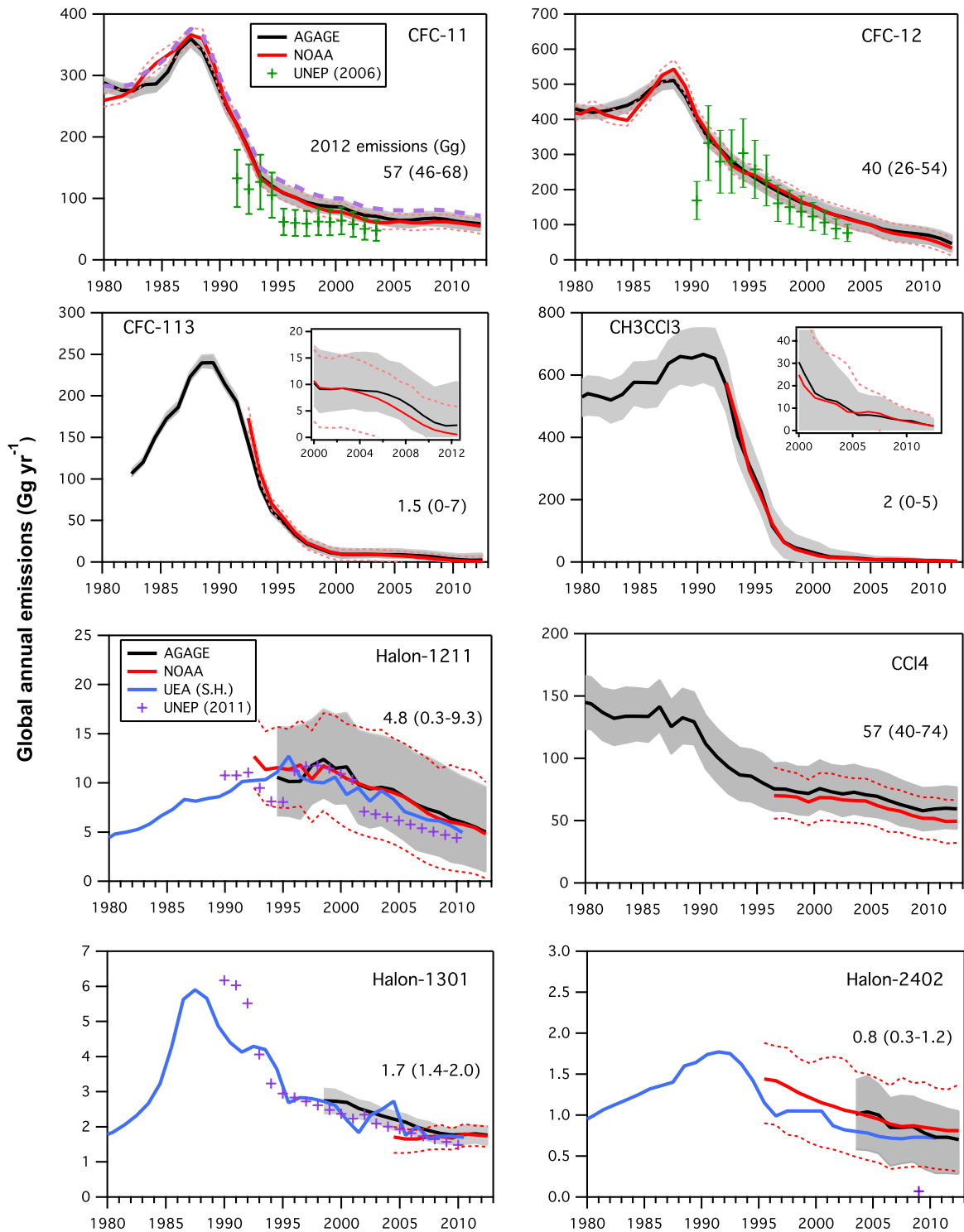


**Figure 1-3.** Top-down and bottom-up global emissions estimates (Gg yr<sup>-1</sup>) for ozone-depleting substances. Top-down emissions from AGAGE (black) and NOAA (red) atmospheric data were calculated using a global 12-box model (Cunnold et al., 1983; Rigby et al., 2013). *(continued next page)*

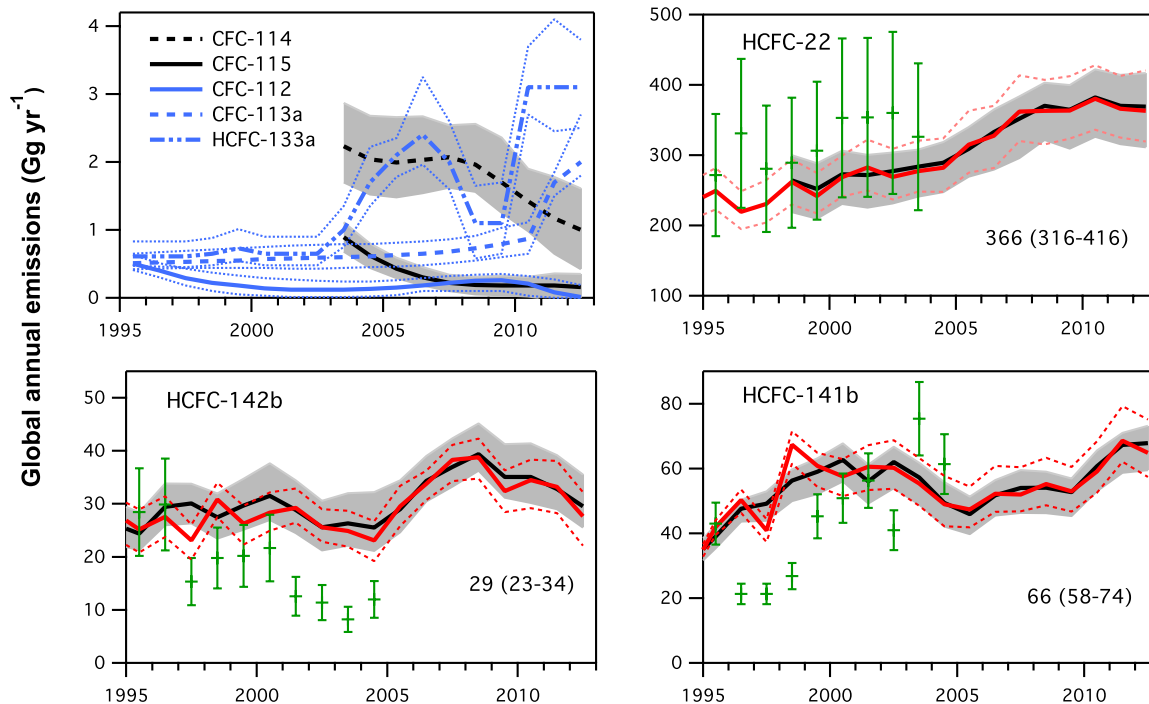


**(Figure 1-3, continued)** Additionally, for CFC-112, CFC-113a, HCFC-133a, and halons the emissions were calculated using UEA data from the Southern Hemisphere (S.H.) (Cape Grim archived air (blue); Laube et al., 2014). Lifetimes and ranges were taken from Newland et al. (2013), Laube et al. (2014), and SPARC (2013). Shaded bands indicate overall uncertainties derived from uncertainties in measurement, lifetimes, and prior emissions estimates. Mean values given in the text, and shown in figures for 2012, were calculated as the mean of AGAGE and NOAA estimates (when available). Ranges were taken from AGAGE data as shown in this figure unless AGAGE and NOAA ranges differed by more than 10%, in which case an average range was reported (e.g., CFC-113). CFC-11 emissions were also calculated using an older lifetime estimate of 45 years instead of 52 years (dashed violet line). Bottom-up estimates include UNEP (2006) (green) and UNEP (2011b) (violet). Note the x-axis ranges are not the same for all panels.

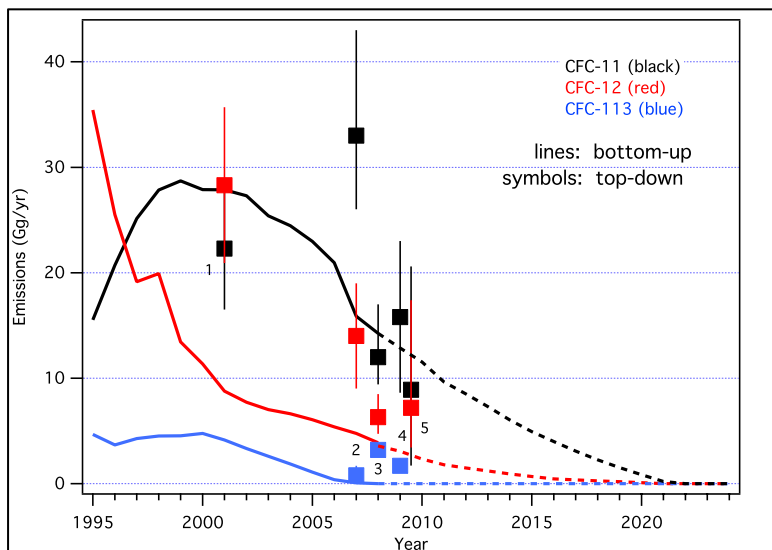


**Figure 1-4.** Regional emission estimates of CFC-11, CFC-12, and CFC-113 from China. Top-down estimates in years indicated were taken from <sup>1</sup>Palmer et al. (2003), <sup>2</sup>Vollmer et al. (2009), <sup>3</sup>Kim et al. (2010), <sup>4</sup>An et al. (2012), and <sup>5</sup>Fang et al. (2012). Bottom-up estimates (solid and dashed lines) are from Wan et al. (2009).

### Box 1-1. Lifetimes and Removal Processes

The total lifetime ( $\tau_{\text{Total}}$ ) of a trace species is defined as the ratio of its global atmospheric burden ( $C_{\text{Global}}$ ) to its total global loss rate ( $L_{\text{Total}}$ )

$$\tau_{\text{Total}} = C_{\text{Global}}/L_{\text{Total}}$$

where  $L_{\text{Total}}$  is the sum of the loss rates for various removal processes

$$L_{\text{Total}} = L_{\text{Atm}} + L_{\text{Soil}} + L_{\text{Ocean}} + \dots L_{\text{X}}$$

$L_{\text{Atm}}$  represents the loss rate for processes occurring in the atmosphere (gas-phase reaction and photolysis),  $L_{\text{Soil}}$  is the loss rate due to soil uptake, and  $L_{\text{Ocean}}$  is the rate for loss to the oceans (additional loss rates are represented by  $L_{\text{X}}$ ). Lifetimes are not constant values because they depend on the abundance of a chemical relative to the distribution of its sinks (and hence can vary with emission magnitude and location). Steady-state lifetimes refer to a lifetime when the emission and removal rates of a species are equal. A discussion of lifetimes and methods for defining their uncertainties is given in SPARC (2013).

Loss rates are associated with partial lifetimes such that

$$L_{\text{Total}} = C_{\text{Global}}/\tau_{\text{Total}} = C_{\text{Global}} \times (1/\tau_{\text{Atm}} + 1/\tau_{\text{Soil}} + 1/\tau_{\text{Ocean}} + \dots 1/\tau_{\text{X}})$$

$$\frac{1}{\tau_{\text{Total}}} = \frac{1}{\tau_{\text{Atm}}} + \frac{1}{\tau_{\text{Soil}}} + \frac{1}{\tau_{\text{Ocean}}} + \dots \frac{1}{\tau_{\text{X}}}$$

where  $(\tau_{\text{Atm}})^{-1} = (\tau_{\text{OH}})^{-1} + (\tau_{\text{O}_3})^{-1} + (\tau_{\text{Cl}})^{-1} + (\tau_{\text{NO}_3})^{-1} + (\tau_{\text{O}(\text{1D})})^{-1} + (\tau_{\text{J}})^{-1}$

The atmospheric lifetime can also be separated into partial troposphere, stratosphere, and mesosphere lifetimes using the total global atmospheric burden and the loss rate integrated over the different atmospheric regions such that

$$\frac{1}{\tau_{\text{Atm}}} = \frac{1}{\tau_{\text{Trop}}} + \frac{1}{\tau_{\text{Strat}}} + \frac{1}{\tau_{\text{Meso}}}$$

Species with total lifetimes greater than ~0.5 years are well-mixed in the troposphere and, for the purposes of this Assessment, are considered long-lived. In this case,  $\tau_{\text{Total}}$  is considered to be independent of the location of emission, and is considered to be a global lifetime that represents the compound's persistence in the Earth's atmosphere. The lifetime of a long-lived species due to reaction with tropospheric OH radicals is estimated relative to the corresponding tropospheric OH partial lifetime of methyl chloroform ( $\text{CH}_3\text{CCl}_3$ , MCF) such that

$$\tau_{\text{OH}}^{\text{RH}} = \frac{k_{\text{MCF}}(272 \text{ K})}{k_{\text{RH}}(272 \text{ K})} \times \tau_{\text{OH}}^{\text{MCF}}$$

where  $\tau_{\text{OH}}^{\text{RH}}$  is the OH partial lifetime for compound RH,  $k_{\text{RH}}(272 \text{ K})$  and  $k_{\text{MCF}}(272 \text{ K})$  are the rate coefficients for the reactions of OH with RH and MCF at 272 K, respectively, and  $\tau_{\text{OH}}^{\text{MCF}} = 6.1$  years (see Table 1-3).

Very short-lived substances (VSLS) (i.e., compounds with atmospheric lifetimes less than ~0.5 years) typically have non-uniform tropospheric distributions, because this time period is comparable to or shorter than the characteristic time of mixing processes in the troposphere. Local atmospheric lifetimes of VSLS, therefore, depend on where and when the compound is emitted, as well as local atmospheric conditions (Table 1-5, page 1.35). The concept of a single global lifetime, an Ozone Depletion Potential (ODP), or a Global Warming Potential (GWP) is inappropriate for VSLS, as discussed in Chapter 5.

Since the last Assessment, SPARC (Stratosphere-Troposphere Processes And their Role in Climate)—a core project of the World Climate Research Programme (WCRP)—initiated a study of the “Lifetimes of Stratospheric Ozone-Depleting Substances, Their Replacements, and Related Species” (SPARC, 2013). The study included 27 long-lived key ozone-depleting substances (ODSs), replacement compounds, and greenhouse gases (see Table 1-3). Including CFC-11 was of particular importance since it is the reference species used in defining the ODPs of other ODSs. The lifetime evaluation was warranted because of advancements in

**(Box 1-1, continued)**

the ability of models to simulate atmospheric circulation (leading to better estimates of age of air) and new measurement data from ground-based networks, high-altitude sampling, and satellite observations. The recommended steady-state atmospheric lifetimes were derived using results from state-of-the-art models and measurement-based estimates. The report also provides an in-depth analysis of the uncertainties in these lifetimes. The SPARC-recommended atmospheric steady-state lifetimes and estimated range of lifetimes given in Table 1-3 were obtained from a weighted average of the lifetimes derived from different methods, as described in SPARC (2013).

**1.2.1.2 HALONS****Observations**

Halon-1211 (CBrClF<sub>2</sub>), halon-2402 (CBrF<sub>2</sub>CBrF<sub>2</sub>), and halon-1202 (CBr<sub>2</sub>F<sub>2</sub>) mole fractions continued to decline from peak values observed in the early and mid-2000s (Table 1-1; Figure 1-1; Newland et al., 2013). Recent trends in halon-1211, halon-1301, and halon-2402 agree with those anticipated in the A1-2010 scenario (Daniel and Velders et al., 2011). Although globally averaged mole fractions of halon-1301 (CF<sub>3</sub>Br) continued to increase (reaching 3.26 ppt in 2012), the summed contribution of halons to total atmospheric bromine peaked around 2007. A decrease in global total bromine from halons was not evident at the time of the last Assessment, but is now significant, with an average rate of decline of  $-0.06$  ppt yr<sup>-1</sup> between 2008 and 2012.

Over the 2008–2012 period, estimates of the global abundances of halon-1301 and -1211 varied by 1–2% among global networks (Table 1-1). For halon-2402, Southern Hemispheric mole fractions from the University of East Anglia (UEA; Newland et al., 2013) were 7.5% lower than the NOAA scale.

**Lifetimes and emissions**

The new recommended steady-state lifetime of halon-1301 is 72 years (increased from 65 years) (SPARC, 2013). Revised lifetimes for halon-1202, halon-1211, and halon-2402, obtained using a 2-D model, are reported in this Assessment based on UV absorption cross section measurements made since the SPARC (2013) assessment (Papanastasiou et al., 2013). These halons are removed exclusively by photolysis in the troposphere and stratosphere. The lifetime uncertainty due solely to the uncertainty in the new cross section data for these substances (Table 1-3) is considerably smaller than reported in SPARC (2013), where the uncertainties were derived by averaging various 3-D approaches and observational data.

Global emission estimations derived from measured global mole fractions peaked around 1988 for halon-1301, 1993 for halon-2402, and 1995–1998 for halon-1211 (Figure 1-3). Emissions of halon-1211 and halon-2402 have been decreasing in recent years, while those of halon-1301 have remained approximately constant (Figure 1-3). This is broadly consistent with emission estimates from inventories (UNEP, 2011b). Continued emissions of halons are expected from banks (Box 5-1), since the primary use for these chemicals is in fire extinguishers. Therefore any impact of the 2010 global phase-out of halon production will likely not be observed in the atmosphere immediately. Top-down and bottom-up emissions estimates agree reasonably well for halon-1211 and halon-1301, but a large discrepancy continues to exist for halon-2402, which was predominantly produced and used in the former Soviet Union (McCulloch, 1992).

In 2010 halon banks were estimated by the Halons Technical Options Committee (HTOC); (UNEP, 2011b) as 43 Gg for halon-1301 and as 65 Gg for halon-1211. For the same year Newland et al. (2013) estimated an identical bank size for halon-1301, but only 37 Gg for halon-1211. The difference for halon-1211 may be partially explained by the relatively large uncertainty in the halon-1211 lifetime range (10–39 years), which translates into large uncertainties in emissions and bank sizes. With banks likely much larger than current emissions, it may take decades before halon-1211 and halon-1301 banks are depleted.

### 1.2.1.3 CARBON TETRACHLORIDE (CCl<sub>4</sub>)

#### **Observations**

The global surface mean mole fraction of carbon tetrachloride (CCl<sub>4</sub>) continued to decline from 2008 to 2012 (Table 1-1). The AGAGE and UCI networks report rates of decline of 1.2–1.3% from 2011–2012, whereas the rate of decline reported by the NOAA network was 1.6%. These relative declines in mole fractions at Earth's surface are comparable to declines in column abundances from remote sensing instruments of 1.2–1.3% yr<sup>-1</sup> (Table 1-2).

#### **Lifetimes and emissions**

Historically, CCl<sub>4</sub> was used as a solvent and as a feedstock for production of CFCs and their replacements. Current production is limited to feedstock, process agent use (e.g., in chlor-alkali production plants), and minor other essential uses (UNEP, 2013b; Fraser et al., 2014). Sinks for CCl<sub>4</sub> include loss in the stratosphere (Sander, 2011; SPARC, 2013), degradation in the oceans (Krysell et al., 1994; Yvon-Lewis and Butler, 2002; Lee et al., 2012), and degradation in soils (Happell and Roche, 2003; Liu, 2006; Rhew et al., 2008; Mendoza et al., 2011). A revised best estimate of the partial lifetime with respect to stratospheric loss, including the results of Laube et al. (2013) and Volk et al. (1997), is 44 years (SPARC, 2013), updated from 35 years. The partial lifetime with respect to oceanic uptake is still 94 (82–191) years (Yvon-Lewis and Butler, 2002). The soil sink partial lifetime is estimated to be approximately 195 (108–907) years (Montzka and Reimann et al., 2011). The sum of these three updated partial loss rates results in a total lifetime estimate of 26 years, which is unchanged from the previous Assessment (Montzka and Reimann et al., 2011). If the soil sink was negligible this would result in total lifetime of ~30 years.

Since the last Assessment, the discrepancy between bottom-up and top-down CCl<sub>4</sub> emission estimates has not been resolved. Global emissions determined from AGAGE and NOAA atmospheric data, using a total lifetime of 26 years, averaged 57 (40–74) Gg in 2012. After 2005 these top-down emission estimates are considerably higher than bottom-up emissions (derived from reported production minus feedstock use and destruction) (Figure 1-6).

A further indication of ongoing CCl<sub>4</sub> emissions (mostly in the Northern Hemisphere) is provided by the difference in mean mole fraction between hemispheres (Northern Hemisphere minus Southern Hemisphere, or NH–SH), which has been virtually stable at about 1.3 ppt since 2006. This is between the NH–SH difference of CFC-11 (~2 ppt), with annual emissions of 57 (46–68) Gg (410 (330–490) Mmol) in 2012, and CFC-113, with virtually no interhemispheric gradient and only small annual emissions of 1.5 (0–7) Gg (9 (0–40) Mmol) in 2012 (Figure 1-5). This suggests that significant sources of CCl<sub>4</sub> remain in the NH, although the higher oceanic sink in the SH, caused by the larger ocean area, may also account for some of this difference (Montzka and Reimann et al., 2011).

Emissions of CCl<sub>4</sub> could potentially arise from old industrial sites and from feedstock usage. The magnitude of emissions from CCl<sub>4</sub> feedstock uses are highly uncertain (UNEP, 2012) but have been estimated to be approximately 0.5%–2% of the feedstock production (1–4 Gg yr<sup>-1</sup> in 2012, Figure 1-6). Emissions from CCl<sub>4</sub> used as a process agent have also been suggested (UNEP, 2013b; Fraser et al., 2014). Fraser et al. (2014) detected enhanced abundances of CCl<sub>4</sub> downwind of industrial waste sites in Melbourne (Australia) and provided evidence that significant amounts of CCl<sub>4</sub> could be emitted from contaminated soils, toxic waste treatment facilities, and possibly chlor-alkali production plants. This finding is also supported by de Blas et al. (2013), who observed similar enhancements at an industrial site in Spain. On the other hand, UNEP (2013b) reported that CCl<sub>4</sub> emissions from process agent use are small and declining (<1 Gg yr<sup>-1</sup>). Although it is possible that unreported fugitive emissions (e.g., in the manufacture of polymers) exist (UNEP, 2013b), it is unlikely that these sources can explain the 30–70 Gg yr<sup>-1</sup> discrepancy between the top-down and bottom-up emission estimates.

The contributions of regional CCl<sub>4</sub> sources to global emissions are not well known. This is particularly true for developing countries, since the density of long-term surface measurements in these countries is still low. For North America, CCl<sub>4</sub> emissions between 0 and 0.4 Gg yr<sup>-1</sup> were derived from regional

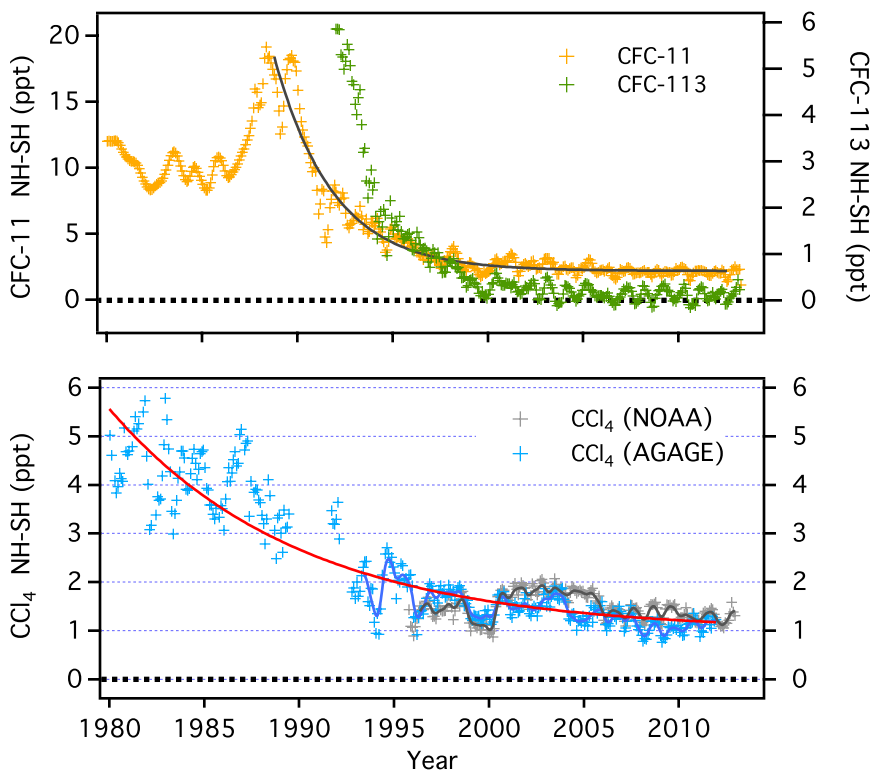


**Figure 1-5.** Trends in mean hemispheric mole fraction differences (NH minus SH ppt) for CFC-11 and CFC-113 (upper panel, NOAA data) and CCl<sub>4</sub> (lower panel; AGAGE data: blue symbols and blue line; NOAA data: gray symbols and black line). The red line is a fit to the AGAGE data.

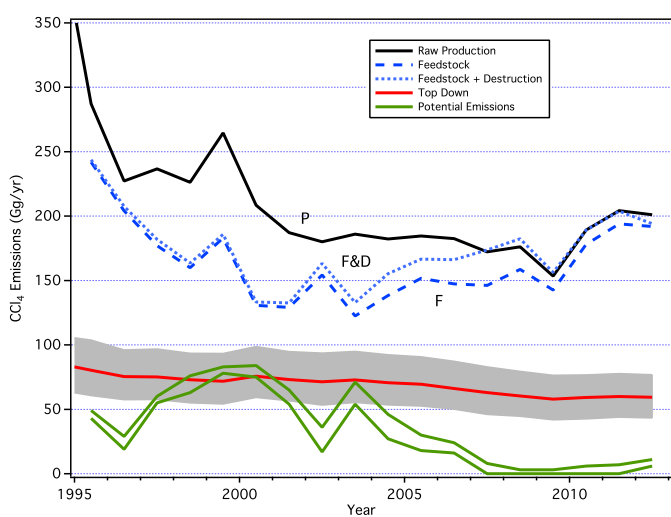


**Figure 1-6.** CCl<sub>4</sub> emissions derived from atmospheric measurements (red line and shading) and potential emissions estimated from production data (green lines). The lower potential emissions estimate (lower green line) was derived from the difference between total CCl<sub>4</sub> production reported to UNEP (solid black line labeled “P”) and the sum of feedstock and amounts destroyed (dotted blue line labeled “F&D”), and also includes estimates of underreported feedstock production. The upper potential emissions estimate (upper green line) was derived similarly, but was augmented by fugitive emissions of 2% of reported CCl<sub>4</sub> feedstock use, and assuming an efficiency of only 75% for reported destruction. Production magnitudes related to feedstock

alone are indicated with the dashed blue line labeled “F”. Top-down estimates (red line) were derived using AGAGE data and a 12-box model as in Figure 1-2. The shaded region represents the uncertainty in the top-down emissions resulting from measurement uncertainty, prior emissions, and a range of lifetimes. A range of partial lifetimes with respect to stratospheric loss, loss to soils, and loss to the oceans, was considered. The mean total lifetime for CCl<sub>4</sub> was 26 years and the range was 22–32 years.

campaigns and extrapolated to the entire U.S. by Hurst et al. (2006), Millet et al. (2009), and Miller et al. (2012) between 2003 and 2009. Xiao et al. (2010a) used monthly means and their uncertainties from globally distributed sites and a global transport model to estimate emissions for several regions, constrained by the global total. They estimated  $\text{CCl}_4$  emissions of  $4.9 \pm 1.4 \text{ Gg yr}^{-1}$  for North America during 1995–2004. More significantly, their study indicated that S.E. Asia was responsible for ~53% ( $37\text{--}42 \text{ Gg yr}^{-1}$ ) of the average global  $\text{CCl}_4$  emissions from 1996–2004. Palmer et al. (2003) (with a campaign downwind of China) and Vollmer et al. (2009) (with high-frequency observations at a site near Beijing) found that emissions from China in the early to mid-2000s were in the range of  $15.0\text{--}17.6 \text{ Gg yr}^{-1}$ , which is 20–25% of the global emissions estimated by top-down methods during that period. Furthermore, based on measurements at Cape Grim (Tasmania), Xiao et al. (2010a) and Fraser et al. (2014) estimated Australian  $\text{CCl}_4$  emissions of  $0.3\text{--}0.4 \text{ Gg}$  in the late 1990s, declining to  $0.1\text{--}0.2 \text{ Gg}$  in the early 2010s.

In summary, the mismatch between bottom-up inventories and global top-down estimates of  $\text{CCl}_4$  is still unresolved. There are, however, indications that some of the discrepancy could be explained by additional sources unrelated to reported production, such as contaminated soils and industrial waste (Fraser et al., 2014), although their global significance is highly uncertain. Additional explanations could include underreported emissions and incorrect partial lifetimes (stratosphere, ocean, or soil).

#### 1.2.1.4 METHYL CHLOROFORM ( $\text{CH}_3\text{CCl}_3$ )

##### **Observations**

The global mole fraction of methyl chloroform (1,1,1-trichloroethane,  $\text{CH}_3\text{CCl}_3$ ) has been declining steadily since reaching a maximum in the early 1990s (Figure 1-1). At  $\sim 5.4 \pm 0.3 \text{ ppt}$  in 2012, the global mean mole fraction is only 4% of its maximum. Thus, the contribution of  $\text{CH}_3\text{CCl}_3$  to future changes in total Cl will likely be small. Atmospheric  $\text{CH}_3\text{CCl}_3$  continues to be used to study the variability of the OH radical (Prinn et al., 2005; Montzka et al., 2011).

##### **Lifetimes and emissions**

Using atmospheric data and a global lifetime of 5.0 years (SPARC, 2013), global emissions of  $\text{CH}_3\text{CCl}_3$  are estimated to have been  $< 10 \text{ Gg yr}^{-1}$  since 2005 and decreased to  $\sim 2 \text{ Gg}$  in 2012 (Figure 1-3). This behavior is consistent with the historical uses of this controlled chemical as a solvent, with generally rapid release to the atmosphere. However, small remaining banks and potential emissions from its feedstock usage could lead to ongoing emissions. Small but non-zero emissions have been reported for different years during the last decade for the U.S. ( $2.4\text{--}2.8 \text{ Gg yr}^{-1}$ ) by Millet et al. (2009) and Miller et al. (2012) as well as for China ( $1.7\text{--}3.3 \text{ Gg yr}^{-1}$ ) by Vollmer et al. (2009) and Li et al. (2011).

#### 1.2.1.5 HYDROCHLOROFLUOROCARBONS (HCFCs)

##### **Observations**

The global surface mean mole fractions of the three most abundant hydrochlorofluorocarbons (HCFC-22,  $\text{CHClF}_2$ ; HCFC-141b,  $\text{CH}_3\text{CCl}_2\text{F}$ ; HCFC-142b,  $\text{CH}_3\text{CClF}_2$ ) continue to increase (Table 1-1). However, the growth rates in 2012 differed significantly from those in 2008 (Figures 1-1, 1-7). Between 2008 and 2012 the growth rate declined by  $\sim 30\%$  for HCFC-22 and by nearly 60% for HCFC-142b. In contrast, recent trends in HCFC-141b show a substantial increase ( $\sim 70\%$ ) in the growth rate since 2008. Whereas the increase in HCFC-141b was anticipated under the A1-2010 scenario (Figure 1-1), the slower increases of HCFC-22 and HCFC-142b were not.

Trends in total column HCFC-22 are also available from remote sensing instruments (updated from Gardiner et al., 2008; Zander et al., 2008; Brown et al., 2011) and are similar to those derived from surface data (Table 1-2). On the other hand, trends for HCFC-142b and HCFC-141b derived from satellite observations (ACE-FTS) do not agree with those measured at the surface (Table 1-2). For HCFC-141b, the ACE-FTS column measurements are subject to interference from other trace gases, such as CFC-114

and HFC-23, particularly at lower altitudes (Brown et al., 2011), which may explain some of the discrepancy.

For HCFC-124 ( $\text{CHClFCF}_3$ ) AGAGE measurements indicate a 9% decline in the global mole fraction between 2009 and 2012 (update of Prinn et al., 2000 and Miller et al., 2008). Laube et al. (2014) reported first measurements of HCFC-133a ( $\text{CH}_2\text{ClCF}_3$ ), which is used in the production of pharmaceuticals and is an intermediate in HFC-134a production (Miller and Batchelor, 2012; UNEP, 2012). Mole fractions of HCFC-133a in the Southern Hemisphere increased slowly from the 1970s to 2003, then increased more rapidly from 2004 to 2008, and after a period of little change from 2008–2010, increased rapidly again to 0.365 ppt in 2012 (Laube et al., 2014; Figure 1-1 and Table 1-1).

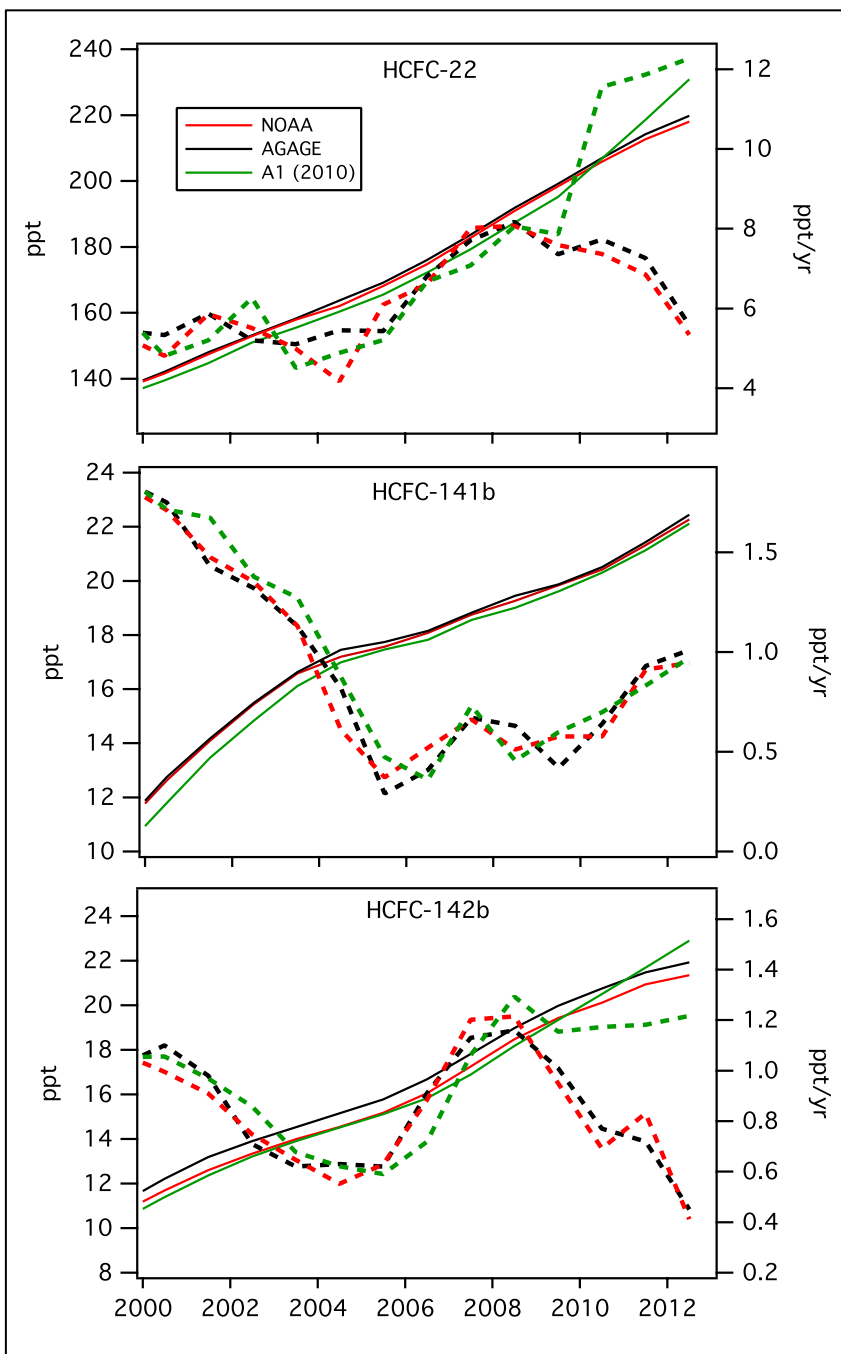


**Figure 1-7.** Recent trends for HCFC-22, HCFC-141b, and HCFC-142b estimated from AGAGE and NOAA global network data and the A1-2010 scenario: global mean mole fraction estimates (solid lines, left axis) and growth rates (dashed lines, right axis).

### Lifetimes and emissions

With a large bank of HCFC-22 thought to exist in refrigeration systems, emissions are expected to continue, but should decline as new refrigerants are being adopted as a consequence of the freeze of HCFC production and consumption for dispersive uses in 2013 in developing (Article 5) countries. Global emissions of HCFC-22, calculated using surface measurements of HCFC-22, peaked in 2010 at 381 (331–431) Gg and were 366 (316–416) Gg in 2012 (Figure 1-3) (i.e., stable within the uncertainties).

The estimated lifetime of HCFC-142b was revised from 17.2 to 18.0 years (+5%) since the previous Assessment (SPARC, 2013). Global HCFC-142b emissions peaked at 39 (34–44) Gg yr<sup>-1</sup> in 2008 and have since declined by 27% to 29 (23–34) Gg in 2012. This decline in emissions follows reduced production and consumption in non-Article 5 (non-A5) countries and a leveling off of production and consumption in Article 5 (A5) countries (Figure 1-8) (UNEP, 2014). Total global production in 2011 was only half that of 2009. On the other hand, feedstock use of HCFC-142b has increased markedly in recent years in both A5 and non-A5 countries. Emissions estimated from feedstock use vary, but are generally thought to be low (UNEP, 2013b).

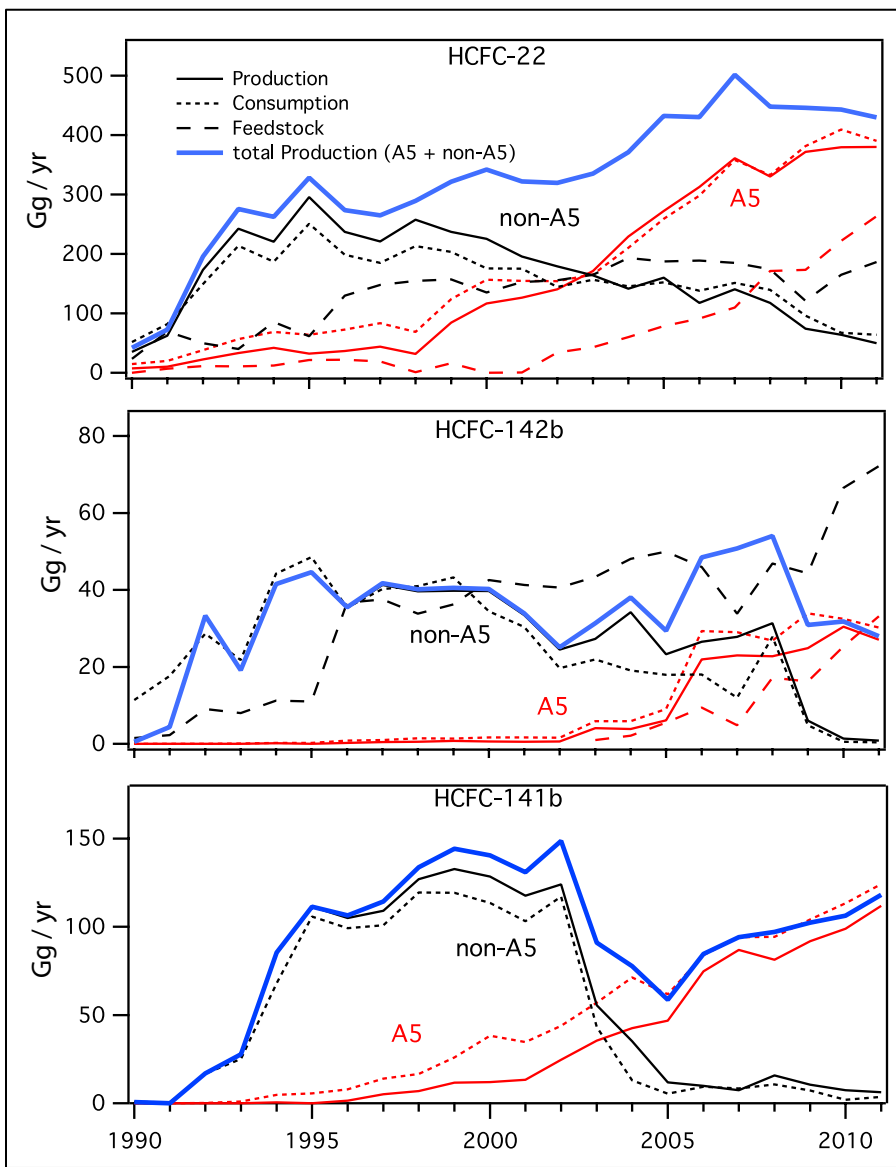


**Figure 1-8.** History of production, consumption, and feedstock use of HCFC-22, -142b, and -141b in Article 5 countries (red) and non-Article 5 countries (black) (UNEP, 2014). Total production (non-A5+A5) (blue) does not include feedstock production. Feedstock data for HCFC-141b are not shown because HCFC-141b feedstock use (15 Gg in 2010; UNEP, 2012) is thought to be small compared to that of HCFC-22 and HCFC-142b.

Current global HCFC-141b emissions are approaching the same level they were during peak production in the early 2000s (Figure 1-8). While production has decreased in non-A5 countries over the last decade, it has increased substantially in A5 countries since 2005 (UNEP, 2014). Regional studies indicate that China was responsible for about 15–30% of global HCFC-141b emissions in 2008–2009 (Wan et al., 2009; Stohl et al., 2010; Li et al., 2011; Fang et al., 2012).

Global and regional studies suggest a shift of HCFC emissions from midlatitudes to lower latitudes. Montzka et al. (2009) found a trend toward smaller intrahemispheric gradients as global emissions increased for HCFC-22, -141b, and -142b from 1996 to 2007. An updated gradient analysis using data through 2012 shows similar patterns to those described by Montzka et al. (2009), suggesting that recent shifts of production and consumption from non-A5 countries to A5 countries (Figure 1-8), which mostly are at lower latitudes, continue to be mirrored by higher emissions in these regions.

Recently, Saikawa et al. (2012) estimated regional HCFC-22 emissions between 1995 and 2009 using globally distributed surface data. They found a distinctive increase in emissions from Article 5 countries in Asia in recent years. A number of regional studies, along with bottom-up emission estimates and consideration of total HCFC production trends, suggest an increase in HCFC-22 emissions particularly from China in recent years (Figure 1-9) (Yokouchi et al., 2006; Stohl et al., 2010; Vollmer et al., 2009; Li et al., 2011; An et al., 2012; Fang et al., 2012). Apart from Vollmer et al. (2009) the temporal increase of the Chinese bottom-up emissions estimate from Wan et al. (2009) is consistent with several measurement-based studies (Figure 1-9). An et al. (2012) used an extension of the data set used by Vollmer et al. (2009) and found emissions that were comparable to those from Wan et al. (2009) (Figure

1-9). The reason for the difference between these two studies could be due to improvements in the regional transport simulation and in the inversion method used by An et al. (2012).

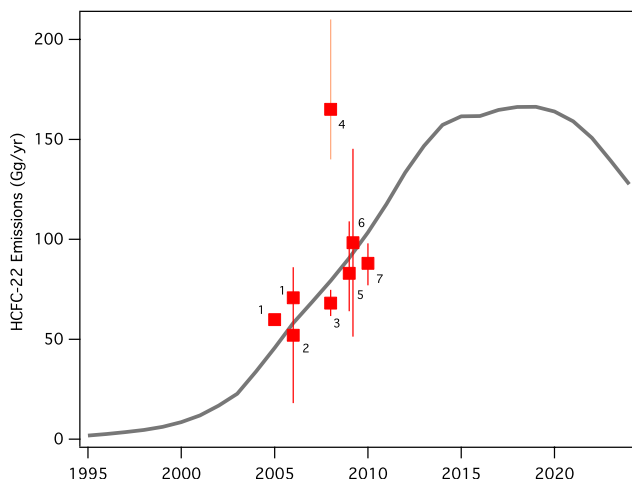


**Figure 1-9.** HCFC-22 emissions from China estimated by bottom-up (solid line; Wan et al., 2009) and top-down methods (filled squares): <sup>1</sup>Stohl et al. (2009); <sup>2</sup>Yokouchi et al. (2006); <sup>3</sup>Stohl et al. (2010); <sup>4</sup>Vollmer et al. (2009); <sup>5</sup>Li et al. (2011); <sup>6</sup>An et al. (2012); <sup>7</sup>Fang et al. (2012).

### 1.2.1.6 METHYL CHLORIDE (CH<sub>3</sub>Cl)

#### Observations

The global surface mean mole fraction of methyl chloride (CH<sub>3</sub>Cl) determined by the NOAA and AGAGE global networks was 540 ppt with a range from 537.1 to 542.2 ppt in 2012 (Table 1-1) and contributed ~16% to the total tropospheric chlorine. Only small changes were observed since the last Assessment, showing an enhanced interannual variability from 2011 to 2012 but an overall decline from 2008 to 2012 (Table 1-1, Figure 1-1).

Spatial and temporal variations in the distribution of CH<sub>3</sub>Cl in the upper troposphere and stratosphere were assessed by Santee et al. (2013) using 8 years of Microwave Limb Sounder (MLS) satellite data. They found a correlation of enhanced CH<sub>3</sub>Cl levels with regional biomass burning events, giving additional evidence for the importance of this highly fluctuating anthropogenically influenced source on the CH<sub>3</sub>Cl budget.

### **Sources and sinks**

While production and consumption of this primarily natural compound are not controlled by the Montreal Protocol, CH<sub>3</sub>Cl shares many natural sources and sinks with CH<sub>3</sub>Br, which is controlled. Sources of CH<sub>3</sub>Cl include the ocean, biomass burning, fungi, salt marshes, wetlands, rice paddies, mangroves, and tropical forests (Table 1-4). As with CH<sub>3</sub>Br, the budget for CH<sub>3</sub>Cl remains unbalanced, with sinks outweighing sources (Table 1-4).

Since the last Assessment, the magnitude of the tropical source has been better defined. Individual studies have shown that tropical sources of CH<sub>3</sub>Cl are significant. Saito et al. (2013) used an isotope tracer technique to separate the production of CH<sub>3</sub>Cl from the degradation associated with tropical plants. They confirmed earlier studies (Yokouchi et al., 2002, 2007; Blei et al., 2010; Saito et al., 2008; Gebhardt et al., 2008) suggesting that tropical plants are a substantial net source of CH<sub>3</sub>Cl. The modeling results of Xiao et al. (2010b) also suggest a substantial CH<sub>3</sub>Cl source from the tropics. These studies together suggest an average tropical terrestrial flux of  $2040 \pm 610$  Gg yr<sup>-1</sup> (Table 1-4).

Sinks of CH<sub>3</sub>Cl include reaction with hydroxyl radicals, uptake by soils, degradation in oceans, and photolysis in the stratosphere (Tables 1-3 and 1-4). Recently, Hu (2012) estimated a global soil uptake rate for CH<sub>3</sub>Cl of 1058 (664–1482) Gg yr<sup>-1</sup>. This rate was determined by scaling with the soil uptake rate for CH<sub>3</sub>Br, as suggested by Rhew et al. (2011). The oceanic uptake and emission of CH<sub>3</sub>Cl were recently revised by Hu et al. (2013) (Table 1-4), where the coastal ocean uptake and emissions were explicitly considered along with the open ocean fluxes and more degradation rate constant measurements.

#### **1.2.1.7 METHYL BROMIDE (CH<sub>3</sub>Br)**

##### **Observations**

The global surface mean mole fraction of methyl bromide (CH<sub>3</sub>Br) continued to decline since the last Assessment. The surface global mean mole fractions determined by NOAA and AGAGE networks was  $7.0 \pm 0.1$  ppt in 2012 (Table 1-1). This represents a decline of around 25% from the 9.2 ppt observed in the mid-1990s (Yvon-Lewis et al., 2009). When data from ice core measurements from Butler et al. (1999), Saltzman et al. (2004), Trudinger et al. (2004), and Saltzman et al. (2008) are averaged, a natural background in the Southern Hemisphere of  $5.5 \pm 0.2$  ppt results, which is consistent with the previous Assessment. Under the assumption that no natural interhemispheric gradient existed, this would signify that mole fractions of around 7 ppt in 2012 are still 27% above the natural background.

##### **Sources and sinks**

CH<sub>3</sub>Br has both natural and anthropogenic sources. Our estimate of global sinks and sources for CH<sub>3</sub>Br is not balanced, with known sinks outweighing known sources (Table 1-4). This imbalance persists from pre-phase-out (1995–1998) through the most recent years (Hu et al., 2012).

The primary anthropogenic source of CH<sub>3</sub>Br has been from its use as a fumigant. Non-quarantine and pre-shipment (non-QPS) fumigation uses (mainly in agriculture) were the dominating anthropogenic source of atmospheric CH<sub>3</sub>Br in the past, but are subject to phase-out and currently only limited amounts are still allowed for applications in critical-use exemptions. Quarantine and pre-shipment (QPS) uses, which are mainly related to pest control during transport and storage, are exempted from the phase-out and consumption from QPS uses was approximately stable in the last two decades (UNEP, 2014). Therefore, the declining atmospheric abundance of CH<sub>3</sub>Br is the result of reductions in consumption for non-QPS uses (Figure 1-10). Accordingly, the non-QPS consumption became lower than the QPS consumption in 2009 and by 2012 it was only 43% of the QPS consumption, or 30% of the total fumigation use (Figure 1-10). Estimated emissions from non-QPS uses became lower than QPS uses after 2006, as emission factors are higher for QPS uses (84%) than for non-QPS uses (65%) (UNEP, 2007). These QPS/non-QPS uses do not include consumption as a chemical feedstock (Montzka and Reimann et al., 2011) or the application of CH<sub>3</sub>Br as a transient in the conversion of methane to fuel (Ding et al., 2013), as CH<sub>3</sub>Br is assumed to be released only in minor quantities from these processes.

**Table 1-4. Sources and sinks for atmospheric CH<sub>3</sub>Cl and CH<sub>3</sub>Br in Gg yr<sup>-1</sup>** (adapted from Hu, 2012). The best values are shown with their possible ranges in parentheses. n.q. = not quantified. QPS = quarantine and pre-shipment. For CH<sub>3</sub>Cl, figures represent the current knowledge. For CH<sub>3</sub>Br changes in anthropogenic sources between 1995–1998 and 2012 are derived from reported information.

Source / Sink	CH <sub>3</sub> Cl (Gg yr <sup>-1</sup> )	CH <sub>3</sub> Br (Gg yr <sup>-1</sup> )	
		1995 – 1998	2012
<b>SOURCES</b>			
<b>Anthropogenic Sources</b>			
Leaded Gasoline	n.q.	3 (0.6–6) <sup>18-21</sup>	0–3
Coal Combustion; Waste Incineration; Industrial Activity	162 (29–295) <sup>1</sup>	n.q.	n.q.
Fumigation – QPS <sup>a</sup>	n.q.	8.1 (7.5–8.7)	7.4 (6.9–7.8)
Fumigation – non-QPS <sup>b</sup>	n.q.	39.9 (28.2–55.9)	2.5 (1.7–3.5)
Biomass Burning – Indoor Biofuel Use <sup>c</sup>	113 (56–169)	6 (3–9)	6 (3–9)
Biomass Burning – Open Field Burning <sup>e</sup>	355 (142–569)	17 (7–27) <sup>d</sup>	17 (7–27)
Ocean	700 (510–910) <sup>2</sup>	32 (22–44) <sup>22</sup>	32 (22–44) <sup>22</sup>
<b>Terrestrial sources</b>			
Tropical and Subtropical Plants; Tropical Leaf Litter <sup>f</sup>	2040 (1430–2650) <sup>3-9</sup>	n.q.	n.q.
Mangroves	12 (11–12) <sup>10</sup>	1.3 (1.2–1.3) <sup>10</sup>	1.3 (1.2–1.3) <sup>10</sup>
Rapeseed	n.q.	4.9 (3.8–5.8) <sup>23</sup>	5.1 (4.0–6.1) <sup>23</sup>
Fungus	145 (128–162) <sup>7,11</sup>	2.2 (1–5.7) <sup>7,24</sup>	2.2 (1–5.7) <sup>7,24</sup>
Salt Marshes	85 (1.1–170) <sup>12,13</sup>	7 (0.6–14) <sup>26</sup>	7 (0.6–14) <sup>26</sup>
Wetland	27 (5.5–48) <sup>14,15</sup>	0.6 (–0.1–1.3) <sup>24</sup>	0.6 (–0.1–1.3) <sup>24</sup>
Rice Paddies	3.7 (2.7–4.9) <sup>16</sup>	0.7 (0.1–1.7) <sup>24</sup>	0.7 (0.1–1.7) <sup>24</sup>
Shrublands	15 (9–21) <sup>17</sup>	0.7 (0.5–0.9) <sup>17</sup>	0.7 (0.5–0.9) <sup>17</sup>
<b>Subtotal (Sources)</b>	<b>3658</b>	<b>123</b>	<b>84</b>
<b>SINKS<sup>g</sup></b>			
Reaction with OH <sup>h</sup>	2832 (2470–3420)	74 (63–83)	56 (48–63)
Loss in Soil	1058 (664–1482)	40 (25–54)	30 (19–41)
Loss in Ocean	370 (296–445) <sup>2</sup>	43 (27–58) <sup>22</sup>	33 (20–44) <sup>22</sup>
Loss in Stratosphere	146	5	4
<b>Subtotal (Sinks)</b>	<b>4406</b>	<b>162</b>	<b>123</b>
<b>Net (Sources – Sinks)</b>	<b>–748</b>	<b>–39</b>	<b>–39</b>

a. Data for fumigation — QPS consumptions of CH<sub>3</sub>Br were downloaded from UNEP ([http://ozone.unep.org/Data\\_Reporting/Data\\_Access](http://ozone.unep.org/Data_Reporting/Data_Access)) and the emission ratio is 84% (78%–90%) from UNEP (2007).

b. Data for fumigation — non-QPS consumptions of CH<sub>3</sub>Br were downloaded from UNEP ([http://ozone.unep.org/Data\\_Reporting/Data\\_Access](http://ozone.unep.org/Data_Reporting/Data_Access)) and the emission ratio is 65% (46%–91%) from UNEP (2007) and UNEP (2011c).

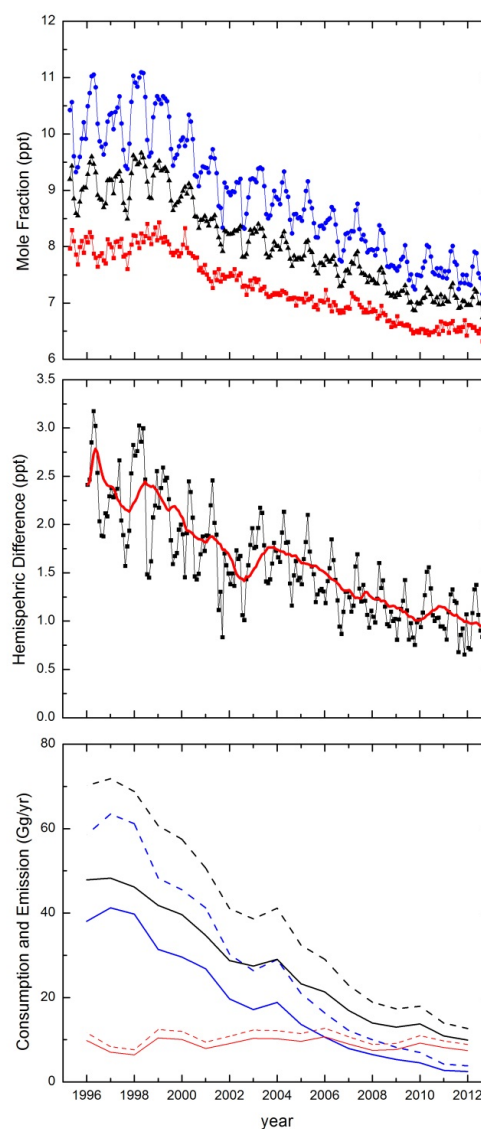
(continued next page)

**Table 1-4, continued.**

- c. Emissions of indoor biofuel use were estimated based on the total dry matter burned for indoor biofuel use in 1995 (Yevich and Logan, 2003) and emission factors from Andreae and Merlet (2001).
- d. Average biomass burning emissions were determined using the dry matter burned (van der Werf et al., 2010) and emission factors from Andreae and Merlet (2001).
- e. Mean of observations with range of  $\pm 1\sigma$ .
- f. Average value from Hu (2012).
- g. For sinks, partial lifetimes from Table 1-3 were used. For the calculation of the atmospheric burden ( $B_a$ ) the following equation was used:  $B_a = \chi_a n_{tr}/r$ , where  $\chi_a$  is the sea-level mole fraction ( $\text{CH}_3\text{Cl}$  540 ppt in 2012;  $\text{CH}_3\text{Br}$  9.2 ppt in 1995-1998 and 7.0 ppt in 2012),  $n_{tr}$  is the number of moles in the troposphere ( $1.446 \times 10^{20}$  moles), and  $r$  is the fraction of the total amount of the substance that resides in the troposphere ( $r = 0.95$  for  $\text{CH}_3\text{Br}$  and 0.887 for  $\text{CH}_3\text{Cl}$ ; Lal et al., 1994).
- h. The sink due to the reaction with Cl-radicals is not included.

<sup>1</sup>McCulloch et al. (1999), <sup>2</sup>Hu et al. (2013), <sup>3</sup>Yokouchi et al. (2007), <sup>4</sup>Blei et al. (2010), <sup>5</sup>Saito et al. (2008), <sup>6</sup>Gebhardt et al. (2008), <sup>7</sup>Lee-Taylor et al. (2001), <sup>8</sup>Xiao et al. (2010b), <sup>9</sup>Yoshida et al. (2004), <sup>10</sup>Manley et al. (2007), <sup>11</sup>Watling and Harper (1998), <sup>12</sup>Rhew et al. (2000), <sup>13</sup>Cox et al. (2004), <sup>14</sup>Varner et al. (1999), <sup>15</sup>Dimmer et al. (2001), <sup>16</sup>Lee-Taylor and Redeker (2005), <sup>17</sup>Rhew et al. (2001), <sup>18</sup>Thomas et al. (1997), <sup>19</sup>Chen et al. (1999), <sup>20</sup>Baker et al. (1998), <sup>21</sup>Bertram and Kolowich (2000), <sup>22</sup> adapted from Hu et al. (2012) according to footnote g, <sup>23</sup>Mead et al. (2008), <sup>24</sup> Lee-Taylor and Holland (2000), <sup>26</sup>Montzka and Reimann et al. (2011).

**Figure 1-10.** Upper panel: Trends since 1995 in methyl bromide (upper) mole fractions with NH (●) SH (■) and global (▲) NOAA data (Montzka et al., 2003, updated). Middle panel: Interhemispheric differences (NH-SH) as monthly means (•) and as a running average (—). Lower panel: consumption (dashed lines) as reported in the UNEP database (UNEP, 2014) for non-QPS uses (---), QPS uses (- - -) and total (---), and emission (solid lines) from non-QPS uses (—), QPS uses (—) and total (—). Soil fumigation emission rates estimated as 65% (46–91%) of reported consumption rates (UNEP 2007). QPS emission rates estimated as 84% (78–90%) of reported consumption rates (UNEP 2007).



The total controlled and non-controlled fumigation emission is estimated to have accounted for 30 (22–40)% of the total global CH<sub>3</sub>Br emissions during 1996–1998, before industrial production and consumption were reduced. By 2012, the total fumigation-related emissions, from controlled and non-controlled uses of CH<sub>3</sub>Br, is estimated to have been reduced to 8 (7–10)% of the total global CH<sub>3</sub>Br emissions.

Other anthropogenic sources of CH<sub>3</sub>Br include the combustion of leaded gasoline, biomass burning, and emissions from certain crop species (e.g., canola/rapeseed, rice, mustard and cabbage) (references in Table 1-4). Biomass burning emissions are separated into open field burning, which can be anthropogenic or natural and indoor biofuel combustion (Yvon-Lewis et al., 2009; Hu, 2012). The combined burning emissions from these sources are comparable to the estimates in the previous Assessment (Table 1-4).

Natural sources of CH<sub>3</sub>Br include the ocean, freshwater wetlands, fungus, tropical plants and leaf litter, and coastal saltmarshes (Table 1-4). Individual studies have shown that tropical sources are small or not significant (Gebhart et al., 2008; Blei et al., 2010). These studies were confirmed recently by Saito et al. (2013), who showed that the uptake of CH<sub>3</sub>Br associated with tropical plants was nearly equal to its emission, resulting in only a small net source for CH<sub>3</sub>Br from tropical plants. The variability in the magnitude of these tropical plant emissions has made them difficult to quantify over the global tropical region and they are therefore not included in the Table 1-4. An updated distribution of net fluxes from open and coastal oceans and of degradation rate constants has resulted in ocean emissions being revised downward from 42 Gg yr<sup>-1</sup> (Montzka and Reimann et al., 2011) to 33 (20–44) Gg yr<sup>-1</sup> (Table 1-4).

Since sink rates scale with the atmospheric burden, the rates of uptake by oceans, reaction with OH, photolysis, and soil microbial degradation continue to decline as the atmospheric concentrations have decreased (Table 1-4). In a recent study, Nilsson et al. (2013) proposed a significantly (~60%) faster reaction rate of CH<sub>3</sub>Br with OH radicals than was recommended in SPARC (2013). However, due to the significant difference between the new reaction rate constant and the consistent values in the existing literature, no major change in the recommended rate constant could be justified. The rate constant recommended in SPARC (2013) is only slightly different from that used in previous Assessments. The partial CH<sub>3</sub>Br lifetime with respect to reaction with OH and photolysis is 1.8 years, vs. 1.7 years in the previous Assessment. The partial lifetime for soil uptake, estimated at 3.35 years in the last Assessment, has been substantiated by results of Rhew et al. (2010) and Rhew (2011). The partial lifetime with respect to oceanic uptake has been revised upward to 3.1 (2.3–5.0) years (Hu et al., 2012) from the 2.2–2.4 years reported in the last Assessment based on Yvon-Lewis et al. (2009). However, when combined with the small reduction in the partial lifetime with respect to reaction with OH (discussed above) and the unchanged soil sink from the last Assessment, the overall lifetime remains unchanged at 0.8 years.

The reduction in the atmospheric abundance of CH<sub>3</sub>Br since the time that the oceanic uptake rate was re-examined results in a lower uptake rate in Table 1-4 than that reported above by Hu et al. (2012). As a result of the decrease in atmospheric CH<sub>3</sub>Br, the natural oceanic source is now comparable to the oceanic sink; this is consistent with the model prediction reported by Butler (1994) and Yvon-Lewis et al. (2009) and the near-equilibrium conditions observed in 2010 and reported by Hu et al. (2012).

### 1.3 VERY SHORT-LIVED HALOGENATED SUBSTANCES (VSLS)

As in previous Assessments, we consider VSLS to include very short-lived halogenated source gases (SGs), halogenated organic and inorganic product gases (PGs) arising from SG degradation, and other sources of tropospheric inorganic halogens.

Various lines of evidence suggest that VSLS may be transported from the boundary layer into the stratosphere, where they contribute to stratospheric halogen loading (Gettelman et al., 2009; Brioude et al., 2010; Montzka and Reimann et al., 2011; Marecal et al., 2012). Evaluating this contribution requires knowledge of VSLS tropospheric degradation and removal (Box 1-2), and the spatial and temporal variability of emissions, loss processes (Table 1-5), and transport processes (Box 1-3). These factors have consequences for the calculation of Ozone Depletion Potentials (ODPs) for VSLS, as the traditional concept of a single, geographically independent and time-independent value does not apply (Chapter 5: Section 5.3, Table 5-4).



### Box 1-3. Transport of Ozone-Depleting Substances to the Stratosphere in the Tropics

Ozone-depleting substances (ODSs) are transported to the stratosphere primarily in tropical regions where ascent through the troposphere is dominated by convection (Figure 1). Outflow from convective clouds, typically between 12–14 km (Folkins and Martin, 2005), can inject boundary layer air that may be rich in ODSs into the tropical tropopause layer (TTL) (e.g., Gettelman and Forster, 2002; Fueglistaler et al., 2009; Randel and Jensen, 2013). Here, over several kilometers, a transition occurs from the well-mixed, convectively dominated troposphere to a region of slow ascent controlled by the ascending branch of the stratospheric Brewer-Dobson circulation. The TTL is here defined as the layer between the level of maximum convective outflow (~12 km altitude, 345K potential temperature) and the cold-point tropopause (CPT, ~17 km, 380K). The level of zero radiative heating (LZRH) marks the transition from clear-sky radiative cooling to clear-sky radiative heating ( $Q_{\text{clear}}$ , ~15 km, 360K), and above which (in the “upper TTL”) air masses may cross the CPT to enter the “tropical stratosphere” or “stratospheric overworld.” For long lived and thus well-mixed halogenated source gases (see Section 1.2), the details of their troposphere-to-stratosphere transport are of minor importance. However, for very short-lived substances (VSLS), whose lifetimes may be comparable to tropospheric transport timescales, transport processes—along with physical and chemical processes that occur in the TTL—may strongly impact their stratospheric source gas and product gas injections.

The convective transport of air masses to the TTL is zonally asymmetric and exhibits significant seasonal and also interannual variability (e.g., Fueglistaler et al., 2004; Ashfold et al., 2012). Preferential transport into the TTL takes place in strong convective source regions. Examples include boreal winter over the Maritime Continent (e.g., Hosking et al., 2010; Bergman et al., 2012)—located within the tropical warm pool, between the Indian and Pacific Oceans—and also boreal summer within Indian monsoon regions (e.g., Devasthale and Grassl, 2009; Devasthale and Fueglistaler, 2010) and Southeast Asia (e.g., Wright et al., 2011; Chen et al., 2012). Air detrained into the lower TTL enters a region of large-scale subsidence and will mostly descend into the mid-troposphere. Air detrained above the LZRH can ascend through the upper TTL, where vertical velocities and residence times vary in both space and time. As zonal variation in these transport timescales can be large, the location at which air enters the TTL, along with its horizontal transport through regions of upwelling/downwelling in relation to the fluctuating LZRH, strongly impact transport into the stratosphere (e.g., Gettelman et al., 2004; Tzella and Legras, 2011; Bergman et al., 2012). In addition to these circulations, the TTL is also characterized by two-way exchange with the extratropics, which may strongly impact the abundance and seasonality of trace gases in the TTL, including ozone (e.g., Ploeger et al., 2012).

For particularly short-lived VSLS (i.e., those with a local lifetime of several days or less at the surface), significant transport to the upper TTL is unlikely unless emitted close to deep convection (Hossaini et al., 2012a). Residence times in this layer are estimated to be in the range of 24–45 days (Montzka and Reimann et al., 2011). For VSLS with comparable or shorter local lifetimes, significant source gas (SG) to product gas (PG) conversion could take place. If product gases are subsequently removed from this layer, for example due to adsorption onto cirrus ice followed by sedimentation, the net stratospheric input of halogen from VSLS will be reduced. Particularly deep overshooting convection can transport air masses directly up to or above the tropopause (e.g., Pommereau, 2010), providing rapid transport through the upper TTL. These events could allow even the shortest-lived VSLS to be transported to the stratospheric overworld, though they are relatively rare (Liu and Zipser, 2005; Takahashi and Luo, 2014) and at present their global-scale impact on stratospheric composition is uncertain. In addition to transport into the overworld, quasi-horizontal transport from the base of the TTL may provide a rapid transport route for VSLS to enter the extratropical lowermost stratosphere (i.e., above the tropopause but below the 380 K isentrope) (Levine et al., 2007). **(continued next page)**

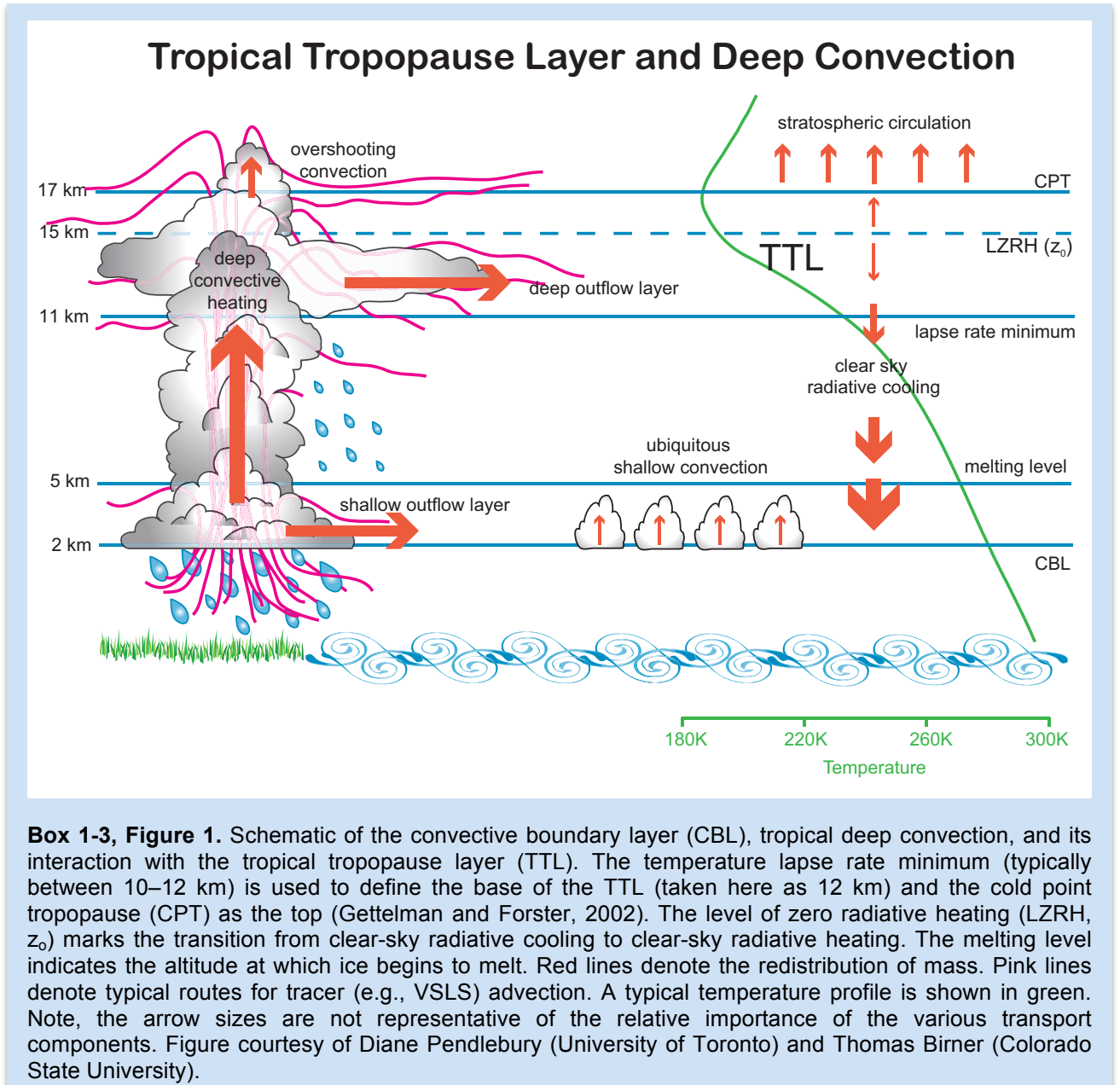


**Table 1-5. Lifetime estimates for halogenated very short-lived (VSL) source gases.** Local lifetimes for the tropospheric tropical and midlatitude regions were calculated using the OH and temperature climatology from Spivakovsky et al. (2000) and Prather and Remsberg (1993), respectively. Photolysis lifetimes were calculated using solar fluxes taken from the TOMCAT chemical transport model (e.g., Hossaini et al., 2012a). For the tropics, annually averaged values are reported along with the seasonal range of lifetimes given in parentheses. For midlatitudes, seasonally averaged local lifetimes (summer, fall, winter, spring) are reported. VSLs with new kinetic or photolysis laboratory studies available since the last Assessment are highlighted in bold, with local lifetimes calculated using the WMO (2011) method given in the footnotes.

Compound	WMO (2011) Local Lifetime (days) <sup>1</sup>	Loss Process	Local Lifetime <sup>2</sup> Tropics (25°S–25°N) (days)		Local Lifetime Midlatitude (25°N–65°N) (days)								Notes
			Boundary Layer	10 km	Boundary Layer				10 km				
					Su	F	W	Sp	Su	F	W	Sp	
<b>Chlorocarbons</b>													
CH <sub>2</sub> Cl <sub>2</sub>	144	OH	109 (98–133)	179 (171–185)	95	235	725	155	180	480	1070	430	3, 7
CHCl <sub>3</sub>	149	OH	112 (100–136)	190 (182–197)	97	240	750	160	190	515	1145	460	4, 7
CH <sub>3</sub> CH <sub>2</sub> Cl	39	OH	30 (27–37)	47 (45–49)	26	65	200	43	47	125	280	111	5, 7
CH <sub>2</sub> ClCH <sub>2</sub> Cl	65	OH	47 (42–58)	90 (86–93)	41	103	320	69	90	250	555	225	4, 7
CH <sub>3</sub> CH <sub>2</sub> CH <sub>2</sub> Cl	14	OH	11 (10–14)	14 (14–15)	10	24	70	15	14	37	80	32	5, 7
CHClCCl <sub>2</sub>	4.9	OH	5 (4–6)	3 (3–4)	4	9	27	6	3	8	16	6	3, 7
CCl <sub>2</sub> CCl <sub>2</sub>	90	OH	67 (60–81)	119 (114–123)	58	145	450	96	120	325	725	290	3, 7
CH <sub>3</sub> CHClCH <sub>3</sub>	18	OH	15 (14–19)	17 (17–18)	13	32	95	21	17	44	95	38	5, 7
<b>Bromocarbons</b>													
CH <sub>2</sub> Br <sub>2</sub>	123	OH	94 (84–114)	150 (144–155)	80	200	620	135	150	405	890	360	3
	5000	<i>J</i>	–	–	–	–	–	–	–	–	–	–	
	123	<i>Total</i>	94 (84–114)	150 (144–155)	80	200	620	135	150	405	890	360	
CHBr <sub>3</sub>	76	OH	40 (36–48)	46 (44–48)	34	84	250	54	45	117	250	101	6, 9
	36	<i>J</i>	23 (21–26)	27 (25–30)	25	59	130	33	28	70	135	40	
	24	<i>Total</i>	15 (13–17)	17 (16–18)	14	35	86	20	17	44	88	29	
CH <sub>2</sub> BrCl	137	OH	103 (92–125)	174 (167–180)	89	220	685	147	175	470	1050	420	3, 7
CHBrCl <sub>2</sub>	121	OH	65 (58–79)	82 (79–85)	56	137	410	89	81	210	460	185	6, 7
	222	<i>J</i>	108 (104–111)	114 (111–117)	120	305	610	160	130	300	550	165	
	78	<i>Total</i>	41 (37–46)	48 (46–49)	38	94	245	57	50	124	250	87	

(continued next page)

Compound	WMO (2011) Local Lifetime (days) <sup>1</sup>	Loss Process	Local Lifetime <sup>2</sup> Tropics (25°S–25°N) (days)		Local Lifetime Midlatitude (25°N–65°N) (days)								Notes
			Boundary Layer	10 km	Boundary Layer				10 km				
					Su	F	W	Sp	Su	F	W	Sp	
CHBr <sub>2</sub> Cl	94	OH	50 (45–61)	59 (57–61)	43	105	310	67	58	150	325	130	6, 7
	161	<i>J</i>	91 (87–94)	55 (54–57)	120	360	820	170	72	195	415	97	
	59	<i>Total</i>	32 (30–37)	28 (28–29)	32	81	225	48	32	85	182	56	
CH <sub>3</sub> CH <sub>2</sub> Br	41	OH	32 (29–40)	45 (43–47)	28	69	210	45	45	118	260	103	3, 7
CH <sub>2</sub> BrCH <sub>2</sub> Br	70	OH	51 (46–62)	95 (91–99)	44	111	350	74	97	265	590	235	4, 7
n-C <sub>3</sub> H <sub>7</sub> Br	12.8	OH	11 (10–13)	12 (12–13)	9	23	67	15	12	30	65	26	3, 7
Iso-C <sub>3</sub> H <sub>7</sub> Br	16.7	OH	14 (13–17)	15 (15–16)	12	30	88	19	15	38	81	33	3, 7
<b>Iodocarbons</b>													
CH <sub>3</sub> I	158	OH	114 (102–139)	223 (213–231)	99	250	780	165	230	620	1395	560	4
	7	<i>J</i>	4.2 (4.0–4.5)	3.6 (3.5–3.7)	4.3	9.6	19	5.6	3.5	7.5	13	4.6	
	7	<i>Total</i>	4.0 (3.8–4.3)	3.5 (3.4–3.6)	4.1	9.2	19	5.4	3.4	7.4	13	4.6	
CF <sub>3</sub> I	4	<i>J</i>	0.97 (0.9–1.0)	0.85 (0.84–0.9)	0.9	2	4	1.1	0.7	1.6	2.9	1	3, 8
CH <sub>3</sub> CH <sub>2</sub> I	17.5	OH	16 (14–19)	14 (13–14)	14	33	94	21	13	34	71	28	4
	5	<i>J</i>	3.6 (3.3–3.8)	2.9 (2.8–2.9)	3.7	8.2	16.4	4.8	2.9	6.0	9.9	3.7	
	4	<i>Total</i>	2.9 (2.7–3.2)	2.4 (2.3–2.4)	2.9	6.6	13.9	3.9	2.4	5.1	8.7	3.3	

**Notes:**

- Instantaneous local lifetimes for OH reactive loss were calculated with  $[\text{OH}] = 1 \times 10^6 \text{ molecule cm}^{-3}$  and  $T = 275 \text{ K}$ ; photolysis lifetimes taken from WMO (2011).
- Annually averaged local lifetimes with the range in seasonal lifetimes given in parentheses.
- OH reaction rate coefficient taken from JPL 10-6.
- OH reaction rate coefficient taken from Atkinson et al. (2008).
- OH reaction rate coefficient taken from Yujing and Mellouki (2001).
- OH reaction rate coefficient taken from Orkin et al. (2013b); the instantaneous local lifetimes calculated as in WMO (2011) (see footnote 1) are 21 days (48 day OH reaction partial lifetime and 36 day partial lifetime for photolysis) for CHBr<sub>3</sub>, 60 days for CHBrCl<sub>2</sub>, and 80 days for CHBr<sub>2</sub>Cl.
- Photolysis is a negligible loss process; total local lifetime = local partial lifetime for OH reaction.
- OH reaction is a negligible loss process; total local lifetime = local partial lifetime for photolysis.
- Photolysis rates calculated using UV absorption cross sections from Papanastasiou et al. (2014); photolysis rates calculated using recommendations in Sander et al. (2011) are ~15% greater, see Papanastasiou et al. (2014).

### 1.3.1 Abundance, Trends, and Emissions of Very Short-Lived Source Gases

#### 1.3.1.1 CHLORINE-CONTAINING VERY SHORT-LIVED SOURCE GASES

This section focuses on the chlorinated VSLS most widely reported in the background atmosphere, i.e., dichloromethane ( $\text{CH}_2\text{Cl}_2$ ), trichloromethane ( $\text{CHCl}_3$ ), tetrachloroethene ( $\text{CCl}_2\text{CCl}_2$ , shortened to  $\text{C}_2\text{Cl}_4$ ), trichloroethene ( $\text{C}_2\text{HCl}_3$ ), and 1,2-dichloroethane ( $\text{CH}_2\text{ClCH}_2\text{Cl}$ ). Long-term global observations are available from the AGAGE (updated from O'Doherty et al., 2001, and Simmonds et al., 2006) and NOAA networks for  $\text{CH}_2\text{Cl}_2$  and  $\text{C}_2\text{Cl}_4$ , and from AGAGE only for  $\text{CHCl}_3$ . Annual weighted sums of these globally distributed measurements are given in Table 1-6 and long-term trends are shown in Figure 1-11. It is notable that considerable differences exist between  $\text{CH}_2\text{Cl}_2$  mole fractions reported by the two networks. These equate to an 11.2 ppt difference in tropospheric chlorine in 2012 (Table 1-6). Possible causes include differences in calibration scales and in measurement locations; the relatively short atmospheric lifetime of this compound (3–6 months in the tropics, Table 1-5) means that it shows large hemispheric and regional variability. However the observed relative growth in  $\text{CH}_2\text{Cl}_2$  between 2001 and 2012 is comparable between the AGAGE (62%) and NOAA (67%) networks (i.e., during the period of onset of  $\text{CH}_2\text{Cl}_2$  increases). In contrast,  $\text{C}_2\text{Cl}_4$  abundances have decreased by 63% since the beginning of observations in 1994. AGAGE observations of  $\text{C}_2\text{Cl}_4$  are only available from 2004 onward but both relative (–35%) and absolute (–0.6 ppt) changes compare well to NOAA trends in this period (–35%, –0.6 ppt). For  $\text{CHCl}_3$ , no significant trends are apparent since the beginning of the record in 1994. Over the 5-year period between 2008 and 2012, we estimate that changes in the abundances of the three VSLS discussed above equate to an increase of  $1.3 \pm 0.2$  ppt  $\text{Cl yr}^{-1}$ , and that total tropospheric chlorine from  $\text{CH}_2\text{Cl}_2$ ,  $\text{CHCl}_3$ ,  $\text{CCl}_2\text{CCl}_2$ ,  $\text{C}_2\text{HCl}_3$ , and  $\text{CH}_2\text{ClCH}_2\text{Cl}$  increased from 84 (70–117) ppt to 91 (76–125) ppt, as shown in Table 1-7.

Other chlorinated VSLS such as vinyl chloride, 1,1-dichloroethane, 1,1-dichloroethene, 1,2-dichloropropane, 1,1,2-trichloroethane, 1,1,2,2-tetrachloroethane, hexachlorobutadiene, and chlorobenzene have been detected in urban air (e.g., Logue et al., 2010), but there is no observational evidence for these compounds in background air, the upper troposphere, or stratosphere.

Estimated global emissions for  $\text{CH}_2\text{Cl}_2$ ,  $\text{CHCl}_3$ , and  $\text{C}_2\text{Cl}_4$ , calculated using a global 12-box model and using the observed mole fractions discussed above, are shown in Table 1-6. Emissions derived using either the NOAA or AGAGE observations (which have different station locations) are within the uncertainties of each other.

**Table 1-6. Annual global mean mole fractions of chlorinated VSLS, and estimated emissions.** Emissions from AGAGE and NOAA atmospheric data were calculated using a global 12-box model (Cunnold et al., 1983; Rigby et al., 2013, 2014), identical to the global emissions shown in Figure 1-3 for longer-lived ODSs.

Formula	Annual Mean Mole Fraction (ppt)			Growth (2011–2012)		Annual Global Emissions ( $\text{Gg yr}^{-1}$ )			Laboratory
	2008	2011	2012	(ppt $\text{yr}^{-1}$ )	(% $\text{yr}^{-1}$ )	2008	2011	2012	
$\text{CH}_2\text{Cl}_2$	21.7	23.9	25.1	1.2	5.0	$633 \pm 142$	$681 \pm 167$	$752 \pm 177$	AGAGE, in situ <sup>1</sup>
	24.8	28.4	30.7	2.3	8.1	$709 \pm 135$	$791 \pm 182$	$841 \pm 183$	NOAA
$\text{CHCl}_3$	7.21	7.39	7.53	0.14	1.9	$272 \pm 51$	$277 \pm 51$	$285 \pm 53$	AGAGE, in situ
$\text{C}_2\text{Cl}_4$	1.55	1.24	1.16	–0.08	–6.5	$213 \pm 40$	$167 \pm 31$	$160 \pm 30$	AGAGE, in situ
	1.66	1.26	1.18	–0.08	–6.6	$230 \pm 50$	$164 \pm 38$	$157 \pm 33$	NOAA

<sup>1</sup> AGAGE calibrations as specified in CDIAC (2014) and related primary publications.

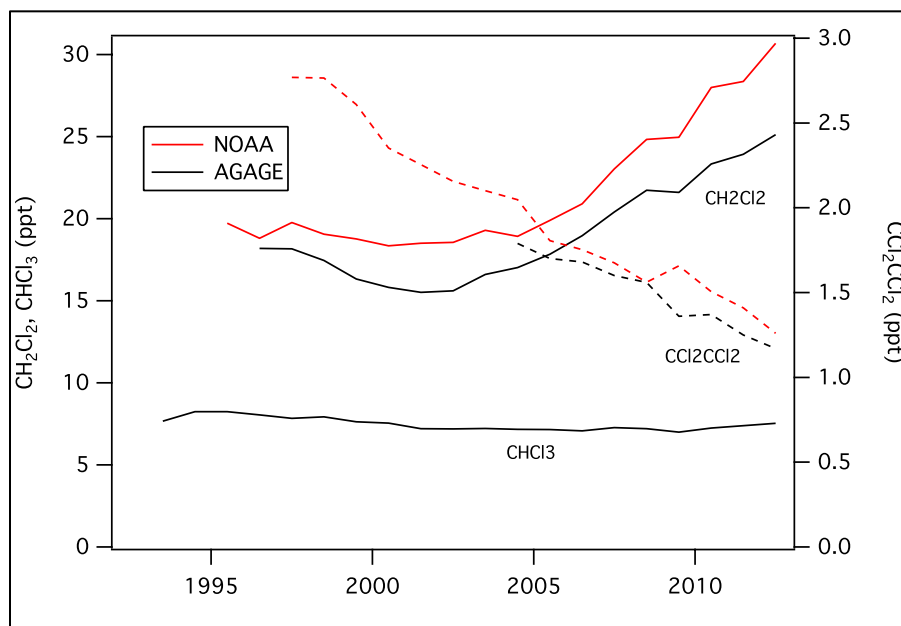


**Figure 1-11.** Global abundances of CH<sub>2</sub>Cl<sub>2</sub>, CHCl<sub>3</sub>, and C<sub>2</sub>Cl<sub>4</sub> as measured by the ground-based AGAGE (Simmonds et al., 2006, updated) and NOAA (Montzka et al., 2011, updated) networks. Global annual mean estimates were derived as weighted averages of monthly mean surface data from globally distributed observing sites (NOAA) and from the AGAGE 12-box model (AGAGE).

The atmospheric sources of chlorinated VSLS have been discussed in detail in Montzka and Reimann et al. (2011). In summary, anthropogenic emissions dominate strongly over natural sources with the exception of CHCl<sub>3</sub> and C<sub>2</sub>H<sub>5</sub>Cl. The anthropogenic emissions of CHCl<sub>3</sub> have been found to show a strong seasonality possibly affecting emission estimates (Gentner et al., 2010). Since the last Assessment various regional studies have confirmed anthropogenic and natural sources for chlorinated VSLS. For CH<sub>2</sub>Cl<sub>2</sub>, CHCl<sub>3</sub>, C<sub>2</sub>HCl<sub>3</sub>, C<sub>2</sub>Cl<sub>4</sub>, and CH<sub>2</sub>ClCH<sub>2</sub>Cl, observation-based studies have reported emissions most likely related to industrial and commercial processes in North America (e.g., Millet et al., 2009; Russo et al., 2010; Miller et al., 2012) as well as East Asia (e.g., Shao et al., 2011; Xue et al., 2011; Bian et al., 2013). Natural sources including biomass burning (CHCl<sub>3</sub>, C<sub>2</sub>H<sub>5</sub>Cl, and CH<sub>2</sub>ClCH<sub>2</sub>Cl), phytoplankton production (CH<sub>2</sub>Cl<sub>2</sub>), and soils (CHCl<sub>3</sub>) such as drained peat land pasture soils or blanket peat bogs have also been reported (Simmonds et al., 2010; Ooki and Yokouchi, 2011; Simpson et al., 2011; Khan et al., 2012; Fraser et al., 2014). For CHCl<sub>3</sub> up to ~50% can be accounted for by anthropogenic sources (Trudinger et al., 2004; Worton et al., 2006). For C<sub>2</sub>H<sub>5</sub>Cl there are indications for both industrial and natural sources (e.g., Low et al., 2003; Simpson et al., 2011), but similar to C<sub>2</sub>HCl<sub>3</sub> and CH<sub>2</sub>ClCH<sub>2</sub>Cl, no reliable global emission estimate is available to date.

### 1.3.1.2 BROMINE-CONTAINING VERY SHORT-LIVED SOURCE GASES

Very short-lived brominated trihalomethanes (e.g., CHBr<sub>3</sub>, CHBrCl<sub>2</sub>, and CHBr<sub>2</sub>Cl) and dibromomethane (CH<sub>2</sub>Br<sub>2</sub>) have primarily natural oceanic sources (Law and Sturges et al., 2007), with a small anthropogenic source from drinking water and cooling water chlorination for the trihalomethanes (Worton et al., 2006). There are also small anthropogenic sources of the VSLS 1-bromopropane (n-propyl bromide) and 1,2-dibromoethane (Montzka and Reimann et al., 2011); no new observations of these compounds have been reported since the last Assessment.

The atmospheric local lifetimes for CHBr<sub>3</sub>, CHBrCl<sub>2</sub>, and CHBr<sub>2</sub>Cl are revised from the previous Assessment (Table 1-5). This is due to new rate coefficient data for the OH reaction with CHBr<sub>3</sub>, CHBrCl<sub>2</sub>,

**Table 1-7. Summary of observations of VSLS source gases from the marine boundary layer (MBL) to the tropical tropopause layer (TTL).** All table entries are mole fractions, with units of parts per trillion (ppt). Note that many of the upper troposphere measurements were made at least one decade ago. For those gases that show trends (notably CH<sub>2</sub>Cl<sub>2</sub> and CCl<sub>2</sub>CCl<sub>2</sub>), these data may no longer be appropriate for the present-day atmosphere. The mole fractions in the LZRH (used to derive the stratospheric input of VSLS chlorine source gases, see Table 1-9) have therefore been scaled to reflect their measured trends in the MBL; the new values are shown in bold. The scaling factor is the ratio of the current MBL mole fraction to that reported in the last Assessment (shown in italics in the MBL column), which are considered concurrent with the higher-altitude data.

	Marine Boundary Layer (MBL)		Lower TTL		LZRH (z <sub>0</sub> ) <sup>a</sup>		Upper TTL		Tropical Tropopause	
Height range			12–14 km		14.5–15.5 km		15.5–16.5 km		16.5–17.5 km	
Potential Temperature Range			340–355 K		355–365 K		365–375 K		375–385 K	
	Median <sup>b</sup>	Range <sup>c</sup>	Mean <sup>b</sup>	Range <sup>c</sup>	Mean <sup>b</sup>	Range <sup>c</sup>	Mean <sup>b</sup>	Range <sup>c</sup>	Mean <sup>b</sup>	Range <sup>c</sup>
CH <sub>2</sub> Cl <sub>2</sub>	28.4 (17.5)	21.8–34.4	17.1	7.8–38.1	14.3 <b>(23.2)</b>	10.8–27.8 <b>(17.5–27.8)</b>	13.2	9.8–28.6	12.6	7.2–30.4
CHCl <sub>3</sub>	7.5	7.3–7.8	6.8	5.3–8.2	5.7	3.5–7.9	4.8	3.5–6.6	4.9	3.3–6.4
CH <sub>2</sub> ClCH <sub>2</sub> Cl	3.7	0.7–14.5	3.6	0.8–7.0	2.7	1.6–4.9	2.2	1.2–4.0	2.0	0.6–4.3
CHClCCl <sub>2</sub>	0.5	0.05–2	0.08	0.0–0.7	0.03	0.00–0.17	0.02	0.00–0.05	0.03	0.00–0.17
CCl <sub>2</sub> CCl <sub>2</sub>	1.3 (1.8)	0.8–1.7	1.1	0.7–1.3	0.9 <b>(0.7)</b>	0.4–1.3 <b>(0.3–1.3)</b>	0.6	0.3–0.9	0.5	0.1–1.0
CH <sub>2</sub> Br <sub>2</sub>	0.9	0.6–1.7	0.89	0.6–1.2	0.74	0.59–0.99	0.66	0.43–0.83	0.52	0.3–0.86
CHBr <sub>3</sub>	1.2	0.4–4.0	0.56	0.2–1.1	0.22	0.00–0.63	0.14	0.01–0.29	0.08	0.00–0.31
CH <sub>2</sub> BrCl	0.10	0.07–0.12	0.12	0.13–0.16	0.10	0.06–0.13	0.11	0.1–0.12	0.07	0.05–0.11
CHBr <sub>2</sub> Cl	0.3	0.1–0.8	0.11	0.04–0.26	0.06	0.03–0.11	0.05	0.01–0.11	0.02	0.00–0.14
CHBrCl <sub>2</sub>	0.3	0.1–0.9	0.21	0.14–0.30	0.09	0.06–0.18	0.12	0.11–0.14	0.06	0.03–0.12
other brominated SG <sup>d</sup>					<0.2		<0.2		<0.2	
CH <sub>3</sub> I	0.8	0.3–2.1	0.16	0.00–0.38	0.04	0.00–0.10	0.00	0.00–0.01	0.01	0.00–0.06
Total Cl	93.4 <sup>e</sup> <b>91<sup>f</sup></b>	70–134 <sup>e</sup> <b>76–125<sup>f</sup></b>	67	36–103	55 <b>(72)</b>	38–95 <b>(50–95)</b>	48	38–89	46	26–93
Anthrop. Cl <sup>g</sup>	76	55–115	48	22–96	39 <b>(64)</b>	27–72 <b>(34–85)</b>	34	24–68	32	17–73
Total Br	7.3	2.8–18.0	4.1	2.2–6.7	2.7	1.4–4.6	2.0	1.1–3.2	1.4	0.7–3.4
Total I	0.8	0.3–2.1	0.16	0.00–0.38	0.04	0.00–0.10	0.00	0.00–0.01	0.01	0.00–0.06

<sup>a</sup> LZRH(z<sub>0</sub>) corresponds to the level of zero clear-sky radiative heating (see Box 1-3, Figure 1). As in the previous Assessment, this level is at about 15 km or 360 K, where there is a transition from clear-sky radiative cooling to clear-sky radiative heating. In general, air masses above this level are expected to enter the stratosphere.

<sup>b</sup> Note that calibration scales for VSLS differ among different research groups (see C.E. Jones et al., 2011; Hall et al., 2014). Abundances in the MBL are calculated from AGAGE and NOAA global 2012 data for CH<sub>2</sub>Cl<sub>2</sub>, CHCl<sub>3</sub>, and CCl<sub>2</sub>CCl<sub>2</sub>, from the compilation of Ziska et al. (2013) for CHBr<sub>3</sub>, CH<sub>2</sub>Br<sub>2</sub>, and CH<sub>3</sub>I (20°N to 20°S), from Brinckmann et al. (2012) for CH<sub>2</sub>BrCl, and from the last Assessment (Montzka and Reimann et al., 2011) for all other MBL data. Data in and above the upper troposphere have been compiled from observations during the PEM-Tropics A and B, TC4, Pre-AVE, and CR-AVE aircraft campaigns (Schauffler et al., 1999), from the SHIVA, HIPPO, and ATTREX aircraft campaigns (Tegtmeier et al., 2013), and from balloon observations (Laube et al., 2008, Brinckmann et al., 2012). See below for definition of field mission acronyms.

<sup>c</sup> The stated observed range represents the smallest mean minus 1 standard deviation and the largest mean plus 1 standard deviation.

<sup>d</sup> Estimated maximum contribution from species like C<sub>2</sub>H<sub>3</sub>Br, C<sub>2</sub>H<sub>4</sub>Br, and C<sub>3</sub>H<sub>7</sub>Br (Montzka and Reimann et al., 2011).

<sup>e</sup> Average median value and range.

<sup>f</sup> Mean value and range.

<sup>g</sup> The anthropogenic fraction of VSLS (Anthrop. Cl) has been calculated from the sum of 90% of CH<sub>2</sub>Cl<sub>2</sub>, 50% of CHCl<sub>3</sub>, and 100% of CH<sub>2</sub>ClCH<sub>2</sub>Cl.

PEM-Tropics = Pacific Exploratory Missions-Tropics A (1996) and B (1999); TC4 = Tropical Composition, Cloud and Climate Coupling missions (2007); Pre-AVE = Pre-Aura Validation Experiment (2004); CR-AVE = Costa Rica-Aura Validation Experiment (2006); SHIVA = Stratospheric Ozone: Halogen Impacts in a Varying Atmosphere (SHIVA); HIPPO = HIAPER (High-Performance Instrumented Airborne Platform for Environmental Research) Pole-to-Pole Observations (2009–2011); ATTREX = Airborne Tropical Tropopause Experiment (2011).

and  $\text{CHBr}_2\text{Cl}$  reported by Orkin et al. (2013b), measured over a more applicable temperature range than previous studies, and improved temperature-dependent UV absorption spectrum data for  $\text{CHBr}_3$  reported by Papanastasiou et al. (2014). The new data result in a decrease of the calculated partial lifetime due to OH reaction for  $\text{CHBr}_3$ ,  $\text{CHBrCl}_2$ , and  $\text{CHBr}_2\text{Cl}$  by ~35% from those given in the previous Assessment, and an overall decrease in the atmospheric photolysis rate of  $\text{CHBr}_3$  of the order of ~15% in the tropical troposphere, the region most critical for transport to the stratosphere. The combination of these new laboratory data implies that photolysis accounts for 50 to 70% of the  $\text{CHBr}_3$  removal in the tropical troposphere (see Papanastasiou et al., 2014), which is less than obtained using the JPL10-6 recommendations used in the previous Assessment.

The relatively short local lifetimes of brominated VSLs, combined with spatially and temporally varying sources, means that determining global budgets for these gases requires extensive global-scale observations. For example, Ashfold et al. (2014) found that around two thirds of the measured  $\text{CHBr}_3$  at a site in Borneo may be due to emissions in a region covering less than 1% of the tropics.

A number of emission estimates for brominated halocarbons have been reported since the last Assessment. Ziska et al. (2013) derived the first global climatology for  $\text{CHBr}_3$  and  $\text{CH}_2\text{Br}_2$  from a global database of measured halocarbon mole fractions, and determined a lower global flux of bromine from the oceans to the atmosphere than other estimates (Table 1-8). However the authors acknowledged that coastal (e.g., Carpenter et al., 2009; Liu et al., 2011) and other elevated emissions were likely underestimated in their climatology. Coastal VSLs emissions exhibit significant variability due to differing types and

**Table 1-8. Fluxes of total bromine from bromoform ( $\text{CHBr}_3$ ) and dibromomethane ( $\text{CH}_2\text{Br}_2$ ) in  $\text{Gg}(\text{Br})\text{yr}^{-1}$ , and iodine from methyl iodide ( $\text{CH}_3\text{I}$ ) in  $\text{Gg}(\text{I})\text{yr}^{-1}$ . Values in italics originate from regional studies while all other values are global studies.**

Reference	$\text{CHBr}_3$ Flux ( $\text{Gg Br yr}^{-1}$ )			$\text{CH}_2\text{Br}_2$ Flux ( $\text{Gg Br yr}^{-1}$ )			$\text{CH}_3\text{I}$ Flux ( $\text{Gg I yr}^{-1}$ )		
	Global	Open Ocean	Coastal	Global	Open Ocean	Coastal	Global	Open Ocean	Coastal
Bell et al. (2002)							272		
<i>Yokouchi et al. (2005)</i>	820 <sup>a</sup>								
Warwick et al. (2006a) <sup>d,e</sup>	560 <sup>d</sup>	280 <sup>d</sup>	280 <sup>d</sup>	100					
Butler et al. (2007)	800	150	650	280	50	230	550	270	280
<i>Carpenter et al. (2009)</i>			200						
O'Brien et al. (2009)	820 <sup>a</sup>								
Palmer and Reason (2009)		120 <sup>c</sup>							
Liang et al. (2010) <sup>e</sup>	430	260	170	57	34	23			
<i>Jones et al. (2010)<sup>f</sup></i>							300	240	60
Youn et al. (2010) <sup>g</sup>							236		
Pyle et al. (2011) <sup>h</sup>	362								
Ordóñez et al. (2012) <sup>e</sup>	506			62			270		
Ziska et al. (2013) <sup>i</sup>	120–200			62–78			157–184		
<i>Ashfold et al. (2014)</i>	213 (tropics only)								
<i>Liu et al. (2013)<sup>j</sup></i>		19–304			9–62				

<sup>a</sup> Scaled to  $\text{CH}_2\text{Br}_2$  emissions from Ko and Poulet et al. (2003) based on global loss rates and an estimated global burden.

<sup>b</sup> Scaled to  $\text{CH}_2\text{Br}_2$  emissions from Warwick et al. (2006b). <sup>c</sup> Tropical ocean only. <sup>d</sup> Modeling study: “Scenario 5”: 70% of emissions in the tropics; August/September. <sup>e</sup> Top-down estimates based on modeling of airborne measurements primarily in the Pacific and North American troposphere and lower stratosphere.  $\text{CH}_3\text{I}$  estimate based upon Bell et al. (2002) inventory.

<sup>f</sup> Bottom-up estimate from north and tropical Atlantic data only. “Coastal”  $\text{CH}_3\text{I}$  emissions include shelf and upwelling fluxes.

<sup>g</sup> Based upon Bell et al. (2002) global inventory. <sup>h</sup> Update of “Scenario 5” from Warwick et al. (2006b). South East Asian emissions scaled to give better agreement with ground-based observations. <sup>i</sup> Net flux (source – sink) reported in Ziska et al. (2013) based on compiled sea-air flux data from the Halocat database (<https://halocat.geomar.de/>). Range represents global extrapolation of data using the robust fit (lower) or ordinary least squares (upper) technique. <sup>j</sup> Extrapolated global open ocean fluxes reported by (Liu et al., 2013) are based on 5 cruises in the Atlantic.

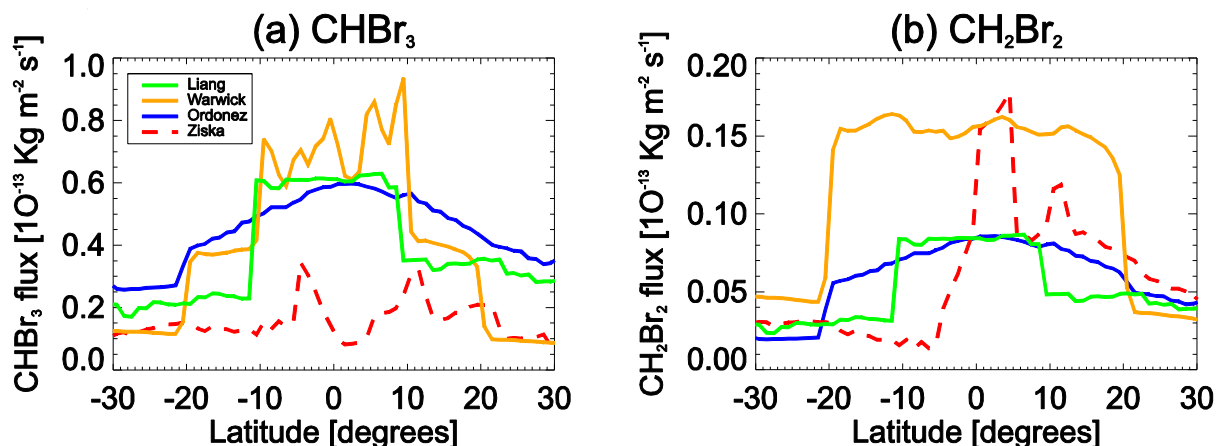


**Figure 1-12.** Latitudinal dependence of zonally averaged (a) CHBr<sub>3</sub> and (b) CH<sub>2</sub>Br<sub>2</sub> emissions (10<sup>-13</sup> kg m<sup>-2</sup> s<sup>-1</sup>) between 30°N and 30°S from recent top-down emission inventories (Warwick et al., 2006a [updated in Pyle et al., 2011]; Liang et al., 2010; Ordoñez et al., 2012) and bottom-up derived emission inventories (Ziska et al., 2013). The figure is modified from Hossaini et al. (2013).

amounts of macroalgae (Leedham et al., 2013), thus global extrapolation of coastal emissions is subject to high uncertainty. Liu et al. (2013) suggested that the Atlantic Ocean has comparable or possibly higher Br VLS seawater concentrations than the Pacific Ocean, in contrast to an earlier study (Butler et al., 2007). These differing results may be due to differences in the locations of the observations and amount of data from each region. Several authors (e.g., Mattsson et al., 2013; Ziska et al., 2013) have also noted the existence of negative saturation anomalies (i.e., net flux from the atmosphere to the ocean) for CHBr<sub>3</sub> and CH<sub>2</sub>Br<sub>2</sub>, mostly in polar seas. Sparse data in these regions means that they may not be properly accounted for in global emission estimates. Although studies have attempted to map VLS emissions by linking them to chlorophyll *a* (Ordoñez et al., 2012), brominated VLS in seawater do not exhibit robust relationships with oceanic pigments (Roy, 2010; Roy et al., 2011; He et al., 2013), likely due to complex production mechanisms and interconversion processes (Lin and Manley, 2012; Hughes et al., 2013; Wever and van der Horst, 2013).

Ordoñez et al. (2012) assessed the ocean fluxes of CHBr<sub>3</sub> and CH<sub>2</sub>Br<sub>2</sub> using a global chemistry-climate model combined with surface and aircraft observations. Global estimates were in the range of previous top-down emission estimates (e.g., Warwick et al., 2006a; Liang et al., 2010; Ordoñez et al., 2012) (Table 1-8). Hossaini et al. (2013) evaluated four global emission estimates, and found that no single inventory provided a satisfactory match between model and observations in all locations. For the tropics, the relatively low emissions of Ziska et al. (2013) provided the best fit with the limited available data. Discrepancies between top-down and bottom-up emission inventories (Figure 1-12 and Table 1-8) indicate that there are still insufficient data to constrain VLS budgets to within a factor of 2–3.

### 1.3.1.3 IODINE-CONTAINING VERY SHORT-LIVED SOURCE GASES

#### *Methyl iodide (CH<sub>3</sub>I)*

The ocean contributes over 80% of global CH<sub>3</sub>I emissions with small contributions from rice production and other land sources (Redeker et al., 2000; Bell et al., 2002; Youn et al., 2010). Known oceanic production processes include photochemical degradation of organic matter in seawater (e.g., Richter and Wallace, 2004) and phytoplankton production (e.g., Brownell et al., 2010). Observed surface seawater concentrations of CH<sub>3</sub>I show best agreement with global model simulations that include a photochemical production pathway or both a photochemical and biological production pathway (Stemmler et al., 2013). CH<sub>3</sub>I has potential anthropogenic sources since it is registered as a pesticide (as a replacement for CH<sub>3</sub>Br) in a number of countries including the U.S., Japan, and Mexico. However the manufacturer has withdrawn it from the U.S. market.

Long-term time-series from the late 1990s of atmospheric CH<sub>3</sub>I from several remote marine sites are now available (Yokouchi et al., 2012) and show a decreasing trend before 2003, but increases in CH<sub>3</sub>I from 2003/2004 to 2009/2010 by several tens of percent. The interannual variation was linked with the Pacific Decadal Oscillation (PDO), suggesting that CH<sub>3</sub>I emissions are affected by global-scale sea surface temperature oscillations (Yokouchi et al., 2012). Seasonally, CH<sub>3</sub>I atmospheric mole fractions at remote marine locations outside of the polar regions tend to maximize in summer (Archer et al., 2007; Yokouchi et al., 2011, 2012), whereas winter maxima are observed in the Arctic due to long-range transport and slower atmospheric photooxidation (Yokouchi et al., 2012).

Globally, CH<sub>3</sub>I emissions are not well constrained (Table 1-8). Recent top-down model estimates (Youn et al., 2010; Ordoñez et al., 2012), based on the CH<sub>3</sub>I emission distribution of Bell et al. (2002), are about a factor of two lower than the global bottom-up estimate of Butler et al. (2007). While these model studies showed good agreement between simulated and observed marine boundary layer (MBL) mole fractions in some locations, there were regional discrepancies, indicating uncertain sources or sinks and/or model meteorology. A new global climatology (Ziska et al., 2013) has been calculated by interpolating available data onto a 1° × 1° grid, and results in even lower emissions of 158–184 Gg I yr<sup>-1</sup>, depending on the fit used. The approach used may underrepresent locally elevated emissions. Quantifying emissions is challenging because oceanic and atmospheric abundances vary significantly in space and time, and there are also differences between measurement calibrations (up to about a factor of 2) (C.E. Jones et al., 2011) used by different research groups, although these are not as large as discrepancies in emission estimates.

### **Other iodine-containing VSLS**

Recent observations indicate that the combined ocean-to-atmosphere flux of iodine-containing dihalomethanes (CH<sub>2</sub>ICl, CH<sub>2</sub>I<sub>2</sub>, and CH<sub>2</sub>IBr) provides a global iodine source of ~330 ± 190 Gg I yr<sup>-1</sup>, comparable to that of CH<sub>3</sub>I (Table 1-8), and a surface iodine atom source 3–4 times higher than CH<sub>3</sub>I due to the rapid photolysis rates of these compounds (Jones et al., 2010). A number of studies have shown however that total organic iodine—including CH<sub>3</sub>I, CH<sub>2</sub>ICl, CH<sub>2</sub>IBr, and CH<sub>2</sub>I<sub>2</sub>—cannot account for observations of IO in the MBL (Jones et al., 2010; Mahajan et al., 2010; Mahajan et al., 2012; Großmann et al., 2013), as they contribute only about 20% of the necessary reactive iodine flux. Laboratory measurements suggest that instead, inorganic emissions, namely I<sub>2</sub> and HOI (Carpenter et al., 2013), are the dominant contributors to MBL reactive iodine chemistry. These compounds are too reactive to be transported out of the MBL, though will be important contributors to particulate iodine, which has been observed in the upper troposphere and lower stratosphere (Murphy and Thomson, 2000).

### **1.3.2 Dynamics and Transport of VSLS**

The last Assessment contained a comprehensive discussion of relevant dynamical processes controlling the transport of VSLS from the boundary layer (BL) to the tropical tropopause layer (TTL) and from the TTL into the stratosphere. Since then, theoretical and modeling studies have been performed that additionally constrain our understanding of the location and magnitude of the troposphere-stratosphere transport of VSLS, the relative importance of source gas injection (SGI) versus product gas injection (PGI), and the total contribution of VSLS to stratospheric bromine, chlorine, and iodine; also, new observations of both very short-lived source gases (SGs) and product gases (PGs) have been made.

Models continue to implicate the Maritime Continent as a strong convective source region where VSLS may be transported to the stratosphere rapidly (Levine et al., 2007; Aschmann et al., 2009; Pisso et al., 2010; Ashfold et al., 2012). However, uncertainties in parameterization of the boundary layer and convective transport (Hoyle et al., 2011; Schofield et al., 2011; Liang et al., 2014) limit the ability of models to calculate absolute amounts of VSLS reaching the stratosphere. The representation of very deep convection that penetrates the tropical tropopause (Liu and Zipser, 2005) is limited in global models (Hosking et al., 2010; Feng et al., 2011). A key constraint on the stratospheric SGI of VSLS is whether regions with particularly high surface mixing ratios are also preferred source regions for stratospheric air,

or whether a VSLS is sufficiently long-lived to be transported into these regions. Because transport processes also vary seasonally, the ODP (Ozone Depletion Potential; see Chapter 5) of a VSLS is dependent on both emission location and season (Pisso et al., 2010; Brioude et al., 2010).

Lagrangian transport calculations, combined with observed sea-to-air fluxes of VSLS in the Maritime Continent, have been used to infer the magnitudes of stratospheric SGI and PGI from  $\text{CHBr}_3$ ,  $\text{CH}_2\text{Br}_2$ , and  $\text{CH}_3\text{I}$  (Tegtmeier et al., 2012, 2013). These results suggest sporadic injections of halogens from VSLS above the tropopause that are an order of magnitude larger than the global mean. These rare enhancements are highly localized in space and time and thus not representative of the global scale. However, they highlight a large variance that is not captured by coarse global-scale models. The “snapshot” nature of observations during individual field campaigns makes an assessment of the relative importance of various geographical regions challenging. For VSLS, this is exacerbated by uncertainties in the magnitude of tropical emissions and how they are distributed with respect to convectively active regions. Based on global model simulations, Liang et al. (2014) found that the largest stratospheric input of bromine from VSLS occurred over the tropical Indian Ocean, where the modeled surface mixing ratio of  $\text{CHBr}_3$  and  $\text{CH}_2\text{Br}_2$  was large. Critically, these results depend on the validity of assumed surface emissions which, in sparsely sampled regions such as the Indian Ocean, are difficult to verify.

Interannual variability of VSLS troposphere-stratosphere transport is likely related to phases of the El Niño-Southern Oscillation (ENSO), through its impact on sea surface temperature (SST) (Aschmann et al., 2011; Ashfold et al., 2012). Using a model driven by offline meteorological analyses, Aschmann et al. (2011) reported 20% more  $\text{CHBr}_3$  and 6% more  $\text{CH}_2\text{Br}_2$  reaching the stratosphere during a strong El Niño event (relative to an ENSO-neutral year). While enhanced SGI is expected to be positively correlated with convective activity, PGI may be anticorrelated because inorganic PGs (e.g., HBr) are highly soluble and can be physically removed from the troposphere in convective rainfall. Liang et al. (2014) suggest that the net transport of bromine from VSLS into the stratosphere is largest under low convective conditions, because the associated increase in PGI (2–3 ppt) greatly exceeds the minor reduction in SGI.

### 1.3.2.1 SOURCE GAS INJECTION (SGI)

Source gases deliver halogens to the stratosphere in the same form as they were emitted at the surface. For a given SG, the efficiency of SGI is determined by its tropospheric loss rate versus timescales for troposphere-to-stratosphere transport. New aircraft observations of VSL SGs, especially the brominated gases, have been reported in tropical regions. These include observations from five aircraft missions spanning the global troposphere over different seasons and multiple years: HIAPER (High-performance Instrumented Airborne Platform for Environmental Research) Pole-to-Pole Observations (HIPPO 1–5) campaigns, 2009–2011; the Stratospheric Ozone: Halogen Impacts in a Varying Atmosphere (SHIVA) campaign in 2011, located in the previously poorly-sampled Maritime Continent region; and CARIBIC flights over the West Atlantic, Africa, and Southeast Asia. Aircraft observations during these campaigns were made at altitudes up to the lower TTL. Higher-altitude observations around the tropical tropopause have been made during the ongoing NASA Airborne Tropical Tropopause Experiment (ATTREX) campaign. These compiled data are reported in Table 1-7.

#### ***SGI from chlorinated VSLS***

The majority of upper tropospheric data for the chlorinated VSLS shown in Table 1-7 were measured around a decade ago. Taken together with the surface data, the measurements apparently indicate a strong vertical gradient of  $\text{CH}_2\text{Cl}_2$  within the troposphere, which is inconsistent with its relatively long lifetime compared to the analogous brominated SGs (see Table 1-5). The reason for this is most likely the temporal disparity between the (current) surface data and the higher-altitude data. Recent data from the HIPPO 1–5 campaign (Wofsy et al., 2011) show mean  $\text{CH}_2\text{Cl}_2$  mixing ratios in the lower TTL of 23.5 (14.8–49.8) ppt, larger than the range of 14.9 (11.7–18.4) ppt reported in the last Assessment. The  $\text{CHCl}_3$  mean mixing ratio in the lower TTL was 6.0 (4.7–8.2) ppt, within the range of

7.1 (5.9–9.2) ppt reported previously. No new observations of chlorinated VSLS have been reported above the level of zero radiative heating (LZRH), where previous measurements suggested a SGI of 55 (38–80) ppt of chlorine from VSLS (Montzka and Reimann et al., 2011). For  $\text{CH}_2\text{Cl}_2$  and  $\text{C}_2\text{Cl}_4$ , gases that show observable trends in the boundary layer (Figure 1-11), we therefore scale mole fractions around the LZRH by the ratio of current MBL abundances to those reported in the last Assessment, which were concurrent with the compiled upper tropospheric data. We therefore suggest an increase in the VSLS chlorine SGI from 55 ppt to 72 (50–95) ppt, to take into account likely increases in  $\text{CH}_2\text{Cl}_2$  abundances near the tropopause.

### ***SGI from brominated VSLS***

The estimated stratospheric SGI of bromine from VSLS, based on available observations around the tropical tropopause, is unchanged since the last Assessment (Table 1-7). Observations of the major brominated VSLS,  $\text{CHBr}_3$  and  $\text{CH}_2\text{Br}_2$ , during HIPPO 1–5 show tropical mean mole fractions of 0.47 (0.14–1.13) ppt and 0.84 (0.58–1.09) ppt in the lower TTL, respectively. These values are generally in close agreement with the compiled mean and range reported in the last Assessment. Over Borneo, aircraft observations made during the SHIVA campaign show a total of 4.35 ( $\pm 0.6$ ) ppt of organic bromine from  $\text{CHBr}_3$ ,  $\text{CH}_2\text{Br}_2$ ,  $\text{CH}_2\text{BrCl}$ ,  $\text{CHBr}_2\text{Cl}$ , and  $\text{CHBrCl}_2$  at approximately 12 km (Sala et al., 2014). Similarly, a total of 4.2 ppt was obtained at 10–13 km from observations of the same suite of VSLS made during CARIBIC flights over Southeast Asia (Wisher et al., 2014). These estimates are in close agreement with the 4.3 (2.8–6.5) ppt of organic bromine reported in the last Assessment. At higher altitudes, in 2008 Brinckmann et al. (2012) reported balloon-borne observations of these five VSLS over Teresina, Brazil, up to the tropical tropopause. Around the LZRH, total organic bromine from VSLS was observed to be 2.25 ppt, in reasonable agreement with the 2.7 (1.4–4.6) ppt reported in the last Assessment. At 17.5 km, total organic bromine from VSLS was observed to be 1.35 ppt and thus within the previously reported range of 0.7–3.4 ppt.

Global model simulations suggest SGI contributes on average ~50% and ~90% of the total bromine reaching the stratosphere from  $\text{CHBr}_3$  and  $\text{CH}_2\text{Br}_2$ , respectively (Aschmann et al., 2011; Hossaini et al., 2012a). Somewhat lower estimates of 21% ( $\text{CHBr}_3$ ) and 74% ( $\text{CH}_2\text{Br}_2$ ) were derived from a single set of balloon-borne observations (Brinckmann et al., 2012). For global models, explicit representation of SGI requires a sound treatment of VSLS emissions. The modeled contribution of VSLS to stratospheric bromine has been shown to vary by a factor of ~2 (Hossaini et al., 2013) when using the different available emission inventories (Liang et al., 2010; Pyle et al., 2011; Ordoñez et al., 2012; Ziska et al., 2013).

The proximity of emissions to convective source regions likely leads to geographical variation in SGI efficiency (Aschmann et al., 2009; Tegtmeier et al., 2012, 2013). The spatial distribution and seasonality of the primary tropospheric oxidant, the hydroxyl radical (OH), also leads to a significant variation in the lifetimes of less photolabile VSLS (Table 1-5). Over the West Pacific warm pool, an [OH] minimum has been inferred (Rex et al., 2014) based on reported low levels of tropospheric ozone from sonde, satellite, and aircraft data, in qualitative agreement with earlier observations (e.g., Kley et al., 1996). The lifetime of  $\text{CH}_2\text{Br}_2$  was calculated to be up to a factor of 3 longer within this “OH hole” relative to typical Atlantic conditions (Figure 1-13), suggesting that regionally, a larger fraction of  $\text{CH}_2\text{Br}_2$  may escape tropospheric oxidation to reach the TTL over the warm pool. Once in the TTL, the local lifetime of  $\text{CH}_2\text{Br}_2$  can be long (~500 days) due to the strong temperature dependence of the  $\text{CH}_2\text{Br}_2 + \text{OH}$  reaction, meaning stratospheric SGI is likely (Hossaini et al., 2010). Future changes to tropospheric [OH], for example due to a projected methane increase/decrease, could alter the local lifetime and SGI of  $\text{CH}_2\text{Br}_2$  substantially (Hossaini et al., 2012b) (Figure 1-14).

### ***SGI from iodinated VSLS***

Available high-altitude  $\text{CH}_3\text{I}$  observations in the last Assessment showed that mixing ratios in the TTL at 15 km were generally below 0.1 ppt, leading to the conclusion that no more than 0.05 ppt of iodine

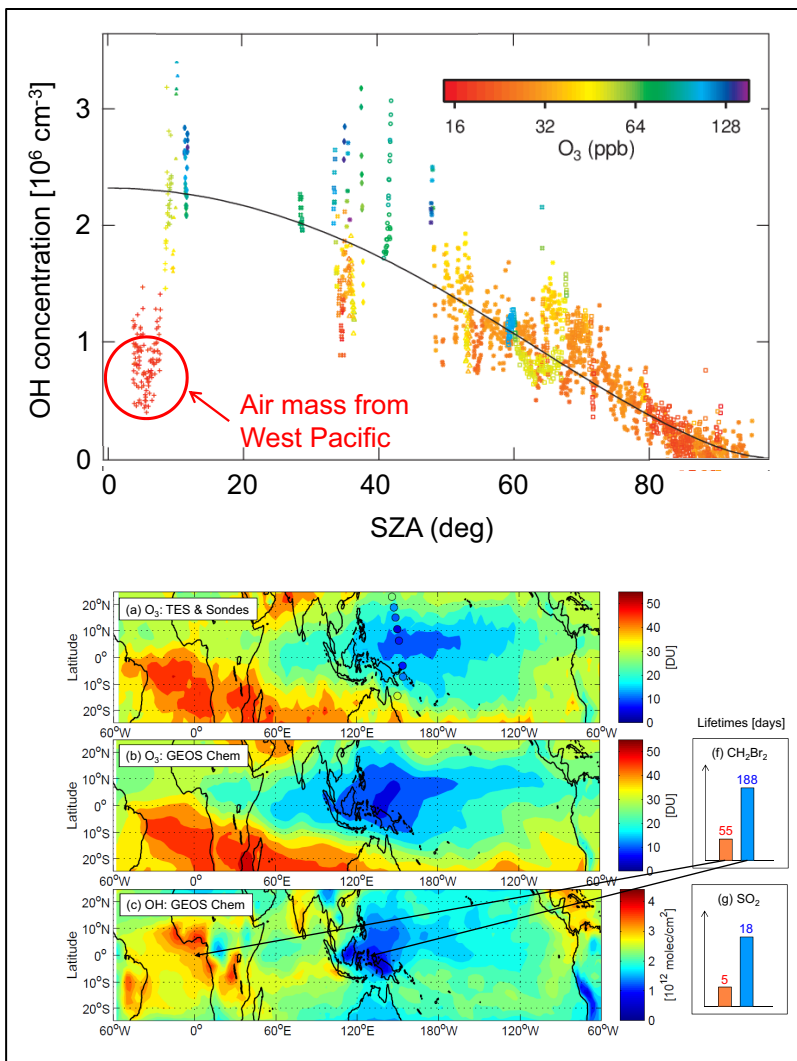


**Figure 1-13.** Top: Observed  $[\text{OH}]$  ( $10^6 \text{ molecules cm}^{-3}$ ) and  $\text{O}_3$  mixing ratio (ppb) as a function of solar zenith angle (SZA) from the NASA Stratospheric Tracers of Atmospheric Transport (STRAT) aircraft mission (1995–1996) near Hawaii. Observations are taken above 11 km altitude. Analysis of back trajectories revealed an air mass originating from the West Pacific region containing relatively low  $\text{O}_3$  and  $[\text{OH}]$ . The black line denotes the compact relation described in Hanisco et al. (2001). Bottom: Observed  $\text{O}_3$  columns from satellite and sonde data, along with the modeled OH column from GEOS CHEM. This analysis indicates an “OH hole” region in the maritime continent, where the lifetime of  $\text{CH}_2\text{Br}_2$  is significantly enhanced. Modified from Rex et al. (2014).

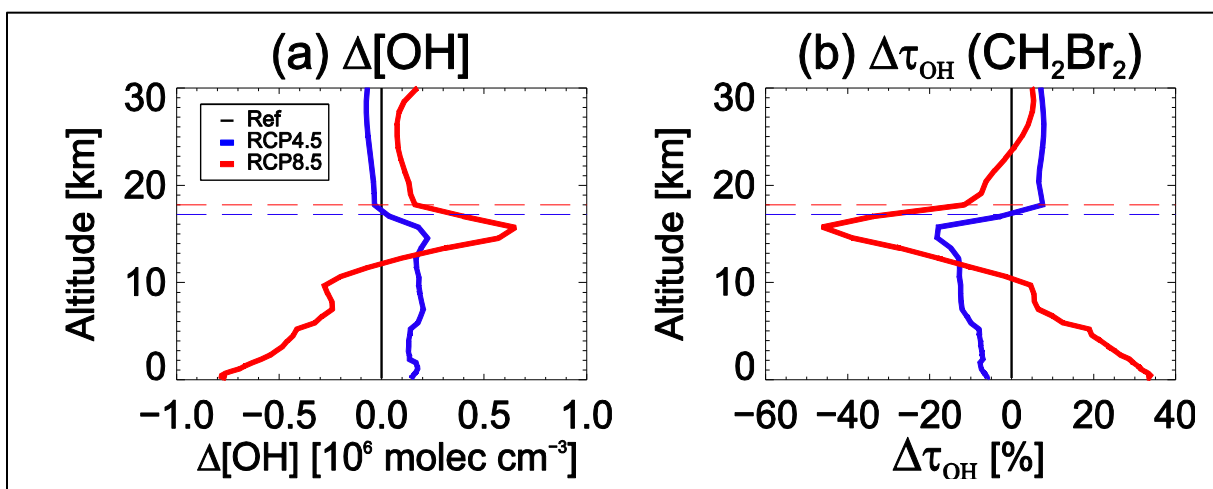


**Figure 1-14.** Modeled 2100 change in (a) OH abundance ( $\text{molecules cm}^{-3}$ ) and (b)  $\text{CH}_2\text{Br}_2$  lifetime due to OH oxidation,  $\tau_{\text{OH}}$ , (%) under projected IPCC RCP 4.5 and 8.5 climate scenarios (relative to 2000). The dashed lines denote cold-point tropopause under each scenario. Modified from Hossaini et al. (2012a).

enters the stratosphere as CH<sub>3</sub>I at the CPT. New high-altitude observations in the East Pacific region, along with associated modeling (Tegtmeier et al., 2013) are consistent with this conclusion, showing 0.01–0.02 ppt of CH<sub>3</sub>I around the tropical CPT. The authors inferred considerably larger mixing ratios in the tropical West Pacific with 0.08 ppt CH<sub>3</sub>I at the tropical CPT, calculated using a Lagrangian transport model and observed sea-air fluxes of CH<sub>3</sub>I. The annual modeled mean over the inner tropical latitude bands between ~20°S and 20°N was ~0.05 ppt. Based on observed correlations between large oceanic CH<sub>3</sub>I emissions and strong vertical uplift, however, a small amount of air was projected to carry larger amounts of CH<sub>3</sub>I, with 5.5% of air at the tropical CPT calculated to have mixing ratios larger than 0.2 ppt.

Shorter-lived iodinated VSLs (e.g., CH<sub>2</sub>ICl) with lifetimes of hours to a few days are unlikely to reach the stratosphere in significant amounts. Hossaini et al. (2012a) estimated with a global model that on average <1% of the surface mixing ratio of an idealized 6-hour lifetime tracer in the MBL was able to reach the CPT over the tropical West Pacific. However, such compounds contribute to longer-lived inorganic iodine product gases (Box 1-2; Saiz-Lopez et al., 2012), which could release reactive iodine at higher altitude.

### **1.3.2.2 PRODUCT GAS INJECTION (PGI)**

The degradation of VSL SGs in the troposphere is expected to produce a range of organic and inorganic PGs. If these PGs evade tropospheric removal processes, such as dry/wet deposition, they may be transported to the stratosphere via PGI. Observational evidence for PGI is limited, and in general global models have limited representation of the multi-phase and microphysical processes that, coupled with sub-grid scale transport processes, determine the efficiency of PGI. Since the last Assessment, observations of inorganic PGs have been made in tropical regions, though observations in the TTL remain sparse. A number of recent modeling studies have also attempted to further constrain estimates of PGI from brominated VSLs.

#### ***PGI from chlorinated VSLs***

The estimate of total stratospheric PGI from chlorinated VSLs is essentially unchanged since the last Assessment, at 25 (0–50) ppt Cl. This estimate is derived from observations of hydrogen chloride (HCl) and phosgene (COCl<sub>2</sub>) observed around the LZRH (Marcy et al., 2007; Mebarki et al., 2010; Brown et al., 2011) of up to 20 and 32 ppt Cl, respectively. As noted in previous Assessments, chlorinated PGs are also produced following the breakdown of long-lived SGs in the stratosphere, and thus the possibility of “double counting” exists if they are recirculated into the troposphere (Montzka and Reimann et al., 2011). Thus, between 0 and 100% of the observed COCl<sub>2</sub> and HCl could originate from VSLs. Recent aircraft observations report evidence for episodic enhancements of ClO in the TTL (up to 40 ppt) in air of tropospheric origin (von Hobe et al., 2011). Heterogeneous chlorine activation, also observed around the tropopause at midlatitudes (Thornton et al., 2007), may occur on ice and/or liquid aerosol particles (von Hobe et al., 2011) at cold TTL temperatures.

#### ***PGI from brominated VSLs***

Although there is now evidence for free tropospheric BrO originating from surface sources of VSLs, with tropospheric BrO columns of around  $1\text{--}3 \times 10^{13}$  molecules cm<sup>-2</sup> (Fitzenberger et al., 2000; Richter et al., 2002; Van Roozendaal et al., 2002; Sinnhuber et al., 2005; Theys et al., 2007, 2011; Parrella et al., 2013), observational evidence for PG as BrO in the TTL is sparse (Dorf et al., 2008), and likely around the limit of detection (~1 ppt) for remote sensing instruments at the LZRH. Estimates of PGI from VSLs bromine are therefore derived from modeling studies. Such calculations of PGI are particularly sensitive to assumptions regarding partitioning of Br<sub>y</sub>, wet scavenging, and heterogeneous recycling. Soluble inorganic bromine (Br<sub>y</sub>) species, particularly HBr, are subject to wet deposition processes (Liang et al., 2010; Marecal et al., 2012) and have high uptake coefficients on ice (Crowley et al., 2010). HBr and HCl adsorbed to ice can be converted via heterogeneous reactions with hypohalous

acids (HOX) or halogen nitrates (XONO<sub>2</sub>) to gas phase Br<sub>2</sub>, BrCl, and/or Cl<sub>2</sub>, which are readily photolyzed to halogen atoms (see Box 1-2).

Previous global modeling studies simplified tropospheric removal of Br<sub>y</sub> by assuming a fixed and uniform loss rate (Sinnhuber and Folkins, 2006; Warwick et al., 2006a; Hossaini et al., 2010). In the last Assessment, PGI from CHBr<sub>3</sub> and CH<sub>2</sub>Br<sub>2</sub> was estimated at 0.4–3.9 ppt Br based on a model sensitivity study (Hossaini et al., 2010) in which the prescribed “washout lifetime” of Br<sub>y</sub> varied between 10 days and infinity (i.e., no tropospheric removal of Br<sub>y</sub>). More recent models speciate Br<sub>y</sub> in an explicit or semi-implicit manner and/or use a more complex representation of the dehydration processes (e.g., Aschmann et al., 2011; Hossaini et al., 2012a), and show that scavenging of Br<sub>y</sub> from VLS (Br<sub>y</sub><sup>VLS</sup>) is a minor loss process in the TTL, removing <10% (Aschmann et al., 2011; Aschmann and Sinnhuber, 2013; Liang et al., 2014). Models also indicate that organic PGs, such as CBr<sub>2</sub>O and CHBrO, for which no observations exist, may also reach the TTL, although their contribution to the total bromine PGI is expected to be minor (Hossaini et al., 2010; Marecal et al., 2012). The tropospheric chemistry and speciation of organic PGs, which are likely sensitive to background NO<sub>x</sub> and HO<sub>x</sub> loading (Krysztofiak et al., 2012), was discussed in Ko and Poulet et al. (2003).

Based on the modeling work discussed above, PGI makes a non-negligible contribution to stratospheric bromine loading from VLS but critically depends on how rapidly SGs can ascend through the troposphere, where the likelihood of Br<sub>y</sub> washout decreases with altitude and may be minor once in the TTL (e.g., Aschmann et al., 2011). Independent model estimates of total PGI of bromine from CHBr<sub>3</sub> and CH<sub>2</sub>Br<sub>2</sub> are 2.5 ppt Br (Liang et al., 2010), ~1.1 ppt Br (Hossaini et al., 2012b), 1.5 ppt Br (Aschmann and Sinnhuber, 2013), and ≥4 ppt Br (Liang et al., 2014). These models contain a more comprehensive treatment of Br<sub>y</sub> than the calculations that formed the basis of the previous Assessment. However, care should be taken when making a direct comparison of these estimates due to variation in the modeling approaches. For example, only Aschmann and Sinnhuber (2013) considered the adsorption of HBr onto ice within the TTL, and the assumed VLS emissions varied between these studies.

As in Montzka and Reimann et al. (2011), we estimate that PGI from minor brominated VLS not considered in the studies mentioned above, such as CHBr<sub>2</sub>Cl, CHBrCl<sub>2</sub>, and CH<sub>2</sub>BrCl, could contribute around 0 to 0.3 ppt Br. Therefore, overall we conclude that total PGI could range from 1.1 to 4.3 ppt Br, compared to the 0.4 to 4.2 ppt Br reported in the last Assessment.

#### ***PGI from iodinated VLS or other iodine sources***

There are no new observations of inorganic iodine (I<sub>y</sub>) in the TTL since the last Assessment, when available Differential Optical Absorption Spectroscopy (DOAS) measurements (Bösch et al., 2003; Butz et al., 2009) suggested upper limits of 0.1 ppt IO and 0.1 ppt OIO and a total I<sub>y</sub> level of <0.15 ppt. New observations of IO in the free troposphere suggest that similar levels are present (Puentedura et al., 2012; Dix et al., 2013). Such low levels of IO are challenging to retrieve accurately but indicate that most of the IO vertical column is above the MBL. This is surprising since the majority of sources are very short lived (Section 1.3.1.3), and could have implications for our understanding of iodine sources and/or the I<sub>x</sub> (I + IO) lifetime with respect to irreversible uptake of reactive iodine to aerosol surfaces. Combined with uncertainties in transport and in iodine chemistry (Saiz-Lopez et al., 2012), the quantity of iodinated PGI is not known, up to the upper limits previously reported for IO and OIO in the TTL of 0.1 ppt (Butz et al., 2009).

### **1.3.2.3 TOTAL VLS HALOGEN INPUT INTO THE STRATOSPHERE**

As discussed above, VLS contribute to stratospheric halogen loading by both SGI and PGI. Observations of SGs around the tropopause provide some constraint on the magnitude of SGI. Observational evidence for PGI is, however, still rather limited and as such its contribution remains a significant uncertainty. An updated estimate of SGI, PGI, and the total (SGI + PGI) contribution of VLS to stratospheric halogen loading is given in Table 1-9 and is based on available SG/PG observations in the tropics and recent model studies.

**TABLE 1-9. Summary of estimated VLSL source gas (SG) and product gas (PG) contributions to stratospheric halogens, based on observations and model results.**

Halogen or Compound	Best Estimate (ppt Cl, Br, or I)
<b>Chlorine</b>	
VSL SGs	72 (50–95)
HCl PG	10 (0–20)
COCl <sub>2</sub> PG	15 (0–30)
<b>Total chlorine</b>	<b>95 (50–145)</b>
<b>Bromine</b>	
VSL SGs	0.7–3.4
PG sum	1.1–4.3
<b>Total bromine</b>	<b>5 (2–8)</b>
<b>Iodine</b>	
CH <sub>3</sub> I SG	< 0.05
PG sum	< 0.1
<b>Total iodine</b>	<b>&lt; 0.15</b>

**Total input from chlorinated VLSL**

As in the previous Assessment, “the best estimate” of total chlorine from VLSL reaching the stratosphere is obtained by summing the observed contribution from SGs (Table 1-7) at the tropopause and adding the estimated PG contribution from COCl<sub>2</sub> and HCl. This gives a best estimate and range of 95 (50–145) ppt. The anthropogenic fraction of VLSL chlorinated SG to the total SG at the tropopause is estimated to be around 70% (Table 1-7). Assuming this applies also to PGs, then we estimate ~70% of the total chlorine from VLSL entering the stratosphere is from anthropogenic sources.

**Total input from brominated VLSL**

The best estimate of bromine from VLSL that reaches the stratosphere,  $Br_y^{VLSL}$ , is based on SG observations around the tropical tropopause, two BrO profiles measurements in the TTL (Dorf et al., 2008), and an estimated PGI contribution from recent global modeling. A range is derived by summing the lower limits of SGI and PGI estimates as well as the upper limits (Table 1-9). This leads to a total estimated range of 2–8 ppt  $Br_y^{VLSL}$ , which is slightly narrower than the reported range of 1–8 ppt in the last Assessment, due to constraints on recent model estimates of PGI (Liang et al., 2010; Hossaini et al., 2012a; Aschmann and Sinnhuber, 2013; Liang et al., 2014).

An alternative approach to estimating  $Br_y^{VLSL}$  is to use observations of stratospheric BrO combined with model estimates of the BrO/ $Br_y$  ratio to calculate total stratospheric  $Br_y$ , and subtract the contribution of long-lived SGs. Uncertainties in the absolute mole fractions of long-lived source gases—CH<sub>3</sub>Br and the halons—are small (< 5%) (see Section 1.2). The overall uncertainty in the BrO/ $Br_y$  ratio is dominated by uncertainties in chemical kinetics, which are estimated to be 10 to 30% (Hendrick et al., 2008; McLinden et al., 2010; Salawitch et al., 2010; Parrella et al., 2012). Based on balloon-borne observations over Kiruna (68°N) and photochemical modeling, Kreycey et al. (2013) inferred that the  $j(\text{BrONO}_2)/k(\text{BrO}+\text{NO}_2)$  ratio (i.e., the ratio of bromine nitrate photolysis to production), could be larger by a factor of 1.7 (+0.4, -0.2) than that obtained using JPL recommendations. This result changes modeled BrO/ $Br_y$  ratios such that the total  $Br_y$  derived from BrO observations is reduced by about 1–2 ppt under conditions of high stratospheric NO<sub>x</sub> levels (for which most  $Br_y$  assessments are made), although the impact could be near zero in regions where BrONO<sub>2</sub> is not important. While not affecting the trend in

$Br_y$  (see Section 1.4.2.2), this study implies that  $Br_y^{VSLs}$  estimated from BrO observations could be smaller than considered previously.

Table 1-10 is an update from the previous Assessment and contains compiled  $Br_y^{VSLs}$  estimates from ground-, balloon-, aircraft- and satellite-based measurements of BrO, with associated uncertainties. Resolution of the measured total BrO columns from satellite UV-visible instruments into their stratospheric and tropospheric contributions depends upon assumptions regarding the presence of BrO in the troposphere and the spatial inhomogeneity of stratospheric BrO. Theys et al. (2011), Choi et al. (2012), and Sihler et al. (2012) have recently addressed many of the issues associated with retrieval of tropospheric BrO from the satellite sensors Ozone Monitoring Instrument (OMI), Global Ozone Monitoring Experiment (GOME-2), and Scanning Imaging Absorption Spectrometer for Atmospheric Cartography (SCIAMACHY), with results that support realistic separation of tropospheric fractions of the measured total BrO columns.

The three new estimates of  $Br_y^{VSLs}$  in Table 1-10 are based on measurements of BrO from the Aura Microwave Limb Sounder (MLS) instrument (Millán et al., 2012), SCIAMACHY (Parrella et al., 2013), and from a balloon-borne Submillimeterwave Heterodyne Limb Sounder (SLS) (Stachnik et al., 2013). These estimates of 5 (0.5–9.5) ppt, 7 (1–13) ppt, and 6 (3–9) ppt, respectively, fall within the previously reported range and support the “ensemble” value of 6 (3–8) ppt from the last Assessment (Montzka and Reimann, 2011). However, the discussion above regarding the  $j(\text{BrONO}_2)/k(\text{BrO}+\text{NO}_2)$  ratio suggests that the lower bound of this estimate should be revised downward, giving a higher uncertainty

**Table 1-10. Estimates of inorganic bromine from very short-lived substances ( $Br_y^{VSLs}$ ) contribution to stratospheric bromine derived from BrO measurements.** Update of Table 1-14 from the previous Assessment (Montzka and Reimann et al., 2011), extended with new results.

Data Source	$Br_y^{VSLs}$		References
	Central Value (ppt)	Range (ppt)	
Compilation of ground-based column BrO, aircraft & balloon BrO profiles, satellite BrO profiles from SCIAMACHY, MLS, and OSIRIS, and GOME and OMI satellite column BrO	6	3–8	Montzka and Reimann et al. (2011)
MLS satellite BrO profiles 55°S–55°N, 10–4.6 hPa	5	0.5–9.5	Millán et al. (2012)
SCIAMACHY satellite BrO profiles, 80°S–80°N, 15–30 km	7	1–13	Parrella et al. (2013)
SLS balloon BrO profiles Ft. Sumner, New Mexico (34°N)	6	3–9	Stachnik et al. (2013)
<b>Ensemble</b>	<b>6 (3–8)<sup>a</sup></b>		
<b>New, adjusted ensemble</b>	<b>5 (2–8)<sup>b</sup></b>		

SCIAMACHY, Scanning Imaging Absorption Spectrometer for Atmospheric Cartography; MLS, Microwave Limb Sounder; OSIRIS, Optical Spectrograph and InfraRed Imager System; GOME, Global Ozone Monitoring Experiment; OMI, Ozone Monitoring Instrument; SLS, Submillimeterwave Heterodyne Limb Sounder.

<sup>a</sup> Average and range of the central values of the 15 published estimates of  $Br_y^{VSLs}$ .

<sup>b</sup> Ensemble values, with mean and lower bound adjusted downwards by ~1 ppt to account for larger  $j(\text{BrONO}_2)/k(\text{BrO}+\text{NO}_2)$  ratio (Kreycky et al., 2013).

range, since it is not yet clear how the new results of Kreycy et al. (2013) affect individual measurements. We therefore suggest a new ensemble value for  $\text{Br}_y^{\text{VLS}}$  from BrO of 5 (2–8) ppt. This new ensemble range is the same as that based on SG observations and model PGI estimates (see above). Based on the similarity between these estimates from two different approaches, and the increased confidence in PGI estimates from models, we merge them to a best estimate of 5 (2–8) ppt  $\text{Br}_y^{\text{VLS}}$ . This inferred quantity of  $\text{Br}_y^{\text{VLS}}$  comprises a significant fraction of total stratospheric  $\text{Br}_y$  and is large enough to significantly affect the balance of ozone in the lower stratosphere, particularly at high latitudes (e.g., Feng et al., 2007) (see Section 1.3.3).

#### **Total input from iodinated VLS**

The best estimate of iodine from VLS that reaches the stratosphere, based on observed  $\text{CH}_3\text{I}$  around the tropopause and observed upper limits of stratospheric IO and OIO (Butz et al., 2009), is  $<0.15$  ppt, which is unchanged from the last Assessment.

### **1.3.3 Potential Influence of VLS on Ozone**

A number of modeling studies have shown that inclusion of  $\text{Br}_y^{\text{VLS}}$  in the stratosphere improves agreement between modeled and observed  $\text{O}_3$  trends (Salawitch et al., 2005; Feng et al., 2007; Sinnhuber et al., 2009). These models show that the influence of  $\text{Br}_y^{\text{VLS}}$  is largest during periods of elevated stratospheric aerosol, such as following large volcanic eruptions (e.g., Mt. Pinatubo in 1991), when heterogeneous halogen activation is enhanced. Therefore, proposed geoengineering strategies to combat climate change, such as stratospheric sulfate injections, may enhance the impact of VLS on  $\text{O}_3$  (Tilmes et al., 2012). In a volcanic quiescent year (2000) and relative to a model run with no VLS, Feng et al. (2007) reported a column  $\text{O}_3$  decrease of  $\sim 10$  Dobson units (DU) at midlatitudes due to 6 ppt of  $\text{Br}_y^{\text{VLS}}$  in the lower stratosphere during 2000.

Recent chemistry-climate model (CCM) studies have also included brominated VLS (e.g., Ordoñez et al., 2012). Braesicke et al. (2013) reported up to a  $\sim 20\%$  reduction in  $\text{O}_3$  in the lower stratosphere in polar regions between a model run with and without  $\text{Br}_y^{\text{VLS}}$  under 2000 stratospheric conditions.

The impact of chlorinated VLS on  $\text{O}_3$  trends has not been assessed, though relative to bromine it is likely to be small at present. Globally and annually averaged, the chemical effectiveness of bromine relative to chlorine for global  $\text{O}_3$  destruction, the alpha factor, is estimated to be  $\sim 60$  (Sinnhuber et al., 2009). The alpha factor for iodine is expected to be significantly larger, with an estimated range of 150–300 (Ko and Poulet et al., 2003). However, at the low levels of stratospheric iodine inferred from observed  $\text{CH}_3\text{I}$  around the tropopause and observed IO/OIO (Butz et al., 2009), models suggest that iodine is a very minor sink for  $\text{O}_3$  (Bösch et al., 2003).

### **1.3.4 New Anthropogenic VLS**

A number of short-lived compounds have been proposed as replacements for long-lived ozone-depleting substances (ODSs) and radiatively active hydrofluorocarbons (HFCs). Several of these substances are halogenated VLS (i.e., lifetimes  $<0.5$  years) and were chosen due to their low Ozone Depletion Potentials (ODPs) and Global Warming Potentials (GWPs). An updated summary of the lifetimes of the proposed replacement substances is given in Table 1-11. These compounds are discussed further in Chapter 5.

**Table 1-11. Local lifetimes of in-use and potential short-lived replacement compounds for long-lived ODSs.** Local lifetimes were calculated for OH reactive loss with the OH and temperature climatology from Spivakovsky et al. (2000) and Prather and Remsberg (1993), respectively, unless noted otherwise. Note that local lifetimes are estimates because the actual lifetimes of short-lived gases are dependent on their emission location and season as well as local atmospheric conditions (e.g., OH concentration and temperature).

Compound	WMO (2011) <sup>a</sup> Local Lifetime (days)	Tropics (25°S–25°N) Annually Averaged Local Lifetime (days)		Midlatitude (25°N–65°N) Annually Averaged Local Lifetime (days)		Notes
		BL	10 km	BL	10 km	
		<b>Hydrocarbons</b>				
CH <sub>2</sub> =CHCH <sub>3</sub> (propene)	0.35	0.31	0.27	0.47	0.50	1
(CH <sub>3</sub> ) <sub>2</sub> C=CH <sub>2</sub> (isobutene)	0.20	0.18	0.15	0.27	0.29	1
CH <sub>3</sub> CH <sub>2</sub> CH <sub>3</sub> (propane, R-600)	12.5	9.9	13.6	16	27	2
(CH <sub>3</sub> ) <sub>2</sub> CHCH <sub>3</sub> (isobutane, R-600a)	6.0	5.2	5.6	8.1	10.7	1
CH <sub>3</sub> CH <sub>2</sub> CH <sub>2</sub> CH <sub>2</sub> CH <sub>3</sub> (n-pentane)	3.4	2.7	3.3	4.3	6.5	3
c-CH <sub>2</sub> CH <sub>2</sub> CH <sub>2</sub> CH <sub>2</sub> CH <sub>2</sub> (cyclopentane)	2.7	2.2	2.7	3.5	5.3	3
(CH <sub>3</sub> ) <sub>2</sub> CHCH <sub>2</sub> CH <sub>3</sub> (isopentane)	3.4	2.9	3.1	4.5	6.0	3
CH <sub>3</sub> OCHO (methyl formate)	72	60	73	95	143	4
(CH <sub>3</sub> ) <sub>2</sub> CHOH (isopropanol)	2.0	1.9	1.5	2.9	2.7	2
CH <sub>3</sub> OCH <sub>2</sub> OCH <sub>3</sub> (methylal)	2.2	1.7	1.5	2.6	2.8	5
<b>Hydrofluorocarbons</b>						
CH <sub>3</sub> CH <sub>2</sub> F (HFC-161)	66	51	76	83	154	2
CH <sub>2</sub> FCH <sub>2</sub> F (HFC-152)	146	114	165	183	335	2
CH <sub>3</sub> CHFCH <sub>3</sub> (HFC-281ea)	23	19	23	30	46	2
<b>Unsaturated Fluorocarbons</b>						
CH <sub>2</sub> =CHF	2.1	2.0	1.4	3.1	2.6	2
CH <sub>2</sub> =CF <sub>2</sub>	4.0	3.7	3.0	5.7	5.4	2
CF <sub>2</sub> =CF <sub>2</sub>	1.1	1.0	0.7	1.6	1.3	2
CH <sub>2</sub> =CHCH <sub>2</sub> F	0.7	0.6	0.5	1.0	0.8	2
CH <sub>2</sub> =CHCF <sub>3</sub>	7.6	7.2	5.5	11	10	2
CH <sub>2</sub> =CFCF <sub>3</sub> (HFC-1234yf)	10.5	9.6	8.4	15	16	2
CF <sub>2</sub> =CFCH <sub>2</sub> F		~2	~2	~2	~2	6
CF <sub>2</sub> =CHCHF <sub>2</sub>		<5	<5	<5	<5	6
CHF=CFCHF <sub>2</sub>		<5	<5	<5	<5	6
CF <sub>2</sub> =CHCF <sub>3</sub>		~2	~2	~2	~2	6
(E)-CHF=CHCF <sub>3</sub> (HFC-1234ze(E))	16.4	15.0	12.8	23	24	2
(E)-CHF=CFCF <sub>3</sub>	4.9	4.5	3.7	6.9	6.8	2
(Z)-CHF=CFCF <sub>3</sub>	8.5	8.0	6.2	12	11	2
CF <sub>2</sub> =CFCF <sub>3</sub>	4.9	4.7	3.3	7.1	6.0	2
CH <sub>2</sub> =CHCF <sub>2</sub> CF <sub>3</sub>	7.9	7.5	5.8	11.4	10.5	2
CH <sub>2</sub> =CHCF <sub>2</sub> CF <sub>2</sub> CF <sub>3</sub>		~8	~6	~10	~10	7
(E)-CF <sub>3</sub> CH=CHCF <sub>3</sub>		~22	~16	~30	~30	8
(Z)-CF <sub>3</sub> CH=CHCF <sub>3</sub>		21.2	16.3	32	30	9
CF <sub>2</sub> =CFCF=CF <sub>2</sub>	1.1	1.0	0.8	1.5	1.6	10
(E)-CF <sub>3</sub> CH=CHCF <sub>2</sub> CF <sub>3</sub>		~22	~16	~30	~30	11
<b>Unsaturated Chlorocarbons</b>						
CH <sub>2</sub> =CHCl	1.5	1.5	0.9	2.2	1.6	2

(continued next page)

Compound	WMO (2011) <sup>a</sup> Local Lifetime (days)	Tropics (25°S–25°N) Annually Averaged Local Lifetime (days)		Midlatitude (25°N–65°N) Annually Averaged Local Lifetime (days)		Notes
		BL	10 km	BL	10 km	
		CH <sub>2</sub> =CCl <sub>2</sub>	0.9	0.9	0.5	
CClH=CClH		4.4	3.2	6.7	5.9	12
CHCl=CCl <sub>2</sub>	4.9	4.7	3.3	7.1	6.0	2, 13
CCl <sub>2</sub> =CCl <sub>2</sub>	90	66	119	109	245	2
CF <sub>2</sub> =CFCl	1.4	1.4	0.8	2.1	1.4	14
(E)-CF <sub>3</sub> CH=CHCl	26	24	21	37	39	15
(Z)-CF <sub>3</sub> CH=CHCl		~25	~20	~40	~40	16
CF <sub>3</sub> CCl=CH <sub>2</sub>		~25	~20	~40	~40	16
CF <sub>2</sub> =CFCF <sub>2</sub> Cl	~5	~5	~3	~7	~6	17
CF <sub>2</sub> =CFCF <sub>2</sub> CFCl <sub>2</sub>	~5	~5	~3	~7	~6	17
<b>Unsaturated Bromocarbons</b>						
CFBr=CF <sub>2</sub>	1.4	1.3	0.9	2.0	1.6	18
CHBr=CF <sub>2</sub>	2.3	2.3	1.5	3.4	2.7	18
CH <sub>2</sub> =CBrCF <sub>3</sub>	2.7	2.6	1.8	3.9	3.3	18
CH <sub>2</sub> =CBrCF <sub>2</sub> CF <sub>3</sub>	3.1	3.0	2.0	4.6	3.6	18
CH <sub>2</sub> =CHCF <sub>2</sub> CF <sub>2</sub> Br	6.5	6.2	4.7	9.5	8.6	18
<b>Fluorinated Ethers, HFE</b>						
CH <sub>3</sub> OCH <sub>2</sub> CF <sub>3</sub> (HFE-263fb2)	23	19	24	30	47	19, 20
CH <sub>3</sub> OCHF <sub>2</sub> CF <sub>3</sub> (HFE-254eb2)	88	69	99	111	200	2
CH <sub>3</sub> OCH <sub>2</sub> CF <sub>2</sub> CF <sub>3</sub> (HFE-365mcf3)	21	17	21	27	42	20, 21
CH <sub>3</sub> CH <sub>2</sub> OCF <sub>2</sub> CHF <sub>2</sub> (HFE-374pc2)	64	50	71	80	142	2
CF <sub>3</sub> CH <sub>2</sub> OCH <sub>2</sub> CF <sub>3</sub> (HFE-356mff)	105	79	132	129	270	2
CH <sub>3</sub> OCH(CF <sub>3</sub> ) <sub>2</sub> (HFE-356mm1)	61	49	64	79	128	22
<b>Fluorinated Ketones</b>						
CF <sub>3</sub> CF <sub>2</sub> C(O)CF(CF <sub>3</sub> ) <sub>2</sub> (FK 5-1-12)	7–14					23
(CF <sub>3</sub> ) <sub>2</sub> CFC(O)CF(CF <sub>3</sub> ) <sub>2</sub>						24
CF <sub>3</sub> CF <sub>2</sub> CF <sub>2</sub> C(O)CF(CF <sub>3</sub> ) <sub>2</sub>						24
<b>Fluorinated Alcohols</b>						
CH <sub>2</sub> FCH <sub>2</sub> OH	12.9	11	11	18	22	2
CHF <sub>2</sub> CH <sub>2</sub> OH	51	42	53	66	103	2
CF <sub>3</sub> CH <sub>2</sub> OH	142	111	161	180	325	2
C <sub>2</sub> F <sub>5</sub> CH <sub>2</sub> OH	143	111	165	180	335	2
C <sub>4</sub> F <sub>9</sub> CH <sub>2</sub> OH	142	111	164	178	330	2
CF <sub>3</sub> CHF <sub>2</sub> CF <sub>2</sub> CH <sub>2</sub> OH	112	85	137	138	280	1
<b>Special Compounds</b>						
CF <sub>3</sub> CF <sub>2</sub> CF <sub>2</sub> I (1-iodo-heptafluoropropane)	<2					25
CH <sub>3</sub> I (methyl iodide)	7	4.0	3.5	9.6	7.1	26
COF <sub>2</sub> (carbonyl fluoride)	5–10					27
PBr <sub>3</sub>	<0.01					28
NH <sub>3</sub>	Few days					2, 29
CH <sub>3</sub> CH <sub>2</sub> Br (bromoethane)	41	32	45	52	90	30

(continued next page)

**Notes:**

- a OH reactive loss partial lifetime was estimated with an OH abundance of  $1 \times 10^6$  molecule  $\text{cm}^{-3}$  and a temperature of 275 K.
1. OH reaction rate coefficient taken from Atkinson et al. (2008).
  2. OH reaction rate coefficient taken from JPL 10-6 (Sander et al., 2011).
  3. OH reaction rate coefficient taken from Calvert et al. (2008).
  4. OH reaction rate coefficient taken from Le Calvé et al. (1997).
  5. OH reaction rate coefficient taken from Porter et al. (1997).
  6. No experimental data available for the OH reaction; lifetime estimate was based on reactivity trends of fluorinated ethenes.
  7. No experimental data available for the OH reaction; lifetime estimated to be similar to that of  $\text{CH}_2=\text{CHCF}_2\text{CF}_3$ .
  8. No experimental data available for the OH reaction; lifetime estimated to be similar to that of (*Z*)- $\text{CF}_3\text{CH}=\text{CHCF}_3$ .
  9. OH reaction rate coefficient taken from Baasandorj et al. (2011).
  10. OH reaction rate coefficient taken from Acerboni et al. (2001).
  11. Lifetime estimated to be similar to that of (*E*)- $\text{CF}_3\text{CH}=\text{CHCF}_3$ .
  12. OH reaction rate coefficient from Zhang et al. (1991).
  13. Photolysis lifetime taken from Table 2-4 in Ko and Poulet et al. (2003).
  14. OH reaction rate coefficient taken from Abbatt and Anderson (1991).
  15. Room temperature OH reaction rate coefficient taken from Sulbaek Andersen et al. (2008).
  16. Local lifetime estimated as similar to that of (*E*)- $\text{CF}_3\text{CH}=\text{CHCl}$ .
  17. Local lifetime estimated as similar to that of  $\text{CF}_3\text{CF}=\text{CF}_2$ .
  18. OH reaction rate coefficient taken from Orkin et al. (2002).
  19. OH reaction rate coefficient taken from Oyaro et al. (2005).
  20. Only room temperature rate coefficient data available; OH reaction lifetime calculated assuming  $E/R = 500$  K.
  21. OH reaction rate coefficient taken from Oyaro et al. (2004).
  22. OH reaction rate coefficient from Chen et al. (2005b).
  23. Estimated local lifetime range due to UV photolysis taken from Taniguchi et al. (2003).
  24. Lifetime estimated to be similar to that of  $\text{CF}_3\text{CF}_2\text{C}(\text{O})\text{CF}(\text{CF}_3)_2$ .
  25. Estimated local lifetime taken from WMO (2011).
  26. Losses due to OH reaction and UV photolysis, see Table 1-5.
  27. Estimated local lifetime range due to heterogeneous uptake taken from Wallington et al. (1994).
  28. Local lifetime taken from Table 2-1 in Law and Sturges et al. (2007); OH reaction rate coefficient taken from Jourdain et al. (1982); the local lifetime is probably determined by UV photolysis.
  29. Local lifetime taken from IPCC/TEAP (2005); determined by washout rate.
  30. See Table 1-5.

## 1.4 CHANGES IN ATMOSPHERIC HALOGENS

### 1.4.1 Tropospheric and Stratospheric Chlorine Changes

#### 1.4.1.1 TROPOSPHERIC CHLORINE CHANGES

Total organic chlorine ( $\text{CCl}_y$ ) in the troposphere peaked in 1993–1994 at  $3660 \pm 23$  ppt and has then continuously declined for 20 years, initially at a rate of around 1% per year, reducing to a rate of around  $0.5\% \text{ yr}^{-1}$  in recent years (Figure 1-15). By mid-2012, tropospheric organic Cl from anthropogenic (CFCs, HCFCs, and chlorinated solvents, including methyl chloroform) and natural (mainly  $\text{CH}_3\text{Cl}$ ) sources had declined to 3300 ppt (Figure 1-15 and Table 1-12). This is a decrease of 1.5% since the 2010 Assessment report and of almost 10% when compared to the 1993 peak value, due to decreases in the anthropogenic Cl gases. In 2012, the CFCs and HCFCs accounted for 61% and 9%, respectively, of  $\text{CCl}_y$  in long-lived gases in the lower atmosphere. Table 1-12, updated from the 2010 Assessment, shows the contribution of halocarbons to the total chlorine budget for three milestones: 2004, 2008 and 2012.

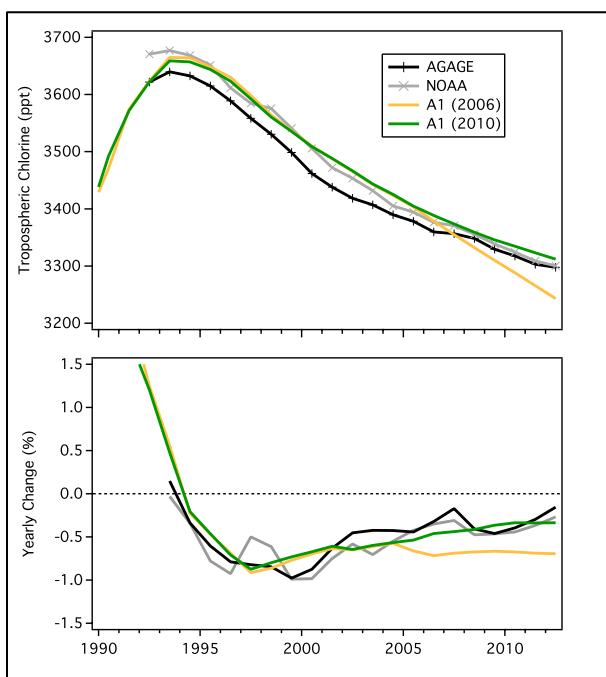


**Figure 1-15.** Total organic chlorine ( $\text{CCl}_y$ ) from the NOAA (gray) and AGAGE (black) global measurement networks. Quantities are based on global mean mole fractions of CFC-11, CFC-12, CFC-113,  $\text{CH}_3\text{CCl}_3$ ,  $\text{CCl}_4$ ,  $\text{CH}_3\text{Cl}$ , HCFC-22, HCFC-141b, HCFC-142b, and halon-1211 determined by the respective networks. CFC-114, CFC-115, CFC-112, and CFC-113a were estimated from measurements of Cape Grim archive air samples (Prinn et al., 2000; Laube et al., 2014) and included in records from both networks. NOAA HCFC and halon-1211 data were included in the AGAGE record for years 1992–1993 to provide a more complete total chlorine record. An additional 75–91 ppt was added to NOAA and AGAGE records to account for the sum of  $\text{CHCl}_3$ ,  $\text{CH}_2\text{Cl}_2$ ,  $\text{C}_2\text{Cl}_4$ , and  $\text{COCl}_2$  (see Table 1-12).

**Table 1-12. Contributions of long-lived halocarbons to total chlorine in the troposphere.**

	Total Cl (ppt) *			Contribution to Total (%)			Average Rate of Change of Total Cl ** (ppt yr <sup>-1</sup> )		
	2004	2008	2012	2004	2008	2012	2000–2004	2004–2008	2008–2012
All CFCs	2126	2078	2024	62.6	62.0	61.34	-7.7 (1.3)	-12.0 (1.0)	-13.5 (0.5)
$\text{CCl}_4$	376	358	339	11.1	10.7	10.3	-4.0 (0.6)	-4.4 (0.5)	-4.9 (0.7)
HCFCs	212	249	286	6.3	7.4	8.7	8.3 (0.4)	9.2 (0.2)	9.2 (0.3)
$\text{CH}_3\text{CCl}_3$	66	32	16	1.9	1.0	0.5	-17.6 (1.1)	-8.4 (0.5)	-4.1 (0.2)
$\text{CH}_3\text{Cl}$	535	545	540	15.8	16.3	16.4	-0.3 (2.8)	2.5 (0.9)	-1.7 (1.3)
halon-1211	4.33	4.24	3.96	0.13	0.13	0.12	0.05 (0.01)	-0.02 (0.01)	-0.07 (0.02)
Total Cl	3397	3352	3300				-21.0 (1.8)	-15.6 (1.3)	-13.4 (0.9)
							-0.60%	-0.46%	-0.40%

\* Chlorine mid-year mole fractions were derived using AGAGE, NOAA, and archive data (see Figures 1-1, 1-15).

\*\* Total and relative Cl changes over 5-year periods, as indicated. Uncertainties (in parentheses) are one standard deviation based on trends determined from different global networks. Relative changes in total chlorine (in percent) were calculated relative to values at the beginning of each period (3484 ppt in 2000).

Values for past years differ slightly from previous Assessments because of updated calibration information, different methods for determining global mean mole fractions, rounding errors, and the inclusion of CFC-112 and CFC-113a (Laube et al., 2014). Total Cl also includes 77, 84, and 91 ppt as VSLS in 2004, 2008, and 2012, respectively. Average trends in total Cl are based only on controlled species (not  $\text{CH}_3\text{Cl}$  and VSLS).

### 1.4.1.2 STRATOSPHERIC CHLORINE CHANGES

Most chlorine enters the stratosphere as organic chlorine ( $\text{CCl}_y$ ) in long-lived source gases and undergoes photochemical oxidation to inorganic forms ( $\text{Cl}_y$ ) as air is transported to higher altitudes within the stratosphere. In the upper stratosphere, total chlorine, i.e., the sum of  $\text{CCl}_y$  and  $\text{Cl}_y$ , lags the tropospheric  $\text{CCl}_y$  time series by up to 6 years owing to timescales for air to be transported to higher altitudes after crossing the tropopause, depicted in Figure 1-16. It is expected that total chlorine will continue to decrease in the stratosphere, with a time-delay as compared to tropospheric observations. The leveling off of inorganic chlorine occurred in 1996–1997 in the stratosphere (Rinsland et al., 2003).

The most abundant chlorine-containing gases in the stratosphere are the “reservoirs” HCl and  $\text{ClONO}_2$ , which can generate chlorine-containing radicals including ClO. Peak stratospheric abundances of  $\text{ClONO}_2$ , HCl, and ClO occur near 25–30 km, 50–60 km, and 25–45 km (daytime)/38–45 km (night-time), respectively (Froidevaux et al., 2006; Sato et al., 2012; Kreyling et al., 2013).

Table 1-13 summarizes observed trends of HCl,  $\text{ClONO}_2$ , and ClO derived from ground-based and satellite measurements of partial and total columns. Over a broad latitudinal range, observed upper stratospheric HCl, which is the dominant  $\text{Cl}_y$  compound in this region, shows trends of  $-0.5$  to  $-0.8\% \text{ yr}^{-1}$  for various time periods between 1997 and 2010. Between 1997 to 2013 and averaged over  $50^\circ\text{N}$  to  $50^\circ\text{S}$ , HCl trends of  $-0.5$  to  $-0.6\% \text{ yr}^{-1}$  are derived from HALOE (Halogen Occultation Experiment) data from January 1997 to November 2005 and ACE-FTS (Atmospheric Chemistry Experiment Fourier Transform Spectrometer) data from February 2004 to February 2013 (A. Jones et al., 2011) (Figure 1-17). These measurements are made between 35 to 45 km, an altitude range particularly suitable for analysis due to the sensitivity of both instruments and because most source gases have been converted to inorganic species, primarily HCl. HALOE and ACE-FTS measurements are biased with respect to each other, due to non-uniform (time-dependent in the case of HALOE) sampling, and different time periods used. However the data shown in Figure 1-17 indicate a trend in HCl similar in magnitude to other observations over different time periods and locations (Table 1-13) and with the observed decrease in tropospheric  $\text{CCl}_y$  of 0.5 to 1% per year on average since 1993–1994 (Figure 1-15).

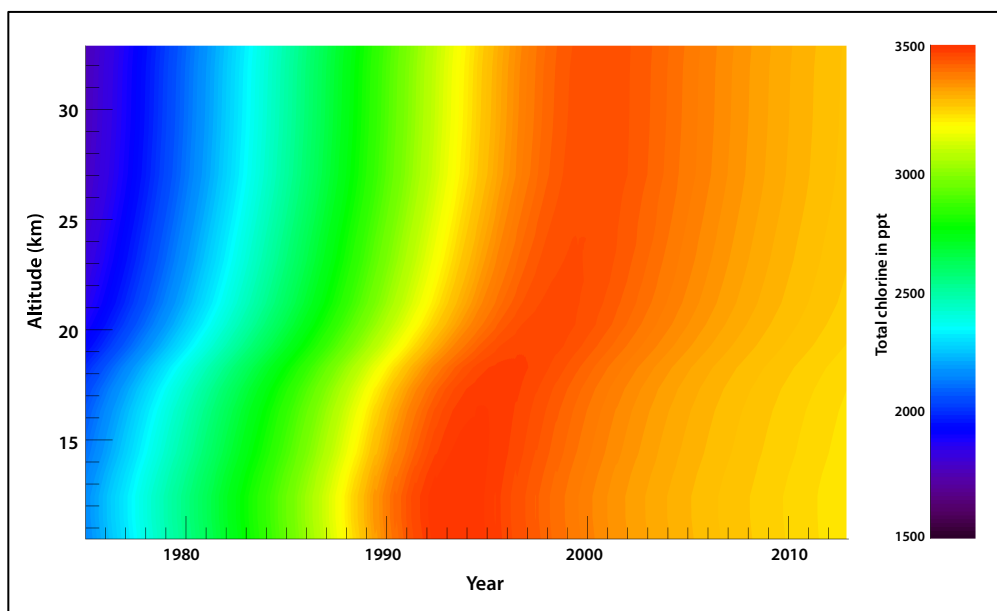


**Figure 1-16.** Midlatitude total chlorine evolution in the stratosphere, calculated using the vertical distribution of mean age (derived from observations of the age tracers  $\text{SF}_6$  and  $\text{CO}_2$ ) and assumptions on the width of the age spectrum. Tropospheric data from NOAA (using the data shown in Figure 1-15) are used exclusively as the basis of the calculation (updated from Engel et al., 2002).

**Table 1-13. Observed inorganic chlorine changes in the upper atmosphere.**

Data Source/ Location	Cl <sub>y</sub> Species	Altitude Region	Rate of Change (yr <sup>-1</sup> )	Time Period	Reference
Ground-based microwave instrument (reanalysis) Mauna Kea, Hawaii (19.8°N, 204.5°E)	ClO	33 – 37 km	-0.64 ± 0.15%	1995–2012	Connor et al. (2013)
Aura MLS + Odin SMR 20°S–20°N	ClO	35 – 45 km	-0.71 ± 0.78%	Dec 2001–Nov 2008	A. Jones et al. (2011)
Aura MLS 60°S–60°N	HCl	50 – 65 km	-0.78 ± 0.08%	Aug 2004–Jan 2006	Froidevaux et al. (2006)
ACE-FTS (v3.0) 30°S–30°N	HCl	50 – 54 km	-0.7 ± 0.1%	2004–2010	Brown et al. (2011)
HALOE and ACE-FTS 30°N–50°N, 30°S–50°S, and 20°N–20°S	HCl	35 – 45 km	-0.51% (NH), -0.52% (SH), -0.58% (tropics)	1997–2008	A. Jones et al. (2011)
17 FTIR NDACC stations (80.1°N–77.8°S)	HCl	Total column	Between -0.36 ± 0.67% and -1.56 ± 0.64%	2000–2009, station dependent	Kohlhepp et al. (2012)
17 FTIR NDACC stations (80.1°N–77.8°S)	ClONO <sub>2</sub>	Total column	Between -0.07 ± 0.52% and -4.56 ± 0.78%	2000–2009, station dependent, without Ny Alesund	Kohlhepp et al. (2012)

MLS = Microwave Limb Sounder; SMR = Sub-millimetre Radiometer; ACE-FTS = Atmospheric Chemistry Experiment Fourier Transform Spectrometer; HALOE = Halogen Occultation Experiment; FTIR = Fourier Transform Infrared; NDACC = Network for the Detection of Atmospheric Composition Change.

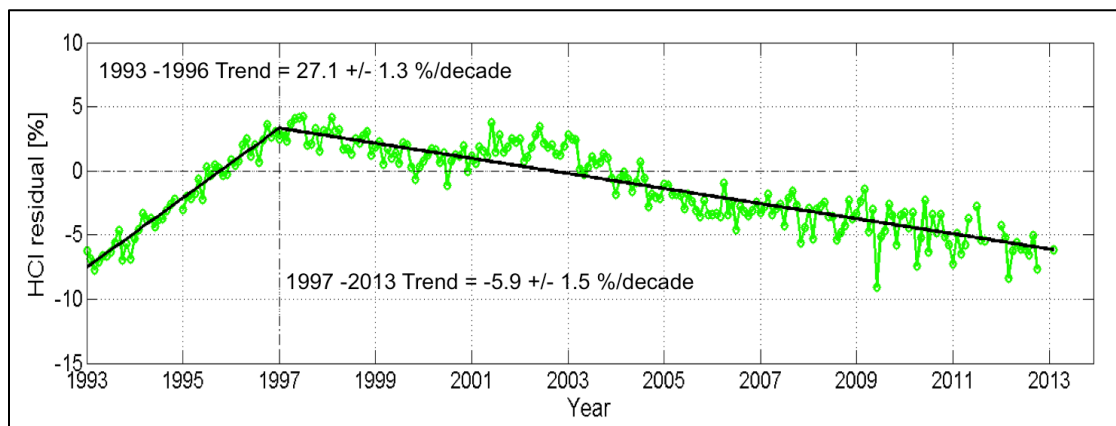


**Figure 1-17.** Time series of HCl anomalies at 35–45 km, averaged over 50°S–50°N. The anomalies represent de-seasonalized monthly averaged data for the all-instrument average (green) produced from HALOE v19 data from January 1997 to November 2005 and ACE-FTS v3.0/3.5 data from February 2004 to February 2013 (Ashley Jones, University of Toronto, extended from A. Jones et al., 2011). The anomalies are calculated by subtracting the climatological average value for each of the 12 months (calculated over the time span of each instrument) from each individual month (as in A. Jones et al., 2011). The vertical black dot-dash line at 1997 indicates the turnaround date. The solid black lines indicate the fitted trend to the all-instrument average before and after 1997. Trend values are given in percent per decade and uncertainties are 2 standard deviations.

Ground-based column data are more sensitive to HCl in the lower stratosphere, and are therefore potentially susceptible to short-term variability. At some ground-based stations, the total-column trends of HCl and ClONO<sub>2</sub> show significant differences, with much faster ClONO<sub>2</sub> decreases than HCl at low and high latitudes (Kohlhepp et al., 2012). However the mean annual cycles of HCl and ClONO<sub>2</sub> and the overall trend in the stratospheric chlorine content reported by Kohlhepp et al. (2012) were in agreement with five model calculations, also reported in the study, which were driven by baseline scenarios from WMO (2003) and WMO (2007).

Recently, Mahieu et al. (2013) updated the long-term Jungfraujoch HCl column measurement time series (Figure 1-18), and this update significantly impacts the derived trend ( $-0.7\% \text{ yr}^{-1}$  for 1997–2011 instead of  $-1.1\% \text{ yr}^{-1}$  for 1997–2007). Surprisingly, a flattening or even a positive trend (at the  $2\text{-}\sigma$  uncertainty level) is found for the 2007–2011 time period, although these changes are relatively small in relation to the atmospheric variability. A change in atmospheric circulation over this period, with more frequent sampling of northerly air masses at the Jungfraujoch, is a possible explanation (Mahieu et al., 2013). Previous Assessments have also noted abrupt unexplained variations in HCl trends, i.e., which differ over short time periods from lagged tropospheric chlorine trends (Montzka and Fraser et al., 2003). The overall changes reported here for HCl, in Figure 1-17 and Table 1-13, and in previous Assessments are however generally consistent with expectations based on trends in tropospheric long-lived chlorine gases.

## 1.4.2 Tropospheric and Stratospheric Bromine Changes

### 1.4.2.1 TROPOSPHERIC BROMINE CHANGES

Total organic bromine in the troposphere has declined by about 2 ppt since it peaked in 1998 (Figure 1-19), at an average rate of  $-0.86 \pm 0.05\% \text{ Br yr}^{-1}$  from 1998–2012, and at  $-0.95 \pm 0.13\% \text{ Br yr}^{-1}$  from 2008–2012. The majority of this decline results from reduced industrial production and emission of CH<sub>3</sub>Br, although the rate of CH<sub>3</sub>Br decline has slowed from  $\sim 0.14 \text{ ppt yr}^{-1}$  during the last Assessment to  $0.08 \pm 0.02 \text{ ppt yr}^{-1}$  since 2008. During 2008–2012 total bromine from CH<sub>3</sub>Br and the halons decreased from  $15.8 \pm 0.2 \text{ ppt}$  to  $15.2 \pm 0.2 \text{ ppt}$  at an average rate of  $0.14 \pm 0.02 \text{ ppt yr}^{-1}$ , based on two independent networks of surface observations (see Table 1-1). In the last Assessment, there were tentative signs of a decline in total Br from halons, from a peak around 2007; this decline is now larger and more robustly determined, decreasing at an average rate of  $0.06 \pm 0.02 \text{ ppt Br yr}^{-1}$  since 2008 (see Table 1-1). Halon-1301

is the only anthropogenic bromocarbon that is still increasing, although the growth has slowed in recent years to  $0.03 \pm 0.01 \text{ ppt yr}^{-1}$ .

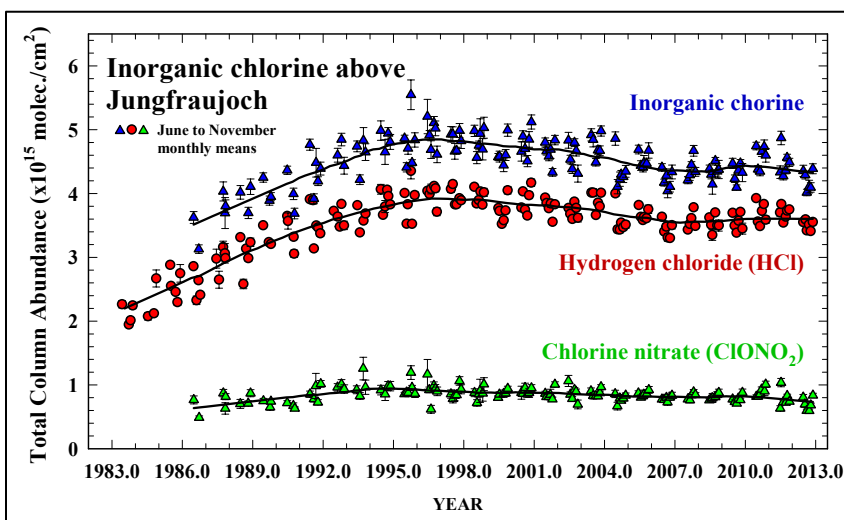


**Figure 1-18.** Time series (1983–2012) of monthly-mean total column HCl (red circles) and ClONO<sub>2</sub> (green triangles), as measured above the Jungfraujoch station (46.5°N). Cl<sub>y</sub> total columns (blue triangles) were obtained by summing the corresponding HCl and ClONO<sub>2</sub> data points. To avoid the significant variability affecting measurements in winter and spring, the time series were derived from June to November data. Least-square fits were applied to these data sets (black curves) to provide trends estimates. Updated from Montzka and Reimann et al. (2011).

variability affecting measurements in winter and spring, the time series were derived from June to November data. Least-square fits were applied to these data sets (black curves) to provide trends estimates. Updated from Montzka and Reimann et al. (2011).

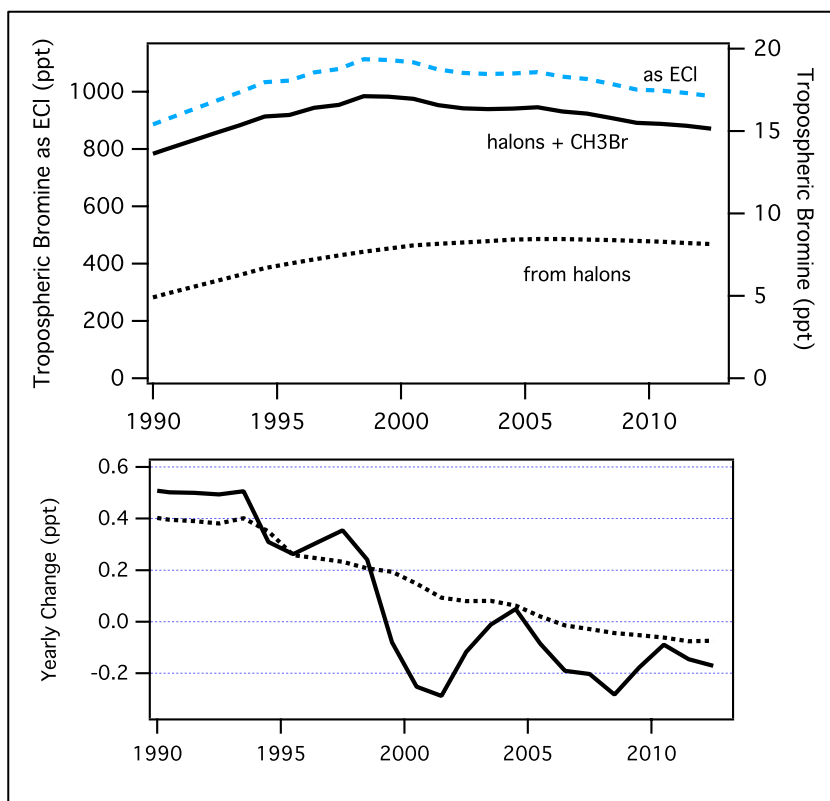


**Figure 1-19.** Tropospheric bromine expressed as bromine from halons, bromine from halons plus CH<sub>3</sub>Br, and as Equivalent Chlorine (ECI, using  $\alpha = 65$ ) (upper panel) and annual changes in Br-halons and Br-halons+CH<sub>3</sub>Br (lower panel). Sums are derived from the NOAA/AGAGE/UEA averaged data set.

#### 1.4.2.2 STRATOSPHERIC BROMINE CHANGES

Total stratospheric inorganic bromine ( $Br_y$ , which includes Br, BrO, BrONO<sub>2</sub>, HOBr, BrCl, HBr, BrONO, and Br<sub>2</sub>) can be determined through modeled estimates of the inorganic product gases arising from bromine source gases (see Section 1.3.2.2). Another method, as discussed in 1.3.2.3, is to use measurements of BrO in the stratosphere and estimate the concentrations of  $Br_y$  based on the calculated BrO/ $Br_y$  concentration ratios (e.g., Dorf et al., 2006; Millán et al., 2012). Figure 1-20 shows the updated stratospheric  $Br_y$  time series inferred from ground-based DOAS (Differential Optical Absorption Spectroscopy) BrO measurements at Lauder (45°S) and Harestua (60°N), and balloon-borne measurements (Dorf et al., 2006). The long-term time series of stratospheric BrO vertical column density measured at Harestua is shown in Figure 1-21 (update of Hendrick et al., 2008). The newly inferred trend values based on Harestua data alone, of  $+2.2 \pm 0.3\% \text{ yr}^{-1}$  between 1995 and 2001 and of  $-0.6 \pm 0.1\% \text{ yr}^{-1}$  between 2001 and 2012, are consistent with the previous estimates of Hendrick et al. (2008) of  $+2.5 \pm 0.5\% \text{ yr}^{-1}$  and  $-0.9 \pm 0.4\% \text{ yr}^{-1}$ , respectively, who identified a negative trend of stratospheric BrO of about  $1\% \text{ yr}^{-1}$  from 2001 from observations in both hemispheres. The stratospheric  $Br_y$  decline is consistent with the observed temporal changes in total tropospheric bromine discussed above.

Recent BrO measurements imply a mean stratospheric  $Br_y$  burden of 20 (16–23) ppt in 2011 (Figure 1-20, Kreygy et al. (2013)). The estimated relative contribution to this burden from controlled uses of halons (~8.4 ppt in 2007, accounting for the mean age of stratospheric air) and CH<sub>3</sub>Br (~0.3 ppt in 2007 from regulated agricultural use (non-QPS)) is within the range of the last Assessment's estimate of 40–45%, although it is declining slowly. Without accounting for the age of air, the estimated relative contributions to  $Br_y$  entering the stratosphere in 2012 from controlled uses are ~8.1 ppt for halons and ~0.15 ppt from regulated agricultural use (non-QPS) of CH<sub>3</sub>Br. Thus, VSLS bromocarbons, natural sources of CH<sub>3</sub>Br, and QPS uses of CH<sub>3</sub>Br (which are not controlled by the Montreal Protocol) contribute more than half of the stratospheric  $Br_y$  burden.

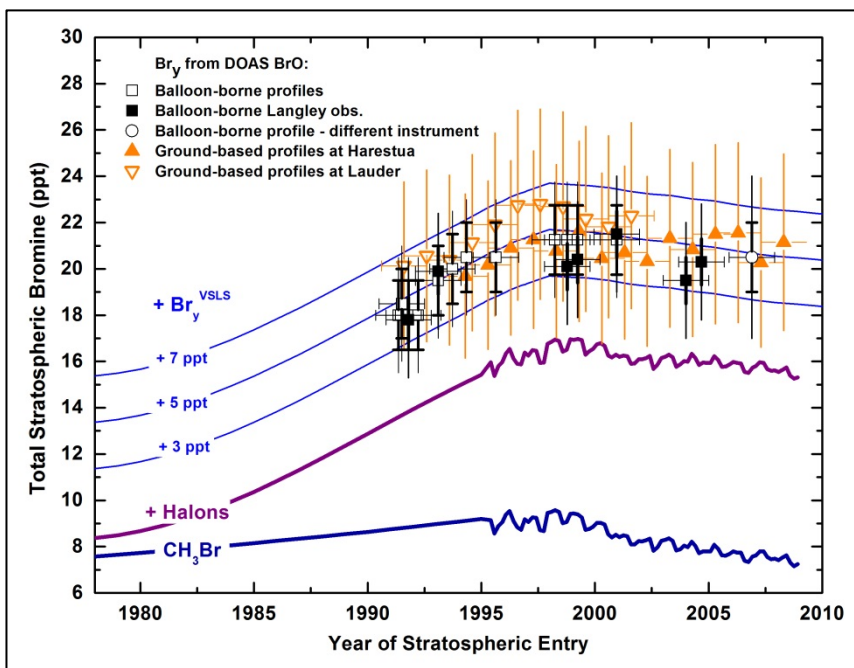
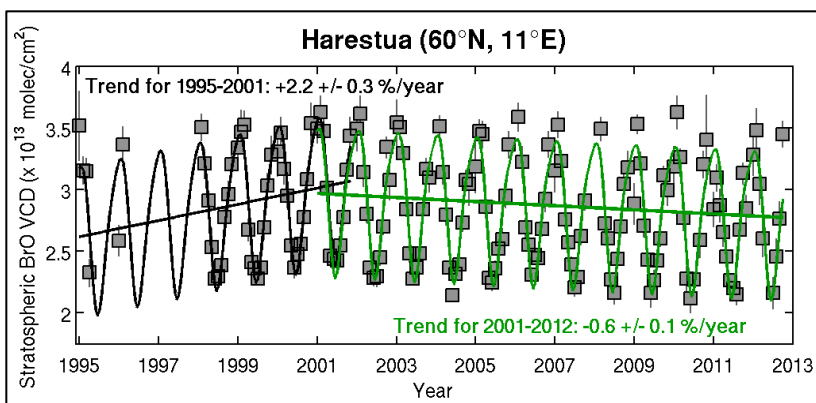


**Figure 1-20.** Changes in total stratospheric  $\text{Br}_y$  (ppt) derived from balloon-borne BrO observations (squares) (update of Dorf et al. (2006)) and annual mean mixing ratios calculated from ground-based UV-visible measurements of stratospheric BrO made at Harestua ( $60^\circ\text{N}$ ) and Lauder ( $45^\circ\text{S}$ ) (filled and open orange triangles, respectively) (adapted from Hendrick et al. (2007) and Hendrick et al. (2008)), using a common BrO absorption cross section. These stratospheric trends are compared to trends in measured bromine (ppt) at Earth's surface with additional constant amounts of  $\text{Br}_y$  added (thin lines). Dark blue line shows global tropospheric

bromine from methyl bromide as measured in firm air (pre-1995, including consideration of a changing interhemispheric gradient; Butler et al., 1999) and ambient air (after 1995, Montzka et al., 2003) with no correction for tropospheric  $\text{CH}_3\text{Br}$  loss. Purple line shows global tropospheric bromine from the sum of methyl bromide plus halons (Butler et al. (1999) and Fraser et al. (1999) through 1995; Montzka et al. (2003) thereafter). Thin blue lines show bromine from  $\text{CH}_3\text{Br}$ , halons, plus additional constant amounts of 3, 5, and 7 ppt Br. Total inorganic bromine is derived from (i) stratospheric measurements of BrO and photochemical modeling that accounts for BrO/ $\text{Br}_y$  partitioning from slopes of Langley BrO observations above balloon float altitude (filled squares); and (ii) lowermost stratospheric BrO measurements (open squares and circles). For the balloon-borne observations, bold/faint error bars correspond to the precision/accuracy of the estimates, respectively. For the ground-based measurements (triangles), the error bars correspond to the total uncertainties in the  $\text{Br}_y$  estimates. For stratospheric data, the date corresponds to the time when the air was last in the troposphere, i.e., sampling date minus estimated mean age of the stratospheric air parcel. For tropospheric data, the date corresponds to the sampling time, i.e., no corrections are applied for the time required to transport air. This figure updates Figure 1-21 from the previous Assessment (Montzka and Reimann et al., 2011).

**Figure 1-21.** Times series of monthly averaged ground-based UV-visible BrO vertical column densities (VCDs) at Harestua ( $60^\circ\text{N}$ ) (update of Hendrick et al., 2008). The gray error bars correspond to the standard error of the monthly mean. The black and green thick solid lines represent the trend analyses for the 1995–2001 and 2001–2012 periods, respectively. The thick straight lines correspond to the linear trend



for both periods. The full data set has been optimized using improved DOAS settings (mainly: new fitting window (342–357 nm),  $\text{O}_3$  cross sections at 218K and 243K from Brion, Daumont, and Malicet (Brion et al., 1998; Daumont et al., 1992; Malicet et al., 1995), Taylor expansion of  $\text{O}_3$  slant column densities in wavelength and vertical optical depth as in Pukite et al. (2010), and  $\text{O}_4$  cross sections from Greenblatt et al. (1990)).

### 1.4.3 Tropospheric and Stratospheric Iodine Changes

#### 1.4.3.1 TROPOSPHERIC IODINE CHANGES

More than a decade of atmospheric CH<sub>3</sub>I observations at several remote sites, ranging in location from 82.5°N to 40.4°S, have revealed an increase from 2003–2004 to 2009–2010 by several tens of percent, with a decreasing trend before 2003 (Yokouchi et al., 2012). The interannual variability of the observations corresponded with the Pacific Decadal Oscillation (PDO), suggesting that CH<sub>3</sub>I emissions are affected by SST-related processes on a global- and decadal scale.

#### 1.4.3.2 STRATOSPHERIC IODINE CHANGES

There are no new observations of inorganic iodine in the upper troposphere/lower stratosphere (UTLS) since the last Assessment, when available measurements (Bösch et al., 2003; Butz et al., 2009) suggested upper limits of 0.1 ppt IO and 0.1 ppt OIO in the UTLS and a total inorganic stratospheric iodine (I<sub>y</sub>) level of <0.15 ppt.

### 1.4.4 Changes in Ozone-Depleting Halogen Abundance in the Stratosphere Based Upon Long-Lived Source Gas Measurements: Equivalent Chlorine (ECI) and Equivalent Effective Stratospheric Chlorine (EESC)

Changes in the stratospheric burden of total inorganic halogens (Cl and Br) can be estimated from changes in the calculated abundance of Equivalent Effective Stratospheric Chlorine (EESC) (Daniel and Velders, 2007); changes in total tropospheric halogen (Cl and Br) abundance can be addressed with the Equivalent Chlorine (ECI) metric (WMO, 1992). At its peak in 1994–1995, the total abundance of ECI was ~4450 ppt. By 2012 ECI had decreased by nearly 10%, to ~4030 ppt.

EESC is a sum of chlorine and bromine derived from ODS tropospheric abundances weighted to reflect their potential influence on ozone. The EESC abundance and temporal behavior is derived for specific regions of the stratosphere (here, as in previous Assessments, for polar and midlatitude regions), because it is dependent on transport timescales and respective trace gas decomposition rates (see Montzka and Reimann et al. (2011) for further details). We continue to use the formulation of EESC introduced by Newman et al. (2007), which includes a variety of parameters such as transport times (expressed as mean ages of air), the efficiency of different halogens to deplete ozone (expressed as alpha factors), mixing processes, and age-of-air-dependent ODS decomposition rates (i.e., fractional release factors, FRFs), to predict inorganic halogen abundances and changes in the stratosphere based on tropospheric measurements of chlorinated and brominated source gases.

EESC has continued to decrease in both the midlatitude and polar stratosphere (Figure 1-22, upper panel), by  $16.2 \pm 0.4\%$  and  $8.9 \pm 1.2\%$ , respectively, between the times of its peak values through to 2012. Midlatitude EESC is calculated at a mean age of 3 years and polar EESC at 5.5 years, with the latter being generally larger due to enhanced ODS decomposition with increasing mean age. Using the average of model-derived fractional release factors from Newman et al. (2007), as used in the last Assessment, and from a new observation-based study by Laube et al. (2013), we find that between 2008 and 2012, EESC declined by 4.15% in midlatitudes and 3.2% in polar latitudes. As in the previous Assessment, we find that no single chemical class dominated these declines in EESC. In the polar stratosphere, CH<sub>3</sub>CCl<sub>3</sub> was still the main contributor to this change (–1.3%), with similar contributions from CH<sub>3</sub>Br (–1.1%) and long-lived CFCs (–0.9%). CCl<sub>4</sub> was a more minor contributor to the decline (change of –0.4%), whereas both HCFCs (+0.3%) and halons (+0.2%) were counteracting as they were still increasing. In the midlatitude stratosphere, the CH<sub>3</sub>CCl<sub>3</sub> change (–1.25%) was less pronounced relative to the total, reflecting its decreasing contribution to total tropospheric Cl, with the EESC changes

mostly influenced by  $\text{CH}_3\text{Br}$  ( $-1.4\%$ ). CFCs contributed  $-1.0\%$ ,  $\text{CCl}_4$   $-0.55\%$ , halons were contributors to an EESC decrease for the first time (change of  $-0.25\%$ ), and increases in HCFCs contributed  $+0.2\%$ .

EESC calculations displayed in the lower panel of Figure 1-22 show changes in EESC relative to peak levels observed in the mid-1990s and amounts inferred for 1980 (Hofmann and Montzka, 2009), and are calculated separately using the FRFs from Newman et al. (2007) and Laube et al. (2013). The new FRFs do not appreciably change our understanding of the relative decline in EESC over time. We find 38–41% recovery to 1980 levels in midlatitudes (2008: 28%) and 16–21% recovery in polar latitudes (2008: 10%) by 2012. We note that ozone depletion is likely to have already been significant before the benchmark recovery date (1980).

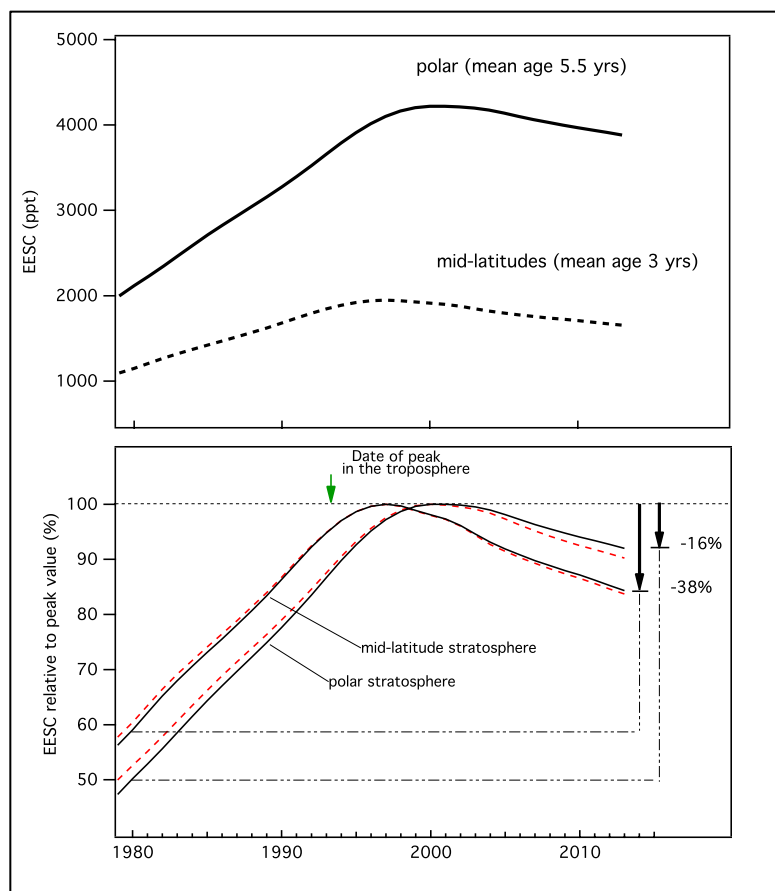


**Figure 1-22.** The Equivalent Effective Stratospheric Chlorine (EESC) was calculated for the midlatitude and polar stratosphere based on global mean mole fractions measured at the surface. Mean ages of 3 years (midlatitude) and 5.5 years (polar) were used along with spectral widths equal to one-half of the mean age. Surface data included CFC-11, CFC-12, CFC-113, CFC-114, CFC-115, CFC-112, CFC-113a,  $\text{CH}_3\text{CCl}_3$ ,  $\text{CCl}_4$ , HCFC-22, HCFC-141b, HCFC-142b, halon-1211, halon-1301, halon-1202, halon-2402,  $\text{CH}_3\text{Br}$ , and  $\text{CH}_3\text{Cl}$ . Surface data were derived from NOAA and AGAGE global networks and from global means estimated from Cape Grim archive air samples (see Figure 1-1). Calibration scale adjustments were made as necessary. The lower panel shows EESC relative to peak levels. Percentages on the right indicate the observed changes in EESC relative to the changes needed for EESC to return to 1980 levels (note that in 1980, more than half the EESC abundance was already from anthropogenic origin). Here, two EESC cases are shown: (1) using age-of-air-dependent fractional release factors (FRF) from Newman et al. (2007) (black lines), and (2) using age-of-air-dependent FRF from Laube et al. (2013) (red lines). FRFs for CFC-112 and CFC-113a were derived as in Laube et al. (2014) for both cases. EESC returned 38–41% (midlatitude) and 16–21% (polar) of the way toward 1980 levels by the end of 2012.

Using the different FRFs (Newman et al., 2007; Laube et al., 2013), however, results in fairly significant differences in the absolute magnitude of reactive halogens as EESC, and different relative contributions of different gases to the EESC decline. The dominating limitations and uncertainties in EESC estimates are related to the methods used to derive inorganic halogen abundances in the stratosphere, which in turn relate to a limited understanding of ODS decomposition rates (expressed as FRFs), and mixing processes (Newman et al., 2007). Calculations of FRFs are dependent upon the methods used to calculate stratospheric mean ages of air (including assumptions on age spectra), interannual variability (especially in the Arctic winter), and long-term changes in stratospheric circulation (Engel et al., 2009; Stiller et al., 2012). Further, the relationship between a trace gas and the EESC derived from it could change with time if the tropospheric trends of the respective ODSs change (Laube et al., 2013); for trends changing by a few percent per year, the impact on the FRF is expected to be a few percent.

The study by Laube et al. (2013), who derived FRFs for 10 major ODSs (CFC-11, CFC-12, CFC-113, HCFC-22, HCFC-141b, HCFC-142b, CCl<sub>4</sub>, CH<sub>3</sub>CCl<sub>3</sub>, halon-1211, and halon-1301), translates into a 22% reduction of the total abundance of EESC from these compounds in midlatitudes and 24% in polar latitudes in 2008, compared to WMO (2011). In terms of the relative importance of different ODS groups, using the Laube et al. (2013) fractional release leads to an increased relative contribution to total EESC from halons and solvents, and a decrease for CFCs and HCFCs, compared to WMO (2011). This would affect future projections depending on the temporal evolution of the individual ODSs; note that in Figure 1-22 the curves derived from the two fractional release data sets diverge most in recent years. In addition it should be noted that no VSLs are included in the EESC. This compound group quickly releases a large portion of its halogen in the lower stratosphere with fractional release factors close to one at relatively low mean ages (Pfeilsticker et al., 2000; Schauffler et al., 2003; Laube et al., 2008). The relative impact of VSLs on stratospheric Equivalent Chlorine is likely to be larger when using the Laube et al. (2013) fractional release.

#### 1.4.5 Fluorine in the Troposphere and Stratosphere

Although the sum of fluorine from ODSs is declining, the tropospheric abundance of fluorine (F) (derived from CFCs -11, -12, -113, -114, -115; HCFCs -22, -141b, -142b, -124; halons -1211, -1301, -2402; HFCs -23, -32, -125, -134a, -143a, -152a, -227ea, -236fa, -245fa, -365mfc, -4310mee; C<sub>1</sub>-C<sub>8</sub> perfluorocarbons (PFCs); SF<sub>6</sub>; SF<sub>5</sub>CF<sub>3</sub>; SO<sub>2</sub>F<sub>2</sub>, and NF<sub>3</sub>) was still increasing between 2009 and 2012 at a mean annual rate of 1.2% yr<sup>-1</sup> or 33 ppt yr<sup>-1</sup> and reached 2801 ppt in 2012. This recent growth in F, which is caused by the rising abundances of fluorine-containing replacement compounds (such as HFCs), is higher than that observed from 1995–2005 (29 ppt yr<sup>-1</sup>), but lower than that of the 1980s (81 ppt yr<sup>-1</sup>) during the period of unrestricted production and use of ODSs.

In the stratosphere, the reservoir species or product gases HF (hydrogen fluoride), COF<sub>2</sub> (carbonyl fluoride), and COClF (carbonyl chlorofluoride) are currently produced by major ODSs and other source gases. In order to estimate recent changes in stratospheric fluorine product gases, only source gases with stratospheric lifetimes of <100 years were considered (Table 1-3). This subset of fluorinated source gases decreased in the troposphere with a change of around -0.5% yr<sup>-1</sup> during 2009–2012. Therefore, the recent stratospheric fluorine changes are likely to be between these two ranges (-0.5% to +1.2% yr<sup>-1</sup>).

The stratospheric fluorine reservoir species HF, COF<sub>2</sub>, and COClF are monitored by ACE-FTS (Brown et al., 2011; 2014), while the ground-based Network for the Detection of Atmospheric Composition Change (NDACC) Fourier Transform Infrared (FTIR) network (Kohlhepp et al., 2012) provides time series of the more abundant HF and COF<sub>2</sub> only. Using ACE-FTS occultation measurements, trends of total stratospheric fluorine were determined by Brown et al. (2014). Total stratospheric fluorine mole fractions increased from 2004 to 2009 by 24.3 ± 3.1 and 28.3 ± 2.7 ppt yr<sup>-1</sup> (or 0.96 ± 0.12 and 1.12 ± 0.11% yr<sup>-1</sup>), for the 30–70°S and 30–70°N latitude bands, respectively.

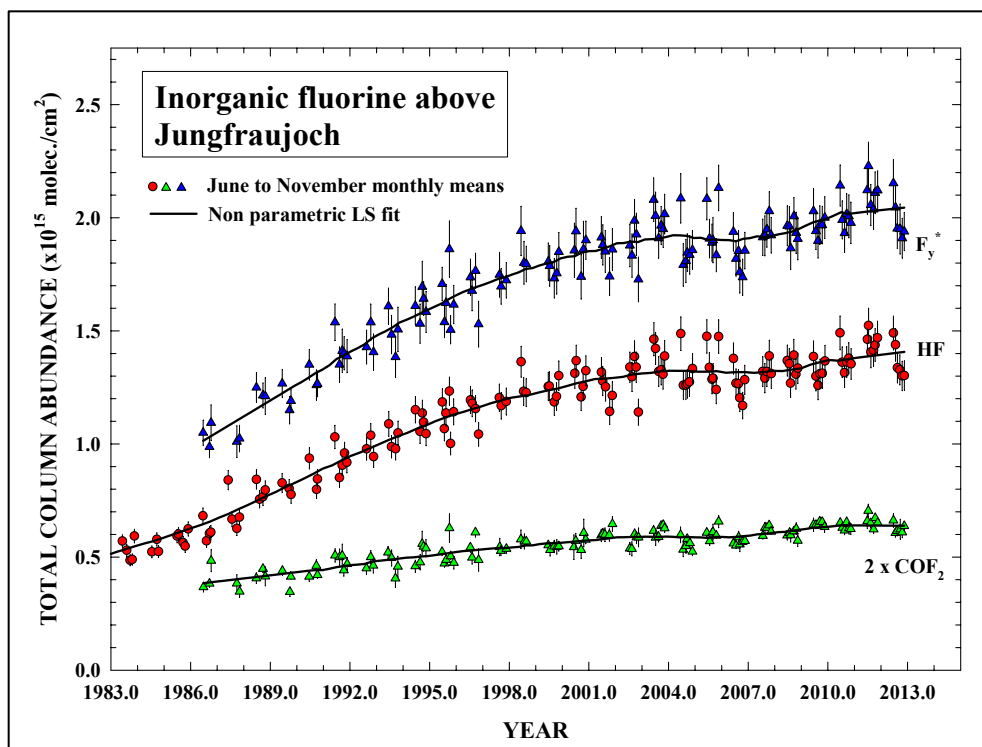


**Figure 1-23.** Time series of monthly-mean total column HF (red circles) and  $2 \times \text{COF}_2$  (green triangles) (molecules per square centimeter), as derived from the Jungfraujoch station ( $46.5^\circ\text{N}$ ) for the June to November months, updated from Montzka and Reimann et al. (2011). The blue triangles correspond to the weighted sum of the HF and  $\text{COF}_2$  total columns, i.e., a very good proxy of the total inorganic fluorine at northern midlatitudes (COCIF is the only fluorine reservoir missing, with a contribution to the  $F_y$  budget estimated to be about 2%).

Kohlhepp et al. (2012) investigated the trend of HF at 16 NDACC stations covering the  $80^\circ\text{N}$  to  $77.8^\circ\text{S}$  latitude range through 2009. For the vast majority of sites, positive linear trends are reported, generally consistent with an increase of HF at rates close to  $1\% \text{ yr}^{-1}$  when considering the 2000 loadings as reference. The Jungfraujoch time series for HF (Duchatelet et al., 2010) and  $\text{COF}_2$  (Duchatelet et al., 2009) have been updated to include all observations up to the end of 2012 (Figure 1-23). The long-term trends for HF,  $\text{COF}_2$ , and their combination ( $F_y^* = \text{HF} + 2 \times \text{COF}_2$ ) above the Jungfraujoch are all positive and remain in line with values reported in Kohlhepp et al. (2012) as well as in Montzka and Reimann et al. (2011). Overall, the remote-sensing measurements of stratospheric F indicate global trends close to a  $1\% \text{ yr}^{-1}$  increase between 2008 and 2012. This is smaller than trends observed during the late 1980s–early 1990s, but within the expected changes for fluorine based on tropospheric trends in ODSs, their substitutes, and other fluorinated gases in recent years.

## 1.5 CHANGES IN OTHER TRACE GASES THAT INFLUENCE STRATOSPHERIC OZONE AND CLIMATE

### 1.5.1 Updates to Mole Fractions, Budgets, Lifetimes, and Observations

In this section, anthropogenically emitted substances that are not covered by the Montreal Protocol but that indirectly affect stratospheric ozone are discussed. These include long-lived greenhouse gases such as  $\text{CH}_4$ ,  $\text{N}_2\text{O}$ , hydrofluorocarbons (HFCs), other fluorinated chemicals (e.g., perfluorocarbons (PFCs),  $\text{SF}_6$ ,  $\text{NF}_3$ ), and some other sulfur-containing gases. HFCs are a focal point because they are potent

greenhouse gases and their increasing abundance in the atmosphere is a direct consequence of the restrictions on ODS production and consumption under the Montreal Protocol. Note that CO<sub>2</sub> is not discussed because it was thoroughly discussed in the recent Intergovernmental Panel on Climate Change (IPCC) 5th Assessment Report (IPCC, 2013).

### 1.5.1.1 F-GASES

F-gases define a class of source gases with fluorine as the only halogen attached either to carbon, sulfur, or nitrogen. F-gases are also called Kyoto Protocol synthetics are almost solely emitted from anthropogenic activities. Stratospheric reservoir species such as HF (hydrogen fluoride) or COF<sub>2</sub> (carbonyl fluoride) are not included here but in Section 1.4.5. F-gases do not deplete ozone but are potent greenhouse gases and therefore have an indirect effect on the ozone budget. They include the HFCs, the PFCs, sulfur hexafluoride (SF<sub>6</sub>), sulfuryl fluoride (SO<sub>2</sub>F<sub>2</sub>), and nitrogen trifluoride (NF<sub>3</sub>). Whereas HFCs have been introduced as replacements for ODSs under the Montreal Protocol for applications such as refrigeration and foam blowing, PFCs are by-products of the aluminum industry or are used in the semiconductor industry (IPCC/TEAP, 2005). Most HFCs and all PFCs are long-lived and have high Global Warming Potentials (GWPs). HFCs, in particular, were the subject of studies that forecasted that they could contribute considerably to climate change in the future (Velders et al., 2012, Rigby et al., 2014). In order to ease this environmental pressure, they are increasingly being replaced by shorter-lived alternatives such as unsaturated HFCs (also named hydrofluoro-olefins, HFOs), or by the non-halogenated gases such as hydrocarbons, CO<sub>2</sub>, or not-in-kind alternatives (UNEP, 2011a, 2013a). In the group of sulfur-containing F-gases, SF<sub>6</sub> is used as insulator gas in electrical switchgear and to a minor extent in various industrial applications (Maiss and Brenninkmeijer, 1998), and SO<sub>2</sub>F<sub>2</sub> is used as a replacement for CH<sub>3</sub>Br in soil and grain fumigation (Mühle et al., 2009). Finally, NF<sub>3</sub> is increasingly used in the semiconductor industry as a replacement for PFCs (Prather and Hsu, 2008, 2010; Fthenakis et al., 2010).

#### ***Update on observations and on atmospheric budget***

Updates of the global mean abundances of F-gases measured by global networks and from archived unpolluted air collected at Cape Grim, Tasmania (Langenfelds et al., 1996) are given in Table 1-14 and Figure 1-24. Global emissions were derived from these observations, their trends, and their loss rates (i.e., lifetimes) as in Section 1.2 for ODSs (Figure 1-25). Regional emissions can be assessed by either extracting information from globally distributed measurements (e.g., Stohl et al., 2009; Rigby et al., 2010) or by using measurements from the source regions (e.g., Miller et al., 2012; Kim et al., 2010; Keller et al., 2012).

#### ***HFC-134a (CH<sub>2</sub>FCF<sub>3</sub>)***

Since the mid-1990s, HFC-134a has been used as replacement refrigerant for CFC-12 in mobile air conditioners, stationary refrigeration, as well as in foam-blowing applications, in aerosol inhalers, and for dry etching (Montzka et al., 1996; O'Doherty et al., 2004). In 2012 HFC-134a was the most abundant HFC and the two independent sampling networks (NOAA, AGAGE) show good agreement in its global mean mole fraction of 67.7 (67.5–67.8) ppt and also in the average annual trend of +5.0 ppt yr<sup>-1</sup> (or 7.6% yr<sup>-1</sup>) in 2011–2012 (Table 1-14). Furthermore, with a radiative forcing of 11 mW m<sup>-2</sup>, HFC-134a was the F-gas with the largest radiative forcing in 2012. As HFC-134a has a high 100-year GWP of 1360 (Chapter 5), low-GWP refrigerants (e.g., HFC-1234yf) are being considered as alternatives for its use in mobile air conditioning and other applications.

Estimated global emissions of 176 ± 39 Gg in 2012 represent an increase of 4% yr<sup>-1</sup> over emissions derived in 2008 (148 ± 24 Gg). Stohl et al. (2009) estimated that regional emissions were highest in Asia and the U.S., followed by Europe, with 29%, 28%, and 17% of the global emissions, respectively. Despite the extrapolations involved with most of these regional studies, results from more recent regional studies are largely in accordance with these findings for the U.S. (Barletta et al., 2011; Miller et al., 2012), Europe (Keller et al., 2012), and Asia (Kim et al., 2010; Stohl et al., 2010; Fang et al., 2012; Yao et al., 2012).

**Table 1-14. Measured mole fractions of selected fluorinated compounds (HFCs, PFCs, SF<sub>6</sub>, NF<sub>3</sub>, SO<sub>2</sub>F<sub>2</sub>, SF<sub>5</sub>CF<sub>3</sub>) and CH<sub>4</sub>, N<sub>2</sub>O, and COS.**

Chemical Formula	Common or Industrial Name	Annual Mean Mole Fraction (ppt)			Change (2011–2012)		Network, Method
		2008	2011	2012	ppt yr <sup>-1</sup>	% yr <sup>-1</sup>	
<b>Hydrofluorocarbons (HFCs)</b>							
CHF <sub>3</sub>	HFC-23	21.9	24.1	25.0	0.9	3.6	AGAGE, in situ (Global)
CH <sub>2</sub> F <sub>2</sub>	HFC-32	2.7	5.2	6.3	1.1	19	AGAGE, in situ (Global)
CHF <sub>2</sub> CF <sub>3</sub>	HFC-125	6.1	9.7	11.2	1.5	7.1	AGAGE, in situ (Global)
CH <sub>2</sub> FCF <sub>3</sub>	HFC-134a	48.1	62.7	67.8	5.1	7.8	AGAGE, in situ (Global)
		47.6	62.7	67.5	4.9	7.5	NOAA, flask & in situ (Global)
		48.4	64.3	68.9	4.6	8.3	UCI, flask (Global)
CH <sub>3</sub> CF <sub>3</sub>	HFC-143a	8.6	12.1	13.4	1.3	11	AGAGE, in situ (Global)
CH <sub>3</sub> CHF <sub>2</sub>	HFC-152a	5.8	6.7	6.9	0.2	2.9	AGAGE, in situ (Global)
		5.6	6.5	6.7	0.2	3.0	NOAA, flask & in situ (Global)
CHF <sub>2</sub> CH <sub>2</sub> CF <sub>3</sub>	HFC-245fa	0.86	1.28	1.44	0.16	12	AGAGE, in situ (Global)
CH <sub>3</sub> CF <sub>2</sub> CH <sub>2</sub> CF <sub>3</sub>	HFC-365mfc	0.44	0.59	0.65	0.06	9.7	AGAGE, in situ (Global)
CHF <sub>3</sub> CHCF <sub>3</sub>	HFC-227ea	0.44	0.66	0.74	0.08	11	AGAGE, in situ (Global)
CF <sub>3</sub> CF <sub>2</sub> (CHF) <sub>2</sub> CF <sub>3</sub>	HFC-43-10mee	0.15	0.20	0.21	0.01	7.9	AGAGE, in situ (Global)
<b>Perfluorocarbons (PFCs)</b>							
CF <sub>4</sub>	PFC-14	77.1	79.0	79.7	0.8	1.0	AGAGE, <i>in situ</i> (Global)
C <sub>2</sub> F <sub>6</sub>	PFC-116	3.9	4.2	4.2	0.1	1.9	AGAGE, <i>in situ</i> (Global)
C <sub>3</sub> F <sub>8</sub>	PFC-218	0.50	0.56	0.57	0.01	2.1	AGAGE, <i>in situ</i> (Global)
c-C <sub>4</sub> F <sub>8</sub>	PFC-318c	<i>1.11</i>	<i>1.20</i>	<i>1.24</i>	<i>0.04</i>	<i>3.2</i>	<i>UEA, Cape Grim</i>
C <sub>4</sub> F <sub>10</sub>	PFC-31-10	0.17	0.17				AGAGE, flask (Global)
		0.174	0.178	0.177	0.00	n.s.	<i>UEA, Cape Grim</i>
C <sub>5</sub> F <sub>12</sub>	PFC-41-12	0.12	0.13				AGAGE, flask (Global)
		<i>0.133</i>	<i>0.136</i>	<i>0.134</i>	<i>0.00</i>	<i>n.s.</i>	<i>UEA, Cape Grim</i>
C <sub>6</sub> F <sub>14</sub>	PFC-51-14	0.26	0.27				AGAGE, flask (Global)
		0.245	0.252	0.252	0.00	<i>n.s.</i>	<i>UEA, Cape Grim</i>
C <sub>7</sub> F <sub>16</sub>	PFC-61-16	0.11	0.12				AGAGE, flask (Global)
		<i>0.095</i>	<i>0.108</i>	<i>0.107</i>	<i>0.00</i>	<i>n.s.</i>	<i>UEA, Cape Grim</i>
C <sub>8</sub> F <sub>18</sub>	PFC-71-18	0.09	0.09				AGAGE, flask (Global)
<b>Other fluorinated compounds</b>							
SF <sub>6</sub>	Sulfur hexafluoride	6.42	7.28	7.58	0.30	4.1	AGAGE, in situ (Global)
		6.46	7.30	7.59	0.29	4.0	NOAA, flask & in situ (Global)

*(continued next page)*

Chemical Formula	Common or Industrial Name	Annual Mean Mole Fraction (ppt)			Change (2011–2012)		Network, Method
		2008	2011	2012	ppt yr <sup>-1</sup>	% yr <sup>-1</sup>	
NF <sub>3</sub>	Nitrogen trifluoride	0.59	0.86				AGAGE, flask (Global)
SO <sub>2</sub> F <sub>2</sub>	Sulfuryl fluoride	1.5	1.7	1.8	0.1	5.4	AGAGE, in situ (Global)
SF <sub>5</sub> CF <sub>3</sub>		<i>0.149</i>	<i>0.152</i>	<i>0.153</i>	<i>0.001</i>	n.s.	<i>UEA, Cape Grim</i>
<b>Other compounds</b>							
CH <sub>4</sub> (ppb)	Methane <sup>1</sup>	1787.9	1803.8	1808.9	5.1	0.28	AGAGE, in situ (Global)
		1787.4	1803.1	1808.3	5.2	0.29	NOAA, flask & in situ (Global)
		1785.3	1798.1	1807.5	9.4	0.52	UCI, flask (Global)
		1785.2	1802.9	1806.5	3.6	0.20	CSIRO, flask (Global)
N <sub>2</sub> O (ppb)	Nitrous oxide	321.6	324.1	325.0	0.85	0.26	AGAGE, in situ (Global)
		321.6	324.2	325.0	0.84	0.26	NOAA, flask & in situ (Global)
		321.4	324.0	324.9	0.93	0.29	CSIRO, flask (Global)
		321.7	324.2	325.1	0.9	0.28	WMO/GAW (Global)
COS (ppt)	Carbonyl sulfide	491	491	493	2	0.4	NOAA, flask & in situ (Global)

Mole fractions in this table represent independent estimates measured by different groups for the years indicated. Results indicated as “Global” are estimates of global surface mean mole fractions. Numbers in italics are from single sites that do not provide a global estimate.

Absolute changes (ppt yr<sup>-1</sup>) are calculated as the difference in annual means; relative changes (% yr<sup>-1</sup>) are the same difference relative to the average between 2011 and 2012 values. Small differences between values from previous Assessments are due to changes in calibration scale and methods for estimating global mean mole fractions from a limited number of sampling sites. n.s.: not significant.

These observations are updated from the following sources: Prinn et al. (2000); O’Doherty et al. (2004); Simpson et al. (2004); Montzka et al. (2007); Simpson et al. (2007); Miller et al. (2008); Montzka et al. (2009); Chevallier et al. (2010); Dlugokencky et al. (2011); Hall et al. (2011); Ivy et al. (2012a); Laube et al. (2012); Oram et al. (2012); Simpson et al. (2012); Sturges et al. (2012); Arnold et al. (2013); Thompson (2014).

AGAGE, Advanced Global Atmospheric Gases Experiment (<http://agage.eas.gatech.edu/>) with AGAGE calibrations as specified in CDIAC (2014) and related primary publications; NOAA, National Oceanic and Atmospheric Administration, U.S. (<http://www.esrl.noaa.gov/gmd/dv/site/>); UEA, University of East Anglia, United Kingdom (<http://www.uea.ac.uk/environmental-sciences/research/marine-and-atmospheric-sciences-group>); UCI, University of California, Irvine, U.S. ([http://ps.uci.edu/~rowlandblake/research\\_atmos.html](http://ps.uci.edu/~rowlandblake/research_atmos.html)); Cape Grim: Cape Grim Baseline Air Pollution Station, Australia; WMO/GAW, World Meteorological Organization, Global Atmosphere Watch, World Data Center for Greenhouse Gases, <http://ds.data.jma.go.jp/gmd/wdogg>.

<sup>1</sup>Global mean estimates for CH<sub>4</sub> from the WMO/GAW network are not included here because the criteria used for data selection in the WMO/GAW global mean mole fraction calculation are inconsistent with other global mean estimates shown. While NOAA, AGAGE, and CSIRO contribute data to the WMO/GAW network, the addition of inland and high-altitude sites in the WMO/GAW global mean leads to estimates for CH<sub>4</sub> that are ~11 ppb larger than those shown here.

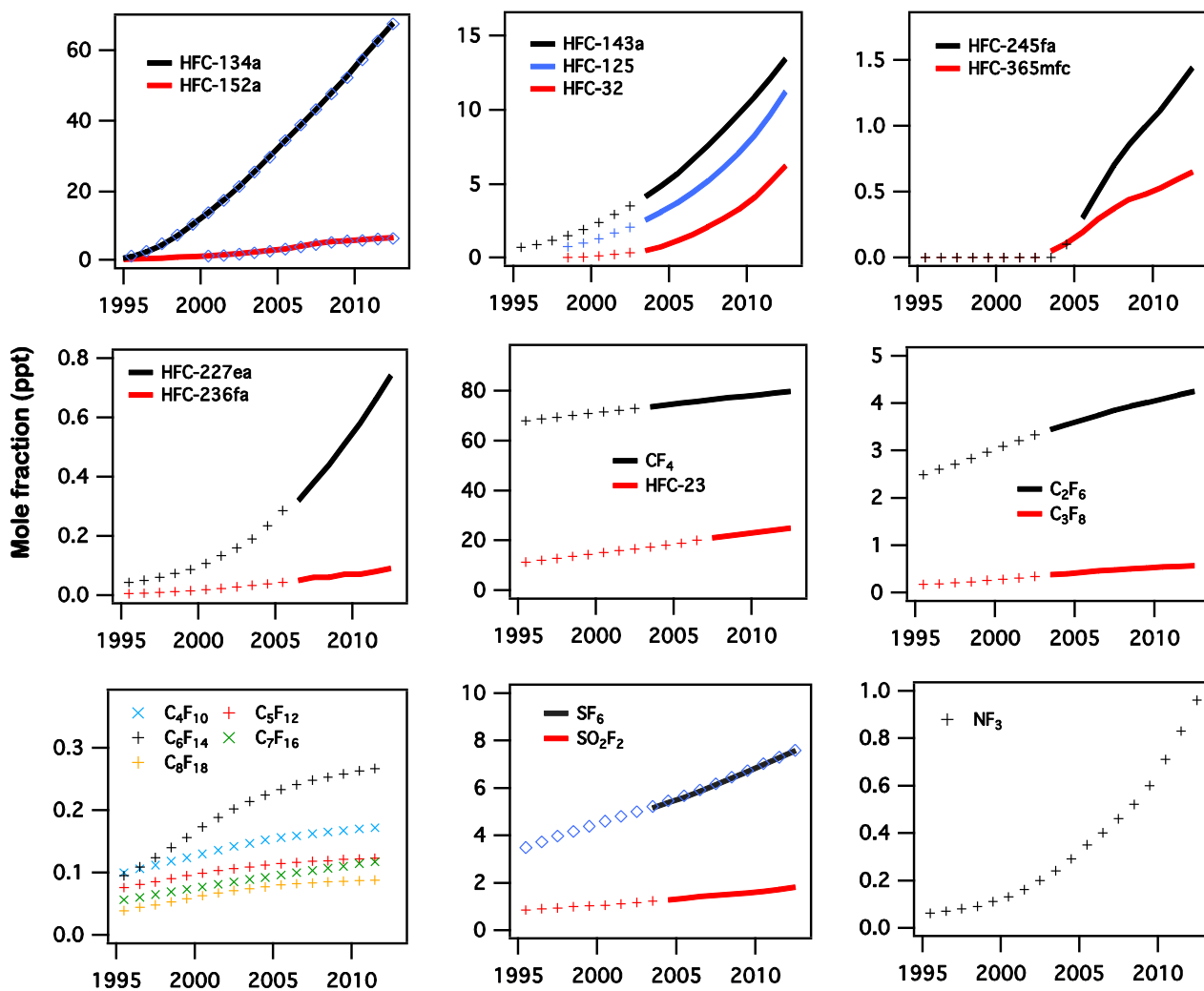


**Figure 1-24.** Global mole fractions of F-gases. Continuous measurements by the AGAGE network are shown as solid lines; NOAA data are shown by blue diamonds. Global mole fractions that have been compiled from grab samples or air archive measurements (e.g., from Cape Grim, Australia) are shown using additional symbols.

### HFC-23 (CHF<sub>3</sub>)

The mean global mole fraction of HFC-23 reached 25 ppt in 2012, and has increased at a rate of  $\sim 1$  ppt yr<sup>-1</sup> or 3.6% yr<sup>-1</sup> in recent years (Table 1-14). At this global abundance, HFC-23 contributed 4.5 mW m<sup>-2</sup> to the atmospheric radiative forcing in 2012. Trends of HFC-23 from ground-based measurements are similar to increases derived from remote sensing instruments (Harrison et al., 2012) (Table 1-2). However, calculated absolute mole fractions are around 30% higher from remote sensing data than from ground-based measurements.

HFC-23 is emitted into the atmosphere nearly exclusively as a by-product from over-fluorination during the production of HCFC-22, with only minor emissions from fire extinguishers, semiconductor industry, refrigeration, and as a feedstock for halon-1301 (Oram et al., 1998; Miller et al., 2010). Many HCFC-22 production facilities have destroyed the co-produced HFC-23 before it was emitted into the atmosphere or optimized the chemical process to minimize its formation (Miller et al., 2010; Han et al.,

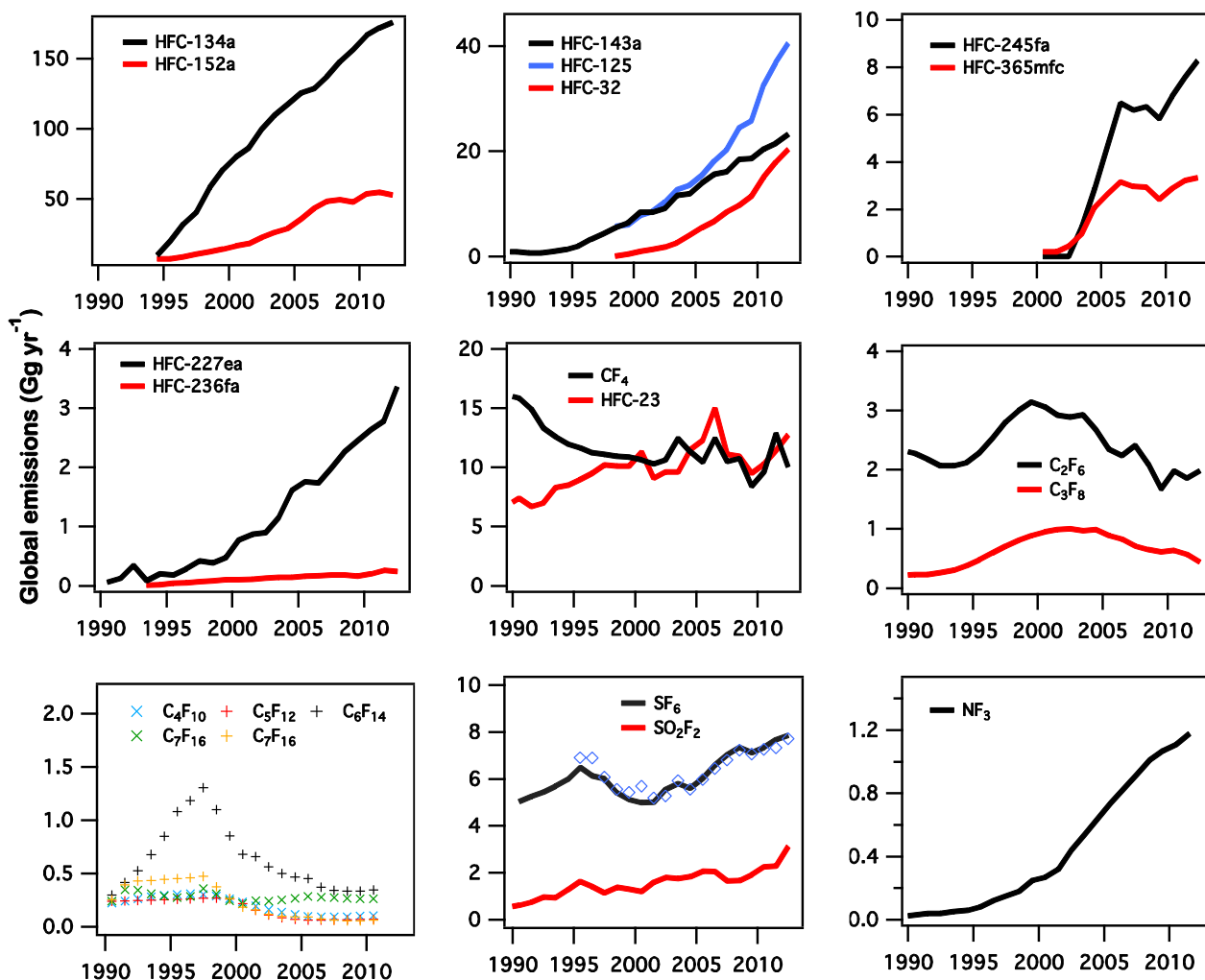


**Figure 1-25.** Global emissions of F-gases estimated by a global 12-box model (as described in Rigby et al. (2013)) using data shown in Figure 1-24 and lifetimes from SPARC (2013).

2012). For developing countries, this capability was facilitated by funding from the Clean Development Mechanism (CDM) under the Kyoto Protocol of the United Nations Framework Convention on Climate Change (UNFCCC).

Global emissions of HFC-23 estimated from measured and derived atmospheric trends reached a maximum of 15 Gg yr<sup>-1</sup> in 2006, fell back to 8.6 Gg in 2009, and subsequently increased again to 12.8 Gg in 2012 (Figure 1-25, update of Miller et al., 2010 and Montzka et al., 2010). Whereas efforts in non-Article 5 countries mitigated an increasing portion of HFC-23 emissions through 2004, the temporal decrease from 2007 to 2009 was likely caused by destruction facilitated by the CDM, even though HCFC-22 production was highest around this time (Figure 1-8). The recent resurgence in emissions since 2009 could be the result of an increase in production of HCFC-22 (see Figure 1-8) with no subsequent incineration of HFC-23 (reference case in Miller and Kuijpers, 2011), or less CDM-aided destruction of existing production in developing countries. Indeed, Miller and Kuijpers (2011) warned that HFC-23 emissions could surpass the historic peak values from 2006 if CDM projects ceased to be supported and feedstock production of HCFC-22 grows unabated.

Current emissions of HFC-23 occur foremost in East Asia. Studies from Yokouchi et al. (2006), Stohl et al. (2010), and Kim et al. (2010) estimate emissions in China to be in the range of 6 to 12 Gg yr<sup>-1</sup> between 2004 and 2008. In contrast, Yao et al. (2012) estimated lower emissions of only 2.8 Gg yr<sup>-1</sup> for China in 2010–2011, based on measurements at one site and a limited catchment area. In Europe, underreported emissions of HFC-23 from some HCFC-22 production facilities were found by Keller et al. (2011), but the difference of around 0.2 Gg yr<sup>-1</sup> was small in comparison to global sources.

#### **HFC-152a (CH<sub>3</sub>CHF<sub>2</sub>)**

HFC-152a is used as a foam-blowing agent and as an aerosol propellant (Grealley et al., 2007). Its growing average global mole fraction reached 6.8 ppt in 2012. The global mole fraction of HFC-152a grew at an average rate of  $0.69 \pm 0.04$  ppt yr<sup>-1</sup> from 2005–2008, but has slowed since 2008 to around 0.28 ppt yr<sup>-1</sup> (Figure 1-24, Table 1-14). Global emissions derived from measured global mole fractions and trends appear to have stabilized at ~50 Gg yr<sup>-1</sup> since 2010 (Figure 1-25). HFC-152a has a relatively small GWP<sub>100</sub> (of 133; Chapter 5) and its direct radiative forcing is small compared to other HFCs.

Currently the U.S. is the world's most important source region for HFC-152a. Estimated U.S. emissions range from 25 (11–50) Gg yr<sup>-1</sup> between 2004–2009 (Miller et al., 2012), to 12.3–15.1 Gg yr<sup>-1</sup> in 2006 (Stohl et al., 2009), to 32 Gg yr<sup>-1</sup> in 2008 (Barletta et al., 2011). European emissions were estimated to be 2.9 Gg in 2009 (Keller et al., 2012). Emissions from China were estimated to be 2.0–2.9 Gg yr<sup>-1</sup> in 2010–2011 by Yao et al. (2012), which was lower than 3.4–5.7 Gg yr<sup>-1</sup> estimated by Yokouchi et al. (2006), Kim et al. (2010), and Stohl et al. (2010) in former years.

#### **HFC-32 (CH<sub>2</sub>F<sub>2</sub>), HFC-125 (CHF<sub>2</sub>CF<sub>3</sub>), HFC-143a (CH<sub>3</sub>CF<sub>3</sub>)**

These three HFCs are mostly used as refrigerants. They are blended in various combinations, for stationary air conditioners as well as for various minor applications (e.g., for fire suppression) replacing HCFC-22 and CFC-115 (IPCC/TEAP, 2005; O'Doherty et al., 2009). Global background mole fractions of HFC-32, HFC-125, and HFC-143a are steadily growing (Table 1-14, Figure 1-24). Current annual growth rates of more than 1 ppt yr<sup>-1</sup> are among the highest for all F-gases, showing the importance of these refrigeration blends in connection with the phase-out of ozone-depleting HCFCs and CFCs. Global estimates of their emissions in 2012 were 19 Gg yr<sup>-1</sup>, 40 Gg yr<sup>-1</sup>, and 24 Gg yr<sup>-1</sup> for HFC-32, HFC-125, and HFC-143a, respectively. During 2009–2012 the emissions approximately doubled for HFC-32 and HFC-125, and increased by ~50% for HFC-143a. The combined radiative forcing of these three substances was 5.4 mW m<sup>-2</sup> in 2012, with highest impact from HFC-125 (2.6 mW m<sup>-2</sup>).

Regional emissions of these three gases have been estimated by several studies in recent years (2004–2011). However, differing time periods and the rapid increase of emissions hinder the direct comparison with total global emission estimates. Estimated emissions from the last decade from East Asia as estimated by Li et al. (2011) and Yao et al. (2012) were of the same order of magnitude as estimated emissions from Europe (O'Doherty et al., 2009; Keller et al., 2012) and from the U.S. (Miller et al., 2012) for different years during this same period.

#### **HFC-245fa (CF<sub>3</sub>CH<sub>2</sub>CHF<sub>2</sub>) and HFC-365mfc (CF<sub>3</sub>CH<sub>2</sub>CF<sub>2</sub>CH<sub>3</sub>)**

HFC-245fa and HFC-365mfc are replacements for HCFC-141b in foam-blowing applications (Vollmer et al., 2006; Stemmler et al., 2007; Vollmer et al., 2011). In 2012 global average mole fractions reached 1.44 and 0.65 ppt for HFC-245fa and HFC-365mfc (Table 1-14), respectively, and were increasing between 2011–2012 at similar rates of 12% and 10% (Table 1-14). The approximately factor-of-two difference in the global mean mole fractions for these two compounds is also reflected in the 2011–2012 growth rates of 0.17 ppt and 0.07 ppt for HFC-245fa and HFC-365mfc, respectively. Global atmospheric-derived emissions of HFC-245fa and HFC-365mfc leveled off after 2006 but showed a renewed increase since 2010 and reached 8.2 Gg yr<sup>-1</sup> for HFC-245fa and 3.1 Gg yr<sup>-1</sup> for HFC-365mfc by 2012 (Figure 1-25).

**HFC-227ea (CF<sub>3</sub>CHF<sub>2</sub>CF<sub>3</sub>)**

HFC-227ea is used in fire suppression, metered dose inhalers, refrigeration, and foam blowing. Vollmer et al. (2011) recently used archived air from both hemispheres to reconstruct the atmospheric history of HFC-227ea. They inferred that the global background mole fraction of HFC-227ea has grown from less than 0.1 ppt in the 1990s to 0.58 ppt in 2010 and that the annual growth rate of HFC-227ea increased from 0.026 ppt yr<sup>-1</sup> in 2000 to 0.069 ppt yr<sup>-1</sup> in 2010 (Vollmer et al., 2011). Global emissions were estimated to be 2.5 Gg yr<sup>-1</sup> in 2010. These results were confirmed by firm air samples from Greenland (Laube et al., 2010), which showed similarly low mole fractions in the 1990s and increasing global emissions of nearly 2 Gg yr<sup>-1</sup> in 2007. In 2012 the global background mole fraction was 0.74 ppt (Table 1-14) and global emissions were estimated at 3.3 Gg yr<sup>-1</sup> (Figure 1-25).

**HFC-43-10mee (CF<sub>3</sub>CF<sub>2</sub>CHFCH<sub>2</sub>CF<sub>3</sub>)**

HFC-43-10mee is used as a cleaning solvent in the electronics industry. First published measurements by Arnold et al. (2014) show a rising global mean mole fraction between 2000 and 2012 (0.04 ± 0.03 ppt to 0.21 ± 0.05 ppt). Based on these measurements, global emissions were estimated as 1.13 ± 0.31 Gg yr<sup>-1</sup> in 2012.

**HFC-1234yf (CH<sub>2</sub>=CF<sub>2</sub>CF<sub>3</sub>) and HFC-1234ze(E) (E-CHF=CHCF<sub>3</sub>)**

HFC-1234yf and HFC-1234ze(E) are unsaturated hydrofluorocarbons (also referred to as hydrofluoro-olefins, HFOs) with estimated tropospheric OH-lifetimes of 8–16 days and 13–24 days, respectively (Table 1-11). These substances have small Global Warming Potentials (GWPs) and are therefore considered as replacement compounds for long-lived HFCs with high GWPs. Whereas HFC-1234ze(E) is already used for foam blowing, HFC-1234yf has only recently been accepted as a replacement for HFC-134a in mobile air conditioners and other refrigeration uses (UNEP, 2011a) (Chapter 5).

Although these unsaturated HFCs degrade within days to weeks in the troposphere, there are concerns regarding the impact of their degradation products on the environment. Whereas HFC-1234ze(E) degrades to short-lived intermediates, the atmospheric degradation of HFC-1234yf almost exclusively yields trifluoroacetic acid (CF<sub>3</sub>C(O)OH, TFA) (Hurley et al., 2008). TFA is resistant to further degradation in the environment and exhibits some herbicidal properties (Boutonnet et al., 1999). Under an upper-limit scenario of full replacement of HFC-134a by HFC-1234yf, Henne et al. (2012) and Pappasavva et al. (2009) estimate that European and U.S. emissions of HFC-1234yf could reach ~20 Gg yr<sup>-1</sup> and 11–25 Gg yr<sup>-1</sup>, respectively. There is currently no imminent danger connected to this potential input of TFA into the environment (Chapter 5). Accumulation of TFA in specific biomes from the long-term usage of HFC-1234yf is discussed in Cahill et al. (2001) and Russell et al. (2012).

**Perfluorocarbons (PFCs)**

Perfluorocarbons (PFCs) exclusively consist of carbon and fluorine. They are not substitutes for ODSs, and they have very long atmospheric lifetimes of up to several thousand years (Table 1-3). In combination with their very large radiative efficiencies, they will have a long-lasting influence on the radiative balance of the atmosphere (Ravishankara et al., 1993; Myrhe et al., 2013). The combined radiative forcing of the PFCs was 6.0 mW m<sup>-2</sup> in 2012, with CF<sub>4</sub> as the main contributor.

Four PFCs were reported in the last Assessment (PFC-14 or CF<sub>4</sub>, PFC-116 or C<sub>2</sub>F<sub>6</sub>, PFC-218 or C<sub>3</sub>F<sub>8</sub>, and PFC-c-318 or c-C<sub>4</sub>F<sub>8</sub>). Ground-based mole fractions and growth rates for CF<sub>4</sub>, C<sub>2</sub>F<sub>6</sub>, and C<sub>3</sub>F<sub>8</sub> were updated from Mühle et al. (2010) and are shown in Table 1-14 and Figure 1-24. CF<sub>4</sub> observations based on remote-sensing techniques (Mahieu et al., 2014) find a comparable trend in the atmospheric abundance as for the ground-based measurements (Table 1-2). Furthermore, mole fractions and trends of c-C<sub>4</sub>F<sub>8</sub> have been updated by Saito et al. (2010) and Oram et al. (2012), with a global mole fraction in 2012 estimated at 1.24 ppt (Table 1-14) and estimated global emissions of 1.1 Gg yr<sup>-1</sup> in 2007 (Oram et al., 2012). PFC-218 was shown to be a minor PFC emission from aluminium smelting, the major PFCs being PFC-14 and PFC-116 (Fraser et al., 2013).

Since the previous Assessment, atmospheric mole fractions and emissions have been newly reported for n-C<sub>4</sub>F<sub>10</sub>, n-C<sub>5</sub>F<sub>12</sub>, n-C<sub>6</sub>F<sub>14</sub>, n-C<sub>7</sub>F<sub>16</sub>, and n-C<sub>8</sub>F<sub>18</sub> in three recent publications (Ivy et al., 2012a, 2012b; Laube et al., 2012). As shown in Table 1-14, the mole fractions of all five long-chain PFCs are currently below 0.3 ppt. Their current growth rates are small and have continued to decrease in recent years, which could be due to the introduction of emission reduction techniques in industrial applications (Tsai et al., 2002). With nearly 1.5 Gg yr<sup>-1</sup> in the 1990s highest emissions from these group of compounds was reached by n-C<sub>6</sub>F<sub>14</sub> (Figure 1-25). In recent years emissions of all these PFCs were stable and smaller than 0.5 Gg yr<sup>-1</sup>.

Lifetime estimates for the perfluorocarbons (PFCs) C<sub>3</sub>F<sub>8</sub>, c-C<sub>3</sub>F<sub>6</sub>, and C<sub>4</sub>F<sub>10</sub> were revised in this Assessment (Table 1-3). PFCs are persistent greenhouse gases removed primarily in the upper-stratosphere and mesosphere (>65 km) mainly by Lyman- $\alpha$  (121.6 nm) photolysis. Lifetime estimates for PFCs (>2000 yr) are typically obtained from model calculations and are highly dependent on transport from the lower atmosphere. The revised lifetime estimates of these three PFCs shown in Table 1-3 are based on a correlation of an increase in Lyman- $\alpha$  absorption cross section with an increase in the -CF<sub>2</sub>-sub-units within the molecule. Baasandorj et al. (2012) reported improved upper-limits for O(<sup>1</sup>D) reactive rate coefficients for C<sub>2</sub>F<sub>6</sub>, c-C<sub>4</sub>F<sub>8</sub>, n-C<sub>5</sub>F<sub>12</sub>, and n-C<sub>6</sub>F<sub>14</sub>, which reduces the calculated contribution of O(<sup>1</sup>D) reaction to their atmospheric loss further from the rate coefficient studies of Zhao et al. (2010) and Ravishankara et al. (1993). Furthermore, the lifetime for C<sub>8</sub>F<sub>18</sub> was estimated to be ~3000 years by (Ivy et al., 2012a), which was adopted in this Assessment.

### **Sulfur hexafluoride (SF<sub>6</sub>)**

The global average mole fraction of sulfur hexafluoride (SF<sub>6</sub>) continues to increase, and reached 7.6 ppt in 2012 (Table 1-14). The global average mole fraction at the surface was increasing at ~0.22 ppt yr<sup>-1</sup> in the early 2000s, but has averaged ~0.28 ppt yr<sup>-1</sup> since 2007 (Rigby et al., 2010; Hall et al., 2011). Due to its long lifetime (3200 years; Table 1-3) combined with a high radiative efficiency, the contribution of SF<sub>6</sub> to radiative forcing is increasing accordingly. The resulting radiative forcing in 2012 was 4.3 mW m<sup>-2</sup>.

Remote sensing techniques have also contributed to the monitoring of SF<sub>6</sub> over the recent years. Brown et al. (2011) using ACE-FTS data, Stiller et al. (2012) using MIPAS global data, and Zander et al. (2008) using ground-based solar spectroscopy at Jungfraujoch all found growth rates which were comparable with the in-situ measurements (Table 1-2).

Global atmospheric-based emissions of SF<sub>6</sub> were estimated by Levin et al. (2010) and Rigby et al. (2010) at 7.2–7.5 Gg yr<sup>-1</sup> in 2008. Emissions since then have increased and were at their highest historic levels in 2012 at almost 8 Gg yr<sup>-1</sup> in 2012 (Figure 1-25). Rigby et al. (2010) found that the rise in global emissions from 2004–2008 was likely mostly due to emissions from Asian developing countries. Consistent with this, Fang et al. (2013) estimated the contribution from East Asia to SF<sub>6</sub> emissions to be 3.8 ± 0.5 Gg yr<sup>-1</sup> in 2009, or a contribution of about 50% to global SF<sub>6</sub> emissions. In addition, based on an extrapolation of results from the northeastern U.S. only, Miller et al. (2012) reported U.S. emissions of 1.4 (0.7–3.0) Gg yr<sup>-1</sup> from 2004–2009, which is equivalent to about 20% of global emissions in 2008.

### **Trifluoromethylsulfurpentafluoride (SF<sub>5</sub>CF<sub>3</sub>)**

This substance was discovered in the atmosphere by Sturges et al. (2000), with a global background mole fraction of 0.12 ppt in 1999 and 0.15 ppt in 2010 (Sturges et al., 2012). SF<sub>5</sub>CF<sub>3</sub> is very long lived, with an estimated lifetime of 650–950 years (Table 1-3). SF<sub>5</sub>CF<sub>3</sub> levels have been stable in recent years and therefore Sturges et al. (2012) concluded that emission sources have ceased. They provide strong indications that SF<sub>5</sub>CF<sub>3</sub> was released as a by-product of the production of perfluorooctanyl sulfonate (PFOS) and similar compounds. Furthermore, they used firm air measurements to place the onset of SF<sub>5</sub>CF<sub>3</sub> emissions in the early 1960s. Baasandorj et al. (2012) reported improved upper limits for the O(<sup>1</sup>D) reactive rate coefficient of SF<sub>5</sub>CF<sub>3</sub>, thereby enhancing knowledge of its atmospheric loss processes from previous studies but not changing its lifetime estimate (Ravishankara et al., 1993; Zhao et al., 2010).

**Nitrogen trifluoride (NF<sub>3</sub>)**

NF<sub>3</sub> is used in the production of flat panel displays, in plasma etching, and in the semiconductor industry as a replacement for PFCs (Weiss et al., 2008; Fthenakis et al., 2010). It was first measured in the atmosphere by Weiss et al. (2008). The measured record was recently extended and revised with a new calibration (Arnold et al., 2012, 2013). Its global tropospheric mole fraction was  $0.86 \pm 0.04$  ppt in 2011 (Table 1-14) with a yearly rate of increase of  $0.10 \pm 0.01$  ppt (11%) between 2010 and 2011.

Global emissions of NF<sub>3</sub> increased continuously from 0.21 Gg yr<sup>-1</sup> in 1998 to 1.18 Gg yr<sup>-1</sup> in 2011 (Arnold et al., 2013; Figure 1-25). With a radiative forcing of just 0.2 mW m<sup>-2</sup>, the effect of NF<sub>3</sub> on climate was still very small in 2011. However, its large atmospheric growth rate and its application in the growing semiconductor industry have a high potential to increase its importance in the future. Therefore, NF<sub>3</sub> was added to the basket of greenhouse gases in the Doha Amendment to the Kyoto Protocol, which covers emissions in a second commitment period of 2013–2020 (UNFCCC, 2014).

The NF<sub>3</sub> lifetime estimate was revised in SPARC (2013) to 569 (454–764) years based on 2-D model calculations that included the NF<sub>3</sub> UV absorption spectrum temperature dependence reported by Papadimitriou et al. (2013a). SPARC (2013) also recommended a revision of the O(<sup>1</sup>D) + NF<sub>3</sub> reaction rate coefficient, although the impact of the revision on the NF<sub>3</sub> lifetime is minor.

**Sulfuryl fluoride (SO<sub>2</sub>F<sub>2</sub>)**

Sulfuryl fluoride (SO<sub>2</sub>F<sub>2</sub>) replaced the ozone-depleting CH<sub>3</sub>Br as a fumigant against animal pests in buildings and other places susceptible to infestation (e.g., flour mills, grain silos, transport containers). The average global mole fraction of SO<sub>2</sub>F<sub>2</sub> has increased to 1.8 ppt in 2012, with a yearly increase (2011–2012) of 0.1 ppt (5%) (update of Mühle et al., 2009; Table 1-14). The total atmospheric lifetime of SO<sub>2</sub>F<sub>2</sub> is  $36 \pm 11$  yr (Mühle et al., 2009), with a partial lifetime for the oceanic uptake of  $40 \pm 13$  yr as its most important contributor. Global emissions calculated from atmospheric observations and the estimated lifetime were 3.1 Gg in 2012. This is an increase of nearly a factor of two in comparison with 2008.

**1.5.1.2 NITROUS OXIDE (N<sub>2</sub>O)**

Nitrous oxide (N<sub>2</sub>O) has both natural and anthropogenic sources and unlike most other chemicals discussed in this section, it has a direct chemical influence on ozone (Ravishankara et al., 2009). The influence of N<sub>2</sub>O on stratospheric ozone and on climate has been the focus of a recent review (UNEP, 2013c). Photochemical degradation of N<sub>2</sub>O in the stratosphere leads predominately to N<sub>2</sub> and O<sub>2</sub>, but about 10% is converted to nitrogen oxides (NO, NO<sub>2</sub>) (UNEP, 2013c), which contribute to stratospheric ozone depletion. Current ODP-weighted emissions of N<sub>2</sub>O from anthropogenic activities are larger than those of any other ozone-depleting species (Ravishankara et al., 2009). Nitrous oxide is also a greenhouse gas, and with the atmospheric burden of CFC-12 decreasing, both of these gases contribute about equally to radiative forcing (Myhre et al., 2013) and are after CO<sub>2</sub> and CH<sub>4</sub> the most important anthropogenic greenhouse gases.

Atmospheric N<sub>2</sub>O has increased from a pre-industrial mole fraction of 271 ppb (Ciais et al., 2013) to 325 ppb in 2012 (Table 1-14) with a fairly constant growth rate of 0.8 ppb yr<sup>-1</sup> over the last decade (3.4 ppb between 2008 and 2012). According to UNEP (2013c), current natural emissions (e.g., from terrestrial, marine, and atmospheric sources) are roughly 11 Tg N<sub>2</sub>O-N yr<sup>-1</sup>. Total gross anthropogenic emissions are estimated to contribute another 6.2 Tg N<sub>2</sub>O-N yr<sup>-1</sup>. Anthropogenic sources include agriculture, biomass burning, and industry (including combustion, production of nitric acid and adipic acid), as well as indirect emissions from reactive nitrogen leaching, runoff, and atmospheric deposition. The observed increase in atmospheric N<sub>2</sub>O over preindustrial levels is largely the result of nitrogen-based fertilizer use (Park et al., 2012). Ciais et al. (2013) have estimated that food production was likely responsible for 80% of the increase in atmospheric N<sub>2</sub>O in recent decades.

The IPCC AR5 report lists total global N<sub>2</sub>O emissions of 17.8 Tg-N yr<sup>-1</sup> in 2006 (Ciais et al., 2013). This value is consistent with global emissions of 17.5 to 20.1 Tg-N yr<sup>-1</sup> estimated between 1999 and 2009 (calculated from atmospheric observations and the estimated lifetime (Thompson et al., 2014)), and also with bottom-up estimates of 17.6 Tg-N yr<sup>-1</sup> from UNEP (2013c). There are, however, substantial

uncertainties associated with both bottom-up and top-down emissions estimates due to uncertain emission factors (bottom-up) and uncertainties in the stratospheric sink (top-down). Revision of emissions factors between AR4 and AR5 resulted in reapportionment of global emissions among anthropogenic sources, but did not significantly affect the global total (Ciais et al., 2013). The global lifetime of N<sub>2</sub>O has also recently been updated from 114 yr to 123 yr with a range of 104–152 yr (SPARC, 2013).

### 1.5.1.3 METHANE (CH<sub>4</sub>)

In addition to its influence on radiative forcing, methane affects the efficiency for ODSs to deplete stratospheric ozone by acting as a sink for reactive chlorine (producing HCl as a reservoir species) and as a source of stratospheric water vapor. In the upper stratosphere, enhanced CH<sub>4</sub> concentrations lead to ozone loss through the HO<sub>x</sub> catalytic cycle, but also reduce ozone loss by sequestering reactive chlorine. In the lower stratosphere and troposphere, additional CH<sub>4</sub> leads to more ozone through photochemical smog chemistry and CH<sub>4</sub> also reacts with OH radicals, which leads to an influence on the lifetimes of ODSs that also react with OH (such as HCFCs and VSLS). In general, an increase in global CH<sub>4</sub> results in an increase in column ozone (Portmann et al., 2012; Revell et al., 2012; Shindell et al., 2013).

Wetlands are the primary natural source of CH<sub>4</sub>, with smaller contributions from sources such as geological seeps and freshwater (Ciais et al., 2013). Anthropogenic sources include agriculture (e.g., rice production, ruminants), landfills, biomass burning, and the extraction and processing of fossil fuels (Kirschke et al., 2013). The global mean mole fraction of CH<sub>4</sub> was 1803 ppb in 2011 (Hartmann et al., 2013) and 1808 ppb in 2012 (Table 1-14). Mole fractions today are more than 2 times greater than those in preindustrial times (1750) (Hartmann et al., 2013). After increasing from ~1750 to the 1980s, global CH<sub>4</sub> mole fractions increased more slowly in the late 1990s and started to stabilize in the early 2000s, but increased again from 1781 ppb in 2007 to 1808 ppb in 2012. Reasons for the growth rate slow-down in the 1990s and renewed increase beginning in 2007 are debated (Rigby et al., 2008; Dlugokencky et al., 2009; Aydin et al., 2011; Bousquet et al., 2011; Kai et al., 2011; Levin et al., 2012; Simpson et al., 2012; Kirschke et al., 2013). The subsequent increase of global CH<sub>4</sub> levels since 2006 is likely due to increased emissions from natural wetlands and fossil fuels, although their relative contributions remain uncertain (Kirschke et al., 2013).

### 1.5.1.4 COS, SO<sub>2</sub>

Carbonyl sulfide (COS) and other sulfur-containing gases such as sulfur dioxide (SO<sub>2</sub>) contribute to stratospheric sulfate aerosols (SSA) (SPARC, 2006).

Sources of SO<sub>2</sub> include fossil fuel combustion, volcanoes, and oxidation of precursors. Fossil fuel combustion accounts for the largest part of the total flux of sulfur gases to the atmosphere, mainly from sources in the Northern Hemisphere (SPARC, 2006). While SO<sub>2</sub> emissions were reduced in the U.S. and Europe in the 1980s and 1990s as part of efforts to reduce acid rain, emissions from East Asia have increased in recent years (Lu et al., 2010).

Sources of COS include the oxidation of dimethyl sulfide (DMS) and carbon disulfide (CS<sub>2</sub>), and ocean-atmosphere gas exchange (SPARC, 2006). Sinks of COS include uptake by terrestrial plants and soils, and oxidation by OH radicals. Current tropospheric mole fractions of COS (~490 ppt, Table 1-14) are substantially higher than preindustrial values of 300–400 ppt (Montzka et al., 2004). Total column COS measurements above Jungfraujoch indicate a decrease in the total column from 1990–2002 followed by an increase from 2002–2008 (update from Zander et al., 2005). A relatively small trend in global COS derived from surface observations (1.8 ppt yr<sup>-1</sup>) was reported in the last Assessment for the period 2000–2008 (Montzka and Reimann et al., 2011). Recent observations from the NOAA surface network updated through 2012 suggest that any systematic changes in global COS since 2000 have been small (<3%), with an increase of 0.4% from 2011–2012 (Table 1-14).

The fraction of COS contributing to SSA is uncertain, but could be about 30% (SPARC, 2006). This is supported by recent work by Hattori et al. (2011), Brühl et al. (2012), and Schmidt et al. (2013). However, it is not yet possible to reconcile these studies with an earlier study from Leung et al. (2002), who concluded that COS is only a minor contributor to SSA.

## 1.6 POLICY-RELEVANT INFORMATION HIGHLIGHTS

### 1.6.1 HCFCs Becoming a Larger Fraction of Tropospheric Chlorine; Bromine from Halons Now Decreasing

As a result of the Montreal Protocol, the overall abundance of controlled ozone-depleting substances (ODSs) in the atmosphere has been decreasing for over 15 years. The reduction in the atmospheric abundance of an ODS in response to controls on production depends principally on two factors: (1) how rapidly an ODS is used and released to the atmosphere after being produced and (2) the lifetime for the removal of the ODS from the atmosphere. Much of the decline in tropospheric chlorine since the peak in the 1990s was due to decreases in methyl chloroform ( $\text{CH}_3\text{CCl}_3$ ), which has a relatively short atmospheric lifetime of about 5 years. This substance still continues to make a significant contribution to declines in total chlorine, although decreases in chlorofluorocarbons (CFCs) are now the largest contributor. Hydrochlorofluorocarbon (HCFC) mixing ratios continue to increase, although at a declining rate.

CFCs still represent the largest fraction of tropospheric chlorine, but their contribution has been decreasing since 2005. The rapid decrease of  $\text{CH}_3\text{CCl}_3$  in the atmosphere means that its relative contribution to the tropospheric ODS abundance is now approaching zero. Since the peak in total tropospheric chlorine, the relative contribution of carbon tetrachloride ( $\text{CCl}_4$ ) has not changed significantly, due to its relatively slow decline. The abundance of methyl chloride ( $\text{CH}_3\text{Cl}$ ), the largest natural contributor to chlorine, has remained fairly constant over the last decades, currently contributing around 17% of tropospheric chlorine. A large proportional change to the total chlorine-containing ODS abundance however comes from HCFCs; their contribution has more than doubled since the mid 1990s.

The largest contributor to the decline in tropospheric bromine is methyl bromide ( $\text{CH}_3\text{Br}$ ), which has both natural and anthropogenic sources. The rate of  $\text{CH}_3\text{Br}$  decline has slowed as phase out of controlled emissions is now almost complete, and the balance of emissions is now overwhelmingly of natural origin, with the remainder mostly from non-controlled emissions. While the contribution of halons to total tropospheric bromine has increased since the mid-1990s, bromine from halons is now showing robust signs of decline. Natural sources contribute over half of the abundance of total tropospheric bromine.

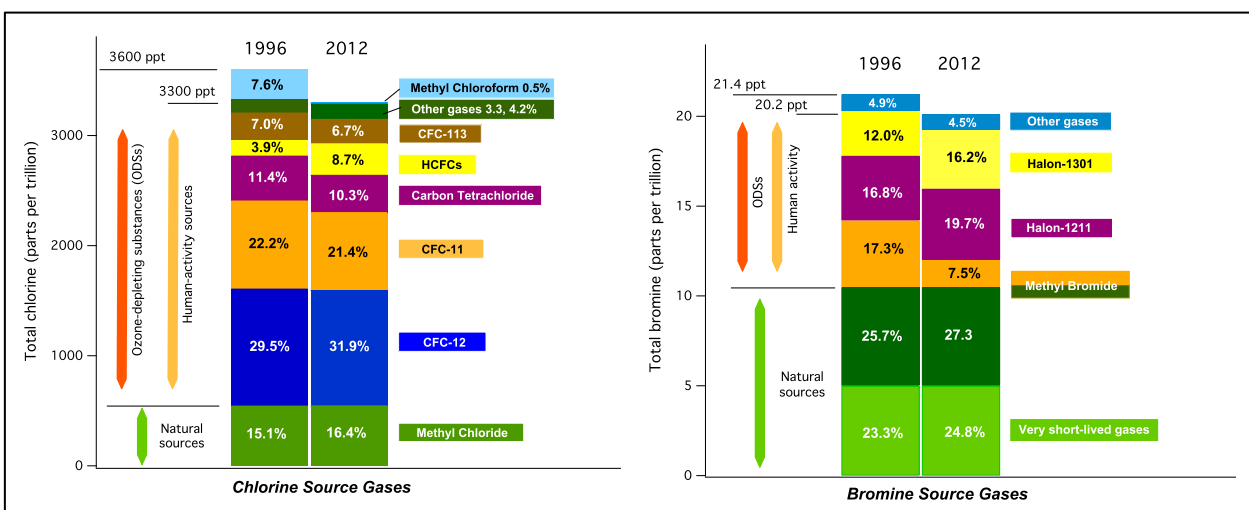


**Figure 1-6-1.** Relative contribution to total tropospheric chlorine and total tropospheric bromine from individual and groups of compounds in 1996 and 2012. The sum of very short-lived species ( $\text{CH}_2\text{Cl}_2$ ,  $\text{CHCl}_3$ ,  $\text{C}_2\text{Cl}_4$ ,  $\text{COCl}_2$ ) is shown as “other gases” for chlorine, while halon-1202 and halon-2402 are included as “other gases” for bromine.

### 1.6.2 VLSL Chlorinated Compounds Become More Relevant for Stratospheric Ozone

The current (2008–2012) increase in tropospheric very short-lived substance (VSL) chlorine source gases is  $\sim 1.3 \pm 0.3$  ppt Cl yr<sup>-1</sup>, compared to the decline in long-lived controlled chlorinated substances of  $13.4 \pm 0.9$  ppt Cl yr<sup>-1</sup>. Averaged over the longer time period of 2004–2013, the combined trend of the three major VSL chlorine source gases CH<sub>2</sub>Cl<sub>2</sub>, C<sub>2</sub>Cl<sub>4</sub>, and CHCl<sub>3</sub> is  $1.8 \pm 0.2$  ppt Cl yr<sup>-1</sup> (Figure 1-6-2). Increased levels of dichloromethane (CH<sub>2</sub>Cl<sub>2</sub>), which has predominantly anthropogenic sources, account for the majority of this change. The globally averaged surface abundance of CH<sub>2</sub>Cl<sub>2</sub> has increased by  $\sim 60\%$  over the last decade. The majority ( $>80\%$ ) of VSL chlorinated gases and associated product gases are expected to reach the stratosphere, based upon observed vertical profiles of CH<sub>2</sub>Cl<sub>2</sub> and model calculations of CH<sub>2</sub>Br<sub>2</sub>, a gas with a similar atmospheric lifetime.

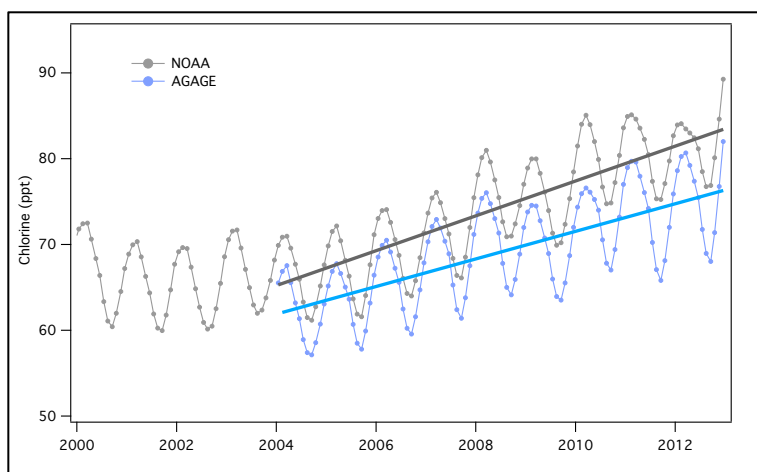


**Figure 1-6-2.** Average global, monthly mean values of total tropospheric chlorine from three VSL gases (CH<sub>2</sub>Cl<sub>2</sub>, C<sub>2</sub>Cl<sub>4</sub>, and CHCl<sub>3</sub>) derived from 12-box model output using NOAA and AGAGE data (Simmonds et al., 2006; Montzka et al., 2011). Linear fits are shown as the thicker lines, starting 2004. The trend from AGAGE:  $1.6 \pm 0.2$  ppt Cl yr<sup>-1</sup>; from NOAA:  $2.0 \pm 0.2$  ppt Cl yr<sup>-1</sup>; average trend:  $1.8$  ppt Cl yr<sup>-1</sup>. A constant 21 ppt, derived from AGAGE data, was used to represent the contribution of CHCl<sub>3</sub>.

### 1.6.3 Radiative Forcing of ODSs and ODS Replacement Compounds

#### *Update on the effect on the radiative budget of F-gases*

In Figure 1-6-3 the radiative forcing values for ODSs and F-gases (source gases with fluorine as the only halogen attached either to carbon, sulfur, or nitrogen; also called Kyoto Protocol synthetics) are compared against those of carbon dioxide (CO<sub>2</sub>), methane (CH<sub>4</sub>), and nitrous oxide (N<sub>2</sub>O). In 2012 the total contribution from the F-gases was  $33 \text{ mW m}^{-2}$ , with  $22 \text{ mW m}^{-2}$  from hydrofluorocarbons (HFCs),  $6 \text{ mW m}^{-2}$  from perfluorocarbons (PFCs), and  $5 \text{ mW m}^{-2}$  from SF<sub>6</sub>, SO<sub>2</sub>F<sub>2</sub>, and NF<sub>3</sub>. The most important single HFC in terms of climate forcing in 2012 was the cooling agent HFC-134a. However, other HFCs used in cooling applications, such as HFC-125, HFC-32, and HFC-143a, are increasing and the sum of their radiative forcing surpassed that of HFC-23 (a by-product of HCFC-22 production) and is now equal to the sum of the PFCs. Radiative forcing from SF<sub>6</sub> has continued its growth at a stable rate of  $0.16\text{--}0.17 \text{ mW yr}^{-1}$  in recent years. SO<sub>2</sub>F<sub>2</sub> and NF<sub>3</sub> currently contribute very little to climate forcing.

In 2012 the total contribution of the F-gases was still small in comparison to the total anthropogenic-induced climate forcing due to the major greenhouse gases ( $1850 \text{ mW m}^{-2}$  for CO<sub>2</sub>,  $490 \text{ mW m}^{-2}$  for CH<sub>4</sub>, and  $170 \text{ mW m}^{-2}$  for N<sub>2</sub>O) and also compared to the total ODS contribution ( $330 \text{ mW m}^{-2}$ ), which has remained virtually stable since the last Assessment.

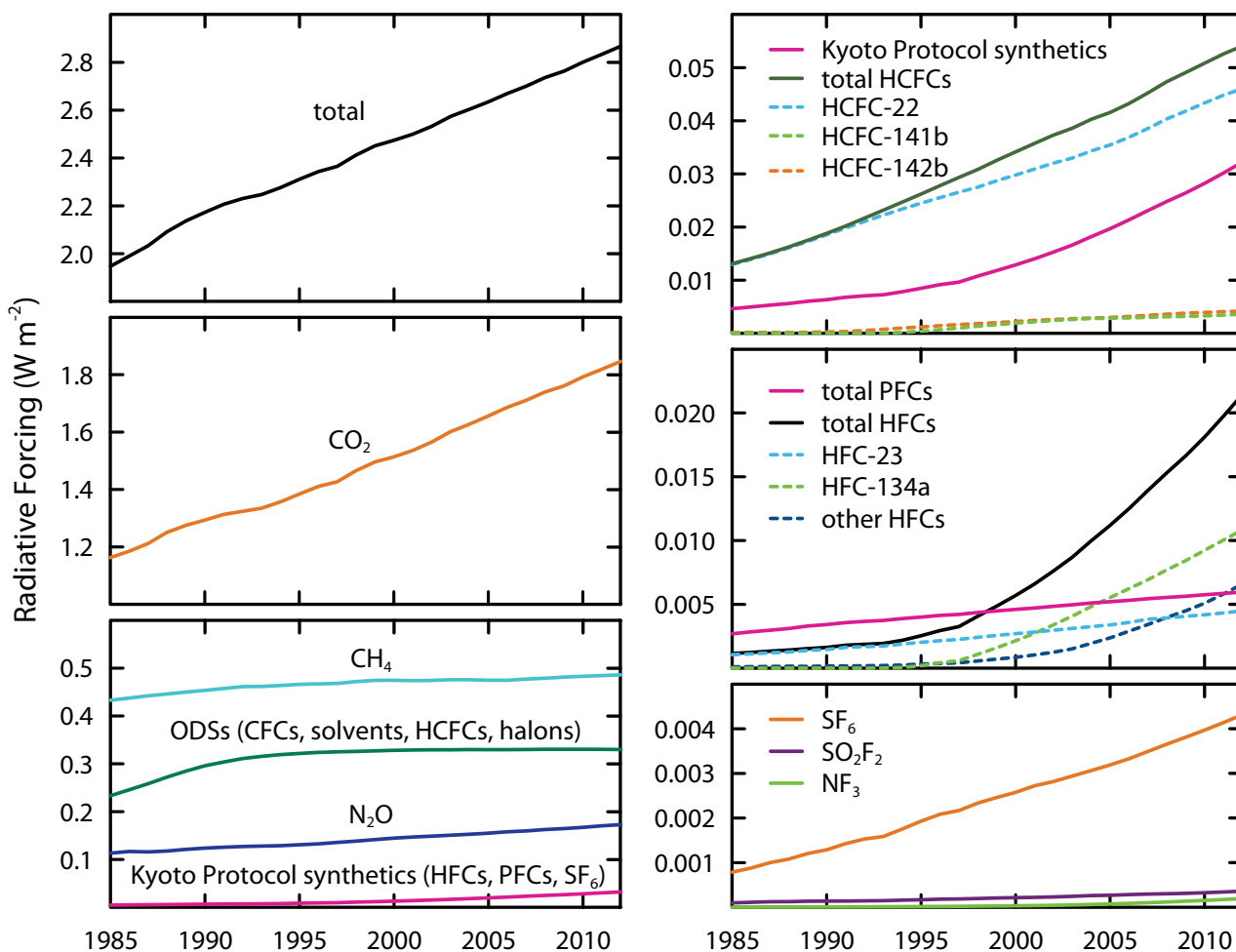


**Figure 1-6-3.** *Left panels:* The evolution of radiative forcing in  $\text{W m}^{-2}$  from the sum of the major greenhouse gases ( $\text{CO}_2$ ,  $\text{CH}_4$ ,  $\text{N}_2\text{O}$ ), the ODSs (CFCs, HCFCs, halons, solvents ( $\text{CH}_3\text{CCl}_3$ ,  $\text{CCl}_4$ )), and the Kyoto Protocol synthetic gases (F-gases (HFCs, PFCs,  $\text{SF}_6$ )). *Right panels:* The evolution of radiative forcing from Kyoto Protocol synthetic gases (and their sums) as well as specified F-gases. Other HFCs combine all measured HFCs from Table 1-14, except HFC-134a and HFC-23. Data are from Table 1-1 and Table 1-14; radiative efficiencies are from Chapter 5. Radiative forcings are calculated according to Myhre et al. (2013). This figure represents an update of Figure 1-25 from the last Assessment (Montzka and Reimann et al., 2011).

#### 1.6.4 GWP-Weighted Emissions of ODS and ODS Replacement Compounds

The emissions of CFCs, HCFCs, and HFCs in terms of their influence on climate (as measured by  $\text{GtCO}_2\text{-equivalent yr}^{-1}$  emissions) were roughly equal in 2012. However, the emissions of HFCs are increasing rapidly, while the emissions of CFCs are going down and those of HCFCs are essentially unchanged. The 100-year GWP weighted emissions for the sum of CFC, HCFC, HFC, halons, and chlorinated solvents emissions was 2.3  $\text{GtCO}_2\text{-eq}$  in 2012. The sum of GWP-weighted emissions of CFCs was  $0.73 \pm 0.25 \text{ GtCO}_2\text{-eq yr}^{-1}$  in 2012 and has decreased on average by  $11.0 \pm 1.2\% \text{ yr}^{-1}$  from 2008 to 2012. The sum of HCFC emissions was  $0.76 \pm 0.12 \text{ GtCO}_2\text{-eq yr}^{-1}$  in 2012 and has been essentially unchanged between 2008 and 2012. Finally, the sum of HFC emissions was  $0.69 \pm 0.12$

GtCO<sub>2</sub>-eq yr<sup>-1</sup> in 2012 and has increased on average by  $6.8 \pm 0.9\%$  yr<sup>-1</sup> from 2008 to 2012. The HFC increase partially offsets the decrease by CFCs. Current emissions of HFCs are, however, less than 10% of peak CFC emissions in the early 1990s ( $>8$  Gt CO<sub>2</sub>-eq yr<sup>-1</sup>).

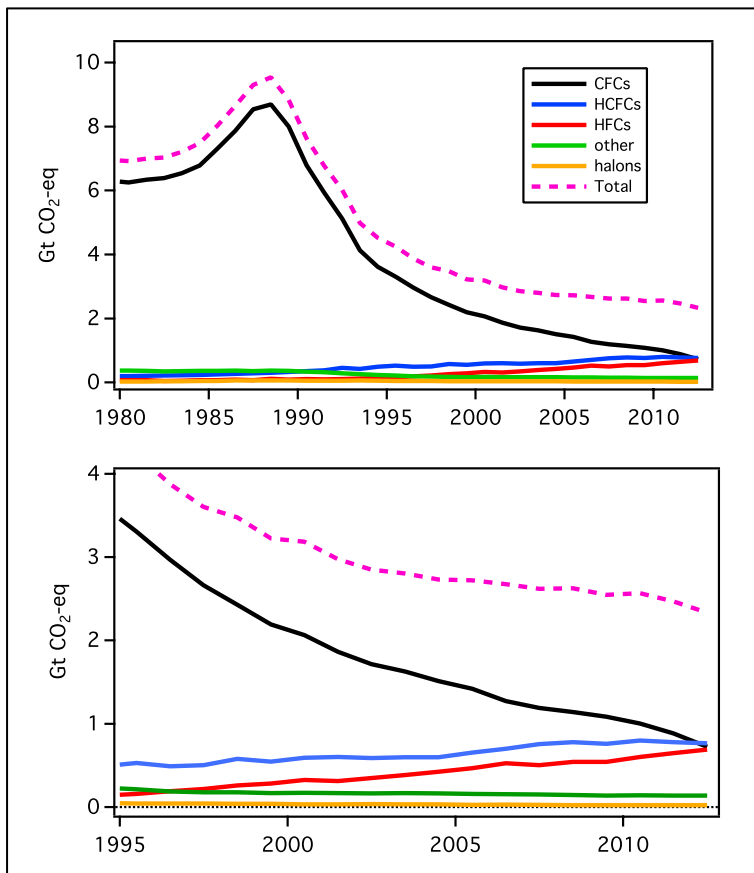


**Figure 1-6-4.** Emissions of ODSs and ODS replacements weighted by 100-yr Global Warming Potential. The lower figure is an expanded version of the upper figure. In 2012, CO<sub>2</sub>-equivalent emissions of CFCs, HCFCs, and HFCs were nearly equal. In this figure, “other” includes CCl<sub>4</sub>, CH<sub>3</sub>CCl<sub>3</sub>, and CH<sub>3</sub>Cl.

### 1.6.5 Ongoing Mismatch between Estimated Sources of CCl<sub>4</sub> from Measurements and from Inventories

Carbon tetrachloride (CCl<sub>4</sub>) accounted for about 10% of total tropospheric Cl in 2012, and during 2009–2012 declined largely as projected in the A1 scenario of the 2010 Assessment. However, estimated sources and sinks remain inconsistent with observations of CCl<sub>4</sub>, so the budget of this key gas remains unclear. When combined with the current estimate of the total atmospheric lifetime of CCl<sub>4</sub> (26 years), the observed CCl<sub>4</sub> trend in the atmosphere ( $-1.1$  to  $-1.4$  ppt yr<sup>-1</sup> in 2012, right panel of Figure 1-6-5) implies sources of 57 (40–74) Gg yr<sup>-1</sup> (red line in left panel of Figure 1-6-5), which cannot be reconciled by estimated emissions from feedstock and other uses (green lines). These industry-based estimates together with a global atmospheric CCl<sub>4</sub> lifetime of 26 years result in calculated CCl<sub>4</sub> mole fractions (dotted black line, right panel) much lower than measured abundances in the past decade, with an increasing divergence. The stable and significant interhemispheric CCl<sub>4</sub> difference of 1.3 ppt in recent years could be an indicator for ongoing anthropogenic emissions in the Northern Hemisphere, although the distribution of CCl<sub>4</sub> sources is not well understood.

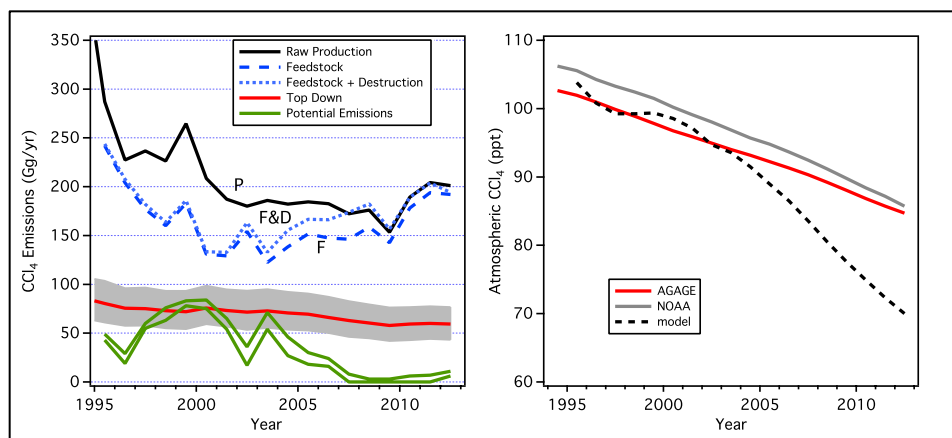


**Figure 1-6-5.** *Left panel:* Global top-down emissions of CCl<sub>4</sub> and global potential emissions of CCl<sub>4</sub>, derived from raw production, feedstock, and destruction. For further explanation see caption of Figure 1-6. *Right panel:* Global mole fractions from NOAA and AGAGE measurements along with the theoretical mole fraction (black dotted line) derived from potential emissions and a global lifetime of 26 years using a 1-box model and observed concentrations in 1994, from 1994 through 2012.

### 1.6.6 Quarantine and Pre-shipment (QPS) Consumption of CH<sub>3</sub>Br Has Exceeded Non-QPS Consumption

Quarantine and pre-shipment (QPS) consumption of methyl bromide (CH<sub>3</sub>Br) exceeded non-QPS consumption in 2009 (Figure 1-6-6). Article 5 and non-Article 5 countries consume similar amounts of CH<sub>3</sub>Br for QPS uses. There was a slight increase in QPS consumption by Article 5 countries in the mid-2000s, with fairly steady consumption since then. QPS consumption by non-Article 5 countries was 34% of the total QPS consumption in 2012. With non-QPS emissions totaling just 30% of the 2012 total fumigation emissions, increases in QPS consumption/emissions will begin to reverse the reductions in tropospheric bromine gained from the reductions in non-QPS production, consumption, and emission.

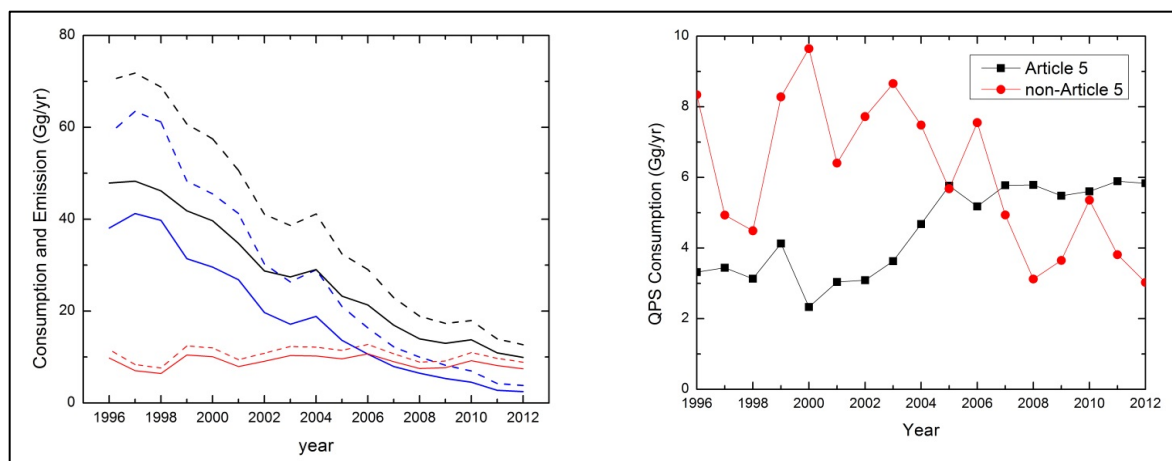


**Figure 1-6-6.** *Left panel:* Trends in methyl bromide consumption (dashed lines) as reported in the UNEP database for non-QPS uses (---), QPS uses (---), and total (---); and trends in methyl bromide emission (solid lines) from non-QPS uses (—), QPS uses (—), and total (—). *Right panel:* Quarantine and pre-shipment (QPS) consumption for Article 5 and non-Article 5 Parties to the Montreal Protocol (UNEP, 2014).

## REFERENCES

- Abbatt, J.P.D., and J.G. Anderson, High-pressure discharge flow kinetics and frontier orbital mechanistic analysis for OH + CH<sub>2</sub>CCl<sub>2</sub>, *cis*-CHClCHCl, *trans*-CHClCHCl, CFCICF<sub>2</sub>, and CF<sub>2</sub>CCl<sub>2</sub> → products, *J. Phys. Chem.*, *95* (6), 2382-2390, doi: 10.1021/j100159a049, 1991.
- Acerboni, G., J.A. Beukes, N.R. Jensen, J. Hjorth, G. Myhre, C.J. Nielsen, and J.K. Sundet, Atmospheric degradation and global warming potentials of three perfluoroalkenes, *Atmos. Environ.*, *35*, 4113-4123, doi: 10.1016/S1352-2310(01)00209-6, 2001.
- An, X.Q., S. Henne, B. Yao, M.K. Vollmer, L.X. Zhou, and Y. Li, Estimating emissions of HCFC-22 and CFC-11 in China by atmospheric observations and inverse modeling, *Sci. China Chem.*, *55* (10), 2233-2241, doi: 10.1007/s11426-012-4624-8, 2012.
- Andreae, M.O., and P. Merlet, Emission of trace gases and aerosols from biomass burning, *Global Biogeochem. Cycles*, *15* (4), 955-966, doi: 10.1029/2000GB001382, 2001.
- Archer, S.D., L.E. Goldson, M.I. Liddicoat, D.G. Cummings, and P.D. Nightingale, Marked seasonality in the concentrations and sea-to-air flux of volatile iodocarbon compounds in the western English Channel, *J. Geophys. Res.*, *112* (C8), C08009, doi: 10.1029/2006JC003963, 2007.
- Arnold, T., J. Mühle, P.K. Salameh, C.M. Harth, D.J. Ivy, and R.F. Weiss, Automated measurement of nitrogen trifluoride in ambient air, *Anal. Chem.*, *84* (11), 4798-4804, doi: 10.1021/ac300373e, 2012.
- Arnold, T., C.M. Harth, J. Mühle, A.J. Manning, P.K. Salameh, J. Kim, D.J. Ivy, L.P. Steele, V.V. Petrenko, J.P. Severinghaus, D. Baggenstos, and R.F. Weiss, Nitrogen trifluoride global emissions estimated from updated atmospheric measurements, *Proc. Natl. Acad. Sci.*, *110* (6), 2029-2034, doi: 10.1073/pnas.1212346110, 2013.
- Arnold, T., D.J. Ivy, C.M. Harth, M.K. Vollmer, J. Mühle, P.K. Salameh, L.P. Steele, P.B. Krummel, R.H.J. Wang, D. Young, C.R. Lunder, O. Hermansen, T.S. Rhee, J. Kim, S. Reimann, S. O'Doherty, P.J. Fraser, P.G. Simmonds, R.G. Prinn, and R.F. Weiss, HFC-43-10mee atmospheric abundances and global emission estimates, *Geophys. Res. Lett.*, *41* (6), 2228-2235, doi: 10.1002/2013GL059143, 2014.
- Aschmann, J., and B.-M. Sinnhuber, Contribution of very short-lived substances to stratospheric bromine loading: Uncertainties and constraints, *Atmos. Chem. Phys.*, *13* (3), 1203-1219, doi: 10.5194/acp-13-1203-2013, 2013.
- Aschmann, J., B.-M. Sinnhuber, E.L. Atlas, and S.M. Schauffler, Modeling the transport of very short-lived substances into the tropical upper troposphere and lower stratosphere, *Atmos. Chem. Phys.*, *9* (23), 9237-9247, doi: 10.5194/acp-9-9237-2009, 2009.
- Aschmann, J., B.-M. Sinnhuber, M.P. Chipperfield, and R. Hossaini, Impact of deep convection and dehydration on bromine loading in the upper troposphere and lower stratosphere, *Atmos. Chem. Phys.*, *11* (6), 2671-2687, doi: 10.5194/acp-11-2671-2011, 2011.
- Ashfold, M.J., N.R.P. Harris, E.L. Atlas, A.J. Manning, and J.A. Pyle, Transport of short-lived species into the Tropical Tropopause Layer, *Atmos. Chem. Phys.*, *12* (14), 6309-6322, doi: 10.5194/acp-12-6309-2012, 2012.
- Ashfold, M.J., N.R.P. Harris, A.J. Manning, A.D. Robinson, N.J. Warwick, and J.A. Pyle, Estimates of tropical bromoform emissions using an inversion method, *Atmos. Chem. Phys.*, *14* (2), 979-994, doi: 10.5194/acp-14-979-2014, 2014.
- Atkinson, R., D.L. Baulch, R.A. Cox, J.N. Crowley, R.F. Hampson, R.G. Hynes, M.E. Jenkin, M.J. Rossi, J. Troe, and T.J. Wallington, Evaluated kinetic and photochemical data for atmospheric chemistry: Volume IV – gas phase reactions of organic halogen species, *Atmos. Chem. Phys.*, *8* (15), 4141-4496, doi: 10.5194/acp-8-4141-2008, 2008.
- Aydin, M., K.R. Verhulst, E.S. Saltzman, M.O. Battle, S.A. Montzka, D.R. Blake, Q. Tang, and M.J. Prather, Recent decreases in fossil-fuel emissions of ethane and methane derived from firn air, *Nature*, *476* (7359), 198-201, doi: 10.1038/nature10352, 2011.
- Baasandorj, M., A.R. Ravishankara, and J.B. Burkholder, Atmospheric chemistry of (*Z*)-CF<sub>3</sub>CH=CHCF<sub>3</sub>: OH radical reaction rate coefficient and global warming potential, *J. Phys. Chem. A*, *115* (38), 10539-10549, doi: 10.1021/jp206195g, 2011.
- Baasandorj, M., B.D. Hall, and J.B. Burkholder, Rate coefficients for the reaction of O(<sup>1</sup>D) with the atmospherically long-lived greenhouse gases NF<sub>3</sub>, SF<sub>3</sub>CF<sub>3</sub>, CHF<sub>3</sub>, C<sub>2</sub>F<sub>6</sub>, *c*-C<sub>4</sub>F<sub>8</sub>, *n*-C<sub>5</sub>F<sub>12</sub>, and *n*-C<sub>6</sub>F<sub>14</sub>, *Atmos. Chem. Phys.*, *12* (23), 11753-11764, doi: 10.5194/acp-12-11753-2012, 2012.
- Baasandorj, M., E.L. Fleming, C.H. Jackman, and J.B. Burkholder, O(<sup>1</sup>D) kinetic study of key ozone depleting substances and greenhouse gases, *J. Phys. Chem. A*, *117* (12), 2434-2445, doi: 10.1021/jp312781c, 2013.
- Baker, J.M., C.E. Reeves, S.A. Penkett, L.M. Cardenas, and P.D. Nightingale, An estimate of the global emissions of methyl bromide from automobile exhausts, *Geophys. Res. Lett.*, *25* (13), 2405-2408, doi: 10.1029/98GL01795, 1998.

- Barletta, B., P. Nissenon, S. Meinardi, D. Dabdub, F. Sherwood Rowland, R.A. VanCuren, J. Pederson, G.S. Diskin, and D.R. Blake, HFC-152a and HFC-134a emission estimates and characterization of CFCs, CFC replacements, and other halogenated solvents measured during the 2008 ARCTAS campaign (CARB phase) over the South Coast Air Basin of California, *Atmos. Chem. Phys.*, *11* (6), 2655-2669, doi: 10.5194/acp-11-2655-2011, 2011.
- Bell, N., L. Hsu, D.J. Jacob, M.G. Schultz, D.R. Blake, J.H. Butler, D.B. King, J.M. Lobert, and E. Maier-Reimer, Methyl iodide: Atmospheric budget and use as a tracer of marine convection in global models, *J. Geophys. Res.*, *107* (D17), 4340, doi: 10.1029/2001JD001151, 2002.
- Bergman, J.W., E.J. Jensen, L. Pfister, and Q. Yang, Seasonal differences of vertical-transport efficiency in the tropical tropopause layer: On the interplay between tropical deep convection, large-scale vertical ascent, and horizontal circulations, *J. Geophys. Res.*, *117* (D5), D05302, doi: 10.1029/2011JD016992, 2012.
- Bertram, F.J., and J.B. Kolowich, A study of methyl bromide emissions from automobiles burning leaded gasoline using standardized vehicle testing procedures, *Geophys. Res. Lett.*, *27* (9), 1423-1426, doi: 10.1029/1999GL011008, 2000.
- Bian, H., P.R. Colarco, M. Chin, G. Chen, J.M. Rodriguez, Q. Liang, D. Blake, D.A. Chu, A. da Silva, A.S. Darmenov, G. Diskin, H.E. Fuelberg, G. Huey, Y. Kondo, J.E. Nielsen, X. Pan, and A. Wisthaler, Source attributions of pollution to the Western Arctic during the NASA ARCTAS field campaign, *Atmos. Chem. Phys.*, *13* (9), 4707-4721, doi: 10.5194/acp-13-4707-2013, 2013.
- Blei, E., C.J. Hardacre, G.P. Mills, K.V. Heal, and M.R. Heal, Identification and quantification of methyl halide sources in a lowland tropical rainforest, *Atmos. Environ.*, *44* (8), 1005-1010, doi: 10.1016/j.atmosenv.2009.12.023, 2010.
- Bösch, H., C. Camy-Peyret, M.P. Chipperfield, R. Fitzenberger, H. Harder, U. Platt, and K. Pfeilsticker, Upper limits of stratospheric IO and OIO inferred from center-to-limb-darkening-corrected balloon-borne solar occultation visible spectra: Implications for total gaseous iodine and stratospheric ozone, *J. Geophys. Res.*, *108* (D15), 4455, doi: 10.1029/2002JD003078, 2003.
- Bousquet, P., B. Ringeval, I. Pison, E.J. Dlugokencky, E.-G. Brunke, C. Carouge, F. Chevallier, A. Fortems-Cheiney, C. Frankenberg, D.A. Hauglustaine, P.B. Krummel, R.L. Langenfelds, M. Ramonet, M. Schmidt, L.P. Steele, S. Szopa, C. Yver, N. Viovy, and P. Ciais, Source attribution of the changes in atmospheric methane for 2006–2008, *Atmos. Chem. Phys.*, *11* (8), 3689–3700, doi: 10.5194/acp-11-3689-2011, 2011.
- Boutonnet, J.C., P. Bingham, D. Calamari, C. de Rooij, J. Franklin, T. Kawano, J.-M. Libre, A. McCulloch, G. Malinverno, J.M. Odom, G.M. Rusch, K. Smythe, I. Sobolev, R. Thompson, and J.M. Tiedje, Environmental risk assessment of trifluoroacetic acid, *Hum. Ecol. Risk Assess.*, *5* (1), 59-124, doi: 10.1080/10807039991289644, 1999.
- Braesicke, P., J. Keeble, X. Yang, G. Stiller, S. Kellmann, N.L. Abraham, A.T. Archibald, P. Telford, and J.A. Pyle, Circulation anomalies in the Southern Hemisphere and ozone changes, *Atmos. Chem. Phys.*, *13* (21), 10677-10688, doi: 10.5194/acp-13-10677-2013, 2013.
- Brinckmann, S., A. Engel, H. Bönisch, B. Quack, and E. Atlas, Short-lived brominated hydrocarbons – observations in the source regions and the tropical tropopause layer, *Atmos. Chem. Phys.*, *12* (3), 1213-1228, doi: 10.5194/acp-12-1213-2012, 2012.
- Brion, J., A. Chakir, J. Charbonnier, D. Daumont, C. Parisse, and J. Malicet, Absorption spectra measurements for the ozone molecule in the 350-830 nm region, *J. Atmos. Chem.*, *30* (2), 291-299, doi: 10.1023/A:1006036924364, 1998.
- Brioude, J., R.W. Portmann, J.S. Daniel, O.R. Cooper, G.J. Frost, K.H. Rosenlof, C. Granier, A.R. Ravishankara, S.A. Montzka, and A. Stohl, Variations in ozone depletion potentials of very short-lived substances with season and emission region, *Geophys. Res. Lett.*, *37* (19), L19804, doi: 10.1029/2010GL044856, 2010.
- Brown, A.T., M.P. Chipperfield, C. Boone, C. Wilson, K.A. Walker, and P.F. Bernath, Trends in atmospheric halogen containing gases since 2004, *J. Quant. Spectrosc. Radiat. Transfer*, *112* (16), 2552-2566, doi: 10.1016/j.jqsrt.2011.07.005, 2011.
- Brown, A.T., M.P. Chipperfield, N.A.D. Richards, C. Boone, and P.F. Bernath, Global stratospheric fluorine inventory for 2004-2009 from Atmospheric Chemistry Experiment Fourier Transform Spectrometer (ACE-FTS) measurements and SLIMCAT model simulations, *Atmos. Chem. Phys.*, *14* (1), 267-282, doi: 10.5194/acp-14-267-2014, 2014.
- Brownell, D.K., R.M. Moore, and J.J. Cullen, Production of methyl halides by *Prochlorococcus* and *Synechococcus*, *Global Biogeochem. Cycles*, *24* (2), GB2002, doi: 10.1029/2009GB003671, 2010.

- Brühl, C., J. Lelieveld, P.J. Crutzen, and H. Tost, The role of carbonyl sulphide as a source of stratospheric sulphate aerosol and its impact on climate, *Atmos. Chem. Phys.*, *12* (3), 1239-1253, doi: 10.5194/acp-12-1239-2012, 2012.
- Butler, J.H., The potential role of the ocean in regulating atmospheric CH<sub>3</sub>Br, *Geophys. Res. Lett.*, *21* (3), 185-188, doi: 10.1029/94GL00071, 1994.
- Butler, J.H., S.A. Montzka, A.D. Clarke, J.M. Lobert, and J.W. Elkins, Growth and distribution of halons in the atmosphere, *J. Geophys. Res.*, *103* (D1), 1503-1511, doi: 10.1029/97JD02853, 1998.
- Butler, J.H., M. Battle, M.L. Bender, S.A. Montzka, A.D. Clarke, E.S. Saltzman, C.M. Sucher, J.P. Severinghaus, and J.W. Elkins, A record of atmospheric halocarbons during the twentieth century from polar firn air, *Nature*, *399* (6738), 749-755, doi: 10.1038/21586, 1999.
- Butler, J.H., D.B. King, J.M. Lobert, S.A. Montzka, S.A. Yvon-Lewis, B.D. Hall, N.J. Warwick, D.J. Mondeel, M. Aydin, and J.W. Elkins, Oceanic distributions and emissions of short-lived halocarbons, *Global Biogeochem. Cycles*, *21*, GB1023, doi: 10.1029/2006GB002732, 2007.
- Butz, A., H. Bösch, C. Camy-Peyret, M.P. Chipperfield, M. Dorf, S. Kreycky, L. Kritten, C. Prados-Roman, J. Schwärzle, and K. Pfeilsticker, Constraints on inorganic gaseous iodine in the tropical upper troposphere and stratosphere inferred from balloon-borne solar occultation observations, *Atmos. Chem. Phys.*, *9* (18), 7229-7242, doi: 10.5194/acp-9-7229-2009, 2009.
- Cahill, T.M., C.M. Thomas, S.E. Schwarzbach, and J.N. Seiber, Accumulation of trifluoroacetate in seasonal wetlands in California, *Environ. Sci. Technol.*, *35* (5), 820-825, doi: 10.1021/es0013982, 2001.
- Calvert, J.G., R.G. Derwent, J.J. Orlando, G.S. Tyndall, and T.J. Wallington, *Mechanisms of Atmospheric Oxidation of the Alkanes*, 1008 pp., Oxford University Press, New York, NY, 2008.
- Carpenter, L.J., C.E. Jones, R.M. Dunk, K.E. Hornsby, and J. Woeltjen, Air-sea fluxes of biogenic bromine from the tropical and North Atlantic Ocean, *Atmos. Chem. Phys.*, *9* (5), 1805-1816, doi: 10.5194/acp-9-1805-2009, 2009.
- Carpenter, L.J., S.M. MacDonald, M.D. Shaw, R. Kumar, R.W. Saunders, R. Parthipan, J. Wilson, and J.M.C. Plane, Atmospheric iodine levels influenced by sea surface emissions of inorganic iodine, *Nature Geosci.*, *6* (2), 108-111, doi: 10.1038/ngeo1687, 2013.
- CDIAC (Carbon Dioxide Information Analysis Center), *The ALE/GAGE/AGAGE Network (DB1001)*, available: <http://cdiac.esd.ornl.gov/ndps/alegag.html>, 2014.
- Chen, B., X.D. Xu, S. Yang, S., and T.L. Zhao, Climatological perspectives of air transport from atmospheric boundary layer to tropopause layer over Asian monsoon regions during boreal summer inferred from Lagrangian approach, *Atmos. Chem. Phys.*, *12* (13), 5827-5839, doi: 10.5194/acp-12-5827-2012, 2012.
- Chen, L., S. Kutsuna, K. Tokuhashi, and A. Sekiya, Kinetics study of the gas-phase reactions of C<sub>2</sub>F<sub>5</sub>OC(O)H and n-C<sub>3</sub>F<sub>7</sub>OC(O)H with OH radicals at 253-328 K, *Chem. Phys. Lett.*, *400* (4-6), 563-568, doi: 10.1016/j.cplett.2004.11.019, 2004a.
- Chen, L., S. Kutsuna, K. Tokuhashi, and A. Sekiya, Kinetics of the gas-phase reaction of CF<sub>3</sub>OC(O)H with OH radicals at 242-328 K, *Int. J. Chem. Kinet.*, *36* (6), 337-344, doi: 10.1002/kin.20004, 2004b.
- Chen, L., S. Kutsuna, K. Tokuhashi, and A. Sekiya, Kinetics study of the gas-phase reactions of -CHF<sub>2</sub>CF<sub>2</sub>OCHF<sub>2</sub> and CF<sub>3</sub>CHF<sub>2</sub>CF<sub>2</sub>OCH<sub>2</sub>CF<sub>2</sub>CF<sub>3</sub> with OH radicals at 253-328 K, *Chem. Phys. Lett.*, *403* (1-3), 180-184, doi: 10.1016/j.cplett.2005.01.002, 2005a.
- Chen, L., S. Kutsuna, K. Tokuhashi, A. Sekiya, R. Tamai, and Y. Hibino, Kinetics and mechanism of (CF<sub>3</sub>)<sub>2</sub>CHOCH<sub>3</sub> reaction with OH radicals in an environmental reaction chamber, *J. Phys. Chem. A*, *109* (21), 4766-4771, doi: 10.1021/jp050491f, 2005b.
- Chen, T.-Y., D.R. Blake, J.P. Lopez, and F.S. Rowland, Estimation of global vehicular methyl bromide emissions: Extrapolation from a case study in Santiago, Chile, *Geophys. Res. Lett.*, *26* (3), 283-286, doi: 10.1029/1998GL900214, 1999.
- Chevallier, F., P. Ciais, T. J. Conway, T. Aalto, B.E. Anderson, P. Bousquet, E.G., Brunke, L. Ciattaglia, Y. Esaki, M. Fröhlich, A. Gomez, A.J. Gomez-Pelaez, L. Haszpra, P.B. Krummel, R.L. Langenfelds, M. Leuenberger, T. Machida, F. Maignan, H. Matsueda, J.A. Morguí, H. Mukai, T. Nakazawa, P. Peylin, M. Ramonet, L. Rivier, Y. Sawa, M. Schmidt, L.P. Steele, S.A. Vay, A.T. Vermeulen, S. Wofsy, and D. Worthy, CO<sub>2</sub> surface fluxes at grid point scale estimated from a global 21 year reanalysis of atmospheric measurements, *J. Geophys. Res.*, *115* (D21), D21307, doi: 10.1029/2010JD013887, 2010.
- Choi, S., Y. Wang, R.J. Salawitch, T. Canty, J. Joiner, T. Zeng, T.P. Kurosu, K. Chance, A. Richter, L.G. Huey, J. Liao, J.A. Neuman, J.B. Nowak, J.E. Dibb, A.J. Weinheimer, G. Diskin, T.B. Ryerson, A. da Silva, J. Curry, D. Kinnison, S. Tilmes, and P.F. Levelt, Analysis of satellite-derived Arctic tropospheric BrO columns in conjunction with aircraft measurements during ARCTAS and ARCPAC, *Atmos. Chem. Phys.*, *12* (3), 1255-1285, doi: 10.5194/acp-12-1255-2012, 2012.

- Christensen, L.K., J. Sehested, O.J. Nielsen, M. Bilde, T.J. Wallington, A. Guschin, L.T. Molina, and M.J. Molina, Atmospheric chemistry of HFE-7200 (C<sub>4</sub>F<sub>9</sub>OC<sub>2</sub>H<sub>5</sub>): Reaction with OH radicals and fate of C<sub>4</sub>F<sub>9</sub>OCH<sub>2</sub>CH<sub>2</sub>O(•) and C<sub>4</sub>F<sub>9</sub>OCHO(•)CH<sub>3</sub> radicals, *J. Phys. Chem. A*, *102* (25), 4839-4845, doi: 10.1021/jp981128u, 1998.
- Ciais, P., and C. Sabine (Co-ordinating Lead Authors), G. Bala, L. Bopp, V. Brovkin, J. Canadell, A. Chhabra, R. DeFries, J. Galloway, M. Heimann, C. Jones, C. Le Quéré, R.B. Myneni, S. Piao, and P. Thornton (Lead Authors), Carbon and other biogeochemical cycles, Chapter 6 in *Climate Change 2013: The Physical Science Basis. Contribution of Working Group I to the Fifth Assessment Report of the Intergovernmental Panel on Climate Change*, edited by T.F. Stocker, D. Qin, G.-K. Plattner, M. Tignor, S.K. Allen, J. Boschung, A. Nauels, Y. Xia, V. Bex, and P.M. Midgley, 1535 pp., Cambridge University Press, Cambridge, U.K. and New York, NY, 2013.
- Clerbaux, C. and D.M. Cunnold (Lead Authors), J. Anderson, A. Engel, P.J. Fraser, E. Mahieu, A. Manning, J. Miller, S.A. Montzka, R. Nassar, R. Prinn, S. Reimann, C.P. Rinsland, P. Simmonds, D. Verdonik, R. Weiss, D. Wuebbles, and Y. Yokouchi, Long-lived compounds, Chapter 1 in *Scientific Assessment of Ozone Depletion, 2006*, Global Ozone Research and Monitoring Project–Report No. 50, Geneva, Switzerland, 2007.
- Connor, B.J., T. Mooney, G. E. Nedoluha, J.W. Barrett, A. Parrish, J. Koda, M.L. Santee, and R.M. Gomez, Re-analysis of ground-based microwave ClO measurements from Mauna Kea, 1992 to early 2012, *Atmos. Chem. Phys.*, *13* (17), 8643-8650, doi: 10.5194/acp-13-8643-2013, 2013.
- Cox, M.L., P.J. Fraser, G.A. Sturrock, S.T. Siems, and L.W. Porter, Terrestrial sources and sinks of halomethanes near Cape Grim, Tasmania, *Atmos. Environ.*, *38* (23), 3839-3852, doi: 10.1016/j.atmosenv.2004.03.050, 2004.
- Crowley, J.N., M. Ammann, R.A. Cox, R.G. Hynes, M.E. Jenkin, A. Mellouki, M.J. Rossi, J. Troe, and T.J. Wallington, Evaluated kinetic and photochemical data for atmospheric chemistry: Volume V – heterogeneous reactions on solid substrates, *Atmos. Chem. Phys.*, *10* (18), 9059-9223, doi: 10.5194/acp-10-9059-2010, 2010.
- Crutzen, P.J., The influence of nitrogen oxides on the atmospheric ozone content, *Quart. J. Roy. Meteorol. Soc.*, *96* (408), 320-325, doi: 10.1002/qj.49709640815, 1970.
- Cunnold, D.M., R.G. Prinn, R.A. Rasmussen, P.G. Simmonds, F.N. Alyea, C.A. Cardelino, A.J. Crawford, P.J. Fraser, and R.D. Rosen, The Atmospheric Lifetime Experiment 3. Lifetime methodology and application to three years of CFCl<sub>3</sub> data, *J. Geophys. Res.*, *88* (C13), 8379-8400, doi: 10.1029/JC088iC13p08379, 1983.
- Daniel, J.S., and G.J.M. Velders (Coordinating Lead Authors), A.R. Douglass, P.M.D. Forster, D.A. Hauglustaine, I.S.A. Isaksen, L.J.M. Kuijpers, A. McCulloch, and T.J. Wallington, Halocarbon scenarios, ozone depletion potentials, and global warming potentials, Chapter 8 in *Scientific Assessment of Ozone Depletion: 2006*, Global Ozone Research and Monitoring Project–Report No. 50, 572 pp., World Meteorological Organization, Geneva, Switzerland, 2007.
- Daniel, J.S., and G.J.M. Velders (Coordinating Lead Authors), H. Akiyoshi, A.F. Bais, E.L. Fleming, C.H. Jackman, L.J.M. Kuijpers, M. McFarland, S.A. Montzka, O. Morgenstern, M.N. Ross, S. Tilmes, D.W. Toohy, M.B. Tully, T.J. Wallington, and D.J. Wuebbles, A Focus on Information and Options for Policymakers, Chapter 5 in *Scientific Assessment of Ozone Depletion: 2010*, Global Ozone Research and Monitoring Project–Report No. 52, World Meteorological Organization, Geneva, Switzerland, 2011.
- Daumont, D., J. Brion, J. Charbonnier, and J. Malicet, Ozone UV spectroscopy. I. Absorption cross-sections at room temperature, *J. Atmos. Chem.*, *15* (2), 145-155, doi: 10.1007/BF00053756, 1992.
- de Blas, M., M. Navazo, L. Alonso, N. Durana, and J. Iza, Trichloroethylene, tetrachloroethylene and carbon tetrachloride in an urban atmosphere: Mixing ratios and temporal patterns, *Intern. J. Environ. Anal. Chem.*, *93* (2), 228-244, doi: 10.1080/03067319.2011.629346, 2013.
- Devasthale, A., and H. Grassl, A daytime climatological distribution of high opaque ice cloud classes over the Indian summer monsoon region observed from 25-year AVHRR data, *Atmos. Chem. Phys.*, *9* (12), 4185-4196, doi: 10.5194/acp-9-4185-2009, 2009.
- Devasthale, A., and S. Fueglistaler, A climatological perspective of deep convection penetrating the TTL during the Indian summer monsoon from the AVHRR and MODIS instruments, *Atmos. Chem. Phys.*, *10* (10), 4573-4582, doi: 10.5194/acp-10-4573-2010, 2010.
- Dimmer, C.H., P.G. Simmonds, G. Nickless, and M.R. Bassford, Biogenic fluxes of halomethanes from Irish peatland ecosystems, *Atmos. Environ.*, *35* (2), 321-330, doi: 10.1016/S1352-2310(00)00151-5, 2001.
- Ding, K., H. Metiu, and G.D. Stucky, The selective high-yield conversion of methane using iodine-catalyzed methane bromination, *ACS Catal.*, *3* (3), 474-477, doi: 10.1021/cs300775m, 2013.
- Dix, B., S. Baidar, J.F. Bresch, S.R. Hall, K.S. Schmidt, S. Wang, and R. Volkamer, Detection of iodine monoxide in the tropical free troposphere, *Proc. Natl. Acad. Sci.*, *110* (6), 2035-2040, doi: 10.1073/pnas.1212386110, 2013.

- Dlugokencky, E.J., L. Bruhwiler, J.W.C. White, L.K. Emmons, P.C. Novelli, S.A. Montzka, K.A. Masarie, P.M. Lang, A.M. Croftwell, J.B. Miller, and L.V. Gatti, Observational constraints on recent increases in the atmospheric CH<sub>4</sub> burden, *Geophys. Res. Lett.*, *36*, L18803, doi: 10.1029/2009GL039780, 2009.
- Dlugokencky, E.J., E.G., Nisbet, R. Fisher, and D. Lowry, Global atmospheric methane: Budget, changes and dangers, *Phil. Trans. R. Soc. A*, *369* (1943), 2058–2072, doi: 10.1098/rsta.2010.0341, 2011.
- Dorf, M., J.H. Butler, A. Butz, C. Camy-Peyret, M.P. Chipperfield, L. Kritten, S.A. Montzka, B. Simmes, F. Weidner, and K. Pfeilsticker, Long-term observations of stratospheric bromine reveal slow down in growth, *Geophys. Res. Lett.*, *33*, L24803, doi: 10.1029/2006GL027714, 2006.
- Dorf, M., A. Butz, C. Camy-Peyret, M.P. Chipperfield, L. Kritten, and K. Pfeilsticker, Bromine in the tropical troposphere and stratosphere as derived from balloon-borne BrO observations, *Atmos. Chem. Phys.*, *8* (23), 7265–7271, doi: 10.5194/acp-8-7265-2008, 2008.
- Duchatelet, P., E. Mahieu, R. Ruhnke, W. Feng, M. Chipperfield, P. Demoulin, P. Bernath, C.D. Boone, K.A. Walker, C. Servais, and O. Flock, An approach to retrieve information on the carbonyl fluoride (COF<sub>2</sub>) vertical distributions above Jungfraujoch by FTIR multi-spectrum multi-window fitting, *Atmos. Chem. Phys.*, *9* (22), 9027–9042, doi: 10.5194/acp-9-9027-2009, 2009.
- Duchatelet, P., P. Demoulin, F. Hase, R. Ruhnke, W. Feng, M.P. Chipperfield, P.F. Bernath, C.D. Boone, K.A. Walker, and E. Mahieu, Hydrogen fluoride total and partial column time series above the Jungfraujoch from long-term FTIR measurements: Impact of the line-shape model, characterization of the error budget and seasonal cycle, and comparison with satellite and model data, *J. Geophys. Res.*, *115* (D22), D22306, doi: 10.1029/2010jd014677, 2010.
- Engel, A., M. Strunk, M. Müller, H.-P. Haase, C. Poss, I. Levin, and U. Schmidt, Temporal development of total chlorine in the high-latitude stratosphere based on reference distributions of mean age derived from CO<sub>2</sub> and SF<sub>6</sub>, *J. Geophys. Res.*, *107* (D12), 4136, doi: 10.1029/2001JD000584, 2002.
- Engel, A., T. Möbius, H. Bönisch, U. Schmidt, R. Heinz, I. Levin, E. Atlas, S. Aoki, T. Nakazawa, S. Sugawara, F. Moore, D. Hurst, J. Elkins, S. Schauffler, A. Andrews, and K. Boering, Age of stratospheric air unchanged within uncertainties over the past 30 years, *Nature Geosci.*, *2* (1), 28–31, doi: 10.1038/ngeo388, 2009.
- Fang, X., J. Wu, S. Su, J. Han, Y. Wu, Y. Shi, D. Wan, X. Sun, J. Zhang, and J. Hu, Estimates of major anthropogenic halocarbon emissions from China based on interspecies correlations, *Atmos. Environ.*, *62*, 26–33, doi: 10.1016/j.atmosenv.2012.08.010, 2012.
- Fang, X., X. Hu, G. Janssens-Maenhout, J. Wu, J. Han, S. Su, J. Zhang, and J. Hu, Sulfur hexafluoride (SF<sub>6</sub>) emission estimates for China: An inventory for 1990–2010 and a projection to 2020, *Environ. Sci. Technol.*, *47* (8), 3848–3855, doi: 10.1021/es304348x, 2013.
- Feng, W., M.P. Chipperfield, M. Dorf, K. Pfeilsticker, and P. Ricaud, Mid-latitude ozone changes: Studies with a 3-D CTM forced by ERA-40 analyses, *Atmos. Chem. Phys.*, *7* (9), 2357–2369, doi: 10.5194/acp-7-2357-2007, 2007.
- Feng, W., M.P. Chipperfield, S. Dhomse, B.M. Monge-Sanz, X. Yang, K. Zhang, and M. Ramonet, Evaluation of cloud convection and tracer transport in a three-dimensional chemical transport model, *Atmos. Chem. Phys.*, *11* (12), 5783–5803, doi: 10.5194/acp-11-5783-2011, 2011.
- Fitzenberger, R., H. Bösch, C. Camy-Peyret, M.P. Chipperfield, H. Harder, U. Platt, B.-M. Sinnhuber, T. Wagner, and K. Pfeilsticker, First profile measurements of tropospheric BrO, *Geophys. Res. Lett.*, *27* (18), 2921–2924, doi: 10.1029/2000GL011531, 2000.
- Folkins, I., and R.V. Martin, The vertical structure of tropical convection and its impact on the budgets of water vapor and ozone, *J. Atmos. Sci.*, *62* (5), 1560–1573. doi: 10.1175/JAS3407.1, 2005.
- Fraser, P.J., D.E. Oram, C.E. Reeves, S.A. Penkett, and A. McCulloch, Southern Hemispheric halon trends (1978–1998) and global halon emissions, *J. Geophys. Res.*, *104* (D13), 15985–15999, doi: 10.1029/1999JD900113, 1999.
- Fraser, P., P. Steele, and M.A. Cooksey, PFC and carbon dioxide emissions from an Australian aluminium smelter using time-integrated stacksampling and GC-MS, GC-FID analysis, in *Light Metals 2013*, edited by B. Sadler, 871–876, John Wiley & Sons, Inc., Hoboken, New Jersey, doi: 10.1002/9781118663189.ch148, 2013.
- Fraser, P.J., B.L. Dunse, A.J. Manning, S. Walsh, R.H.J. Wang, P.B. Krummel, L.P. Steele, L.W. Porter, C. Allison, S. O’Doherty, P.G. Simmonds, J. Mühle, R.F. Weiss, and R.G. Prinn, Australian carbon tetrachloride emissions in a global context, *Environ. Chem.*, *11*, 77–88, doi: 10.1071/EN13171, 2014.
- Froidevaux, L., N.J. Livesey, W.G. Read, R.J. Salawitch, J.W. Waters, B. Drouin, I.A. MacKenzie, H.C. Pumphrey, P. Bernath, C. Boone, R. Nassar, S. Montzka, J. Elkins, D. Cunnold, and D. Waugh, Temporal decrease in upper atmospheric chlorine, *Geophys. Res. Lett.*, *33*, L23812, doi: 10.1029/2006GL027600, 2006.

- Fthenakis, V., D.O. Clark, M. Moalem, P. Chandler, R.G. Ridgeway, F.E. Hulbert, D.B. Cooper, and P.J. Maroulis, Life-cycle nitrogen trifluoride from photovoltaics, *Environ. Sci. Technol.*, *44* (22), 8750–8757, doi: 10.1021/es100401y, 2010.
- Fueglistaler, S., H. Wernli, and T. Peter, Tropical troposphere-to-stratosphere transport inferred from trajectory calculations, *J. Geophys. Res.*, *109* (D3), D03108, doi: 10.1029/2003JD004069, 2004.
- Fueglistaler, S., A.E. Dessler, T.J. Dunkerton, I. Folkins, Q. Fu, and P.W. Mote, Tropical tropopause layer, *Rev. Geophys.*, *47*, RG1004, doi: 10.1029/2008RG000267, 2009.
- Gardiner, T., A. Forbes, M. de Mazière, C. Vigouroux, E. Mahieu, P. Demoulin, V. Velazco, J. Notholt, T. Blumenstock, F. Hase, I. Kramer, R. Sussmann, W. Stremme, J. Mellqvist, A. Strandberg, K. Ellingsen, and M. Gauss, Trend analysis of greenhouse gases over Europe measured by a network of ground-based remote FTIR instruments, *Atmos. Chem. Phys.*, *8* (22), 6719–6727, doi: 10.5194/acp-8-6719-2008, 2008.
- Gebhardt, S., A. Colomb, R. Hofmann, J. Williams, and J. Lelieveld, Halogenated organic species over the tropical South American rainforest, *Atmos. Chem. Phys.*, *8* (12), 3185–3197, doi: 10.5194/acp-8-3185-2008, 2008.
- Gentner, D.R., A.M. Miller, and A.H. Goldstein, Seasonal variability in anthropogenic halocarbon emissions, *Environ. Sci. Technol.*, *44* (14), 5377–5382, doi: 10.1021/es1005362, 2010.
- Gottelman, A., and P.M. de F. Forster, A climatology of the tropical tropopause layer, *J. Meteorol. Soc. Japan.*, *80* (4B), 911–924, doi: 10.2151/jmsj.80.911, 2002.
- Gottelman, A., P.M. de F. Forster, M. Fujiwara, Q. Fu, H. Vömel, L.K. Gohar, C. Johanson, and M. Ammerman, Radiation balance of the tropical tropopause layer, *J. Geophys. Res.*, *109* (D7), D07103, doi: 10.1029/2003JD004190, 2004.
- Gottelman, A., P.H. Lauritzen, M. Park, and J.E. Kay, Processes regulating short-lived species in the tropical tropopause layer, *J. Geophys. Res.*, *114*, D13303, doi: 10.1029/2009JD011785, 2009.
- Greally, B.R., A.J. Manning, S. Reimann, A. McCulloch, J. Huang, B.L. Dunse, P.G. Simmonds, R.G. Prinn, P.J. Fraser, D.M. Cunnold, S. O'Doherty, L.W. Porter, K. Stemmler, M.K. Vollmer, C.R. Lunder, N. Schmidbauer, O. Hermansen, J. Arduini, P.K. Salameh, P.B. Krummel, R.H.J. Wang, D. Folini, R.F. Weiss, M. Maione, G. Nickless, F. Stordal, and R.G. Derwent, Observations of 1,1-difluoroethane (HFC-152a) at AGAGE and SOGE monitoring stations in 1994–2004 and derived global and regional emission estimates, *J. Geophys. Res.*, *112* (D6), D06308, doi: 10.1029/2006JD007527, 2007.
- Greenblatt, G.D., J.J. Orlando, J.B. Burkholder, and A.R. Ravishankara, Absorption measurements of oxygen between 330 and 1140 nm, *J. Geophys. Res.*, *95* (D11), 18557–18582, doi: 10.1029/JD095iD11p18577, 1990.
- Großmann, K., U. Frieß, E. Peters, F. Wittrock, J. Lampel, S. Yilmaz, J. Tschritter, R. Sommariva, R. von Glasow, B. Quack, K. Krüger, K. Pfeilsticker, and U. Platt, Iodine monoxide in the Western Pacific marine boundary layer, *Atmos. Chem. Phys.*, *13* (6), 3363–3378, doi: 10.5194/acp-13-3363-2013, 2013.
- Hall, B.D., G.S. Dutton, D.J. Mondeel, J.D. Nance, M. Rigby, J.H. Butler, F.L. Moore, D.F. Hurst, and J.W. Elkins, Improving measurements of SF<sub>6</sub> for the study of atmospheric transport and emissions, *Atmos. Meas. Tech.*, *4* (11), 2441–2451, doi: 10.5194/amt-4-2441-2011, 2011.
- Hall, B.D., A. Engel, J. Mühle, J.W. Elkins, F. Artuso, E. Atlas, M. Aydin, D.R. Blake, E.-G. Brunke, S. Chiavarini, P.J. Fraser, J. Happell, P.B. Krummel, I. Levin, M. Loewenstein, M. Maione, S.A. Montzka, S. O'Doherty, S. Reimann, G. Rhoderick, E.S. Saltzman, H.E. Scheel, L.P. Steele, M.K. Vollmer, R.F. Weiss, D. Worthy, and Y. Yokouchi, Results from the International Halocarbons in Air Comparison Experiment (IHALACE), *Atmos. Meas. Tech.*, *7* (2), 469–490, doi: 10.5194/amt-7-469-2014, 2014.
- Han, W., Y. Li, H. Tang, and H. Liu, Treatment of the potent greenhouse gas, CHF<sub>3</sub> – An overview, *J. Fluorine Chem.*, *140*, 7–16, doi: 10.1016/j.jfluchem.2012.04.012, 2012.
- Hanisco, T.F., E.J. Lanzendorf, P.O. Wennberg, K.K. Perkins, R.M. Stimpfle, P.B. Voss, J.G. Anderson, R.C. Cohen, D.W. Fahey, R.S. Gao, E.J. Hints, R.J. Salawitch, J.J. Margitan, C.T. McElroy, and C. Midwinter, Sources, sinks, and the distribution of OH in the lower stratosphere, *J. Phys. Chem. A*, *105* (9), 1543–1553, doi: 10.1021/jp002334g, 2001.
- Happell, J.D., and M.P. Roche, Soils: A global sink of atmospheric carbon tetrachloride, *Geophys. Res. Lett.*, *30* (2), 1088, doi: 10.1029/2002GL015957, 2003.
- Harrison, J.J., C.D. Boone, A.T. Brown, N.D.C. Allen, G.C. Toon, and P.F. Bernath, First remote sensing observations of trifluoromethane (HFC-23) in the upper troposphere and lower stratosphere, *J. Geophys. Res.*, *117* (D5), D05308, doi: 10.1029/2011JD016423, 2012.
- Hartmann, D.L., A.M.G. Klein Tank, M. Rusticucci, L.V. Alexander, S. Brönnimann, Y. Charabi, F.J. Dentener, E.J. Dlugokencky, D.R. Easterling, A. Kaplan, B.J. Soden, P.W. Thorne, M. Wild, and P.M. Zhai, Observations: Atmosphere and surface, Chapter 2 in *Climate Change 2013: The Physical Science Basis. Contribution of Working Group I to the Fifth Assessment Report of the Intergovernmental Panel on Climate*

- Change*, edited by T.F. Stocker, D. Qin, G.-K. Plattner, M. Tignor, S.K. Allen, J. Boschung, A. Nauels, Y. Xia, V. Bex, and P.M. Midgley, Cambridge University Press, Cambridge, U.K. and New York, NY, 2013.
- Hattori, S., S.O. Danielache, M.S. Johnson, J.A. Schmidt, H.G. Kjaergaard, S. Toyoda, Y. Ueno, and N. Yoshida, Ultraviolet absorption cross sections of carbonyl sulfide isotopologues  $\text{OC}^{32}\text{S}$ ,  $\text{OC}^{33}\text{S}$ ,  $\text{OC}^{34}\text{S}$  and  $\text{O}^{13}\text{CS}$ : Isotopic fractionation in photolysis and atmospheric implications, *Atmos. Chem. Phys.*, *11* (19), 10293-10303, doi: 10.5194/acp-11-10293-2011, 2011.
- He, Z., G.P. Yang, and X.L. Lu, Distributions and sea-to-air fluxes of volatile halocarbons in the East China Sea in early winter, *Chemosphere*, *90* (2), 747-757, doi: 10.1016/j.chemosphere.2012.09.067, 2013.
- Hendrick, F., M. Van Roozendaal, M.P. Chipperfield, M. Dorf, F. Goutail, X. Yang, C. Fayt, C. Hermans, K. Pfeilsticker, J.P. Pommereau, J.A. Pyle, N. Theys, and M. De Maziere, Retrieval of stratospheric and tropospheric BrO profiles and columns using ground-based zenith-sky DOAS observations at Harestua, 60 degrees N, *Atmos. Chem. Phys.*, *7* (18), 4869-4885, 2007.
- Hendrick, F., P.V. Johnston, M. De Mazière, C. Fayt, C. Hermans, K. Kreher, N. Theys, A. Thomas, and M. Van Roozendaal, One-decade trend analysis of stratospheric BrO over Harestua (60°N) and Lauder (45°S) reveals a decline, *Geophys. Res. Lett.*, *35* (14), L14801, doi: 10.1029/2008GL034154, 2008.
- Henne, S., D.E. Shallcross, S. Reimann, P. Xiao, D. Brunner, S. O'Doherty, and B. Buchmann, Future emissions and atmospheric fate of HFC-1234yf from mobile air conditioners in Europe, *Environ. Sci. Technol.*, *46* (3), 1650-1658, doi: 10.1021/es2034608, 2012.
- Hodson, E.L., D. Martin, and R.G. Prinn, The municipal solid waste landfill as a source of ozone-depleting substances in the United States and United Kingdom, *Atmos. Chem. Phys.*, *10* (4), 1899-1910, doi: 10.5194/acp-10-1899-2010, 2010.
- Hofmann, D.J., and S.A. Montzka, Recovery of the ozone layer: The Ozone Depleting Gas Index, *EOS Transactions*, *90* (1), 1-2, doi: 10.1029/2009EO010001, 2009.
- Hosking, J.S., M.R. Russo, P. Braesicke, and J.A. Pyle, Modelling deep convection and its impacts on the tropical tropopause layer, *Atmos. Chem. Phys.*, *10* (22), 11175-11188, doi: 10.5194/acp-10-11175-2010, 2010.
- Hossaini, R., M.P. Chipperfield, B.M. Monge-Sanz, N.A.D. Richards, E. Atlas, and D.R. Blake, Bromoform and dibromomethane in the tropics: A 3-D model study of chemistry and transport, *Atmos. Chem. Phys.*, *10* (2), 719-735, doi: 10.5194/acp-10-719-2010, 2010.
- Hossaini, R., M.P. Chipperfield, S. Dhomse, C. Ordoñez, A. Saiz-Lopez, N.L. Abraham, A. Archibald, P. Braesicke, P. Telford, N. Warwick, X. Yang, and J. Pyle, Modelling future changes to the stratospheric source gas injection of biogenic bromocarbons, *Geophys. Res. Lett.*, *39* (20), L20813, doi: 10.1029/2012GL053401, 2012a.
- Hossaini, R., M.P. Chipperfield, W. Feng, T.J. Breider, E. Atlas, S.A. Montzka, B.R. Miller, F. Moore, and J. Elkins, The contribution of natural and anthropogenic very short-lived species to stratospheric bromine, *Atmos. Chem. Phys.*, *12* (1), 371-380, doi: 10.5194/acp-12-371-2012, 2012b.
- Hossaini, R., Mantle, H., Chipperfield, M.P., Montzka, S.A., Hamer, P., Ziska, F., Quack, B., Krüger, K., Tegtmeier, S., Atlas, E., Sala, S., Engel, A., Bönisch, H., Keber, T., Oram, D., Mills, G., Ordóñez, C., Saiz-Lopez, A., Warwick, N., Liang, Q., Feng, W., Moore, F., Miller, B.R., Marécal, V., Richards, N.A.D., Dorf, M., and Pfeilsticker, K., Evaluating global emission inventories of biogenic bromocarbons, *Atmos. Chem. Phys.*, *13* (23), 11819-11838, doi: 10.5194/acp-13-11819-2013, 2013.
- Hoyle, C.R., V. Marecal, M.R. Russo, G. Allen, J. Arteta, C. Chemel, M.P. Chipperfield, F. D'Amato, O. Dessens, W. Feng, J.F. Hamilton, N.R.P. Harris, J.S. Hosking, A.C. Lewis, O. Morgenstern, T. Peter, J.A. Pyle, T. Reddman, N.A.D. Richards, P.J. Telford, W. Tian, S. Viciani, A. Volz-Thomas, O. Wild, X. Yang, and G. Zeng, Representation of tropical deep convection in atmospheric models - Part 2: Tracer transport, *Atmos. Chem. Phys.*, *11* (15), 8103-8131, doi: 10.5194/acp-11-8103-2011, 2011.
- Hu, L., The Role of the Ocean in the Atmospheric Budgets of Methyl Bromide, Methyl Chloride and Methane, Doctoral dissertation, Texas A&M University, College Station, TX, U.S.A., 2012.
- Hu, L., S.A. Yvon-Lewis, Y. Liu, and T.S. Bianchi, The ocean in near equilibrium with atmospheric methyl bromide, *Global Biogeochem. Cycles*, *26* (3), GB3016, doi: 10.1029/2011GB004272, 2012.
- Hu, L., S.A. Yvon-Lewis, J.H. Butler, J.M. Lobert, and D.B. King, An improved oceanic budget for methyl chloride, *J. Geophys. Res.*, *118* (2), 715-725, doi: 10.1029/2012JC008196, 2013.
- Hughes, C., M. Johnson, R. Utting, S. Turner, G. Malin, A. Clarke, and P.S. Liss, Microbial control of bromocarbon concentrations in coastal waters of the western Antarctic Peninsula, *Mar. Chem.*, *151*, 35-46, doi: 10.1016/j.marchem.2013.01.007, 2013.
- Hurley, M.D., T.J. Wallington, M.S. Javadi, and O.J. Nielsen, Atmospheric chemistry of  $\text{CF}_3\text{CF}=\text{CH}_2$ : Products and mechanisms of Cl atom and OH radical initiated oxidation, *Chem. Phys. Lett.*, *450* (4-6), 263-267, doi: 10.1016/j.cplett.2007.11.051, 2008.

- Hurst, D.F., J.C. Lin, P.A. Romashkin, B.C. Daube, C. Gerbig, D.M. Matross, S.C. Wofsy, B.D. Hall, and J.W. Elkins, Continuing global significance of emissions of Montreal Protocol-restricted halocarbons in the United States and Canada, *J. Geophys. Res.*, *111*, D15302, doi: 10.1029/2005JD006785, 2006.
- IPCC (Intergovernmental Panel on Climate Change), *Climate Change 2013: The Physical Science Basis: Contribution of Working Group I to the Fifth Assessment Report of the Intergovernmental Panel on Climate Change*, edited by T.F. Stocker, D. Qin, G.-K. Plattner, M. Tignor, S.K. Allen, J. Boschung, A. Nauels, Y. Xia, V. Bex, and P.M. Midgley, 1535 pp., Cambridge University Press, Cambridge, UK and New York, NY, USA, 2013.
- IPCC/TEAP (Intergovernmental Panel on Climate Change/Technology and Economic Assessment Panel), *IPCC/TEAP Special Report on Safeguarding the Ozone Layer and the Global Climate System: Issues Related to Hydrofluorocarbons and Perfluorocarbons*, prepared by Working Groups I and III of the Intergovernmental Panel on Climate Change, and the Technical and Economic Assessment Panel, Cambridge University Press, Cambridge, U.K. and New York, NY, U.S.A., 2005.
- Ivy, D.J., T. Arnold, C.M. Harth, L.P. Steele, J. Mühle, M. Rigby, P.K. Salameh, M. Leist, P.B. Krummel, P.J. Fraser, R.F. Weiss, and R.G. Prinn, Atmospheric histories and growth trends of C<sub>4</sub>F<sub>10</sub>, C<sub>5</sub>F<sub>12</sub>, C<sub>6</sub>F<sub>14</sub>, C<sub>7</sub>F<sub>16</sub> and C<sub>8</sub>F<sub>18</sub>, *Atmos. Chem. Phys.*, *12* (9), 4313-4325, doi: 10.5194/acp-12-4313-2012, 2012a.
- Ivy, D.J., M. Rigby, M. Baasandorj, J.B. Burkholder, and R.G. Prinn, Global emission estimates and radiative impact of C<sub>4</sub>F<sub>10</sub>, C<sub>5</sub>F<sub>12</sub>, C<sub>6</sub>F<sub>14</sub>, C<sub>7</sub>F<sub>16</sub> and C<sub>8</sub>F<sub>18</sub>, *Atmos. Chem. Phys.*, *12* (16), 7635-7645, doi: 10.5194/acp-12-7635-2012, 2012b.
- Jones, A., J. Urban, D.P. Murtagh, C. Sanchez, K.A. Walker, N.J. Livesey, L. Froidevaux, and M.L. Santee, Analysis of HCl and ClO time series in the upper stratosphere using satellite data sets, *Atmos. Chem. Phys.*, *11* (11), 5321-5333, doi: 10.5194/acp-11-5321-2011, 2011.
- Jones, C.E., K.E. Hornsby, R. Sommariva, R.M. Dunk, R. von Glasow, G.B. McFiggans, and L.J. Carpenter, Quantifying the contribution of marine organic gases to atmospheric iodine, *Geophys. Res. Lett.*, *37* (18), L18804, doi: 10.1029/2010GL043990, 2010.
- Jones, C.E., S.J. Andrews, L.J. Carpenter, C. Hogan, F.E. Hopkins, J.C. Laube, A.D. Robinson, T.G. Spain, S.D. Archer, N.R.P. Harris, P.D. Nightingale, S.J. O'Doherty, D.E. Oram, J.A. Pyle, J.H. Butler, and B.D. Hall, Results from the first national UK inter-laboratory calibration for very short-lived halocarbons, *Atmos. Meas. Tech.*, *4* (5), 865-874, doi: 10.5194/amt-4-865-2011, 2011.
- Jourdain, J.L., G. Le Bras, and J. Combourieu, Kinetic study by electron paramagnetic resonance and mass spectrometry of the elementary reactions of phosphorus tribromide with H, O, and OH radicals, *J. Phys. Chem.*, *86* (21), 4170-4175, doi: 10.1021/j100218a016, 1982.
- Kai, F.M., S.C. Tyler, J.T. Randerson, and D.R. Blake, Reduced methane growth rate explained by decreased Northern Hemisphere microbial sources, *Nature*, *476* (7359), 194-197, 2011.
- Keller, C.A., D. Brunner, S. Henne, M.K. Vollmer, S. O'Doherty, and S. Reimann, Evidence for under-reported western European emissions of the potent greenhouse gas HFC-23, *Geophys. Res. Lett.*, *38* (15), L15808, doi: 10.1029/2011GL047976, 2011.
- Keller, C.A., M. Hill, M.K. Vollmer, S. Henne, D. Brunner, S. Reimann, S. O'Doherty, J. Arduini, M. Maione, Z. Ferenczi, L. Haszpra, A.J. Manning, and T. Peter, European emissions of halogenated greenhouse gases inferred from atmospheric measurements, *Environ. Sci. Technol.*, *46* (1), 217-225, doi: 10.1021/es202453j, 2012.
- Kellmann, S., T. von Clarmann, G.P. Stiller, E. Eckert, N. Glatthor, M. Höpfner, M. Kiefer, J. Orphal, B. Funke, U. Grabowski, A. Linden, G.S. Dutton, and J.W. Elkins, Global CFC-11 (CCl<sub>3</sub>F) and CFC-12 (CCl<sub>2</sub>F<sub>2</sub>) measurements with the Michelson Interferometer for Passive Atmospheric Sounding (MIPAS): Retrieval, climatologies and trends, *Atmos. Chem. Phys.*, *12* (24), 11857-11875, doi: 10.5194/acp-12-11857-2012, 2012.
- Khan, M.A.H., M.E. Whelan, and R.C. Rhew, Effects of temperature and soil moisture on methyl halide and chloroform fluxes from drained peatland pasture soils, *J. Environ. Monit.*, *14* (1), 241-249, doi: 10.1039/c1em10639b, 2012.
- Kim, J., S. Li, K.-R. Kim, A. Stohl, J. Mühle, S.-K. Kim, M.-K. Park, D.-J. Kang, G. Lee, C.M. Harth, P.K. Salameh, and R.F. Weiss, Regional atmospheric emissions determined from measurements at Jeju Island, Korea: Halogenated compounds from China, *Geophys. Res. Lett.*, *37*, L12801, doi: 10.1029/2010GL043263, 2010.
- Kirschke, S., P. Bousquet, P. Ciais, M. Saunio, J.G. Canadell, E.J. Dlugokencky, P. Bergamaschi, D. Bergmann, D.R. Blake, L. Bruhwiler, P. Cameron-Smith, S. Castaldi, F. Chevallier, L. Feng, A. Fraser, M. Heimann, E.L. Hodson, S. Houweling, B. Josse, P.J. Fraser, P.B. Krummel, J.-F. Lamarque, R.L. Langenfelds, C. Le Quere, V. Naik, S. O'Doherty, I. Palmer, I. Pison, D. Plummer, B. Poulter, R.G. Prinn, M. Rigby, B. Ringeval, M. Santini, M. Schmidt, D.T. Shindell, I.J. Simpson, R. Spahni, L.P. Steele, S.A. Strode, K. Sudo, S. Szopa, G.R. van der

- Werf, A. Voulgarakis, M. van Weele, R.F. Weiss, J.E. Williams, and G. Zeng, Three decades of global methane sources and sinks, *Nature Geosci.*, *6* (10), 813-823, doi: 10.1038/ngeo1955, 2013.
- Kley, D., P.J. Crutzen, H.G.J. Smit, H. Vömel, S.J. Oltmans, H. Grassl, and V. Ramanathan, Observations of near-zero ozone concentrations over the convective Pacific: Effects on air chemistry, *Science*, *274* (5285), 230-233, doi: 10.1126/science.274.5285.230, 1996.
- Ko, M.K.W., and G. Poulet (Lead Authors), D.R. Blake, O. Boucher, J.H. Burkholder, M. Chin, R.A. Cox, C. George, H.-F. Graf, J.R. Holton, D.J. Jacob, K.S. Law, M.G. Lawrence, P.M. Midgley, P.W. Seakins, D.E. Shallcross, S.E. Strahan, D.J. Wuebbles, and Y. Yokouchi, Very short-lived halogen and sulfur substances, Chapter 2 in *Scientific Assessment of Ozone Depletion: 2002*, Global Ozone Research and Monitoring Project-Report No. 47, World Meteorological Organization, Geneva, Switzerland, 2003.
- Kohlhepp, R., R. Ruhnke, M.P. Chipperfield, M. De Maziere, J. Notholt, S. Barthlott, R.L. Batchelor, R.D. Blatherwick, T. Blumenstock, M.T. Coffey, P. Demoulin, H. Fast, W. Feng, A. Goldman, D.W.T. Griffith, K. Hamann, J.W. Hannigan, F. Hase, N.B. Jones, A. Kagawa, I. Kaiser, Y. Kasai, O. Kirner, W. Kouker, R. Lindenmaier, E. Mahieu, R.L. Mittermeier, B. Monge-Sanz, I. Morino, I. Murata, H. Nakajima, M. Palm, C. Paton-Walsh, U. Raffalski, T. Reddmann, M. Rettinger, C.P. Rinsland, E. Rozanov, M. Schneider, C. Senten, C. Servais, B.-M. Sinnhuber, D. Smale, K. Strong, R. Sussmann, J.R. Taylor, G. Vanhalewyn, T. Warneke, C. Whaley, M. Wiehle, and S.W. Wood, Observed and simulated time evolution of HCl, ClONO<sub>2</sub>, and HF total column abundances, *Atmos. Chem. Phys.*, *12* (7), 3527-3556, doi: 10.5194/acp-12-3527-2012, 2012.
- Kreycy, S., C. Camy-Peyret, M.P. Chipperfield, M. Dorf, W. Feng, R. Hossaini, L. Kritten, B. Werner, and K. Pfeilsticker, Atmospheric test of the  $J(\text{BrONO}_2)/k_{\text{BrO}+\text{NO}_2}$  ratio: Implications for total stratospheric Br<sub>y</sub> and bromine-mediated ozone loss, *Atmos. Chem. Phys.*, *13* (13), 6263-6274, doi: 10.5194/acp-13-6263-2013, 2013.
- Kreyling, D., H. Sagawa, I. Wohltmann, R. Lehmann, and Y. Kasai, SMILES zonal and diurnal variation climatology of stratospheric and mesospheric trace gasses: O<sub>3</sub>, HCl, HNO<sub>3</sub>, ClO, BrO, HOCl, HO<sub>2</sub>, and temperature, *J. Geophys. Res.*, *118* (20), doi: 10.1002/2012JD019420, 2013.
- Krysell, M., E. Fogelqvist, and T. Tanhua, Apparent removal of the transient tracer carbon tetrachloride from anoxic seawater, *Geophys. Res. Lett.*, *21* (23), 2511-2514, doi: 10.1029/94GL02336, 1994.
- Krysztofiak, G., V. Catoire, G. Poulet, V. Maréchal, M. Pirre, F. Louis, S. Canneaux, and B. Josse, Detailed modeling of the atmospheric degradation mechanism of very-short lived brominated species, *Atmos. Environ.*, *59*, 514-532, doi: 10.1016/j.atmosenv.2012.05.026, 2012.
- Kutsuna, S., L. Chen, T. Abe, J. Mizukado, T. Uchimaru, K. Tokuhashi, and A. Sekiya, Henry's law constants of 2,2,2-trifluoroethyl formate, ethyl trifluoroacetate, and non-fluorinated analogous esters, *Atmos. Environ.*, *39* (32), 5884-5892, doi: 10.1016/j.atmosenv.2005.06.021, 2005.
- Lal, S., R. Borchers, P. Fabian, P.K. Patra, and B. H. Subbaraya, Vertical distribution of methyl bromide over Hyderabad, India, *Tellus B*, *46*, 373-377, doi: 10.1034/j.1600-0889.1994.t01-3-00003.x, 1994.
- Langbein, T., H. Sonntag, D. Trapp, A. Hoffmann, W. Malms, E.P. Roth, V. Mors, and R. Zellner, Volatile anaesthetics and the atmosphere: Atmospheric lifetimes and atmospheric effects of halothane, enflurane, isoflurane, desflurane and sevoflurane, *British J. Anaesthesia*, *82* (1), 66-73, doi: 10.1093/bja/82.1.66, 1999.
- Langenfelds, R.L., P.J. Fraser, R.J. Francey, L.P. Steele, L.W. Porter, and C.E. Allison, The Cape Grim Air Archive: The first seventeen years, 1978-1995, in *Baseline Atmospheric Program (Australia) 1994-95*, edited by R.J. Francey, A.L. Dick, and N. Derek, 53-70, Bureau of Meteorology and CSIRO Division of Atmospheric Research, Melbourne, Australia, 1996.
- Laube, J.C., A. Engel, H. Bönisch, T. Möbius, D.R. Worton, W.T. Sturges, K. Grunow, and U. Schmidt, Contribution of very short-lived organic substances to stratospheric chlorine and bromine in the tropics—a case study, *Atmos. Chem. Phys.*, *8* (23), 7325-7334, doi: 10.5194/acp-8-7325-2008, 2008.
- Laube, J.C., P. Martinerie, E. Witrant, T. Blunier, J. Schwander, C.A.M. Brenninkmeijer, T.J. Schuck, M. Bolder, T. Röckmann, C. van der Veen, H. Bönisch, A. Engel, G.P. Mills, M.J. Newland, D.E. Oram, C.E. Reeves, and W.T. Sturges, Accelerating growth of HFC-227ea (1,1,1,2,3,3,3-heptafluoropropane) in the atmosphere, *Atmos. Chem. Phys.*, *10* (13), 5903-5910, doi: 10.5194/acp-10-5903-2010, 2010.
- Laube, J.C., C. Hogan, M.J. Newland, F.S. Mani, P.J. Fraser, C.A.M. Brenninkmeijer, P. Martinerie, D.E. Oram, T. Röckmann, J. Schwander, E. Witrant, G.P. Mills, C.E. Reeves, and W.T. Sturges, Distributions, long term trends and emissions of four perfluorocarbons in remote parts of the atmosphere and firn air, *Atmos. Chem. Phys.*, *12* (9), 4081-4090, doi: 10.5194/acp-12-4081-2012, 2012.
- Laube, J.C., A. Keil, H. Bönisch, A. Engel, T. Röckmann, C.M. Volk, and W.T. Sturges, Observation-based assessment of stratospheric fractional release, lifetimes, and ozone depletion potentials of ten important source gases, *Atmos. Chem. Phys.*, *13* (5), 2779-2791, doi: 10.5194/acp-13-2779-2013, 2013.

- Laube, J.C., M.J. Newland, C. Hogan, C.A.M. Brenninkmeijer, P.J. Fraser, P. Martinerie, D.E. Oram, C.E. Reeves, T. Röckmann, J. Schwander, E. Witrant, and W.T. Sturges, Newly detected ozone-depleting substances in the atmosphere, *Nature Geosci.*, *7* (4), 266–269, doi: 10.1038/ngeo2109, 2014.
- Law, K.S., and W.T. Sturges (Lead Authors), D.R. Blake, N.J. Blake, J.B. Burkholder, J.H. Butler, R.A. Cox, P.H. Haynes, M.K.W. Ko, K. Kreher, C. Mari, K. Pfeilsticker, J.M.C. Plane, R.J. Salawitch, C. Schiller, B.-M. Sinnhuber, R. von Glasow, N.J. Warwick, D.J. Wuebbles, and S.A. Yvon-Lewis, Halogenated very short-lived substances, Chapter 2 in *Scientific Assessment of Ozone Depletion: 2006*, Global Ozone Research and Monitoring Project—Report No.50, World Meteorological Organization, Geneva, Switzerland, 2007.
- Lawler, M.J., B. D. Finley, W.C. Keene, A.A.P. Pszenny, K.A. Read, R. von Glasow, and E.S. Saltzman, Pollution-enhanced reactive chlorine chemistry in the eastern tropical Atlantic boundary layer, *Geophys. Res. Lett.*, *36* (8), L08810, doi: 10.1029/2008GL036666, 2009.
- Le Calvé, S., G. Le Bras, and A. Mellouki, Temperature dependence for the rate coefficients of the reactions of the OH radical with a series of formates, *J. Phys. Chem. A*, *101* (30), 5489–5493, doi: 10.1021/jp970554x, 1997.
- Lee, Y., S. Bae, and W. Lee, Degradation of carbon tetrachloride in modified Fenton reaction, *Korean J. Chem. Eng.*, *29* (6), 769–774, doi: 10.1007/s11814-011-0261-8, 2012.
- Lee-Taylor, J.M., and E.A. Holland, Litter decomposition as a potential natural source of methyl bromide, *J. Geophys. Res.*, *105* (D7), 8857–8864, doi: 10.1029/1999JD901112, 2000.
- Lee-Taylor, J., and K.R. Redeker, Reevaluation of global emissions from rice paddies of methyl iodide and other species, *Geophys. Res. Lett.*, *32*, L15801, doi: 10.1029/2005GL022918, 2005.
- Lee-Taylor, J.M., G.P. Brasseur, and Y. Yokouchi, A preliminary three-dimensional global model study of atmospheric methyl chloride distributions, *J. Geophys. Res.*, *106* (D24), 34221–34233, doi: 10.1029/2001JD900209, 2001.
- Leedham, E.C., C. Hughes, F.S.L. Keng, S.-M. Phang, G. Malin, and W.T. Sturges, Emission of atmospherically significant halocarbons by naturally occurring and farmed tropical macroalgae, *Biogeosciences*, *10* (6), 3615–3633, doi: 10.5194/bg-10-3615-2013, 2013.
- Leung, F.-Y.T., A.J. Colussi, M.R. Hoffmann, and G.C. Toon, Isotopic fractionation of carbonyl sulfide in the atmosphere: Implications for the source of background stratospheric sulfate aerosol, *Geophys. Res. Lett.*, *29* (10), 112–111–112–114, doi: 10.1029/2001GL013955, 2002.
- Levin, I., T. Naegler, R. Heinz, D. Osusko, E. Cuevas, A. Engel, J. Ilmberger, R.L. Langenfelds, B. Neininger, C. von Rohden, L.P. Steele, R. Weller, D.E. Worthy, and S.A. Zimov, The global SF<sub>6</sub> source inferred from long-term high precision atmospheric measurements and its comparison with emission inventories, *Atmos. Chem. Phys.*, *10* (6), 2655–2662, doi: 10.5194/acp-10-2655-2010, 2010.
- Levin, I., C. Veidt, B.H. Vaughn, G. Brailsford, T. Bromley, R. Heinz, D. Lowe, J.B. Miller, C. Poß, and J.W.C. White, No inter-hemispheric δ<sup>13</sup>CH<sub>4</sub> trend observed, *Nature*, *486* (7404), E3–E4, doi: 10.1038/nature11175, 2012.
- Levine, J.G., P. Braesicke, N.R.P. Harris, N.H. Savage, and J.A. Pyle, Pathways and timescales for troposphere-to-stratosphere transport via the tropical tropopause layer and their relevance for very short lived substances, *J. Geophys. Res.*, *112* (D4), D04308, doi: 10.1029/2005JD006940, 2007.
- Li, S., J. Kim, K.R. Kim, J. Mühle, S.K. Kim, M.K. Park, A. Stohl, D.J. Kang, T. Arnold, C.M. Harth, P.K. Salameh, and R.F. Weiss, Emissions of halogenated compounds in East Asia determined from measurements at Jeju Island, Korea, *Environ. Sci. Technol.*, *45* (13), 5668–5675, doi: 10.1021/es104124k, 2011.
- Liang, Q., R.S. Stolarski, S.R. Kawa, J.E. Nielsen, J.M. Rodriguez, A.R. Douglass, J.M. Rodriguez, D.R. Blake, E.L. Atlas, and L.E. Ott, Finding the missing stratospheric Br<sub>y</sub>: A global modeling study of CHBr<sub>3</sub> and CH<sub>2</sub>Br<sub>2</sub>, *Atmos. Chem. Phys.*, *10* (5), 2269–2286, doi: 10.5194/acp-10-2269-2010, 2010.
- Liang, Q., E. Atlas, D. Blake, M. Dorf, K. Pfeilsticker, and S. Schauffler, Convective transport of very-short-lived bromocarbons to the stratosphere, *Atmos. Chem. Phys.*, *14*, 5781–5792, doi: 10.5194/acp-14-5781-2014, 2014.
- Lin, C.Y., and S.L. Manley, Bromoform production from seawater treated with bromoperoxidase, *Limnol. Oceanogr.*, *57* (6), 1857–1866, doi: 10.4319/lo.2012.57.06.1857, 2012.
- Liu, C., and E.J. Zipser, Global distribution of convection penetrating the tropical tropopause, *J. Geophys. Res.*, *110* (D23), D23104, doi: 10.1029/2005JD006063, 2005.
- Liu, X.-F., Evidence of Biodegradation of Atmospheric Carbon Tetrachloride in Soils: Field and Microcosm Studies, Ph.D. thesis, 139 pp., Columbia University, New York, NY, U.S.A., 2006.
- Liu, Y., S.A. Yvon-Lewis, L. Hu, J.E. Salisbury, and J.E. O'Hern, CHBr<sub>3</sub>, CH<sub>2</sub>Br<sub>2</sub>, and CHClBr<sub>2</sub> in U.S. coastal waters during the Gulf of Mexico and East Coast Carbon cruise, *J. Geophys. Res.*, *116* (C10), C10004, doi: 10.1029/2010JC006729, 2011.

- Liu, Y., S.A. Yvon-Lewis, D.C.O. Thornton, J.H. Butler, T.S. Bianchi, L. Campbell, L. Hu, and R.W. Smith, Spatial and temporal distributions of bromoform and dibromomethane in the Atlantic Ocean and their relationship with photosynthetic biomass, *J. Geophys. Res.*, *118* (8), 3950–3965, doi: 10.1002/jgrc.20299, 2013.
- Logue, J.M., M.J. Small, D. Stern, J. Maranche, and A.L. Robinson, Spatial variation in ambient air toxics concentrations and health risks between industrial-influenced, urban, and rural sites, *J. Air Waste Manag. Assoc.*, *60* (3), 271–286, doi: 10.3155/1047-3289.60.3.271, 2010.
- Low, J.C., N.Y. Wang, J. Williams, and R.J. Cicerone, Measurements of ambient atmospheric C<sub>2</sub>H<sub>5</sub>Cl and other ethyl and methyl halides at coastal California sites and over the Pacific Ocean, *J. Geophys. Res.*, *108* (D19), 4608, doi: 10.1029/2003JD003620, 2003.
- Lu, Z., D.G. Streets, Q. Zhang, S. Wang, G.R. Carmichael, Y.F. Cheng, C. Wei, M. Chin, T. Diehl, and Q. Tan, Sulfur dioxide emissions in China and sulfur trends in East Asia since 2000, *Atmos. Chem. Phys.*, *10* (13), 6311–6331, doi: 10.5194/acp-10-6311-2010, 2010.
- Mahajan, A.S., J.M.C. Plane, H. Oetjen, L. Mendes, R.W. Saunders, A. Saiz-Lopez, C.E. Jones, L.J. Carpenter, and G.B. McFiggans, Measurement and modelling of tropospheric reactive halogen species over the tropical Atlantic Ocean, *Atmos. Chem. Phys.*, *10* (10), 4611–4624, doi: 10.5194/acp-10-4611-2010, 2010.
- Mahajan, A.S., J.C. Gómez Martín, T.D. Hay, S.-J. Royer, S. Yvon-Lewis, Y. Liu, L. Hu, C. Prados-Roman, C. Ordóñez, J.M.C. Plane, and A. Saiz-Lopez, Latitudinal distribution of reactive iodine in the Eastern Pacific and its link to open ocean sources, *Atmos. Chem. Phys.*, *12* (23), 11609–11617, doi: 10.5194/acp-12-11609-2012, 2012.
- Mahieu, E., R. Zander, P.F. Bernath, C.D. Boone, and K.A. Walker, Recent trend anomaly of hydrogen chloride (HCl) at northern mid-latitudes derived from Jungfraujoch, HALOE and ACE-FTS Infrared solar observations, in *The Atmospheric Chemistry Experiment ACE at 10: A Solar Occultation Anthology*, edited by P.F. Bernath, 239–249, A. Deepak Publishing, Hampton, Virginia, 2013.
- Mahieu, E., R. Zander, G.C. Toon, M.K. Vollmer, S. Reimann, J. Mühle, W. Bader, B. Bovy, B. Lejeune, C. Servais, P. Demoulin, G. Roland, P.F. Bernath, C.D. Boone, K.A. Walker, and P. Duchatelet, Spectrometric monitoring of atmospheric carbon tetrafluoride (CF<sub>4</sub>) above the Jungfraujoch station since 1989: Evidence of continued increase but at a slowing rate, *Atmos. Meas. Tech.*, *7* (1), 333–344, doi: 10.5194/amt-7-333-2014, 2014.
- Maiss, M., and C.A.M. Brenninkmeijer, Atmospheric SF<sub>6</sub>: Trends, sources and prospects, *Environ. Sci. Technol.*, *32* (20), 3077–3086, doi: 10.1021/es9802807, 1998.
- Malicet, J., D. Daumont, J. Charbonnier, C. Parisse, A. Chakir, and J. Brion, Ozone U.V. spectroscopy. II. Absorption cross-sections and temperature dependence, *J. Atmos. Chem.*, *21* (3), 263–273, doi: 10.1007/BF00696758, 1995.
- Manley, S.L., N.-Y. Wang, M.L. Walser, and R.J. Cicerone, Methyl halide emissions from greenhouse-grown mangroves, *Geophys. Res. Lett.*, *34* (1), L01806, doi: 10.1029/2006GL027777, 2007.
- Marcy, T.P., P.J. Popp, R.S. Gao, D.W. Fahey, E.A. Ray, E.C. Richard, T.L. Thompson, E.L. Atlas, M. Loewenstein, S.C. Wofsy, S. Park, E.M. Weinstock, W.H. Swartz, and M.J. Mahoney, Measurements of trace gases in the tropical tropopause layer, *Atmos. Environ.*, *41* (34), 7253–7261, doi: 10.1016/j.atmosenv.2007.05.032, 2007.
- Marécal, V., M. Pirre, G. Krysztofiak, P.D. Hamer, and B. Josse, What do we learn about bromoform transport and chemistry in deep convection from fine scale modelling?, *Atmos. Chem. Phys.*, *12* (14), 6073–6093, doi: 10.5194/acp-12-6073-2012, 2012.
- Mattsson, E., A. Karlsson, and K. Abrahamsson, Regional sinks of bromoform in the Southern Ocean, *Geophys. Res. Lett.*, *40* (15), 3991–3996, doi: 10.1002/grl.50783, 2013.
- McCulloch, A., Global production and emissions of bromochlorodifluoromethane and bromotrifluoromethane (halons 1211 and 1301), *Atmos. Environ., Part A*, *26* (7), 1325–1329, doi: 10.1016/0960-1686(92)90392-X, 1992.
- McCulloch, A., M.L. Aucott, C.M. Benkovitz, T.E. Graedel, G. Kleiman, P.M. Midgley, and Y.-F. Li, Global emissions of hydrogen chloride and chloromethane from coal combustion, incineration and industrial activities: Reactive Chlorine Emissions Inventory, *J. Geophys. Res.*, *104* (D7), 8391–8403, doi: 10.1029/1999JD900025, 1999.
- McGillen, M.R., E.L. Fleming, C.H. Jackman, and J.B. Burkholder, CFC<sub>11</sub> (CFC-11): UV absorption spectrum temperature dependence measurements and the impact on its atmospheric lifetime and uncertainty, *Geophys. Res. Lett.*, *40* (17), 4772–4776, doi: 10.1002/grl.50915, 2013.
- McLinden, C.A., C.S. Haley, N.D. Lloyd, F. Hendrick, A. Rozanov, B.-M. Sinnhuber, F. Goutail, D.A. Degenstein, E.J. Llewellyn, C.E. Sioris, M. Van Roozendaal, J.P. Pommereau, W. Lotz, and J.P. Burrows, Odin/OSIRIS

- observations of stratospheric BrO: Retrieval methodology, climatology, and inferred Br<sub>y</sub>, *J. Geophys. Res.*, *115*, D15308, doi: 10.1029/2009JD012488, 2010.
- Mead, M.I., I.R. White, G. Nickless, K.-Y. Wang, and D.E. Shallcross, An estimation of the global emission of methyl bromide from rapeseed (*Brassica napus*) from 1961 to 2003, *Atmos. Environ.*, *42* (2), 337-345, doi: 10.1016/j.atmosenv.2007.09.020, 2008.
- Mébarki, Y., V. Catoire, N. Huret, G. Berthet, C. Robert, and G. Poulet, More evidence for very short-lived substance contribution to stratospheric chlorine inferred from HCl balloon-borne in situ measurements in the tropics, *Atmos. Chem. Phys.*, *10* (2), 397-409, doi: 10.5194/acp-10-397-2010, 2010.
- Mendoza, Y., K.D. Goodwin, and J.D. Happell, Microbial removal of atmospheric carbon tetrachloride in bulk aerobic soils, *Appl. Environ. Microbiol.*, *77* (17), 5835-5841, doi: 10.1128/AEM.05341-11, 2011.
- Millán, L., N. Livesey, W. Read, L. Froidevaux, D. Kinnison, R. Harwood, I.A. MacKenzie, and M.P. Chipperfield, New Aura Microwave Limb Sounder observations of BrO and implications for Br<sub>y</sub>, *Atmos. Meas. Tech.*, *5* (7), 1741-1751, doi: 10.5194/amt-5-1741-2012, 2012.
- Miller, B.R., and L.J.M. Kuijpers, Projecting future HFC-23 emissions, *Atmos. Chem. Phys.*, *11* (24), 13259-13267, doi: 10.5194/acp-11-13259-2011, 2011.
- Miller, B.R., R.F. Weiss, P.K. Salameh, T. Tanhua, B.R. Grealley, J. Mühle, and P.G. Simmonds, Medusa: A sample preconcentration and GC/MS detector system for in situ measurements of atmospheric trace halocarbons, hydrocarbons, and sulfur compounds, *Anal. Chem.*, *80* (5), 1536-1545, doi: 10.1021/ac702084k, 2008.
- Miller, B.R., M. Rigby, L.J.M. Kuijpers, P.B. Krummel, L.P. Steele, M. Leist, P.J. Fraser, A. McCulloch, C. Harth, P. Salameh, J. Mühle, R.F. Weiss, R.G. Prinn, R.H.J. Wang, S. O'Doherty, B.R. Grealley, and P.G. Simmonds, HFC-23 (CHF<sub>3</sub>) emission trend response to HCFC-22 (CHClF<sub>2</sub>) production and recent HFC-23 emission abatement measures, *Atmos. Chem. Phys.*, *10* (16), 7875-7890, doi: 10.5194/acp-10-7875-2010, 2010.
- Miller, J.B., S.J. Lehman, S.A. Montzka, C. Sweeney, B.R. Miller, A. Karion, C. Wolak, E.J. Dlugokencky, J. Southon, J.C. Turnbull, and P.P. Tans, Linking emissions of fossil fuel CO<sub>2</sub> and other anthropogenic trace gases using atmospheric <sup>14</sup>CO<sub>2</sub>, *J. Geophys. Res.*, *117*, D08302, doi: 10.1029/2011JD017048, 2012.
- Miller, M., and T. Batchelor, Information paper on feedstock uses of ozone-depleting substances, 72 pp., available at [http://ec.europa.eu/clima/policies/ozone/research/docs/feedstock\\_en.pdf](http://ec.europa.eu/clima/policies/ozone/research/docs/feedstock_en.pdf), 2012.
- Millet, D.B., E.L. Atlas, D.R. Blake, N.J. Blake, G.S. Diskin, J.S. Holloway, R.C. Hudman, S. Meinardi, T.B. Ryerson, and G.W. Sachse, Halocarbon emissions from the United States and Mexico and their global warming potential, *Environ. Sci. Technol.*, *43* (4), 1055-1060, doi: 10.1021/es802146j, 2009.
- Montzka, S.A., R.C. Myers, J.H. Butler, J.W. Elkins, L.T. Lock, A.D. Clarke, and A.H. Goldstein, Observations of HFC-134a in the remote troposphere, *Geophys. Res. Lett.*, *23* (2), 169-172, doi: 10.1029/95GL03590, 1996.
- Montzka, S.A., J.H. Butler, J.W. Elkins, T.M. Thompson, A.D. Clarke, and L.T. Lock, Present and future trends in the atmospheric burden of ozone-depleting halogens, *Nature*, *398*, 690-694, doi: 10.1038/19499, 1999.
- Montzka, S.A., C.M. Spivakovsky, J.H. Butler, J.W. Elkins, L.T. Lock, and D.J. Mondeel, New observational constraints for atmospheric hydroxyl on global and hemispheric scales, *Science*, *288* (5465), 500-503, doi: 10.1126/science.288.5465.500, 2000.
- Montzka, S.A., and P.J. Fraser (Lead Authors), J.H. Butler, P.S. Connell, D.M. Cunnold, J.S. Daniel, R.G. Derwent, S. Lal, A. McCulloch, D.E. Oram, C.E. Reeves, E. Sanhueza, L.P. Steele, G.J.M. Velders, R.F. Weiss, and R.J. Zander, Controlled substances and other source gases, Chapter 1 in *Scientific Assessment of Ozone Depletion: 2002*, Global Ozone Research and Monitoring Project—Report No. 47, Geneva, Switzerland, 2003.
- Montzka, S.A., J.H. Butler, B.D. Hall, D.J. Mondeel, and J.W. Elkins, A decline in tropospheric organic bromine, *Geophys. Res. Lett.*, *30* (15), 1826, doi: 10.1029/2003GL017745, 2003.
- Montzka, S.A., M. Aydin, M. Battle, J.H. Butler, E.S. Saltzman, B.D. Hall, A.D. Clarke, D. Mondeel, and J.W. Elkins, A 350-year atmospheric history for carbonyl sulfide inferred from Antarctic firn air and air trapped in ice, *J. Geophys. Res.*, *109*, D22302, doi: 10.1029/2004JD004686, 2004.
- Montzka, S.A., P. Calvert, B.D. Hall, J.W. Elkins, T.J. Conway, P.P. Tans, and C. Sweeney, On the global distribution, seasonality, and budget of atmospheric carbonyl sulfide (COS) and some similarities to CO<sub>2</sub>, *J. Geophys. Res.*, *112*, D09302, doi: 10.1029/2006JD007665, 2007.
- Montzka, S.A., B.D. Hall, and J.W. Elkins, Accelerated increases observed for hydrochlorofluorocarbons since 2004 in the global atmosphere, *Geophys. Res. Lett.*, *36*, L03804, doi: 10.1029/2008GL036475, 2009.
- Montzka, S.A., L. Kuijpers, M.O. Battle, M. Aydin, K.R. Verhulst, E.S. Saltzman, and D.W. Fahey, Recent increases in global HFC-23 emissions, *Geophys. Res. Lett.*, *37*, L02808, doi: 10.1029/2009GL041195, 2010.
- Montzka, S.A., and S. Reimann (Coordinating Lead Authors), A. Engel, K. Krüger, S. O'Doherty, W.T. Sturges, D.R. Blake, M. Dorf, P.J. Fraser, L. Froidevaux, K. Jucks, K. Kreher, M.J. Kurylo, A. Mellouki, J. Miller, O.-J. Nielsen, V.L. Orkin, R.G. Prinn, R. Rhew, M.L. Santee, and D.P. Verdonik, Ozone-Depleting Substances

- (ODSs) and related chemicals, Chapter 1 in *Scientific Assessment of Ozone Depletion: 2010*, Global Ozone Research and Monitoring Project—Report No. 52, World Meteorological Organization, Geneva, Switzerland, 2011.
- Montzka, S.A., M. Krol, E. Dlugokencky, B. Hall, P. Jöckel, and J. Lelieveld, Small interannual variability of global atmospheric hydroxyl, *Science*, *331* (6013), 67-69, doi: 10.1126/science.1197640, 2011.
- Mühle, J., J. Huang, R.F. Weiss, R.G. Prinn, B.R. Miller, P.K. Salameh, C.M. Harth, P.J. Fraser, L.W. Porter, B.R. Grealley, S. O'Doherty, and P.G. Simmonds, Sulfuryl fluoride in the global atmosphere, *J. Geophys. Res.*, *114*, D05306, doi: 10.1029/2008JD011162, 2009.
- Mühle, J., A.L. Ganesan, B.R. Miller, P.K. Salameh, C.M. Harth, B.R. Grealley, M. Rigby, L.W. Porter, L.P. Steele, C.M. Trudinger, P.B. Krummel, S. O'Doherty, P.J. Fraser, P.G. Simmonds, R.G. Prinn, and R.F. Weiss, Perfluorocarbons in the global atmosphere: Tetrafluoromethane, hexafluoroethane, and octafluoropropane, *Atmos. Chem. Phys.*, *10* (11), 5145-5164, doi: 10.5194/acp-10-5145-2010, 2010.
- Murphy, D.M., and D.S. Thomson, Halogen ions and NO<sup>+</sup> in the mass spectra of aerosols in the upper troposphere and lower stratosphere, *Geophys. Res. Lett.*, *27* (19), 3217-3220, doi: 10.1029/1999GL011267, 2000.
- Myhre, G., and D. Shindell (Coordinating Lead Authors), F.-M. Bréon, W. Collins, J. Fuglestvedt, J. Huang, D. Koch, J.-F. Lamarque, D. Lee, B. Mendoza, T. Nakajima, A. Robock, G. Stephens, T. Takemura, and H. Zhang (Lead Authors), Anthropogenic and natural radiative forcing, Chapter 8 in *Climate Change 2013: The Physical Science Basis. Contribution of Working Group I to the Fifth Assessment Report of the Intergovernmental Panel on Climate Change*, edited by Stocker, T.F., D. Qin, G.-K. Plattner, M. Tignor, S.K. Allen, J. Boschung, A. Nauels, Y. Xia, V. Bex, and P.M. Midgley, 1535 pp., Cambridge University Press, Cambridge, U.K. and New York, NY, 2013.
- Naik, V., A.K. Jain, K.O. Patten, and D.J. Wuebbles, Consistent sets of atmospheric lifetimes and radiative forcings on climate for CFC replacements: HCFCs and HFCs, *J. Geophys. Res.*, *105* (D5), 6903-6914, doi: 10.1029/1999JD901128, 2000.
- Newland, M.J., C.E. Reeves, D.E. Oram, J.C. Laube, W.T. Sturges, C. Hogan, P. Begley, and P.J. Fraser, Southern hemispheric halon trends and global halon emissions, 1978-2011, *Atmos. Chem. Phys.*, *13* (11), 5551-5565, doi: 10.5194/acp-13-5551-2013, 2013.
- Newman, P.A., J.S. Daniel, D.W. Waugh, and E.R. Nash, A new formulation of equivalent effective stratospheric chlorine (EESC), *Atmos. Chem. Phys.*, *7* (17), 4537-4552, doi: 10.5194/acp-7-4537-2007, 2007.
- Nilsson, E.J.K., L.M.T. Joelsson, J. Heimdal, M.S. Johnson, and O.J. Nielsen, Re-evaluation of the reaction rate coefficient of CH<sub>3</sub>Br + OH with implications for the atmospheric budget of methyl bromide, *Atmos. Environ.*, *80*, 70-74, doi: 10.1016/j.atmosenv.2013.07.046, 2013.
- O'Brien, L.M., N.R.P. Harris, A.D. Robinson, B. Gostlow, N. Warwick, X. Yang, and J.A. Pyle, Bromocarbons in the tropical marine boundary layer at the Cape Verde Observatory – measurements and modelling, *Atmos. Chem. Phys.*, *9* (22), 9083-9099, doi: 10.5194/acp-9-9083-2009, 2009.
- O'Doherty, S., D.M. Cunnold, A. Manning, B.R. Miller, R.H.J. Wang, P.B. Krummel, P.J. Fraser, P.G. Simmonds, A. McCulloch, R.F. Weiss, P. Salameh, L.W. Porter, R.G. Prinn, J. Huang, G. Sturrock, D. Ryall, R.G. Derwent, and S.A. Montzka, Rapid growth of hydrofluorocarbon 134a and hydrochlorofluorocarbons 141b, 142b, and 22 from Advanced Global Atmospheric Gases Experiment (AGAGE) observations at Cape Grim, Tasmania, and Mace Head, Ireland, *J. Geophys. Res.*, *109*, D06310, doi: 10.1029/2003JD004277, 2004.
- O'Doherty, S., D.M. Cunnold, B.R. Miller, J. Mühle, A. McCulloch, P.G. Simmonds, A.J. Manning, S. Reimann, M.K. Vollmer, B.R. Grealley, R.G. Prinn, P.J. Fraser, L.P. Steele, P.B. Krummel, B.L. Dunse, L.W. Porter, C.R. Lunder, N. Schmidbauer, O. Hermansen, P.K. Salameh, C.M. Harth, R.H.J. Wang, and R.F. Weiss, Global and regional emissions of HFC-125 (CHF<sub>2</sub>CF<sub>3</sub>) from in situ and air archive atmospheric observations at AGAGE and SOGE observatories, *J. Geophys. Res.*, *114*, D23304, doi: 10.1029/2009JD012184, 2009.
- O'Doherty, S., P.G. Simmonds, D.M. Cunnold, H.J. Wang, G.A. Sturrock, P.J. Fraser, D. Ryall, R.G. Derwent, R.F., Weiss, P. Salameh, B.R. Miller, and R.G. Prinn, In situ chloroform measurements at Advanced Global Atmospheric Gases Experiment atmospheric research stations from 1994 to 1998, *J. Geophys. Res.*, *106* (D17), 20429-20444, doi: 10.1029/2000JD900792, 2001.
- Ooki, A., and Y. Yokouchi, Dichloromethane in the Indian Ocean: Evidence for in-situ production in seawater, *Mar. Chem.*, *124* (1-4), 119-124, doi: 10.1016/j.marchem.2011.01.001, 2011.
- Oram, D.E., Trends of Long-Lived Anthropogenic Halocarbons in the Southern Hemisphere and Model Calculations of Global Emissions, Ph.D. thesis, University of East Anglia, Norwich, U.K., 249 pp., 1999.
- Oram, D.E., W.T. Sturges, S.A. Penkett, A. McCulloch, and P.J. Fraser, Growth of fluoroform (CHF<sub>3</sub>, HFC-23) in the background atmosphere, *Geophys. Res. Lett.*, *25* (1), 35-38, doi: 10.1029/97GL03483, 1998.

- Oram, D.E., F.S. Mani, J.C. Laube, M.J. Newland, C.E. Reeves, W.T. Sturges, S.A. Penkett, C.A.M. Brenninkmeijer, T. Röckmann, and P.J. Fraser, Long-term tropospheric trend of octafluorocyclobutane (c-C<sub>4</sub>F<sub>8</sub> or PFC-318), *Atmos. Chem. Phys.*, *12* (1), 261-269, doi: 10.5194/acp-12-261-2012, 2012.
- Ordoñez, C., J.-F. Lamarque, S. Tilmes, D.E. Kinnison, E.L. Atlas, D.R. Blake, G. Sousa Santos, G. Brasseur, and A. Saiz-Lopez, Bromine and iodine chemistry in a global chemistry-climate model: Description and evaluation of very short-lived oceanic sources, *Atmos. Chem. Phys.*, *12* (3), 1423-1447, doi: 10.5194/acp-12-1423-2012, 2012.
- Orkin, V.L., F. Louis, R.E. Huie, and M.J. Kurylo, Photochemistry of bromine-containing fluorinated alkenes: Reactivity toward OH and UV spectra, *J. Phys. Chem. A*, *106* (43), 10195-10199, doi: 10.1021/jp014436s, 2002.
- Orkin, V.L., V.G. Khamaganov, E.E. Kasimovskaya, and A.G. Guschin, Photochemical properties of some Cl-containing halogenated alkanes, *J. Phys. Chem. A*, *117* (26), 5483-5490, doi: 10.1021/jp400408y, 2013a.
- Orkin, V.L., V.G. Khamaganov, S.N. Kozlov, and M.J. Kurylo, Measurements of rate constants for the OH reactions with bromoform (CHBr<sub>3</sub>), CHBr<sub>2</sub>Cl, CHBrCl<sub>2</sub>, and epichlorohydrin (C<sub>3</sub>H<sub>5</sub>ClO), *J. Phys. Chem. A*, *117* (18), 3809-3818, doi: 10.1021/jp3128753, 2013b.
- Oyaro, N., S.R. Sellevåg, and C.J. Nielsen, Study of the OH and Cl-initiated oxidation, IR absorption cross-section, radiative forcing, and global warming potential of four C<sub>4</sub>-hydrofluoroethers, *Environ. Sci. Technol.*, *38* (21), 5567-5576, doi: 10.1021/es0497330, 2004.
- Oyaro, N., S.R. Sellevåg, and C.J. Nielsen, Atmospheric chemistry of hydrofluoroethers: Reaction of a series of hydrofluoroethers with OH radicals and Cl atoms, atmospheric lifetimes, and global warming potentials, *J. Phys. Chem. A*, *109* (2), 337-346, doi: 10.1021/jp047860c, 2005.
- Palmer, C.J., and C.J. Reason, Relationships of surface bromoform concentrations with mixed layer depth and salinity in the tropical oceans, *Global Biogeochem. Cycles*, *23*, GB2014, doi: 10.1029/2008GB003338, 2009.
- Palmer, P.I., D.J. Jacob, L.J. Mickley, D.R. Blake, G.W. Sachse, H.E. Fuelberg, and C.M. Kiley, Eastern Asian emissions of anthropogenic halocarbons deduced from aircraft concentration data, *J. Geophys. Res.*, *108* (D24), 4753, doi: 10.1029/2003JD003591, 2003.
- Papadimitriou, V.C., R.W. Portmann, D.W. Fahey, J. Mühle, R.F. Weiss, and J.B. Burkholder, Experimental and theoretical study of the atmospheric chemistry and global warming potential of SO<sub>2</sub>F<sub>2</sub>, *J. Phys. Chem. A*, *112* (49), 12657-12666, doi: 10.1021/jp806368u, 2008.
- Papadimitriou, V.C., M.R. McGillen, E.L. Fleming, C.H. Jackman, and J.B. Burkholder, NF<sub>3</sub>: UV absorption spectrum temperature dependence and the atmospheric and climate forcing implications, *Geophys. Res. Lett.*, *40* (2), 440-445, doi: 10.1002/grl.50120, 2013a.
- Papadimitriou, V.C., M.R. McGillen, S.C. Smith, A.M. Jubb, R.W. Portmann, B.D. Hall, E.L. Fleming, C.H. Jackman, and J.B. Burkholder, 1,2-Dichlorohexafluoro-cyclobutane (1,2-c-C<sub>4</sub>F<sub>6</sub>Cl<sub>2</sub>, R-316c) a potent ozone depleting substance and greenhouse gas: Atmospheric loss processes, lifetimes, and ozone depletion and global warming potentials for the (*E*) and (*Z*) stereoisomers, *J. Phys. Chem. A*, *117* (43), 11049-11065, doi: 10.1021/jp407823k, 2013b.
- Papanastasiou, D.K., N. Rontu Carlon, J.A. Neuman, E.L. Fleming, C.H. Jackman, and J.B. Burkholder, Revised UV absorption spectra, ozone depletion potentials, and global warming potentials for the ozone-depleting substances CF<sub>2</sub>Br<sub>2</sub>, CF<sub>2</sub>ClBr, and CF<sub>2</sub>BrCF<sub>2</sub>Br, *Geophys. Res. Lett.*, *40* (2), 464-469, doi: 10.1002/grl.50121, 2013.
- Papanastasiou, D.K., S.A. McKeen, and J.B. Burkholder, The very short-lived ozone depleting substance CHBr<sub>3</sub> (bromoform): Revised UV absorption spectrum, atmospheric lifetime and ozone depletion potential, *Atmos. Chem. Phys.*, *14* (6), 3017-3025, doi: 10.5194/acp-14-3017-2014, 2014.
- Papasavva, S., D.J. Luecken, R.L. Waterland, K.N. Taddonio, and S.O. Andersen, Estimated 2017 refrigerant emissions of 2,3,3,3-tetrafluoropropene (HFC-1234yf) in the United States resulting from automobile air conditioning, *Environ. Sci. Technol.*, *43* (24), 9252-9259, doi: 10.1021/es902124u, 2009.
- Park, S., P. Croteau, K.A. Boering, D.M. Etheridge, D. Ferretti, P.J. Fraser, K.-R. Kim, P.B. Krummel, R.L. Langenfelds, T.D. van Ommen, L.P. Steele, and C.M. Trudinger, Trends and seasonal cycles in the isotopic composition of nitrous oxide since 1940, *Nature Geosci.*, *5* (4), 261-265, doi: 10.1038/ngeo1421, 2012.
- Parrella, J.P., D.J. Jacob, Q. Liang, Y. Zhang, L.J. Mickley, B. Miller, M.J. Evans, X. Yang, J.A. Pyle, N. Theys, and M. Van Roozendaal, Tropospheric bromine chemistry: Implications for present and pre-industrial ozone and mercury, *Atmos. Chem. Phys.*, *12* (15), 6723-6740, doi: 10.5194/acp-12-6723-2012, 2012.
- Parrella, J.P., K. Chance, R.J. Salawitch, T. Canty, M. Dorf, and K. Pfeilsticker, New retrieval of BrO from SCIAMACHY limb: An estimate of the stratospheric bromine loading during April 2008, *Atmos. Meas. Tech.*, *6* (10), 2549-2561, doi: 10.5194/amt-6-2549-2013, 2013.

- Pfeilsticker, K., W.T. Sturges, H. Bösch, C. Camy-Peyret, M.P. Chipperfield, A. Engel, R. Fitzenberger, M. Müller, S. Payan, and B.-M. Sinnhuber, Lower stratospheric organic and inorganic bromine budget for the Arctic winter 1998/99, *Geophys. Res. Lett.*, *27* (20), 3305-3308, 2000.
- Pisso, I., P.H. Haynes, and K.S. Law, Emission location dependent ozone depletion potentials for very short-lived halogenated species, *Atmos. Chem. Phys.*, *10* (24), 12025-12036, doi: 10.5194/acp-10-12025-2010, 2010.
- Ploeger, F., P. Konopka, R. Müller, S. Fueglistaler, T. Schmidt, J.C. Manners, J.-U. Groöf, G. Günther, P.M. Forster, and M. Riese, Horizontal transport affecting trace gas seasonality in the Tropical Tropopause Layer (TTL), *J. Geophys. Res.*, *117* (D9), D09303, doi: 10.1029/2011JD017267, 2012.
- Pommereau, J.-P., Troposphere-to-stratosphere transport in the tropics, *Comptes Rendus Géoscience*, *342* (4-5), 331-338, doi: 10.1016/j.crte.2009.10.015, 2010.
- Porter, E., J. Wenger, J. Treacy, H. Sidebottom, A. Mellouki, S. Téton, and G. LeBras, Kinetic studies on the reactions of hydroxyl radicals with diethers and hydroxyethers, *J. Phys. Chem. A*, *101* (32), 5770-5775, doi: 10.1021/jp971254i, 1997.
- Portmann, R.W., J.S. Daniel, and A.R. Ravishankara, Stratospheric ozone depletion due to nitrous oxide: Influences of other gases, *Phil. Trans. R. Soc. Lond. B. Biol. Sci.*, *367* (1593), 1256-1264, doi: 10.1098/rstb.2011.0377, 2012.
- Prather, M.J., and J. Hsu,  $\text{NF}_3$ , the greenhouse gas missing from Kyoto, *Geophys. Res. Lett.*, *35* (12), L12810, doi: 10.1029/2008GL034542, 2008.
- Prather, M.J., and J. Hsu, Correction to “ $\text{NF}_3$ , the greenhouse gas missing from Kyoto,” *Geophys. Res. Lett.*, *37*, L11807, doi: 10.1029/2010GL043831, 2010.
- Prather, M. J., and E.E. Remsberg (editors), *The Atmospheric Effects of Stratospheric Aircraft: Report of the 1992 Models and Measurements Workshop*, National Aeronautics and Space Administration, NASA Ref. Publ. 1292, available <http://ntrs.nasa.gov>, 1993.
- Prinn, R.G., R.F. Weiss, P.J. Fraser, P.G. Simmonds, D.M. Cunnold, F.N. Alyea, S. O’Doherty, P. Salameh, B.R. Miller, J. Huang, R.H.J. Wang, D.E. Hartley, C. Harth, L.P. Steele, G. Sturrock, P.M. Midgley, and A. McCulloch, A history of chemically and radiatively important gases in air deduced from ALE/GAGE/AGAGE, *J. Geophys. Res.*, *105* (D14), 17751-17792, doi: 10.1029/2000JD900141, 2000.
- Prinn, R.G., J. Huang, R.F. Weiss, D.M. Cunnold, P.J. Fraser, P.G. Simmonds, A. McCulloch, C. Harth, S. Reimann, P. Salameh, S. O’Doherty, R.H.J. Wang, L.W. Porter, B.R. Miller, and P.B. Krummel, Evidence for variability of atmospheric hydroxyl radicals over the past quarter century, *Geophys. Res. Lett.*, *32*, L07809, doi: 10.1029/2004GL022228, 2005.
- Puenteo, O., M. Gil, A. Saiz-Lopez, T. Hay, M. Navarro-Comas, A. Gómez-Pelaez, E. Cuevas, J. Iglesias, and L. Gomez, Iodine monoxide in the north subtropical free troposphere, *Atmos. Chem. Phys.*, *12* (11), 4909-4921, doi: 10.5194/acp-12-4909-2012, 2012.
- Puķite, J., S. Kühn, T. Deutschmann, S. Dörner, P. Jöckel, U. Platt, and T. Wagner, The effect of horizontal gradients and spatial measurement resolution on the retrieval of global vertical  $\text{NO}_2$  distributions from SCIAMACHY measurements in limb only mode, *Atmos. Meas. Tech.*, *3* (4), 1155-1174, 2010.
- Pyle, J.A., M.J. Ashfold, N.R.P. Harris, A.D. Robinson, N.J. Warwick, G.D. Carver, B. Gostlow, L.M. O’Brien, A.J. Manning, S.M. Phang, S.E. Yong, K.P. Leong, E.H. Ung, and S. Ong, Bromoform in the tropical boundary layer of the Maritime Continent during OP3, *Atmos. Chem. Phys.*, *11* (2), 529-542, doi: 10.5194/acp-11-529-2011, 2011.
- Randel, W.J., and E.J. Jensen, Physical processes in the tropical tropopause layer and their role in a changing climate, *Nature Geosci.*, *6* (3), 169-176, doi: 10.1038/ngeo1733, 2013.
- Ravishankara, A.R., S. Solomon, A.A. Turnipseed, and R.F. Warren, Atmospheric lifetimes of long-lived halogenated species, *Science*, *259* (5092), 194-199, doi: 10.1126/science.259.5092.194, 1993.
- Ravishankara, A.R., J.S. Daniel, and R.W. Portmann, Nitrous oxide ( $\text{N}_2\text{O}$ ): The dominant ozone-depleting substance emitted in the 21<sup>st</sup> century, *Science*, *326* (5949), 123-125, doi: 10.1126/science.1176985, 2009.
- Redeker, K.R., and R.J. Cicerone, Environmental controls over methyl halide emissions from rice paddies, *Global Biogeochem. Cycles*, *18*, GB1027, doi: 10.1029/2003GB002092, 2004.
- Reeves, C.E., W.T. Sturges, G.A. Sturrock, K. Preston, D.E. Oram, J. Schwander, R. Mulvaney, J.-M. Barnola, and J. Chappellaz, Trends of halon gases in polar firn air: Implications for their emission distributions, *Atmos. Chem. Phys.*, *5* (8), 2055-2064, doi: 10.5194/acp-5-2055-2005, 2005.
- Revell, L.E., G.E. Bodeker, P.E. Huck, B.E. Williamson, and E. Rozanov, The sensitivity of stratospheric ozone changes through the 21<sup>st</sup> century to  $\text{N}_2\text{O}$  and  $\text{CH}_4$ , *Atmos. Chem. Phys.*, *12* (23), 11309-11317, doi: 10.5194/acp-12-11309-2012, 2012.

- Rex, M., I. Wohltmann, T. Ridder, R. Lehmann, K. Rosenlof, P. Wennberg, D. Weisenstein, J. Notholt, K. Krüger, V. Mohr, and S. Tegtmeier, A Tropical West Pacific OH minimum and implications for stratospheric composition, *Atmos. Chem. Phys.*, *14* (9), 4827-4841, doi: 10.5194/acp-14-4827-2014, 2014.
- Rhew, R.C., Sources and sinks of methyl bromide and methyl chloride in the tallgrass prairie: Applying a stable isotope tracer technique over highly variable gross fluxes, *J. Geophys. Res.*, *116* (G3), G03026, doi: 10.1029/2011JG001704, 2011.
- Rhew, R.C., B.R. Miller, and R.F. Weiss, Natural methyl bromide and methyl chloride emissions from coastal salt marshes, *Nature*, *403*, 292-295, doi: 10.1038/35002043, 2000.
- Rhew, R.C., B.R. Miller, M.K. Vollmer, and R.F. Weiss, Shrubland fluxes of methyl bromide and methyl chloride, *J. Geophys. Res.*, *106* (D18), 20875-20882, doi: 10.1029/2001JD000413, 2001.
- Rhew, R.C., B.R. Miller, and R.F. Weiss, Chloroform, carbon tetrachloride and methyl chloroform fluxes in southern California ecosystems, *Atmos. Environ.*, *42* (30), 7135-7140, doi: 10.1016/j.atmosenv.2008.05.038, 2008.
- Rhew, R.C., C. Chen, Y.A. Teh, and D. Baldocchi, Gross fluxes of methyl chloride and methyl bromide in a California oak-savanna woodland, *Atmos. Environ.*, *44* (16), 2054-2061, doi: 10.1016/j.atmosenv.2009.12.014, 2010.
- Richter, U., and D.W.R. Wallace, Production of methyl iodide in the tropical Atlantic Ocean, *Geophys. Res. Lett.*, *31* (23), L23S03, doi: 10.1029/2004GL020779, 2004.
- Richter, A., F. Wittrock, A. Ladstätter-Weißenmayer, and J.P. Burrows, GOME measurements of stratospheric and tropospheric BrO, *Adv. Space Res.*, *29* (11), 1667-1672, doi: 10.1016/S0273-1177(02)00123-0, 2002.
- Rigby, M., R.G. Prinn, P.J. Fraser, P.G. Simmonds, R.L. Langenfelds, J. Huang, D.M. Cunnold, L.P. Steele, P.B. Krummel, R.F. Weiss, S. O'Doherty, P.K. Salameh, H.J. Wang, C.M. Harth, J. Mühle, and L.W. Porter, Renewed growth of atmospheric methane, *Geophys. Res. Lett.*, *35*, L22805, doi: 10.1029/2008GL036037, 2008.
- Rigby, M., J. Mühle, B.R. Miller, R.G. Prinn, P.B. Krummel, L.P. Steele, P.J. Fraser, P.K. Salameh, C.M. Harth, R.F. Weiss, B.R. Grealley, S. O'Doherty, P.G. Simmonds, M.K. Vollmer, S. Reimann, J. Kim, K.-R. Kim, H.J. Wang, J.G.J. Olivier, E.J. Dlugokencky, G.S. Dutton, B.D. Hall, and J.W. Elkins, History of atmospheric SF<sub>6</sub> from 1973 to 2008, *Atmos. Chem. Phys.*, *10* (21), 10305-10320, doi: 10.5194/acp-10-10305-2010, 2010.
- Rigby, M., R.G. Prinn, S. O'Doherty, S.A. Montzka, A. McCulloch, C.M. Harth, J. Mühle, P.K. Salameh, R.F. Weiss, D. Young, P.G. Simmonds, B.D. Hall, G.S. Dutton, D. Nance, D.J. Mondeel, J.W. Elkins, P.B. Krummel, L.P. Steele, and P.J. Fraser, Re-evaluation of the lifetimes of the major CFCs and CH<sub>3</sub>CCl<sub>3</sub> using atmospheric trends, *Atmos. Chem. Phys.*, *13* (5), 2691-2702, doi: 10.5194/acp-13-2691-2013, 2013.
- Rigby, M., R.G. Prinn, S. O'Doherty, B.R. Miller, D. Ivy, J. Mühle, C.M. Harth, P.K. Salameh, T. Arnold, R.F. Weiss, P.B. Krummel, L.P. Steele, P.J. Fraser, D. Young, and P.G. Simmonds, Recent and future trends in synthetic greenhouse gas radiative forcing, *Geophys. Res. Lett.*, *41* (7), doi: 10.1002/2013GL059099, 2014.
- Rinsland, C.P., E. Mahieu, R. Zander, N.B. Jones, M.P. Chipperfield, A. Goldman, J. Anderson, J.M. Russell III, P. Demoulin, J. Notholt, G.C. Toon, J.-F. Blavier, B. Sen, R. Sussmann, S.W. Wood, A. Meier, D.W.T. Griffith, L.S. Chiou, F.J. Murcray, T.M. Stephen, F. Hase, S. Mikuteit, A. Schulz, and T. Blumenstock, Long-term trends of inorganic chlorine from ground-based infrared solar spectra: Past increases and evidence for stabilization, *J. Geophys. Res.*, *108* (D8), 4252, doi: 10.1029/2002JD003001, 2003.
- Rinsland, C.P., E. Mahieu, P. Demoulin, R. Zander, C. Servais, and J.-M. Hartmann, Decrease of the carbon tetrachloride (CCl<sub>4</sub>) loading above Jungfraujoch, based on high resolution infrared solar spectra recorded between 1999 and 2011, *J. Quant. Spectrosc. Radiat. Transfer*, *113* (11), 1322-1329, doi: 10.1016/j.jqsrt.2012.02.016, 2012.
- Rowland, F.S., S.C. Tyler, D.C. Montague, and Y. Makide, Dichlorodifluoromethane, CCl<sub>2</sub>F<sub>2</sub>, in the Earth's atmosphere, *Geophys. Res. Lett.*, *9* (4), 481-484, doi: 10.1029/GL009i004p00481, 1982.
- Roy, R., Short-term variability in halocarbons in relation to phytoplankton pigments in coastal waters of the central eastern Arabian Sea, *Estuar. Coast. Shelf Sci.*, *88* (3), 311-321, doi: 10.1016/j.ecss.2010.04.011, 2010.
- Roy, R., A. Pratihary, G. Narvenkar, S. Mochamadkar, M. Gauns, and S.W.A. Naqvi, The relationship between volatile halocarbons and phytoplankton pigments during a *Trichodesmium* bloom in the coastal eastern Arabian Sea, *Estuar. Coast. Shelf Sci.*, *95* (1), 110-118, doi: 10.1016/j.ecss.2011.08.025, 2011.
- Russell, M.H., G. Hoogeweg, E.M. Webster, D.A. Ellis, R.L. Waterland, and R.A. Hoke, TFA from HFO-1234yf: Accumulation and aquatic risk in terminal water bodies, *Environ. Toxicol. Chem.*, *31* (9), 1957-1965, doi: 10.1002/etc.1925, 2012.
- Russo, R.S., Y. Zhou, M.L. White, H. Mao, R. Talbot, and B.C. Sive, Multi-year (2004-2008) record of nonmethane hydrocarbons and halocarbons in New England: Seasonal variations and regional sources, *Atmos. Chem. Phys.*, *10* (10), 4909-4929, doi: 10.5194/acp-10-4909-2010, 2010.

- Saikawa, E., M. Rigby, R.G. Prinn, S.A. Montzka, B.R. Miller, L.J.M. Kuijpers, P.J.B. Fraser, M.K. Vollmer, T. Saito, Y. Yokouchi, C.M. Harth, J. Mühle, R.F. Weiss, P.K. Salameh, J. Kim, S. Li, S. Park, K.-R. Kim, D. Young, S. O'Doherty, P.G. Simmonds, A. McCulloch, P.B. Krummel, L.P. Steele, C. Lunder, O. Hermansen, M. Maione, J. Arduini, B. Yao, L.X. Zhou, H.J. Wang, J.W. Elkins, and B. Hall, Global and regional emission estimates for HCFC-22, *Atmos. Chem. Phys.*, *12* (21), 10033-10050, doi: 10.5194/acp-12-10033-2012, 2012.
- Saito, T., Y. Yokouchi, Y. Kosugi, M. Tani, E. Philip, and T. Okuda, Methyl chloride and isoprene emissions from tropical rain forest in Southeast Asia, *Geophys. Res. Lett.*, *35* (19), L19812, doi: 10.1029/2008GL035241, 2008.
- Saito, T., Y. Yokouchi, A. Stohl, S. Taguchi, and H. Mukai, Large emissions of perfluorocarbons in East Asia deduced from continuous atmospheric measurements, *Environ. Sci. Technol.*, *44* (11), 4089-4095, doi: 10.1021/es1001488, 2010.
- Saito, T., Y. Yokouchi, E. Phillip, and T. Okuda, Bidirectional exchange of methyl halides between tropical plants and the atmosphere, *Geophys. Res. Lett.*, *40* (19), 5300-5304, doi: 10.1002/grl.50997, 2013.
- Saiz-Lopez, A., J.M.C. Plane, A.R. Baker, L.J. Carpenter, R. von Glasow, J.C.G. Martín, G. McFiggans, and R.W. Saunders, Atmospheric chemistry of iodine, *Chem. Rev.*, *112* (3), 1773-1804, doi: 10.1021/cr200029u, 2012.
- Sala, S., H. Bönisch, T. Keber, D.E. Oram, G. Mills, and A. Engel, Deriving an atmospheric budget of total organic bromine using airborne in-situ measurements from the Western Pacific during SHIVA, *Atmos. Chem. Phys.*, *14* (13), 6903-6923, doi: 10.5194/acp-14-6903-2014, 2014.
- Salawitch, R.J., D.K. Weisenstein, L.J. Kovalenko, C.E. Sioris, P.O. Wennberg, K. Chance, M.K.W. Ko, and C.A. McLinden, Sensitivity of ozone to bromine in the lower stratosphere, *Geophys. Res. Lett.*, *32*, L05811, doi: 10.1029/2004GL021504, 2005.
- Salawitch, R.J., T. Canty, T. Kurosu, K. Chance, Q. Liang, A. da Silva, S. Pawson, J.E. Nielsen, J.M. Rodriguez, P.K. Bhartia, X. Liu, L.G. Huey, J. Liao, R.E. Stickel, D.J. Tanner, J.E. Dibb, W.R. Simpson, D. Donohoue, A. Weinheimer, F. Flocke, D. Knapp, D. Montzka, J.A. Neuman, J.B. Nowak, T.B. Ryerson, S. Oltmans, D.R. Blake, E.L. Atlas, D.E. Kinnison, S. Tilmes, L.L. Pan, F. Hendrick, M. Van Roozendaal, K. Kreher, P.V. Johnston, R.S. Gao, B. Johnson, T.P. Bui, G. Chen, R.B. Pierce, J.H. Crawford, and D.J. Jacob, A new interpretation of total column BrO during Arctic spring, *Geophys. Res. Lett.*, *37* (21), L21805, doi: 10.1029/2010GL043798, 2010.
- Saltzman, E.S., M. Aydin, W.J. De Bruyn, D.B. King, and S.A. Yvon-Lewis, Methyl bromide in preindustrial air: Measurements from an Antarctic ice core, *J. Geophys. Res.*, *109* (D5), D05301, doi: 10.1029/2003JD004157, 2004.
- Saltzman, E.S., M. Aydin, C. Tatum, and M.B. Williams, 2,000-year record of atmospheric methyl bromide from a South Pole ice core, *J. Geophys. Res.*, *113*, D05304, doi: 10.1029/2007JD008919, 2008.
- Sander, S.P., J. Abbatt, J.R. Barker, J.B. Burkholder, R.R. Friedl, D.M. Golden, R.E. Huie, C.E. Kolb, M.J. Kurylo, G.K. Moortgat, V.L. Orkin, and P.H. Wine, *Chemical Kinetics and Photochemical Data for Use in Atmospheric Studies, Evaluation Number 17*, JPL Publication 10-6, Jet Propulsion Laboratory, Pasadena, Calif., <http://jpldataeval.jpl.nasa.gov/pdf/JPL%2010-6%20Final%2015June2011.pdf>, 2011.
- Santee, M.L., N.J. Livesey, G.L. Manney, A. Lambert, and W.G. Read, Methyl chloride from the Aura Microwave Limb Sounder: First global climatology and assessment of variability in the upper troposphere and stratosphere, *J. Geophys. Res.*, *118* (24), 13532-13560, doi: 10.1002/2013JD020235, 2013.
- Sato, T.O., H. Sagawa, D. Kreyling, T. Manabe, S. Ochiai, K. Kikuchi, P. Baron, J. Mendrok, J. Urban, D. Murtagh, M. Yasui, and Y. Kasai, Strato-mesospheric ClO observations by SMILES: Error analysis and diurnal variation, *Atmos. Meas. Tech.*, *5* (11), 2809-2825, doi: 10.5194/amt-5-2809-2012, 2012.
- Schauffler, S.M., E.L. Atlas, D.R. Blake, F. Flocke, R.A. Lueb, J.M. Lee-Taylor, V. Stroud, and W. Travnicek, Distributions of brominated organic compounds in the troposphere and lower stratosphere, *J. Geophys. Res.*, *104* (D17), 21513-21536, doi: 10.1029/1999jd900197, 1999.
- Schauffler, S.M., E.L. Atlas, S.G. Donnelly, A. Andrews, S.A. Montzka, J.W. Elkins, D.F. Hurst, P.A. Romashkin, G.S. Dutton, and V. Stroud, Chlorine budget and partitioning during the Stratospheric Aerosol and Gas Experiment (SAGE) III Ozone Loss and Validation Experiment (SOLVE), *J. Geophys. Res.*, *108* (D5), 4173, doi: 10.1029/2001JD002040, 2003.
- Schmidt, J.A., M.S. Johnson, S. Hattori, N. Yoshida, S. Nanbu, and R. Schinke, OCS photolytic isotope effects from first principles: Sulfur and carbon isotopes, temperature dependence and implications for the stratosphere, *Atmos. Chem. Phys.*, *13* (3), 1511-1520, doi: 10.5194/acp-13-1511-2013, 2013.
- Schofield, R., K. Kreher, B.J. Connor, P.V. Johnston, A. Thomas, D. Shooter, M.P. Chipperfield, C.D. Rodgers, and G.H. Mount, Retrieved tropospheric and stratospheric BrO columns over Lauder, New Zealand, *J. Geophys. Res.*, *109*, D14304, doi: 10.1029/2003JD004463, 2004.

- Schofield, R., P.V. Johnston, A. Thomas, K. Kreher, B.J. Connor, S. Wood, D. Shooter, M.P. Chipperfield, A. Richter, R. von Glasow, and C.D. Rodgers, Tropospheric and stratospheric BrO columns over Arrival Heights, Antarctica, 2002, *J. Geophys. Res.*, *111*, D22310, doi: 10.1029/2005JD007022, 2006.
- Schofield, R., S. Fueglistaler, I. Wohltmann, and M. Rex, Sensitivity of stratospheric Br<sub>y</sub> to uncertainties in very short lived substance emissions and atmospheric transport, *Atmos. Chem. Phys.*, *11* (4), 1379-1392, doi: 10.5194/acp-11-1379-2011, 2011.
- Shao, M., D. Huang, D. Gu, S. Lu, C. Chang, and J. Wang, Estimate of anthropogenic halocarbon emission based on measured ratio relative to CO in the Pearl River Delta region, China, *Atmos. Chem. Phys.*, *11* (10), 5011-5025, doi: 10.5194/acp-11-5011-2011, 2011.
- Shindell, D.T., O. Pechony, A. Voulgarakis, G. Faluvegi, L. Nazarenko, J.-F. Lamarque, K. Bowman, G. Milly, B. Kovari, R. Ruedy, and G.A. Schmidt, Interactive ozone and methane chemistry in GISS-E2 historical and future climate simulations, *Atmos. Chem. Phys.*, *13* (5), 2653-2689, doi: 10.5194/acp-13-2653-2013, 2013.
- Sihler, H., U. Platt, S. Beirle, T. Marbach, S. Köhl, S. Dörner, J. Verschaeve, U. Frieß, D. Pöhler, L. Vogel, R. Sander, and T. Wagner, Tropospheric BrO column densities in the Arctic derived from satellite: Retrieval and comparison to ground-based measurements, *Atmos. Meas. Tech.*, *5* (11), 2779-2807, doi: 10.5194/amt-5-2779-2012, 2012.
- Simmonds, P.G., A.J. Manning, D.M. Cunnold, A. McCulloch, S. O'Doherty, R.G. Derwent, P.B. Krummel, P.J. Fraser, B. Dunse, L.W. Porter, R.H.J. Wang, B.R. Grealley, B.R. Miller, P. Salameh, R.F. Weiss, and R.G. Prinn, Global trends, seasonal cycles, and European emissions of dichloromethane, trichloroethene, and tetrachloroethene from the AGAGE observations at Mace Head, Ireland, and Cape Grim, Tasmania, *J. Geophys. Res.*, *111*, D18304, doi: 10.1029/2006JD007082, 2006.
- Simmonds, P.G., R.G. Derwent, A.J. Manning, S. O'Doherty, and G. Spain, Natural chloroform emissions from the blanket peat bogs in the vicinity of Mace Head, Ireland over a 14-year period, *Atmos. Environ.*, *44* (10), 1284-1291, doi: 10.1016/j.atmosenv.2009.12.027, 2010.
- Simpson, I.J., S. Meinardi, N.J. Blake, F.S. Rowland, and D.R. Blake, Long-term decrease in the global atmospheric burden of tetrachloroethene (C<sub>2</sub>Cl<sub>4</sub>), *Geophys. Res. Lett.*, *31* (8), L08108, doi: 10.1029/2003GL019351, 2004.
- Simpson, I.J., N.J. Blake, D.R. Blake, S. Meinardi, M.P.S. Andersen, and F.S. Rowland, Strong evidence for negligible methyl chloroform (CH<sub>3</sub>CCl<sub>3</sub>) emissions from biomass burning, *Geophys. Res. Lett.*, *34* (10), L10805, doi: 10.1029/2007GL029383, 2007.
- Simpson, I.J., S.K. Akagi, B. Barletta, N.J. Blake, Y. Choi, G.S. Diskin, A. Fried, H.E. Fuelberg, S. Meinardi, F.S. Rowland, S.A. Vay, A.J. Weinheimer, P.O. Wennberg, P. Wiebring, A. Wisthaler, M. Yang, R.J. Yokelson, and D.R. Blake, Boreal forest fire emissions in fresh Canadian smoke plumes: C<sub>1</sub>-C<sub>10</sub> volatile organic compounds (VOCs), CO<sub>2</sub>, CO, NO<sub>2</sub>, NO, HCN and CH<sub>3</sub>CN, *Atmos. Chem. Phys.*, *11* (13), 6445-6463, doi: 10.5194/acp-11-6445-2011, 2011.
- Simpson, I.J., M.P. Sulbaek Andersen, S. Meinardi, L. Bruhwiler, N.J. Blake, D. Helmig, F.S. Rowland, and D.R. Blake, Long-term decline of global atmospheric ethane concentrations and implications for methane, *Nature*, *488* (7412), 490-494, doi: 10.1038/nature11342, 2012.
- Sinnhuber, B.-M., and I. Folkins, Estimating the contribution of bromoform to stratospheric bromine and its relation to dehydration in the tropical tropopause layer, *Atmos. Chem. Phys.*, *6* (12), 4755-4761, doi: 10.5194/acp-6-4755-2006, 2006.
- Sinnhuber, B.-M., A. Rozanov, N. Sheode, O.T. Afe, A. Richter, M. Sinnhuber, F. Wittrock, J.P. Burrows, G.P. Stiller, T. von Clarmann, and A. Linden, Global observations of stratospheric bromine monoxide from SCIAMACHY, *Geophys. Res. Lett.*, *32* (20), L20810, doi: 10.1029/2005GL023839, 2005.
- Sinnhuber, B.-M., N. Sheode, M. Sinnhuber, M.P. Chipperfield, and W. Feng, The contribution of anthropogenic bromine emissions to past stratospheric ozone trends: A modelling study, *Atmos. Chem. Phys.*, *9* (8), 2863-2871, doi: 10.5194/acp-9-2863-2009, 2009.
- Sioris, C.E., L.J. Kovalenko, C.A. McLinden, R.J. Salawitch, M. Van Roozendaal, F. Goutail, M. Dorf, K. Pfeilsticker, K. Chance, C. von Savigny, X. Liu, T.P. Kurosu, J.-P. Pommereau, H. Bösch, and J. Frerick, Latitudinal and vertical distribution of bromine monoxide in the lower stratosphere from Scanning Imaging Absorption Spectrometer for Atmospheric Cartography limb scattering measurements, *J. Geophys. Res.*, *111*, D14301, doi: 10.1029/2005JD006479, 2006.
- Solomon, S., R.W. Portmann, R.R. Garcia, W. Randel, F. Wu, R. Nagatani, J. Gleason, L. Thomason, L.R. Poole, and M.P. McCormick, Ozone depletion at mid-latitudes: Coupling of volcanic aerosols and temperature variability to anthropogenic chlorine, *Geophys. Res. Lett.*, *25* (11), 1871-1874, doi: 10.1029/98GL01293, 1998.

- SPARC (Stratosphere-troposphere Processes And their Role in Climate), *SPARC Assessment of Stratospheric Aerosol Properties*, edited by L. Thomason and Th. Peter, World Climate Research Program Report 124, SPARC Report 4, WMO/TD- No. 1295, 346 pp., Verrières le Buisson, France, 2006.
- SPARC (Stratosphere-troposphere Processes And their Role in Climate), *SPARC Report on the Lifetimes of Stratospheric Ozone-Depleting Substances, Their Replacements, and Related Species*, edited by M. Ko, P. Newman, S. Reimann, and S. Strahan, SPARC Report No. 6, WCRP-15/2013, 2013.
- Spivakovsky, C.M., J.A. Logan, S.A. Montzka, Y.J. Balkanski, M. Foreman-Fowler, D.B.A. Jones, L.W. Horowitz, A.C. Fusco, C.A.M. Brenninkmeijer, M.J. Prather, S.C. Wofsy, and M.B. McElroy, Three-dimensional climatological distribution of tropospheric OH: Update and evaluation, *J. Geophys. Res.*, *105* (D7), 8931-8980, doi: 10.1029/1999JD901006, 2000.
- Stachnik, R.A., L. Millán, R. Jarnot, R. Monroe, C. McLinden, S. Köhl, J. Pukite, M. Shiotani, M. Suzuki, Y. Kasai, F. Goutail, J.P. Pommereau, M. Dorf, and K. Pfeilsticker, Stratospheric BrO abundance measured by a balloon-borne submillimeterwave radiometer, *Atmos. Chem. Phys.*, *13* (6), 3307-3319, doi: 10.5194/acp-13-3307-2013, 2013.
- Stemmler, K., D. Folini, S. Ubl, M.K. Vollmer, S. Reimann, S. O'Doherty, B.R. Grealley, P.G. Simmonds, and A.J. Manning, European emissions of HFC-365mfc, a chlorine-free substitute for the foam blowing agents HCFC-141b and CFC-11, *Environ. Sci. Technol.*, *41* (4), 1145-1151, doi: 10.1021/es061298h, 2007.
- Stemmler, I., M. Rothe, I. Hense, and H. Hepach, Numerical modelling of methyl iodide in the eastern tropical Atlantic, *Biogeosciences*, *10* (6), 4211-4225, doi: 10.5194/bg-10-4211-2013, 2013.
- Stilller, G.P., T. von Clarmann, F. Haenel, B. Funke, N. Glatthor, U. Grabowski, S. Kellmann, M. Kiefer, A. Linden, S. Lossow, and M. López-Puertas, Observed temporal evolution of global mean age of stratospheric air for the 2002 to 2010 period, *Atmos. Chem. Phys.*, *12* (7), 3311-3331, doi: 10.5194/acp-12-3311-2012, 2012.
- Stohl, A., P. Seibert, J. Arduini, S. Eckhardt, P. Fraser, B.R. Grealley, C. Lunder, M. Maione, J. Mühle, S. O'Doherty, R.G. Prinn, S. Reimann, T. Saito, N. Schmidbauer, P.G. Simmonds, M.K. Vollmer, R.F. Weiss, and Y. Yokouchi, An analytical inversion method for determining regional and global emissions of greenhouse gases: Sensitivity studies and application to halocarbons, *Atmos. Chem. Phys.*, *9* (5), 1597-1620, doi: 10.5194/acp-9-1597-2009, 2009.
- Stohl, A., J. Kim, S. Li, S. O'Doherty, J. Mühle, P.K. Salameh, T. Saito, M.K. Vollmer, D. Wan, R.F. Weiss, B. Yao, Y. Yokouchi, and L.X. Zhou, Hydrochlorofluorocarbon and hydrofluorocarbon emissions in East Asia determined by inverse modeling, *Atmos. Chem. Phys.*, *10* (8), 3545-3560, doi: 10.5194/acp-10-3545-2010, 2010.
- Sturges, W.T., T.J. Wallington, M.D. Hurley, K.P. Shine, K. Sihra, A. Engel, D.E. Oram, S.A. Penkett, R. Mulvaney, and C.A.M. Brenninkmeijer, A potent greenhouse gas identified in the atmosphere: SF<sub>5</sub>CF<sub>3</sub>, *Science*, *289* (5479), 611-613, doi: 10.1126/science.289.5479.611, 2000.
- Sturges, W.T., D.E. Oram, J.C. Laube, C.E. Reeves, M.J. Newland, C. Hogan, P. Martinerie, E. Witrant, C.A.M. Brenninkmeijer, T.J. Schuck, and P.J. Fraser, Emissions halted of the potent greenhouse gas SF<sub>5</sub>CF<sub>3</sub>, *Atmos. Chem. Phys.*, *12* (8), 3653-3658, doi: 10.5194/acp-12-3653-2012, 2012.
- Sulbaek Andersen, M.P., E.J.K. Nilsson, O.J. Nielsen, M.S. Johnson, M.D. Hurley, and T.J. Wallington, Atmospheric chemistry of *trans*-CF<sub>3</sub>CH=CHCl: Kinetics of the gas-phase reactions with Cl atoms, OH radicals, and O<sub>3</sub>, *J. Photochem. Photobiol. A: Chemistry*, *199* (1), 92-97, doi: 10.1016/j.jphotochem.2008.05.013, 2008.
- Sulbaek Andersen, M.P., O.J. Nielsen, B. Karpichev, T.J. Wallington, and S.P. Sander, Atmospheric chemistry of isoflurane, desflurane, and sevoflurane: Kinetics and mechanisms of reactions with chlorine atoms and OH radicals and global warming potentials, *J. Phys. Chem. A*, *116* (24), 5806-5820, doi: 10.1021/jp2077598, 2012.
- Takahashi, H., and Luo, Z.J., Characterizing tropical overshooting deep convection from joint analysis of CloudSat and geostationary satellite observations, *J. Geophys. Res.*, *119* (1), 112-121, doi: 10.1002/2013JD020972, 2014.
- Taniguchi, N., T.J. Wallington, M.D. Hurley, A.G. Guschin, L.T. Molina, and M.J. Molina, Atmospheric chemistry of C<sub>2</sub>F<sub>5</sub>C(O)CF(CF<sub>3</sub>)<sub>2</sub>: Photolysis and reaction with Cl atoms, OH radicals, and ozone, *J. Phys. Chem. A*, *107* (15), 2674-2679, doi: 10.1021/jp0220332, 2003.
- Tegtmeier, S., K. Krüger, B. Quack, E.L. Atlas, I. Pisso, A. Stohl, and X. Yang, Emission and transport of bromocarbons: From the West Pacific ocean into the stratosphere, *Atmos. Chem. Phys.*, *12* (22), 10633-10648, doi: 10.5194/acp-12-10633-2012, 2012.
- Tegtmeier, S., K. Krüger, B. Quack, E. Atlas, D.R. Blake, H. Boenisch, A. Engel, H. Hepach, R. Hossaini, M.A. Navarro, S. Raimund, S. Sala, Q. Shi, and F. Ziska, The contribution of oceanic methyl iodide to stratospheric iodine, *Atmos. Chem. Phys.*, *13* (23), 11869-11886, doi: 10.5194/acp-13-11869-2013, 2013.

- Theys, N., M. Van Roozendael, F. Hendrick, C. Fayt, C. Hermans, J.-L. Barray, F. Goutail, J.-P. Pommereau, and M. De Mazière, Retrieval of stratospheric and tropospheric BrO columns from multi-axis DOAS measurements at Reunion Island (21°S, 56°E), *Atmos. Chem. Phys.*, *7* (18), 4733-4749, doi: 10.5194/acp-7-4733-2007, 2007.
- Theys, N., M. Van Roozendael, F. Hendrick, X. Yang, I. De Smedt, A. Richter, M. Begoin, Q. Errera, P.V. Johnston, K. Kreher, and M. De Mazière, Global observations of tropospheric BrO columns using GOME-2 satellite data, *Atmos. Chem. Phys.*, *11* (4), 1791-1811, doi: 10.5194/acp-11-1791-2011, 2011.
- Thomas, V.M., J.A. Bedford, and R.J. Cicerone, Bromine emissions from leaded gasoline, *Geophys. Res. Lett.*, *24* (11), 1371-1374, doi: 10.1029/97GL01243, 1997.
- Thompson, R.L., F. Chevallier, A.M. Crowell, G. Dutton, R.L. Langenfelds, R.G. Prinn, R.F. Weiss, Y. Tohjima, T. Nakazawa, P.B. Krummel, L.P. Steele, P. Fraser, S. O'Doherty, K. Ishijima, and S. Aoki, Nitrous oxide emissions 1999–2009 from a global atmospheric inversion, *Atmos. Chem. Phys.*, *14* (4), 1801-1817, doi: 10.5194/acp-14-1801-2014, 2014.
- Thornton, B.F., D.W. Toohey, A.F. Tuck, J.W. Elkins, K.K. Kelly, S.J. Hovde, E.C. Richard, K.H. Rosenlof, T.L. Thompson, M.J. Mahoney, and J.C. Wilson, Chlorine activation near the midlatitude tropopause, *J. Geophys. Res.*, *112* (D18), D18306, doi: 10.1029/2006JD007640, 2007.
- Tilmes, S., D.E. Kinnison, R.R. Garcia, R. Salawitch, T. Canty, J. Lee-Taylor, S. Madronich, and K. Chance, Impact of very short-lived halogens on stratospheric ozone abundance and UV radiation in a geo-engineered atmosphere, *Atmos. Chem. Phys.*, *12* (22), 10945-10955, doi: 10.5194/acp-12-10945-2012, 2012.
- Tokuhashi, K., A. Takahashi, M. Kaise, and S. Kondo, Rate constants for the reactions of OH radicals with CH<sub>3</sub>OCF<sub>2</sub>CHFCl, CHF<sub>2</sub>OCF<sub>2</sub>CHFCl, CHF<sub>2</sub>OCHClCF<sub>3</sub>, and CH<sub>3</sub>CH<sub>2</sub>OCF<sub>2</sub>CHF<sub>2</sub>, *J. Geophys. Res.*, *104* (D15), 18681-18688, doi: 10.1029/1999JD900278, 1999.
- Trudinger, C.M., D.M. Etheridge, G.A. Sturrock, P.J. Fraser, P.B. Krummel, and A. McCulloch, Atmospheric histories of halocarbons from analysis of Antarctic firn air: Methyl bromide, methyl chloride, chloroform, and dichloromethane, *J. Geophys. Res.*, *109* (D22), D22310, doi: 10.1029/2004JD004932, 2004.
- Tsai, W.-T., H.-P. Chen, and W.-Y. Hsien, A review of uses, environmental hazards and recovery/recycle technologies of perfluorocarbons (PFCs) emissions from the semiconductor manufacturing processes, *J. of Loss Prevent. Proc.*, *15* (2), 65-75, doi: 10.1016/S0950-4230(01)00067-5, 2002.
- Tzella, A., and B. Legras, A Lagrangian view of convective sources for transport of air across the Tropical Tropopause Layer: Distribution, times and the radiative influence of clouds, *Atmos. Chem. Phys.*, *11* (23), 12517-12534, doi: 10.5194/acp-11-12517-2011, 2011.
- UNEP (United Nations Environment Programme), *Technology and Economic Assessment Panel: Task Force On Emissions Discrepancies Report*, 80 pp., Nairobi, Kenya, [http://montreal-protocol.org/Assessment\\_Panels/TEAP/Reports/TEAP\\_Reports/TEAP-Discrepancy-report.pdf](http://montreal-protocol.org/Assessment_Panels/TEAP/Reports/TEAP_Reports/TEAP-Discrepancy-report.pdf), 2006.
- UNEP (United Nations Environment Programme), *2006 Report of the Methyl Bromide Technical Options Committee: 2006 Assessment*, coordinated by M. Pizano, I. Porter, M. Marcotte, M. Besri, and J. Banks, 453 pp., Nairobi, Kenya, [http://montreal-protocol.org/Assessment\\_Panels/TEAP/Reports/MBTOC/MBTOC-2006-Assessment%20Report.pdf](http://montreal-protocol.org/Assessment_Panels/TEAP/Reports/MBTOC/MBTOC-2006-Assessment%20Report.pdf), 2007.
- UNEP (United Nations Environment Programme), *HFCs: A Critical Link in Protecting Climate and the Ozone Layer*, 36 pp., Nairobi, Kenya, [http://www.unep.org/dewa/Portals/67/pdf/HFC\\_report.pdf](http://www.unep.org/dewa/Portals/67/pdf/HFC_report.pdf), 2011a.
- UNEP (United Nations Environment Programme), *2010 Report Of The Halons Technical Options Committee*, coordinated by D. Catchpole, S. Kopylov, and D. Verdonik, 168 pp., Nairobi, Kenya, [http://montreal-protocol.org/Assessment\\_Panels/TEAP/Reports/HTOC/HTOC-Assessment-Report-2010.pdf](http://montreal-protocol.org/Assessment_Panels/TEAP/Reports/HTOC/HTOC-Assessment-Report-2010.pdf), 2011b.
- UNEP (United Nations Environment Programme), *Report of the Methyl Bromide Technical Options Committee: 2010 Assessment*, coordinated by M. Besri, M. Marcotte, M. Pizano, and I. Porter, 397 pp., Nairobi, Kenya, [http://montreal-protocol.org/Assessment\\_Panels/TEAP/Reports/MBTOC/MBTOC-Assesment-Report-2010.pdf](http://montreal-protocol.org/Assessment_Panels/TEAP/Reports/MBTOC/MBTOC-Assesment-Report-2010.pdf), 2011c.
- UNEP (United Nations Environment Programme), *May 2012 Report of the Technology and Economic Assessment Panel: Volume 1 Progress Report*, 222 pp., Nairobi, Kenya, [http://montreal-protocol.org/Assessment\\_Panels/TEAP/Reports/TEAP\\_Reports/teap-progress-report-may2012.pdf](http://montreal-protocol.org/Assessment_Panels/TEAP/Reports/TEAP_Reports/teap-progress-report-may2012.pdf), 2012.
- UNEP (United Nations Environment Programme), *May 2013 Report of the Technology and Economic Assessment Panel: Decision XXIV/7 Task Force Report, Additional Information on Alternatives to ODS, Volume 2*, 124 pp., Nairobi, Kenya, [http://montreal-protocol.org/Assessment\\_Panels/TEAP/Reports/TEAP\\_Reports/TEAP\\_Task\\_Force%20XXIV-7-May2013.pdf](http://montreal-protocol.org/Assessment_Panels/TEAP/Reports/TEAP_Reports/TEAP_Task_Force%20XXIV-7-May2013.pdf), 2013a.
- UNEP (United Nations Environment Programme), *May 2013 Report of the Technology and Economic Assessment Panel: Volume 1 Progress Report*, 156 pp., Nairobi, Kenya, [http://montreal-protocol.org/Assessment\\_Panels/TEAP/Reports/TEAP\\_Reports/TEAP\\_Progress\\_Report\\_May\\_2013.pdf](http://montreal-protocol.org/Assessment_Panels/TEAP/Reports/TEAP_Reports/TEAP_Progress_Report_May_2013.pdf), 2013b.

- UNEP (United Nations Environment Programme), *Drawing Down N<sub>2</sub>O to Protect Climate and the Ozone Layer. A UNEP Synthesis Report*, 57 pp., Nairobi, Kenya, <http://www.unep.org/pdf/UNEPN2Oreport.pdf>, 2013c.
- UNEP (United Nations Environment Programme), [http://ozone.unep.org/new\\_site/en/ozone\\_data\\_tools\\_access.php](http://ozone.unep.org/new_site/en/ozone_data_tools_access.php), retrieved in May 2014, 2014.
- UNFCCC (United Nations Framework Convention on Climate Change), [http://unfccc.int/kyoto\\_protocol/doha\\_amendment/items/7362.php](http://unfccc.int/kyoto_protocol/doha_amendment/items/7362.php), retrieved in May 2014, 2014.
- van der Werf, G.R., J.T. Randerson, L. Giglio, G.J. Collatz, M. Mu, P.S. Kasibhatla, D.C. Morton, R.S. DeFries, Y. Jin, and T.T. van Leeuwen, Global fire emissions and the contribution of deforestation, savanna, forest, agricultural, and peat fires (1997-2009), *Atmos. Chem. Phys.*, *10* (23), 11707-11735, doi: 10.5194/acp-10-11707-2010, 2010.
- Van Roozendaal, M., T. Wagner, A. Richter, I. Pundt, D.W. Arlander, J.P. Burrows, M. Chipperfield, C. Fayt, P.V. Johnston, J.-C. Lambert, K. Kreher, K. Pfeilsticker, U. Platt, J.-P. Pommereau, B.-M. Sinnhuber, K.K. Tørnkvist, and F. Wittrock, Intercomparison of BrO measurements from ERS-2 GOME, ground-based and balloon platforms, *Adv. Space Res.*, *29* (11), 1661-1666, 2002.
- Varner, R.K., P.M. Crill, and R.W. Talbot, Wetlands: A potentially significant source of atmospheric methyl bromide and methyl chloride, *Geophys. Res. Lett.*, *26* (16), 2433-2436, doi: 10.1029/1999GL900587, 1999.
- Velders, G.J.M., A.R. Ravishankara, M.K. Miller, M.J. Molina, J. Alcamo, J.S. Daniel, D.W. Fahey, S.A. Montzka, and S. Reimann, Preserving Montreal Protocol climate benefits by limiting HFCs, *Science*, *335* (6071), 922-923, doi: 10.1126/science.1216414, 2012.
- Volk, C.M., J.W. Elkins, D.W. Fahey, G.S. Dutton, J.M. Gilligan, M. Loewenstein, J.R. Podolske, K.R. Chan, and M.R. Gunson, Evaluation of source gas lifetimes from stratospheric observations, *J. Geophys. Res.*, *102* (D21), 25543-25564, doi: 10.1029/97JD02215, 1997.
- Vollmer, M.K., S. Reimann, D. Folini, L.W. Porter, and L.P. Steele, First appearance and rapid growth of anthropogenic HFC-245fa (CHF<sub>2</sub>CH<sub>2</sub>CF<sub>3</sub>) in the atmosphere, *Geophys. Res. Lett.*, *33*, L20806, doi: 10.1029/2006GL026763, 2006.
- Vollmer, M.K., L.X. Zhou, B.R. Grealley, S. Henne, B. Yao, S. Reimann, F. Stordal, D.M. Cunnold, X.C. Zhang, M. Maione, F. Zhang, J. Huang, and P.G. Simmonds, Emissions of ozone-depleting halocarbons from China, *Geophys. Res. Lett.*, *36*, L15823, doi: 10.1029/2009GL038659, 2009.
- Vollmer, M.K., B.R. Miller, M. Rigby, S. Reimann, J. Mühle, P.B. Krummel, S. O'Doherty, J. Kim, T.S. Rhee, R.F. Weiss, P.J. Fraser, P.G. Simmonds, P.K. Salameh, C.M. Harth, R.H.J. Wang, L.P. Steele, D. Young, C.R. Lunder, O. Hermansen, D. Ivy, T. Arnold, N. Schmidbauer, K.-R. Kim, B.R. Grealley, M. Hill, M. Leist, A. Wenger, and R.G. Prinn, Atmospheric histories and global emissions of the anthropogenic hydrofluorocarbons HFC-365mfc, HFC-245fa, HFC-227ea, and HFC-236fa, *J. Geophys. Res.*, *116* (D8), D08304, doi: 10.1029/2010JD015309, 2011.
- von Hobe, M., J.-U. Groöf, G. Günther, P. Konopka, I. Gensch, M. Krämer, N. Spelten, A. Afchine, C. Schiller, A. Ulanovsky, N. Sitnikov, G. Shur, V. Yushkov, F. Ravegnani, F. Cairo, A. Roiger, C. Voigt, H. Schlager, R. Weigel, W. Frey, S. Borrmann, R. Müller, and F. Stroh, Evidence for heterogeneous chlorine activation in the tropical UTLS, *Atmos. Chem. Phys.*, *11* (1), 241-256, doi: 10.5194/acp-11-241-2011, 2011.
- Wallington, T.J., W.F. Schneider, D.R. Worsnop, O.J. Nielsen, J. Sehested, W.J. DeBruyn, and J.A. Shorter, The environmental impact of CFC replacements – HFCs and HCFCs, *Environ. Sci. Technol.*, *28* (7), 320A-326A, doi: 10.1021/es00056a002, 1994.
- Wan, D., J. Xu, J. Zhang, X. Tong, and J. Hu, Historical and projected emissions of major halocarbons in China, *Atmos. Environ.*, *43* (36), 5822-5829, doi: 10.1016/j.atmosenv.2009.07.052, 2009.
- Warwick, N.J., J.A. Pyle, G.D. Carver, X. Yang, N.H. Savage, F.M. O'Connor, and R.A. Cox, Global modeling of biogenic bromocarbons, *J. Geophys. Res.*, *111* (D24), D24305, doi: 10.1029/2006JD007264, 2006a.
- Warwick, N.J., J.A. Pyle, and D.E. Shallcross, Global modelling of the atmospheric methyl bromide budget, *J. Atmos. Chem.*, *54* (2), 133-159, doi: 10.1007/s10874-006-9020-3, 2006b.
- Watling, R., and D.B. Harper, Chloromethane production by wood-rotting fungi and an estimate of the global flux to the atmosphere, *Mycol. Res.*, *102* (7), 769-787, doi: 10.1017/S0953756298006157, 1998.
- Weiss, R.F., J. Mühle, P.K. Salameh, and C.M. Harth, Nitrogen trifluoride in the global atmosphere, *Geophys. Res. Lett.*, *35* (20), L20821, doi: 10.1029/2008GL035913, 2008.
- Wever, R., and M.A. van der Horst, The role of vanadium haloperoxidases in the formation of volatile brominated compounds and their impact on the environment, *Dalton Trans.*, *42* (33), 11778-11786, doi: 10.1039/c3dt50525a, 2013.

- Wisher, A., D.E. Oram, J.C. Laube, G.P. Mills, P. van Velthoven, A. Zahn, and C.A.M. Brenninkmeijer, Very short-lived bromomethanes measured by the CARIBIC observatory over the North Atlantic, Africa and Southeast Asia during 2009–2013, *Atmos. Chem. Phys.*, *14* (7), 3557–3570, doi: 10.5194/acp-14-3557-2014, 2014.
- WMO, (World Meteorological Organization), *Scientific Assessment of Ozone Depletion: 1991 Global Ozone Research and Monitoring Project–Report No. 25*, Geneva, Switzerland, 1992.
- WMO (World Meteorological Organization), *Scientific Assessment of Ozone Depletion: 2002*, Global Ozone Research and Monitoring Project–Report No. 47, Geneva, Switzerland, 2003.
- WMO (World Meteorological Organization), *Scientific Assessment of Ozone Depletion: 2006*, Global Ozone Research and Monitoring Project–Report No. 50, 572 pp., Geneva, Switzerland, 2007.
- WMO, (World Meteorological Organization), *Scientific Assessment of Ozone Depletion: 2010*, Global Ozone Research and Monitoring Project–Report No. 52, Geneva, Switzerland, 2011.
- Wofsy, S.C., HIPPO Science Team, and Cooperating Modellers and Satellite Team, HIAPER Pole-to-Pole Observations (HIPPO): Fine-grained, global-scale measurements of climatically important atmospheric gases and aerosols, *Phil. Trans. R. Soc. A*, *369* (1943), 2073–2086, doi: 10.1098/rsta.2010.0313, 2011.
- Worton, D.R., W.T. Sturges, J. Schwander, R. Mulvaney, J.-M. Barnola, and J. Chappellaz, 20<sup>th</sup> century trends and budget implications of chloroform and related tri- and dihalomethanes inferred from firn air, *Atmos. Chem. Phys.*, *6* (10), 2847–2863, doi: 10.5194/acp-6-2847-2006, 2006.
- Wright, J.S., R. Fu, S. Fueglistaler, Y.S. Liu, and Y. Zhang, The influence of summertime convection over Southeast Asia on water vapor in the tropical stratosphere, *J. Geophys. Res.*, *116* (D12), D12302, doi: 10.1029/2010JD015416, 2011.
- Wu, J., X. Fang, J.W. Martin, Z. Zhai, S. Su, X. Hu, J. Han, S., Lu, C., Wang, J., Zhang, and J., Hu, Estimated emissions of chlorofluorocarbons, hydrochlorofluorocarbons, and hydrofluorocarbons based on an interspecies correlation method in the Pearl River Delta region, China, *Sci. Total. Environ.*, *470–471*, 829–834, doi: 10.1016/j.scitotenv.2013.09.071, 2014.
- Xiao, X., R.G. Prinn, P.J. Fraser, R.F. Weiss, P.G. Simmonds, S. O’Doherty, B.R. Miller, P.K. Salameh, C.M. Harth, P.B. Krummel, A. Golombek, L.W. Porter, J.W. Elkins, G.S. Dutton, B.D. Hall, L.P. Steele, R.H.J. Wang, and D.M. Cunnold, Atmospheric three-dimensional inverse modeling of regional industrial emissions and global oceanic uptake of carbon tetrachloride, *Atmos. Chem. Phys.*, *10* (21), 10421–10434, doi: 10.5194/acp-10-10421-2010, 2010a.
- Xiao, X., R.G. Prinn, P.J. Fraser, P.G. Simmonds, R.F. Weiss, S. O’Doherty, B.R. Miller, P.K. Salameh, C.M. Harth, P.B. Krummel, L.W. Porter, J. Mühle, B.R. Grealley, D. Cunnold, R. Wang, S.A. Montzka, J.W. Elkins, G.S. Dutton, T.M. Thompson, J.H. Butler, B.D. Hall, S. Reimann, M.K. Vollmer, F. Stordal, C. Lunder, M. Maione, J. Arduini, and Y. Yokouchi, Optimal estimation of the surface fluxes of methyl chloride using a 3-D global chemical transport model, *Atmos. Chem. Phys.*, *10* (12), 5515–5533, doi: 10.5194/acp-10-5515-2010, 2010b.
- Xue, L.K., T. Wang, I.J. Simpson, A.J. Ding, J. Gao, D.R. Blake, X. Z. Wang, W.X. Wang, H.C. Lei, and D.Z. Jing, Vertical distributions of non-methane hydrocarbons and halocarbons in the lower troposphere over northeast China, *Atmos. Environ.*, *45* (36), 6501–6509, doi: 10.1016/j.atmosenv.2011.08.072, 2011.
- Yao, B., M.K. Vollmer, L.X. Zhou, S. Henne, S. Reimann, P.C. Li, A. Wenger, and M. Hill, In-situ measurements of atmospheric hydrofluorocarbons (HFCs) and perfluorocarbons (PFCs) at the Shangdianzi regional background station, China, *Atmos. Chem. Phys.*, *12* (21), 10181–10193, doi: 10.5194/acp-12-10181-2012, 2012.
- Yevich, R., and J.A. Logan, An assessment of biofuel use and burning of agricultural waste in the developing world, *Global Biogeochem. Cycles*, *17* (4), 1095, doi: 10.1029/2002GB001952, 2003.
- Yokouchi, Y., M. Ikeda, Y. Inuzuka, and T. Yukawa, Strong emission of methyl chloride from tropical plants, *Nature*, *416*, 163–165, doi: 10.1038/416163a, 2002.
- Yokouchi, Y., F. Hasebe, M. Fujiwara, H. Takashima, M. Shiotani, N. Nishi, Y. Kanaya, S. Hashimoto, P. Fraser, D. Toom-Sauntry, H. Mukai, and Y. Nojiri, Correlations and emission ratios among bromoform, dibromochloromethane, and dibromomethane in the atmosphere, *J. Geophys. Res.*, *110*, D23309, doi: 10.1029/2005JD006303, 2005.
- Yokouchi, Y., S. Taguchi, T. Saito, Y. Tohjima, H. Tanimoto, and H. Mukai, High frequency measurements of HFCs at a remote site in east Asia and their implications for Chinese emissions, *Geophys. Res. Lett.*, *33* (21), L21814, doi: 10.1029/2006GL026403, 2006.
- Yokouchi, Y., T. Saito, C. Ishigaki, and M. Aramoto, Identification of methyl chloride-emitting plants and atmospheric measurements on a subtropical island, *Chemosphere*, *69* (4), 549–553, doi: 10.1016/j.chemosphere.2007.03.028, 2007.

- Yokouchi, Y., T. Saito, A. Ooki, and H. Mukai, Diurnal and seasonal variations of iodocarbons ( $\text{CH}_2\text{ClI}$ ,  $\text{CH}_2\text{I}_2$ ,  $\text{CH}_3\text{I}$ , and  $\text{C}_2\text{H}_5\text{I}$ ) in the marine atmosphere, *J. Geophys. Res.*, *116* (D6), D06301, doi: 10.1029/2010JD015252, 2011.
- Yokouchi, Y., Y. Nojiri, D. Toom-Sauntry, P. Fraser, Y. Inuzuka, H. Tanimoto, H. Nara, R. Murakami, and H. Mukai, Long-term variation of atmospheric methyl iodide and its link to global environmental change, *Geophys. Res. Lett.*, *39* (23), L23805, doi: 10.1029/2012GL053695, 2012.
- Yoshida, Y., Y.H. Wang, T. Zeng, and R. Yantosca, A three-dimensional global model study of atmospheric methyl chloride budget and distributions, *J. Geophys. Res.*, *109* (D24), D24309, doi: 10.1029/2004JD004951, 2004.
- Youn, D., K.O. Patten, D.J. Wuebbles, H. Lee, and C.-W. So, Potential impact of iodinated replacement compounds  $\text{CF}_3\text{I}$  and  $\text{CH}_3\text{I}$  on atmospheric ozone: A three-dimensional modeling study, *Atmos. Chem. Phys.*, *10* (20), 10129-10144, doi: 10.5194/acp-10-10129-2010, 2010.
- Young, C.J., M.D. Hurley, T.J. Wallington, and S.A. Mabury, Atmospheric chemistry of  $\text{CF}_3\text{CF}_2\text{H}$  and  $\text{CF}_3\text{CF}_2\text{CF}_2\text{CF}_2\text{H}$ : Kinetics and products of gas-phase reactions with Cl atoms and OH radicals, infrared spectra, and formation of perfluorocarboxylic acids, *Chem. Phys. Lett.*, *473* (4-6), 251-256, doi: 10.1016/j.cplett.2009.04.001, 2009.
- Yujing, M., and A. Mellouki, Rate constants for the reactions of OH with chlorinated propanes, *Phys. Chem. Chem. Phys.*, *3*, 2614-2617, doi: 10.1039/b102971c, 2001.
- Yvon-Lewis, S.A., and J.H. Butler, Effect of oceanic uptake on atmospheric lifetimes of selected trace gases, *J. Geophys. Res.*, *107* (D20), 4414, doi: 10.1029/2001JD001267, 2002.
- Yvon-Lewis, S.A., E.S. Saltzman, and S.A. Montzka, Recent trends in atmospheric methyl bromide: Analysis of post-Montreal Protocol variability, *Atmos. Chem. Phys.*, *9* (16), 5963-5974, doi: 10.5194/acp-9-5963-2009, 2009.
- Zander, R., E. Mahieu, P. Demoulin, P. Duchatelet, G. Roland, C. Servais, M. De Mazière, and C.P. Rinsland, Evolution of a dozen non- $\text{CO}_2$  greenhouse gases above central Europe since the mid-1980s, *Environ. Sci.*, *2* (2-3), 295-303, 2005.
- Zander, R., E. Mahieu, P. Demoulin, P. Duchatelet, G. Roland, C. Servais, M. De Mazière, S. Reimann, and C.P. Rinsland, Our changing atmosphere: Evidence based on long-term infrared solar observations at the Jungfraujoch since 1950, *Sci. Tot. Environ.*, *391* (2-3), 184-195, doi: 10.1016/j.scitotenv.2007.10.018, 2008.
- Zhang, Z., R. Liu, R.E. Huie, and M.J. Kurylo, A gas-phase reactivity study of OH radicals with 1,1-dichloroethene and *cis*- and *trans*-1,2-dichloroethene over the temperature range 240-400 K, *J. Phys. Chem.*, *95* (1), 194-196, doi: 10.1021/j100154a039, 1991.
- Zhao, Z., P.L. Laine, J.M. Nicovich, and P.H. Wine, Reactive and nonreactive quenching of  $\text{O}(^1\text{D})$  by the potent greenhouse gases  $\text{SO}_2\text{F}_2$ ,  $\text{NF}_3$ , and  $\text{SF}_5\text{CF}_3$ , *Proc. Natl. Acad. Sci.*, *107* (15), 6610-6615, doi: 10.1073/pnas.0911228107, 2010.
- Ziska, F., B. Quack, K. Abrahamsson, S.D. Archer, E. Atlas, T. Bell, J.H. Butler, L.J. Carpenter, C.E. Jones, N.R.P. Harris, H. Hepach, K.G. Heumann, C. Hughes, J. Kuss, K. Krüger, P. Liss, R.M. Moore, A. Orlikowska, S. Raimund, C.E. Reeves, W. Reifenhäuser, A.D. Robinson, C. Schall, T. Tanhua, S. Tegtmeier, S. Turner, L. Wang, D. Wallace, J. Williams, H. Yamamoto, S. Yvon-Lewis, and Y. Yokouchi, Global sea-to-air flux climatology for bromoform, dibromomethane and methyl iodide, *Atmos. Chem. Phys.*, *13* (17), 8915-8934, doi: 10.5194/acp-13-8915-2013, 2013.